ADVANCED WARNING OPERATIONS COURSE (AWOC)

- FY13 OBJECTIVES

Severe Track

IC Severe 1 - Conceptual Models

Lesson 1: Conceptual Models for Supercell Tornadic Storms

Learning Objectives

1. Identify the importance of forward flank baroclinic vorticity.
2. Identify favorable storm-scale boundary characteristics which can enhance vertical vorticity

- Through tilting

- And stretching.

3. Identify potential origins of storm-scale vorticity due to the rear-flank downdraft (RFD)

- Downward-tilting of vortex lines along RFD surge

- Baroclinic generation in the RFD (due to buoyancy effects)

- Descending Reflectivity Core (DRC).

4. Identify the role of the RFD on tornado maintenance.

Lesson 2: Hail Storms

Learning Objectives

1. Identify the role of shear and midlevel rotation on updraft strength and hail threat.
2. Identify the role of convective available potential energy (CAPE) in the hail growth zone.

3. Identify favorable hail embryo sources.
4. Identify trajectories which maximize hailstone residence time in the hail growth zone.
5. Identify factors which influence the amount of melting a hailstone undergoes.
6. Identify characteristics of the high precipitation (HP) supercell with a deep convergence zone (DCZ).

Lesson 3: Flash Flooding

Learning Objectives

1. Identify synoptic scale patterns that enhance the heavy rainfall and flash flood potential.
2. Identify meteorological ingredients that enhance the heavy rainfall and flash flood potential.
3. Identify other events and features that provide heavy rain and flash flooding.

Lessons 1-3: Performance Objective

1. The trainee will demonstrate ability to incorporate knowledge of conceptual models to describe convective storm structure and evolution.

IC Severe 2 - Threat Assessment

Lesson 1: Lifting Mechanisms

Learning Objectives

1. Identify regions of potential convective instability.
2. Identify types of lifting mechanisms.
3. Identify the factors in evaluating lift.
4. Identify the effects of orientation of line of forcing and boundary-relative steering-layer flow on convective evolution.

Lesson 2: Short-Term Assessment

Learning Objectives

1. Identify purposes of threat assessment.
2. Identify key job tasks for threat assessment for 0 to 24 hour time period.
3. Identify 3 key job tasks for threat assessment in the 0 to 6 hour time period.

Lesson 3: Threat Assessment of Quasi-Linear Convective Systems (QLCSs)

Learning Objectives

1. Identify some of the key features found in conceptual models of QLCS events.
2. Identify the types of QLCS events that produce the most intense impacts.
3. Identify parameters for evaluating the severity of QLCS events.
4. Identify discrimination capabilities of parameters used in forecasting QLCS events.
5. Identify patterns/parameters that affect longevity of a QLCS.
6. Determine motion of a QLCS (both forward propagating and backward).

Lessons 1-3: Performance Objective

1. Demonstrate processes for continuous evaluation of hazardous weather threats (tornadoes, damaging winds, and hail) to support effective warning methodologies.

Examples:

- Coordinate with SPC and adjacent FOs on watch decisions.
- Utilize full suite of products to issue short-term forecasts of convection
- Monitor mesoscale conditions and provide input to warning decisions based on that data.

IC Severe 3 - Storm Interrogation

Section 1: Locating Updrafts

Locating Updrafts of a Sheared Cell by Satellite

Learning Objectives

1. As a compliment to, or without radar data, use satellite data to locate an updraft to deep, moist convection in a sheared environment.

- Be able to use satellite data during the day or night.

Section 2: Updraft Strength

Estimating Updraft Intensity with Satellite: Part 1

Learning Objectives

1. Use satellite data to qualitatively estimate updraft strength in the absence of radar data based on

- Cloud top growth rates determined from temperature and the D2D cloud height estimation tool

- Temperature and height of the storm equilibrium level.

Estimating Updraft Intensity with Satellite: Part 2

Learning Objectives

1. Utilize the following satellite signatures to assist radar in estimating updraft strength and severe storm potential

- overshooting top characteristics,

- presence of an enhanced-V,

- anvil shape vs. storm-relative anvil-layer flow,

- and anvil top temperatures.

Section 3: Tornadogenesis

Part 1: Near Range Tornadogenesis Signatures Viewed by the WSR-88D

Learning Objectives

1. Recognize how tornado precursor signatures such as the mesocyclone and TVS appear in ranges less than 50 km.
2. Interpret favorable signatures indicating a likely tornado that can only be detected at close ranges.

Part 2: Near Range Tornadogenesis Signatures Viewed by the TDWR

Learning Objectives

1. Familiarize yourself with the applications and weaknesses of using Terminal Doppler Weather Radar (TDWR) for analyzing close range tornadogenesis signatures.
2. Be familiar with the characteristics of the TDWR.

Supercell Collapse Phase

Learning Objectives

1. Define the Supercell Collapse Phase.
2. Identify Collapse Phase Characteristics.
3. Identify Variations in the Collapse Phase.
4. Identify its Significance.
5. Identify Importance of Collapse Phase Recognition to the Warning Decision.

Section 4: Non-Tornadic Wind Event Detection

Extreme Non-Tornadic Wind Damage Events

Learning Objectives

1. Identify volumetric radar characteristics of extreme non-tornadic wind producing supercells within derecho producing MCSs.
2. Understand stormscale mechanisms for the production of extreme winds
3. Understand suggested operational philosophies during warning operations.

Section 5: Quasi-Linear Convective Systems

QLCS Storm-Scale Interrogation and Warning Considerations

Learning Objectives

1. Describe and identify QLCS growth stages and their characteristics (formation to dissipation).
2. Describe what broad QLCS structures/evolution yield the highest severe weather threat

- Understand the evolution of bow echoes and their time dependent severe weather threats.

1. Identify relevant characteristics of QLCS mesovortices

-Origins

-Lifecycle.

Warning Decision Making Issues with Derecho-Producing QLCS Events

Learning Objectives

1. Demonstrate the ability to identify synoptic- and/or mesoscale environments supportive of Quasi-Linear Convective Systems (QLCSs) including derechos.
2. Demonstrate the ability to identify WSR-88D signatures associated with derechos and their associated severe weather hazards in order to facilitate effective impact-based warning decisions by both customers and partners.

IC Severe 4 - Application and Review

AWOC Severe Forecast Challenge

Performance Objectives

Using the instruction provided in AWOC, students will:

1. Demonstrate how to evaluate severe weather risk using: An ingredients-based methodology pattern recognition
2. Exhibit improved severe weather forecast skill for: Tornado, hail, and wind
3. Demonstrate the ability to write an effective severe storm forecast discussion.

AWOC Severe Warning Case ILT Session

Performance Objective

1. The teletraining participant will demonstrate the ability to identify and apply important components of an effective warning methodology that includes threat assessment, storm interrogation strategies, and proper storm-based warning decision.

IC Severe 5 – Simulations

Performance Objectives

1. In accordance with AWOC training, using the WES Simulation Case, the trainee will demonstrate the ability to issue effective storm-based warnings to convey severe weather threats.

Welcome to AWOC Severe!

Each of the following handouts is numbered individually for each lesson, beginning at page one.

1. Conceptual Models for Supercell Tornadic Storms

Instructor Notes: Welcome AWOC students. The title for this lesson is Conceptual Models for Supercell Tornadic Storms. This is the first lesson in Instructional Component 1 in the AWOC Severe Track. Lesson 1 will describe various conceptual models for supercell tornadic storms, including some of the more recent research from VORTEX 2. Our authors are Brad Grant and Les Lemon.

Student Notes:

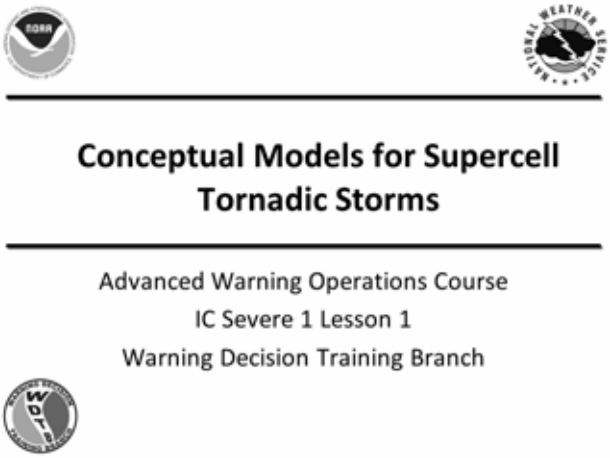

2. Instructional Component 1 Lesson Outline

Instructor Notes: The instruction for IC 1 in Severe Track is broken up into 3 lessons, with the following topics in each lesson: Tornadic supercell storms Hail storms Flash flooding (meteorological and hydrological effects) The learning and performance goals of this IC are the trainee will be able to demonstrate ability to incorporate the knowledge of conceptual models to help describe convective storm structure and evolution with a focus on the three threats listed here. Individual learning objectives are defined for each lesson with respective tests addressing the objectives. You might notice that multicell conceptual models are not explicitly identified in this Instructional Component. The reason is that in IC 2, lesson 3, Threat Assessment of Quasi-Linear Convective Systems , many conceptual models of multicell storms are shown as a part of treating the understanding of the threat assessment process for QLCSs.

Student Notes:

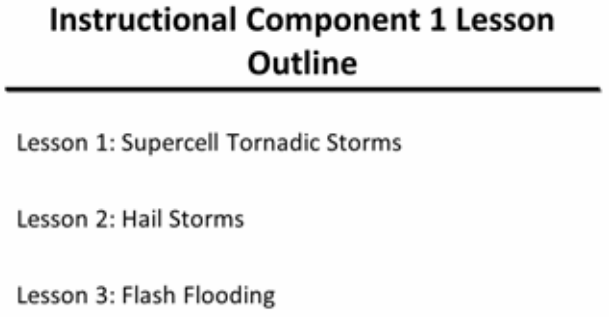

3. Learning Objectives

Instructor Notes: These are the learning objectives for lesson 1. Identify the importance of forward flank baroclinic vorticity. 2. Identify favorable storm-scale boundary characteristics which can enhance vertical vorticity through tilting and stretching.3. Identify potential origins of storm-scale vorticity due to the rear-flank downdraft (RFD) such as downward-tilting of vortex lines along RFD surge, baroclinic generation in the RFD (due to buoyancy effects), and the Descending Reflectivity Core (DRC). And 4) Identify the role of the RFD on tornado maintenance. There will be a test on the learning objectives for this lesson.

Student Notes:

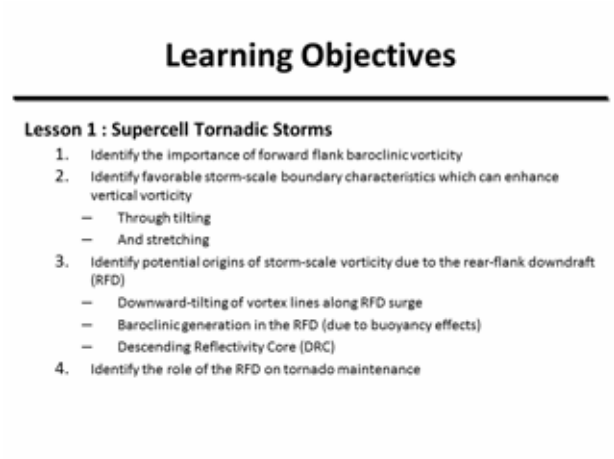

4. Introduction

Instructor Notes: According to Smith et al. (2012), nearly 90% of strong (EF2/3) and virtually all violent (EF4/5) tornadoes in the U.S. are spawned by right-moving supercell thunderstorms. Increased accessibility to advanced computer modeling, observations, and technology such as dual-pol radar have been used to study supercells more than ever before, enabling detailed scientific exploration of supercells and tornadoes, such as the Verification of the Origins of Rotation in Tornadoes Experiment (VORTEX2), conducted in 2009-10. One of the goals of VORTEX 2, which was a successor to VORTEX 1 conducted back in the mid 90s, was to better understand the processes related to tornado formation, in particular, the wind, precipitation, and thermodynamic data and the local environment influential to the tornado life cycle. A better understanding of the tornado life cycle can help tornado warning accuracy, lead time, and false alarm rates. Results from VORTEX 2 are still being formulated but there has been a notable increase in the knowledge concerning the conceptual models of the processes governing tornadic storms. However, the findings have also accentuated gaps in our understanding of tornadogenesis, persistence, and demise. This module attempts to shed more light on supercell tornadoes based on observational evidence from VORTEX 1 and 2.

Student Notes:

Introduction

5. Supercell Tornadoes vs Non Supercell Tornadoes

Instructor Notes: Tornadoes require a high concentration of vertical vorticity (vortex lines) embedded in converging and ascending flow into a convective updraft. The lines in the above figure containing a rotational symbol are “vortex lines” defined as a line that is everywhere tangent to the local vorticity vector. The basic structure shown in a) is that vertical vorticity is already embedded in a line of convergence and waiting for a locally intense updraft to intensify it through stretching. This type of tornado has been called a landspout, but is more appropriately, a non-mesocyclonic tornado. This type of tornado is the only kind that can occur in association with an ordinary cell updraft. The second type of tornado (b) is the type we will discuss in this lesson. They occur in an environment that has little vertical vorticity previous to the storm. In order to get a tornado, a downdraft must tilt vorticity into the vertical position at ground. An updraft cannot accomplish this by itself and so this tornado requires the existence of a downdraft. We call this a mesocyclonic tornado that can accompany supercells. Many tornadoes derive their vorticity from both sources but in disproportionate amounts. And finally, the origin of vorticity for the “mesovortex” associated with the QLCS tornadoes remains somewhat of a mystery.

Student Notes:

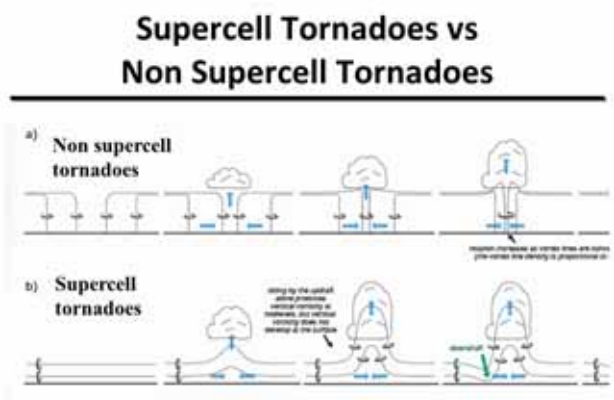

Markowski (2008)

6. Vorticity Sources Required for Supercell Tornadoes

Instructor Notes: Environmental vorticity produced by shear is typically on the order of 10 to the -2 per second in the lower troposphere. In contrast, vorticity can be generated internally in supercell environments and can occur through a variety of ways, principally by horizontal buoyancy gradients (the so-called baroclinicity effects or sometimes correctly termed baroclinity) and these values are at least an order of magnitude larger than environmental vorticity.

Student Notes:

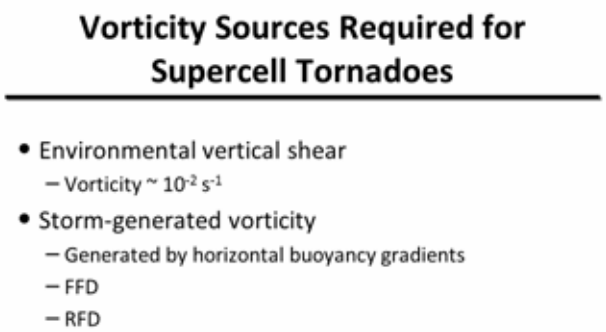

7. Sources of Vertical Vorticity(Streamwise horizontal vorticity stretched into storm updraft)

Instructor Notes: This 3-D figure from COMET (adapted from Klemp, 1987) depicts a classic supercell in its mature phase. The near-surface vortex lines (in blue) represent the environmental vorticity bending toward the storm's updraft in the baroclinic zone of the forward flank downdraft. This diagram, based on simulations in the mid to late 80s, indicates the baroclinic generation of horizontal vorticity in the FFD region. Once vorticity enters the updraft, it is stretched vertically to create much stronger low-level rotation. This process can be an important contributor to low-level storm rotation, which previously was thought led directly to tornadogenesis. However, more recent research suggested that augmented horizontal vorticity from the FFD was usually insufficient for tornadogenesis. In moist, low-level conditions, there might not be a discernible FFD (thus no baroclinicity). The tornadic scale stretching is now believed to come from the RFD via tilting downward of vertical vorticity. Horizontal vorticity enhancements are necessary for low-level mesocyclogenesis. In rare cases where large-scale low-level horizontal vorticity is already very high (e.g., 0–3-km mean horizontal vorticity of 1 × 10 2 s 1 or greater or storm-relative helicity of 500 m2 s 2 or greater) or deep-layer shear is very strong (e.g., 50 m s 1 in the lowest 10 km AGL), forward flank baroclinicity alone may provide sufficient augmentation of the horizontal vorticity associated with the large-scale mean shear for tornadogenesis to occur. Other sources for streamwise vorticity that may become stretched into the updraft originate from behind the cold front boundary.

Student Notes:

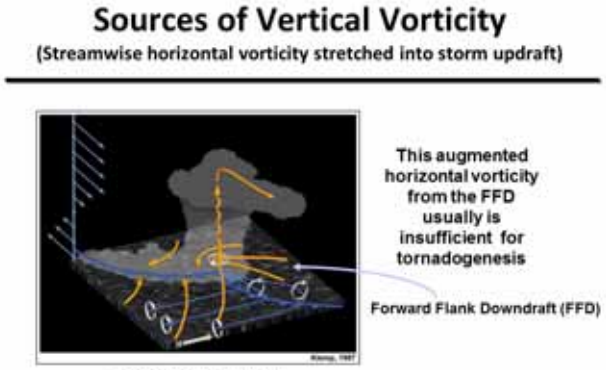

From COMET (1996)

8. Role of Baroclinic Generation of Vorticity

Instructor Notes: VORTEX 1 findings indicated that buoyancy gradients due to convective outflow and other mesoscale thermal boundaries generate baroclinic vorticity which can locally enhance the streamwise vorticity and storm-relative helicity (SRH). Thus, even though the horizontal baroclinic vorticity generated along a supercell's forward flank may be insufficient to support the low-level mesocyclonegenesis necessary for tornadoes, the addition of baroclinic vorticity from a pre-existing outflow boundary may be sufficient. It's important to note that this baroclinically-generated horizontal vorticity remains long after the associated thermal gradient has weakened or dissipated. Numerous baroclinic vorticity zones associated with remnant boundaries could exist virtually undetected across the mesoscale landscape. That's why it's important to review radar reflectivity, storm total precipitation, and high-resolution visible satellite loops from several hours previously to help identify any remnant outflow boundaries.

Student Notes:

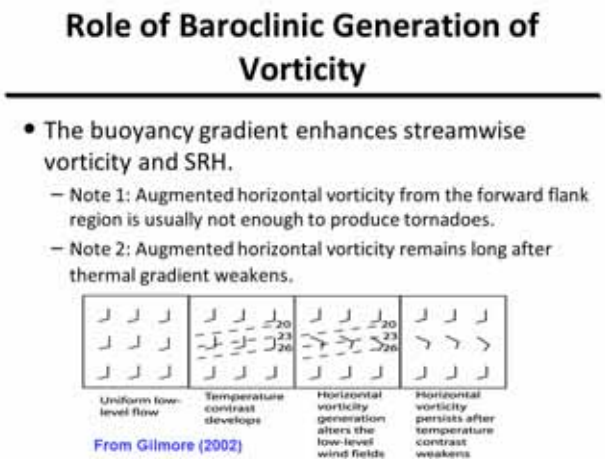

9. Anvil-Generated Baroclinity

Instructor Notes: This is a conceptual model by Markowski et al. (1998) showing enhancement of low-level horizontal vorticity by an anvil-generated baroclinic zone. The amount of horizontal vorticity generated is a function of baroclinity and parcel residence time in the baroclinic zone. Residence time is a function of both storm-relative inflow speed and crossing angle with respect to the baroclinity. Horizontal vorticity will be mostly streamwise if the crossing angle of the storm relative near-surface inflow with respect to the anvil zone is very small (~ 0). The estimated maximum parcel residence time was around two hours for the three cases examined. Their research of proximity hodographs in baroclinic regions revealed that to maximize horizontal vorticity generation in the near-ground inflow, the head of the storm motion vector should lie close to the line drawn from the heads of the 0 to 500 mb mean wind vector and the wind vector near the equilibrium level. This assumes that the baroclinic zone is aligned closely with the anvil edge. Horizontal vorticity generated with a streamwise component can serve to enhance the storm-relative helicity already present in the environment due to the low-level vertical shear. SRH has been shown to be the source for net updraft rotation in supercells. Thus, the observations of anvil-generated baroclinicity had implications for the origin or enhancement of updraft rotation in thunderstorms.

Student Notes:

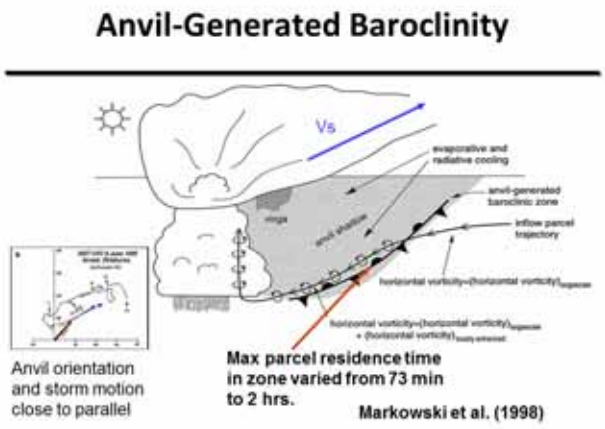

10. Sources of Streamwise Vorticity

Instructor Notes: The sources of streamwise vorticity in supercell thunderstorms are important to understand. Atkins et al. (1999) presented a case which explained the concept showing low-level storm structure (0.5 km AGL) at 1 hour for a boundary simulation and the source region for the low-level meso which is in the yellow square region. Parcels from behind the boundary and in the forward flank regions acquired a streamwise horizontal vorticity which, after tilting and stretching by storm's updraft, aided low-level mesocyclogenesis. In the diagram (a), rainwater mixing ratio greater than 0.1 g kg−1 is shaded gray. The gray contours are rainwater mixing ratio starting at 1.0 g kg−1. Thin black lines are θe (K). Thick black lines are vertical vorticity with contours starting at 0.01 s−1 and a contour interval of 0.01 s−1. The vector field is horizontal vorticity. In diagram (b), positive and negative vertical velocities are gray shades and thick dashed lines, respectively. The contour and shade interval is 2 m s−1 . Thin solid lines are the projection of the 3D trajectory locations. I've drawn arrows to highlight the three principal trajectory projections, blue is the forward flank region, purple is the behind the boundary, and red arrow indicates the inflow region. Numbers at the black dots on the midlevel trajectories are the height of the parcel (AGL). Thick solid lines are vertical vorticity. Note that the preexisting boundary provides an important additional source region of parcels at low levels that have acquired solenoidally generated streamwise vorticity. The next slide shows a slightly different result from VORTEX 2.

Student Notes:

Sources of Streamwise Vorticity

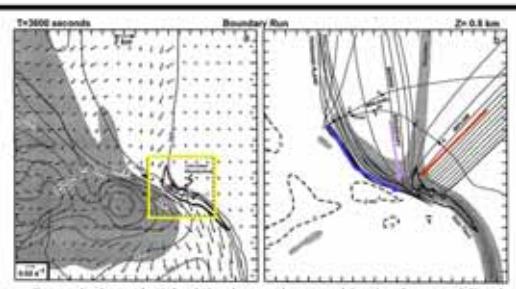

Parcels from behind the boundary and in the forward flank regions acquire streamwise horizontal vorticity; which, after tilting and stretching by storm's updraft can aid low-level mesocyclogenesis (Atkins et al. 1999)

11. Is All Horizontal Vorticity in the Forward Flank Region Streamwise?

Instructor Notes: VORTEX 2 findings suggested baroclinically generated vorticity below .75 km was crosswise (vector points across the thermal gradient), which was at odds in previous numerical simulations. It might have been influenced by surface drag. However, they did find more streamwise vorticity at Z=.75 km and above.

Student Notes:

Is All Horizontal Vorticity in the Forward Flank Region Streamwise?

- Some baroclinic generated vorticity in the Goshen, WY VORTEX 2 storm was oriented crosswise at low-levels

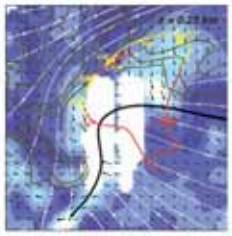

From Markowski et al (2012)

12. Role of the RFD

Instructor Notes: Hi, this is Les Lemon. The purpose of this supercell schematic and the material to come in this lesson is designed to inform the student of our present day understanding of the supercell as well as how it relates to warning issuance and radar detection. This conceptual supercell model was introduced in 1979 but is still largely current today. On the left is the schematic plan view of a supercell storm at the surface. Relevant details will be covered in the next slides. On the right, is the associated schematic depiction of the drafts, flow field, mesocyclone, and tornado within an evolving supercell (precipitation echo is omitted). Major features are labeled including storm relative flow in low-, mid-, and upper-levels throughout. Tornado is seen developing aloft in b) and over the full depth in c). While the RFD is seen as originating at ~ 9 km AGL that is still uncertain. The RFD is conceptualized more as a zone of flow decent where air parcels flow into the RFD while maintaining horizontal momentum, flow across the downdraft while descending, and flow out of the RFD where parcels mix with adjacent updraft. Note that the mesocyclone is seen as having a “divided structure” over the lower ½ to 2/3rds of storm depth similar to an extra-tropical cyclone (ETC). Storm relative, the mesocyclone updraft and storm inflow are on the left similar to the ETC “warm sector”, on the right is the downdraft (RFD) and outflow. Tornadogenesis takes place at the updraft-downdraft (RFD) interface but just inside the updraft. Note the “Forward Flank Downdraft” (FFD) is typical of all thunderstorms and is found in the precipitation cascade region. The RFD is unique to the supercell and is critical to tornadogenesis. The RFD is seen to flow or migrate around the circulation center (tornado location) as the RFD gust front “occludes”. A new updraft is shown in d) originating at the occlusion and may cycle through the process again becoming a cyclic tornado producer. Several features are included with this model, 1) the RFD and is critical role in tornadogenesis, 2) the divided structure of the mesocyclone incorporating both updraft and RFD downdraft, 3) mesocyclone occlusion similar to the ETC. This model also, 4) incorporates the cyclic nature of some supercells and, as a part of 5), the collapse phase of some supercells (not covered here). Note that while the mesocyclone appears as a microcosm of the ETC, its dynamics are very different. Note, that the mesocyclone over most of its life and the lowest ½ to 2/3rds of storm depth is not a “rotating updraft” but an analogue to the ETC.

Student Notes:

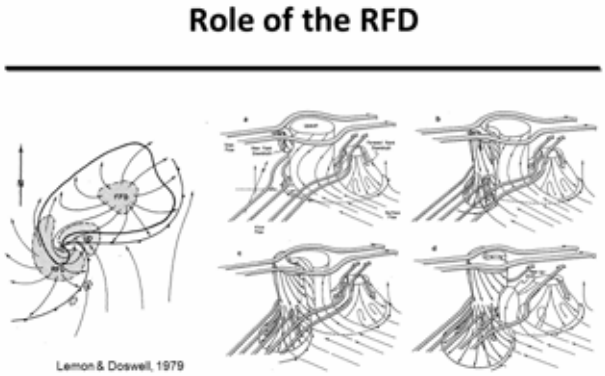

13. Role of the RFD (cont.)

Instructor Notes: This schematic and photo tie the storm structure to the visual cloud and tornado locations. (After Lemon and Deswell, 1979) As in the previous slide, the thick line encompasses the radar echo. The gust front structure and occluding wave are depicted with solid lines and frontal symbols. Updraft (UD) and (Rear Flank Downdraft, RFD; and Forward Flank Downdraft, FFD) are included along with streamlines (surface relative). Tornado location is the encircled T. The photo on the right is taken from east southeast of the tornado, ahead of the RFD gust front and clearly shows the sunlit “clear slot” behind the bowing and occluding RFD gust front. Also seen in the photo is the dark, “horseshoe shaped” rain free cloud-base ahead of the wrapping RFD and is the major storm updraft. The tornado is seen in the distance located at the updraft/RFD downdraft interface.

Student Notes:

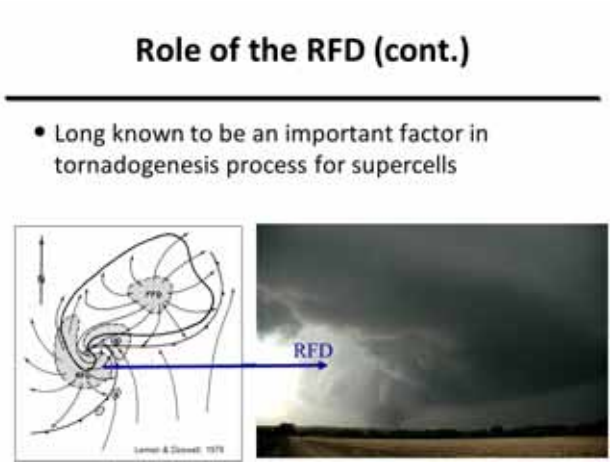

14. Thermodynamics of the RFD Play Big Role in Tornadogenesis

Instructor Notes: Markowski et al. (2002), developed this composite diagram illustrating the general characteristics of RFDs that are associated with supercells that produce “significant” (e.g., EF2 or stronger, or EF0–EF1 tornados persisting for >5 min) are shown in the upper two diagrams. RFDs associated with non-tornadic supercells or those that produce weak, brief tornadoes are shown in the lower diagrams. The thick, dashed contour is the outline of the hook echo, and thin, solid arrows represent idealized streamlines. Again, the bottom two depictions illustrate tornadogenesis failures. In cases where the RFD is characterized with only small theta-e deficits, small CIN, and significant potential CAPE (the above two illustrations) then significant tornadoes often result. But when the dominant RFD outflow is characterized by large theta-e deficits and little potential CAPE, tornado genesis failures or only weak, short-lived tornadoes result as in the lower two frames. Note the above processes can arise with new RFD Internal Surges (RFDIS) and can sustain or end the life of associated tornadoes [Lee et al. (2012); Marquis, et al., (2012)]

Student Notes:

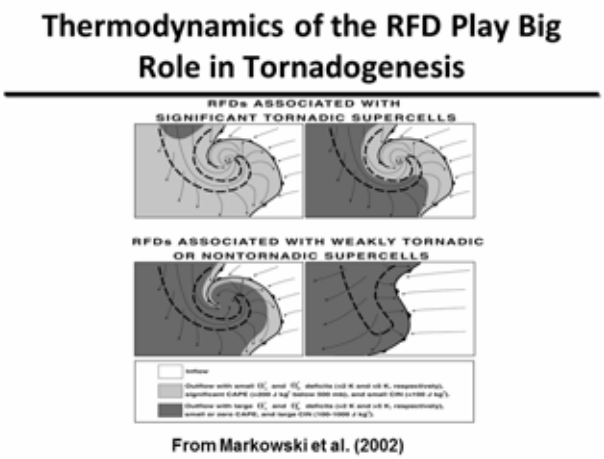

15. Tilting Vertical Vorticity in the Downdraft

Instructor Notes: Here's an illustration showing the development of vorticity in both updraft and downdraft. Vertical vorticity and the mid-level mesocyclone has long been known to originate from the tilting of environmental horizontal vortex lines into the vertical and subsequent vertical stretching in the developing supercell updraft. However, the downward tilting of vortex lines in the RFD resulting in the low-level mesocyclone is of more recent understanding [e.g., Markowski, et al. (2008)]. This results in significant vertical vorticity next to the ground and the low-level mesocyclone. If baroclinity is absent (and turbulent diffusion is neglected), vortex lines are frozen in the fluid and are redistributed by the downdraft as material lines. In this case, the vortex line passing through the low-level vertical vorticity maximum and takes on a U shape rather than an arch. A couplet of counter-rotating vortices straddles the downdraft maximum and often the hook echo. When this and baroclinic vorticity generated from the RFD are converged and stretched, within the updraft, tornadogenesis may result.

Student Notes:

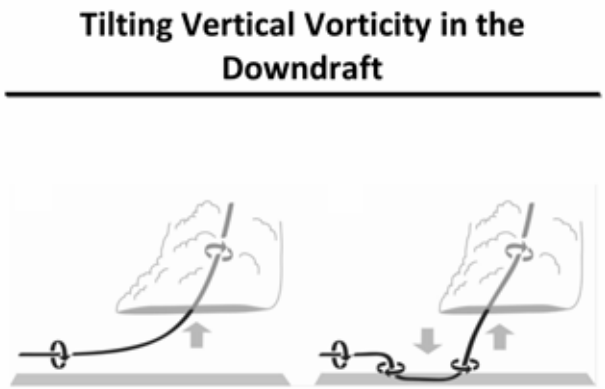

Markowski (2008)

16. Latest Research on the Role of RFDs and Tornadogenesis

Instructor Notes: VORTEX 2 observations reveal the development of arching vortex lines that join counter rotating vortices found to be straddling the hook echo. But this is similar to what had been seen before in VORTEX 1 and thought to suggest significant baroclinic vorticity generation. So, as a horizontal vortex ring forms around the RFD, the upward tilting of the ring begins where the local updraft maximum forms. Upward tilting then progresses forming a cyclonic-anticyclonic vertical vortex pair. The vortex arch matures as does the cyclonic-anticyclonic pair. In some instances a cyclonic tornado arises within the hook with the mesocyclone while an anti-cyclonic tornado arises to the rear of the hook echo at the other end of the vortex arch. Note that you may detect some hook echoes via your radar that actually reveal the counter rotating vortices. Note also that counter rotating tornadoes can actually arise in the hook echo region.

Student Notes:

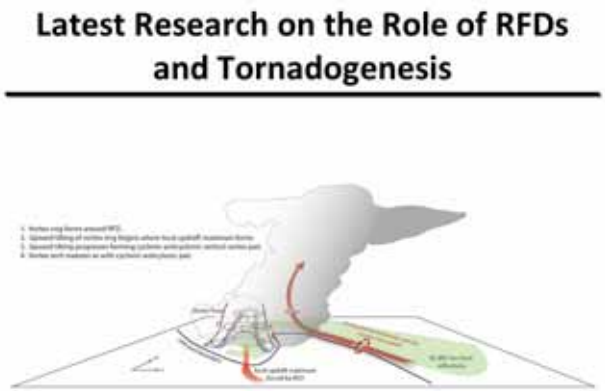

Adapted from Markowski et al (2012)

17. Hook Echo and the RFD

Instructor Notes: This hook echo schematic summarizes some recent and fascinating findings of Lee et al. While they studied several tornadoes via a mobile mesonet, this schematic summarizes observations made very near a large EF-4 tornado that occurred near Bowdle, SD. Embedded within the larger supercell RFDs they sometimes found "RFD Internal Surges" (RFDIS) and "RFDIS Boundaries" (RFDISB). These features are thought to contribute to tornadogenesis, maintenance, and demise through their thermodynamic and kinematic character. RFDISs with relatively strong kinematics and near neutral buoyancy that converge with very large potential buoyancy ahead of the RFD Internal Surge boundary contribute to tornado development and intensification. However, they also found RFDISs with weak kinematics and colder thermodynamics relative to the ambient RFDIS boundary air contributed to tornadogenesis failure or demise. Here, from the Bowdle, SD study we see a schematic hook echo tip region behind the leading RFD Gust Front (RFDGF) during the rapid intensification stage of the Bowdle, tornado. The Bowdle tornado intensification stage may represent an optimal situation combining: 1) RFD thermodynamics with just enough negative buoyancy for baroclinic vorticity generation (in this case the baroclinicity was provided by an RFDIS); 2) an augmented Tornado Cyclone convergence zone (denoted by the stippled vertical vortex sheet) due to the RFDIS and RFDISB interactions with the developing tornadic vortex; and 3) near-neutrally buoyant and very potentially buoyant air converging on the left flank of the tornado.

Student Notes:

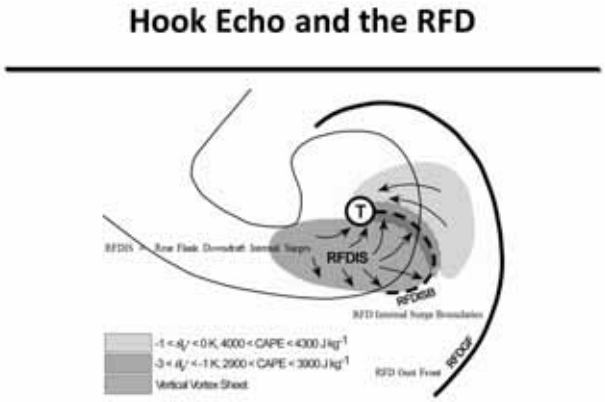

18. What About The RFD Surges and Tornado Development?

Instructor Notes: Fujita (1978) utilized his unprecedented care and detail to describe the relationship between tornadoes and downbursts from his storm damage survey of the Springfield, Illinois event of August 6, 1977. Eighteen tornadoes, 10 downbursts, and 17 microbursts are depicted in this map. Apparently, eight tornadoes formed on the left side of microbursts. No traces of downbursts were found in the vicinity of other tornadoes. Fujita documented very similar relationships in association with many other tornadoes. It is very likely that these microbursts and downbursts were “RFD Internal Surges”. Recall the supercell schematic surface depiction and photo previously showing the tornado to the left of the RFD and “clear slot”. (NWS meteorologists, when doing storm damage surveys, should be aware of these downbursts and microbursts associated with these damaging RFDIS and include them where appropriate.)

Student Notes:

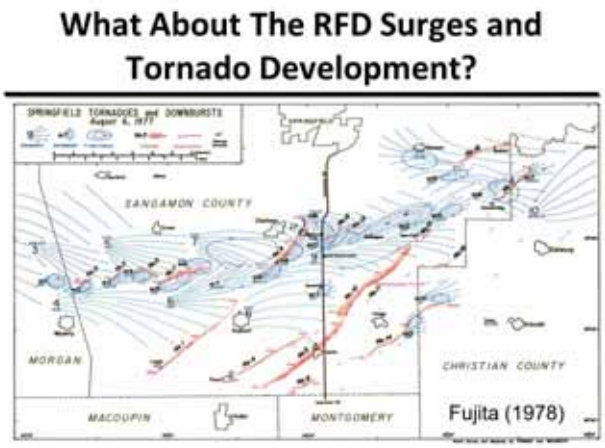

19. Tornado MaintenanceMarquis et al. 2012

Instructor Notes: As previously, a schematic illustration of the evolution of storm-scale features located on the rear-flank of the supercell storm during tornado maturity (t1 to t2) and at the time of demise (t3) in (c) the Crowell and Orleans storms. Figure (d) is a conceptual model of a supercell that does not include a secondary rear-flank downdraft and secondary gust front (adapted from Lemon and Doswell 1979). t2 represents a time immediately before a rapid decline in tornado intensity. A T marks the location of the tornado and an X marks the location of tornado demise at time t3. Black lines indicate the presence of kinematic gust front boundaries, gray shades indicate varying magnitudes of low-level divergence associated with the rear-flank downdraft, and gray contours indicate radar reflectivity. Fine dashed lines indicate that the feature continues beyond the area shown. Long dashed lines indicate uncertainty in the location of the feature. In (C), tornadoes in two other storms persist within a band of low-level convergence in the outflow air (a possible secondary rear-flank gust front), suggesting that tornado maintenance can occur away from the main boundary separating the outflow air and the ambient environment. The Almena case resembles most closely the Lemon and Doswell (1979) model.

Student Notes:

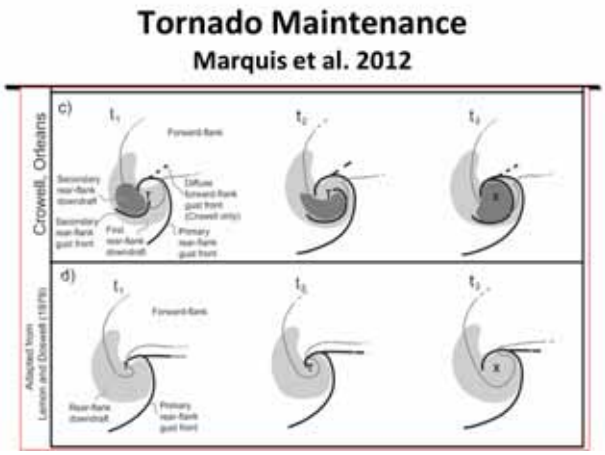

20. Tornado Maintenance (Cont.)Marquis et al. 2012

Instructor Notes: For two other storms in the Marquis et al. (2012) study, Crowell and Orleans, tornadoes persisted within a band of low-level convergence in the outflow air, not along a RFD Internal Surge Boundary, which suggests that tornado maintenance can occur away from the main boundary separating the outflow air and the ambient environment.

Student Notes:

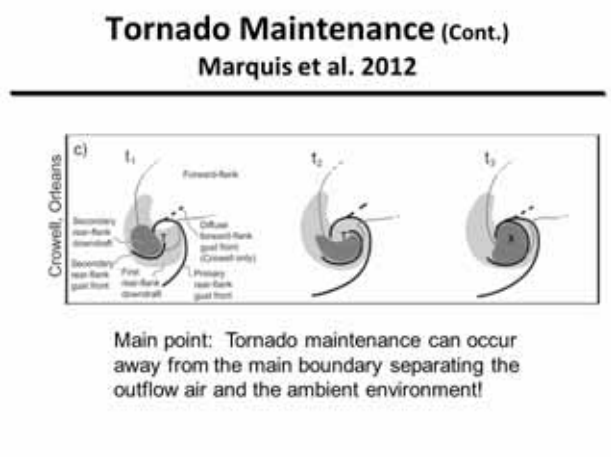

21. Descending Reflectivity Core (DRC) Role in Tornado Production

Instructor Notes: The descending reflectivity core (DRC) is a descending region of precipitation arriving at the surface of some supercells as part of, or very near the hook echo. When a DRC develops, a vorticity couplet straddling the feature is often found. However, whereas earlier studies of this feature seemed to implicate it's importance to low-level tornadogenesis, other studies have not upheld that observation. Tornadogenesis occurred in those studies with or without this feature. In Markowski et al (2012), a DRC was found in the VORTEX 2 Goshen County, Wyoming tornadic supercell to have some seemingly minor importance in altering the mesocyclone circulation and buoyancy fields. This, in turn, appears to promote the low-level mesocyclone occlusion. However, this VORTEX 2 study failed to establish a real importance to the DRC. Much more study is needed.

Student Notes:

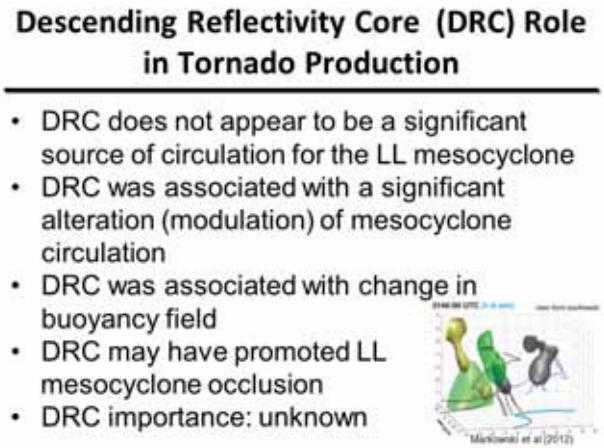

22. RFD Video

Instructor Notes: This is a video by Neal Rasmussen showing an excellent development of the RFD and subsequent tornadogenesis. This video will play continuously until you click the advance slide.

Student Notes:

23. Updraft, RFD, and Tornado-Life Cycle

Instructor Notes: Note the strong divergence to the rear of the funnel/tornado and the descending cloud fragments to your left and the tornado's right flank. Note also that the descending precipitation is being driven or forced to the ground by the RFD in which the rain is embedded.

Student Notes:

24. Relative Roles of FFD and RFD

Instructor Notes: Both the forward flank downdraft (FFD) and rear-flank downdraft (RFD) play important roles in tornadogenesis, sustenance, and demise. The FFD provides baroclinic streamwise horizontal vorticity along the forward flank baroclinic zone which in turn is tilted and stretched. This helps to create the low-level mesocyclone and, at times, the tornado as well. However, this alone appears to be insufficient for tornadogenesis. The FFD also contributes substantially to mesocyclone circulation and tornadic inflow. The RFD contributes to low-level baroclinic horizontal vorticity generation along its rear flank gust front which is turned into the vertical and converges rapidly into the updraft and developing tornado. Further, high potential CAPE associated with both the RFD and RFDIS is ingested by the tornado vortex and stretched. But, because the RFD is often weakly negatively buoyant (contributing to baroclinic vorticity generation) it requires a vertically directed pressure gradient force (VDPGF) to forcibly lift it to its level of free convection (LFC). Once reaching its LFC, that now buoyant air is rapidly accelerates vertically and is stretched, amplifying its vertical vorticity. Interestingly, in the VORTEX 2 Goshen County case only about 1/4th of the tornadic vorticity arose from the near-storm environment, but 3/4ths were generated by the storm itself. However, at this point we can only say with confidence that both the RFD and the FFD are important to tornadogenesis, sustenance, and demise. (Note: A good article describing these roles is at http://journals.ametsoc.org/doi/pdf/10.1175/MWR-D-11-00337.1).

Student Notes:

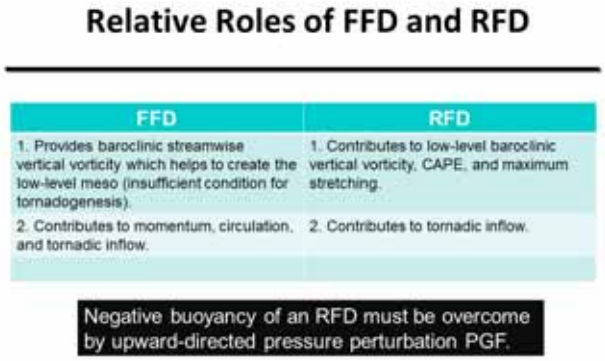

25. Questions About the Roles of FFD and RFD

Instructor Notes: So, perhaps the FFD should be viewed as the main source of circulation, with the RFD being responsible for the rapid descent of the "rear" of the circuits that allows the circuits to become horizontal at their "final" positions? Alternatively, perhaps distinguishing between RFDs and FFDs is no longer fruitful, given that the RFD and FFD typically occur within one large, contiguous region of downdraft, and sometimes there may not even be two distinct downdraft maxima. Obviously, the relative roles of the FFD and the RFD have yet to be satisfactorily resolved. On the one hand, the RFD seems to be more relevant to the tornadogenesis process than the FFD because the RFD has vertical velocities an order of magnitude larger than the FFD and is associated with even larger horizontal gradients of vertical velocity (and therefore much larger vorticity tilting rates) given its closer proximity to the storm updraft. But, the researchers in VORTEX 2 felt that they couldn't dismiss the possibility of the process occurring within the gentle descent of the FFD. The development of only a small vertical vorticity component could be important given the subsequent exponential intensification possible from stretching.

Student Notes:

Questions About the Roles of FFD and RFD

- FFD: Is it the main source of circulation?
- RFD: Does it produce the final orientation of vorticity tilting (upward)?
- RFDs/FFDs continuous?
- Not distinct?

26. Summary

Instructor Notes: Vorticity generated from environment is relevant (for tilting and stretching). Environmental vorticity is important for developing mid-level meso but not low-levels. Analysis from VORTEX 2 suggests that storm-generated vorticity is a dominant contributor to the circulation of the low-level mesocyclone.

Student Notes:

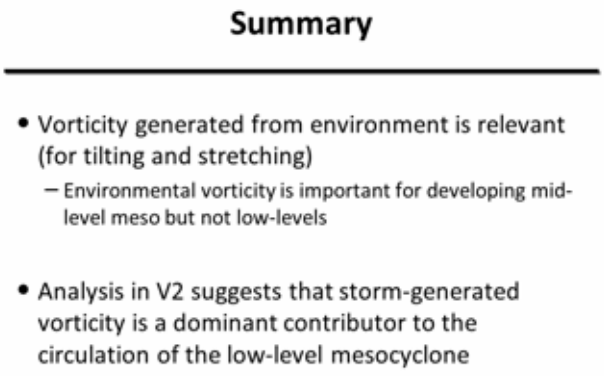

27. Summary (cont.)

Instructor Notes: The low-level mesocyclone region is increasingly dominated by air parcels originating in the RFD outflow (as opposed to the warm sector). The initial rear-flank downdraft produces low level baroclinic vorticity that is tilted upward and stretched. A secondary RFD forms (called the RFDIS) cyclonically wraps around the developing tornado. Kinematic and thermodynamic analyses suggest that horizontal vorticity created in the forward-flank downdraft region and in the RFD region near the hook echo is tilted and then stretched near the developing tornado. Tilting and stretching are enhanced in the developing low-level circulation as the RFDIS develops, intensifies, and wraps around the circulation center. Shortly thereafter, the tornado forms. Tornadic circulations can also persist within a band of low-level convergence in the RFD outflow air, not along the RFDIS boundary. This suggests that tornado maintenance can occur away from the main boundary separating the outflow air and the ambient environment.

Student Notes:

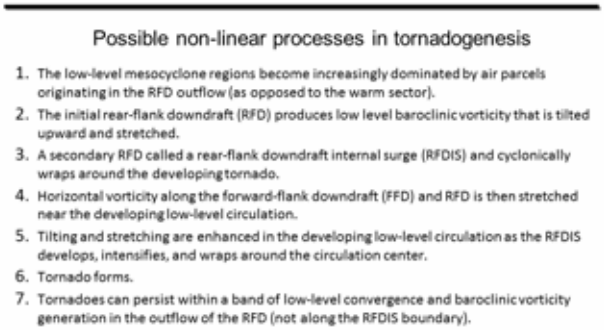

28. Summary (cont.)

Instructor Notes: RFD internal surge (RFDIS) events appear to influence tornado development, intensity, and demise by altering the thermodynamic and kinematic character of the RFD region bounding the pretornadic and tornadic circulations. Significant tornadoes develop and mature when the RFD, modulated by internal surges, is kinematically strong, only weakly negatively buoyant, and very potentially buoyant. The influx of near-neutrally buoyant air with very large potential buoyancy may aid tornado intensification via enhanced vortex stretching. In contrast, the demise of the tornado intercepted by V2 (Bowdle storm) was concurrent with a much cooler RFDIS that replaced more buoyant and far more potentially buoyant RFD air near the tornado. This surge also likely contributed to a displacement of the tornado from the storm updraft. An RFDIS coupled with a convergent, near-neutrally buoyant and very potentially buoyant RFD flow field appeared to play an important role in the rapid intensification stage. Tornado intensification may depend on interaction of RFDIS convergence zone with pre-tornadic circulation as seen in this model.

Student Notes:

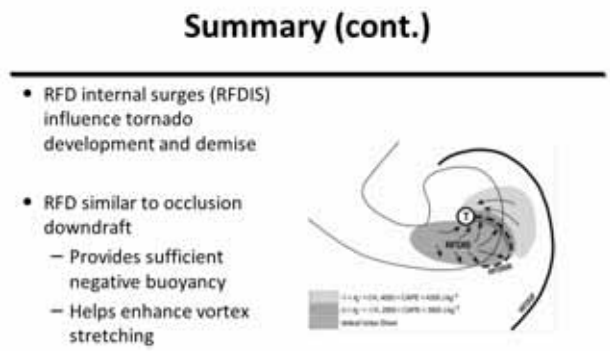

29. What Causes Tornadoes to Die?

Instructor Notes: Tornadoes appear to die when RFD Internal Surges possess large, negative buoyancy. Also, demise may be related to strong cold pool with the RFDIS as it replaces more buoyant and more potential buoyant RFD air surrounding the tornado. Also, it has been found that misalignment of the tornado and storm updraft may be factor. More analysis of RFD datasets are needed.

Student Notes:

What Causes Tornadoes to Die?

- RFDIS with large negative buoyancy
  - Strong cold pool with the RFDIS replaces more buoyant and more potential buoyant RFD air surrounding the tornado
  - Misalignment of tornado and storm updraft
- More analysis of RFD datasets needed

30. Outstanding Questions

Instructor Notes: While our knowledge of tornadoes has definitely increased and a clearer picture of the conceptual models has emerged, there remains some perplexing questions such as : Atmospheric stability and the role of the tornado, How & why do tornadoes form? Tornadogenesis and tornado failure, the role of the RFD in tornadogenesis, what drives the RFD? RFD origin and depth RFD characteristics – bouncy, vorticity, thermodynamics, microphysics.

Student Notes:

Outstanding Questions

- Atmospheric stability and the role of the tornado
- How & why do tornadoes form?
- Tornadogenesis and tornado failure
- The role of the RFD in tornadogenesis
- What drives the RFD?
- RFD origin and depth
- RFD characteristics – bouncy, vorticity, thermodynamics, microphysics, etc.

31. References

Instructor Notes: Please see the reference page for AWOC Severe Track IC1 at http://wdtb.noaa.gov/courses/awoc/index.html

Student Notes:

References

- See the reference page on http://www.wdtb.noaa.gov/courses/awoc

32. Contact Information

Instructor Notes:

Student Notes:

Contact Information

Warning Decision Training Branch
120 David L. Boren Blvd.
Norman, OK 73072
(405) 325-3190

Brad Grant bradford.n.grant@noaa.gov 405-325-2997	Les Lemon les.lemon@noaa.gov 405-325-1013

1. Conceptual Models for Origins and Evolutions of Convective Storms

Instructor Notes: Welcome to the Advanced Warning Operations Course, IC Severe 1, Lesson 2…Hail Storms. This lesson covers hail storm conceptual models and favorable environmental parameters.

Student Notes:

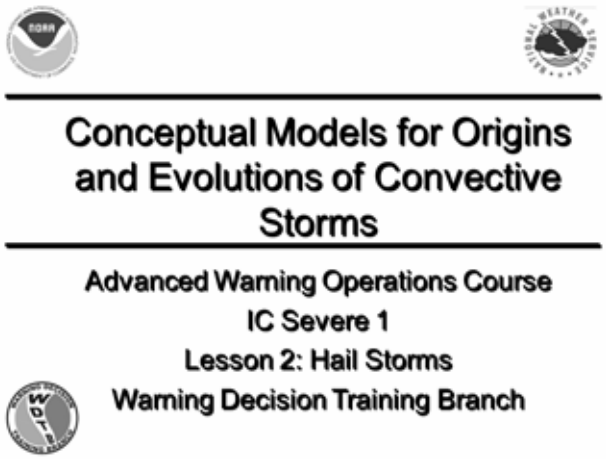

2. Hailstone Size Impact

Instructor Notes: A hailstone's size plays a critical role in its destructive potential. As you can see from this chart, a hailstone's kinetic energy (purple line) increases dramatically with its diameter. That's why the ability to forecast hail size in the warning environment is important. It can be the difference between small hail with little impact and severe or even giant hail with tremendous impact on both life and property.

Student Notes:

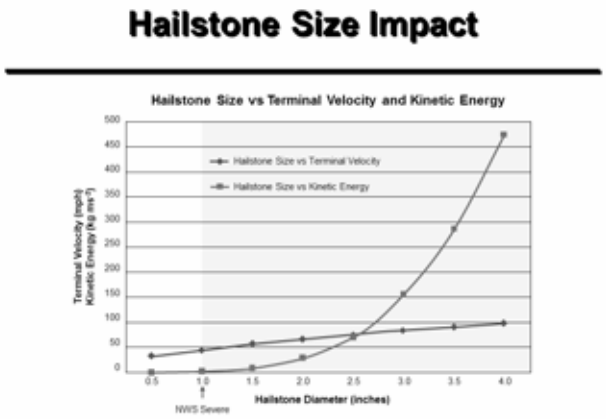

3. Objectives

Instructor Notes: This lesson has six objectives: Identify the role of shear and midlevel rotation on updraft strength and hail threat. Identify the role of Convective Available Potential Energy (CAPE) in hail growth zone. Identify favorable hail embryo sources. Identify trajectories which maximize hailstone residence time in the hail growth zone. Identify factors which influence the amount of melting a hailstone undergoes.

Student Notes:

Objectives

1. Identify the role of shear and midlevel rotation on updraft strength and hail threat.
2. Identify the role of convective available potential energy (CAPE) in the hail growth zone.
3. Identify favorable hail embryo sources.
4. Identify trajectories which maximize hailstone residence time in the hail growth zone.
5. Identify factors which influence the amount of melting a hailstone undergoes.

4. Objectives (cont'd)

Instructor Notes: Identify characteristics of the high precipitation (HP) supercell with a deep convergence zone (DCZ).

Student Notes:

Objectives (cont'd)

6. Identify characteristics of the high precipitation (HP) supercell with a deep convergence zone (DCZ).

5. Role of Shear and Midlevel Rotation on Updraft Strength

Instructor Notes: Let's begin with a discussion of the role of shear and midlevel rotation on updraft strength. Recall from the IC Severe lesson on supercells, that vertical wind shear produces horizontal vorticity that can tilted into the vertical within a strong updraft. This now vertically-oriented vorticity is associated with updraft rotation and is typically strongest in the mid-levels of the updraft. Focusing on the left part of this Flash graphic, regardless of the direction of spin of the rotation, whether cyclonic or anti-cyclonic, centrifugal force is associated with the rotation. The stronger the rotation, the stronger the centrifugal force. Strongly rotating updrafts are identified as mesocyclones on radar. To keep the forces balanced, an opposing pressure gradient force must be present. Again, regardless of the direction of spin, whether cyclonic or anti-cyclonic, dynamically-induced low pressure develops in the mid-levels of the updraft which creates an inward directed pressure gradient force. Focusing now on the right part of the Flash graphic, this low pressure leads to an upward directed pressure gradient force below the circulation, which intensifies the upward vertical motion. It has been shown mathematically that the dynamically induced (via mid-level rotation) contribution towards total updraft velocity can be as large as the contribution due to buoyancy, effectively "doubling the CAPE." Stronger updrafts have the ability to support larger hailstones. Thus, thunderstorm updrafts which contain strong, persistent rotation (i.e., a mesocyclone) are stronger than buoyancy considerations alone would suggest and possess a higher threat of severe hail (all other environmental factors being equal). A mesocyclone, the defining characteristic of a supercell, is a strong indicator of severe hail. In fact, a high percentage of significant (>2-inch diameter) hail events are produced by supercells. Recall that bulk shear through the lower half of a storm's depth (i.e., effective bulk shear) has been found to be an effective discriminator between ordinary and supercell storm types. Effective bulk shear greater than 30-40 knots favors supercells and, thus, is an important ingredient for significant (> 2-inch diameter) hail.

Student Notes:

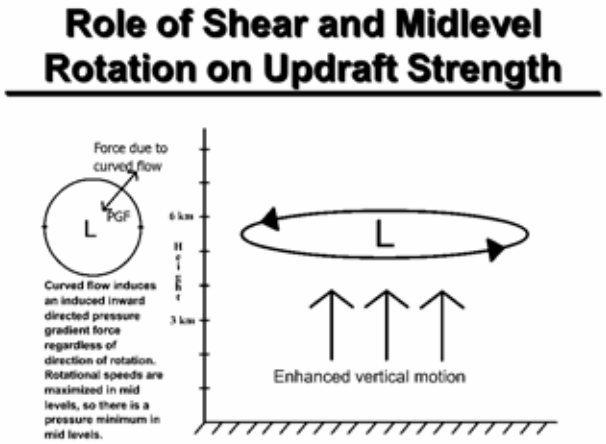

6. Hail Growth Zone Factors – CAPE in the -10° to -30 °C Layer

Instructor Notes: Hailstone formation requires an embryo (ice crystal, graupel, rain drop, etc.) to accumulate ice as it traverses the supercooled water region within a cumulonimbus updraft. Research studies have concluded that the most efficient hailstone growth occurs within the -10o to -30oC temperature range. Thus, a hailstone's size is dependent on its residence time within its parent thunderstorm's "hail growth zone." A factor thought to influence this residence time is CAPE, particularly CAPE in the hail growth zone. All other factors being equal, higher CAPE in the -10o to -30oC layer indicate stronger thunderstorm updrafts within the hail growth zone and the potential to suspend hailstones within this zone for a longer time, leading to larger hail stones. Bear in mind, CAPE in the hail growth zone is just a concept based on a model which uses simplified hail growth trajectories and hasn't been rigorously tested as a forecast parameter on a national scale. Hail forecasting is still an immature science.

Student Notes:

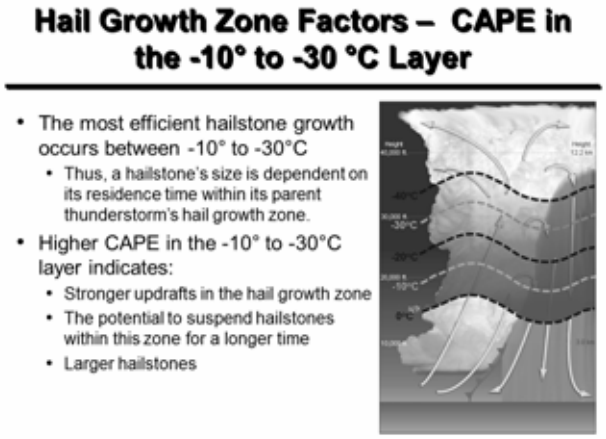

7. Hail Growth Zone Factors – “Thin CAPE” Example

Instructor Notes: This is a sounding from Wallop’s Island, VA. The red line represents the path of a parcel lifted from the surface, the blue lines delineate the -10oC and -30oC isotherms, and the blinking red area represents the CAPE in the hail growth zone. Surface-based CAPE was over 1000 J/kg, but its profile was quite narrow since it was stretched through a large depth. Lapse rates in the -10oC to -30oC layer were essentially moist adiabatic, contributing to relatively low CAPE in the hail growth zone. Thus, this can be labeled a “thin” CAPE profile. Consequently, even with significant CAPE and shear, there were no hail reports with this event. Bear in mind, supercells have the capability of producing significant hail even with a “thin CAPE” profile.

Student Notes:

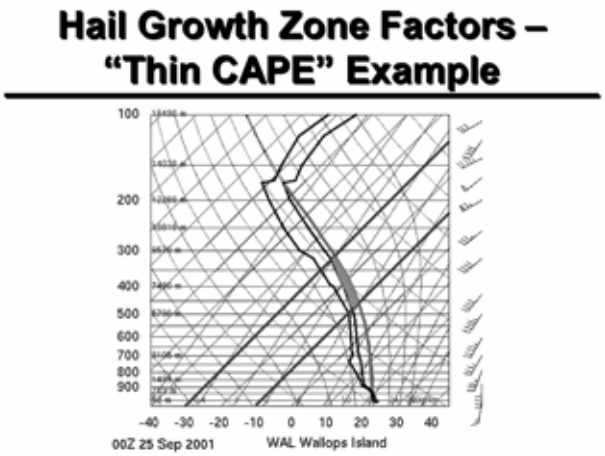

8. Hail Growth Zone Factors – “Thick CAPE” Example

Instructor Notes: This is a sounding from Omaha, NE. Surface-based CAPE was large and its profile was “thick,” much of it residing within -10oC to -30oC hail growth zone. Lapse rates in the hail growth zone were basically greater than moist adiabatic as well. Supercells containing giant hail pounded southern Nebraska. A storm at Aurora, NE produced a 7” diameter hailstone which was the U.S record at the time.

Student Notes:

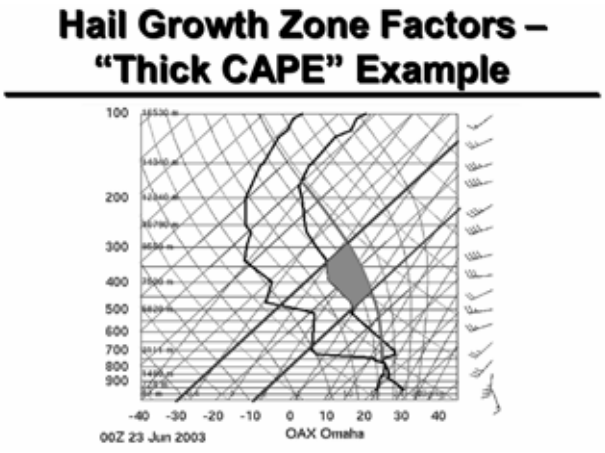

9. Most Favorable Hail Embryo Sources

Instructor Notes: A thunderstorm can possess many different hail embryo sources, all of which can operate simultaneously, but we are going to focus on the three most favorable sources for embryo growth. The first is within developing cumulus towers on the flanks of the parent storm or within the newer updrafts of a multicell storm. The second is near the stagnation point in the midlevels of an intense updraft. And the third source is from drops shed from growing or melting hail. The first two are primary hail embryo sources, while the last one is a secondary source; secondary because hail already has to be within the storm.

Student Notes:

10. Most Favorable Hail Embryo Sources – Growing Cumulus Towers/Flanking Lines

Instructor Notes: Growing cumulus towers and flanking lines near the main updraft of the parent storm provide an ideal incubator for young hail embryos because their updraft velocities are not too strong which allows the embryos to grow to appreciable size before they are advected downwind into the main updraft of the parent storm, where they can then grow into hailstones.

Student Notes:

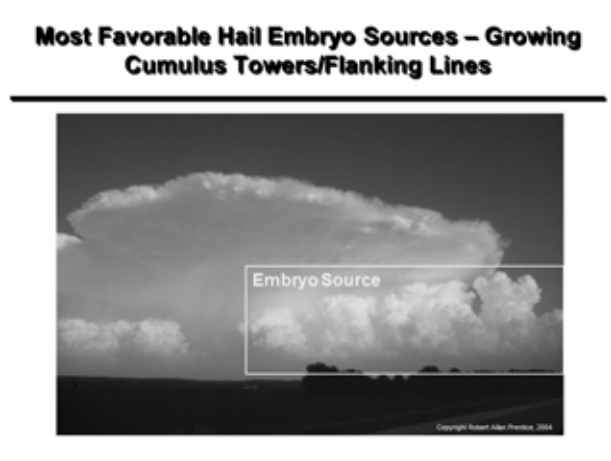

11. Most Favorable Hail Embryo Sources – Stagnation Point

Instructor Notes: The stagnation point which is found in the midlevels on the upwind-side of an intense updraft is an important source for hail embryo growth. The stagnation point develops because the updraft behaves like an obstacle to the flow, resulting in a dynamically-induced high pressure on the upwind side of the updraft and a region of little or no horizontal flow which occurs where the midlevel flow splits and is diverted around the updraft. Realize that the updraft is porous; that is, it isn't a rigid obstacle to the flow, but rather it diverts a certain percentage of the mid-level flow. Some of the flow still enters and mixes with the updraft. The stagnation point is important for embryo growth because the edges of the main updraft are a region where graupel particles and ice crystals can reside in the hail growth zone long enough to grow into hailstones.

Student Notes:

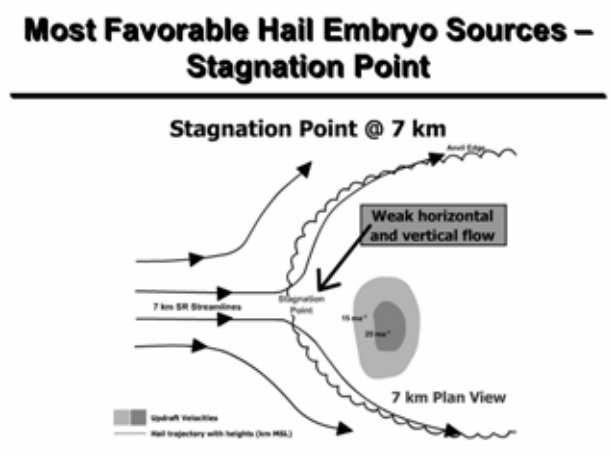

12. Most Favorable Hail Embryo Sources – Shed Drops

Instructor Notes: Hailstones greater than 9 mm in diameter have been found to shed liquid drops during both the wet growth and melting processes. These shed drops can then become hail embryos within the supercooled water region of an updraft. Dual-pol radar allows for the detection of drop-shedding regions. This Flash animation demonstrates how drops are shed from a melting hailstone. Of course, during the melting process drops must be lofted back into the supercooled water region to grow into hailstones.

Student Notes:

13. Hail Trajectories

Instructor Notes: Recall that a hailstone's size is heavily dependent on its residence time within the most efficient hail growth zone of supercooled water between -10° to -30°C. Strong, wide, persistent updrafts and storm relative winds which aren't too strong are most favorable because they allow a hailstone's terminal velocity to be balanced by the updraft for an extended time in the hail growth zone. Thus, the importance of determining which hailstone trajectories maximize residence time in the hail growth zone is obvious. Problem is, hailstone trajectories have been found to be extremely diverse within convective storms and many different trajectories can occur simultaneously within the same storm. The diversity of the trajectories becomes even more complicated when the storm size, updraft strength, and wind shear increase. A hailstone can grow up to the size of about a golf ball via a single trip through the updraft of a pulse thunderstorm (Knight and Knight 2001), but larger sizes require trajectories that recycle the hailstone. An example of this occurs in a multicell thunderstorm when a newer updraft ingests hail fall at its base from an older updraft. A supercell thunderstorm allows for numerous recycling trajectories, but the bulk of the trajectory studies to date have found relatively simple paths through or around the main updraft. The largest hailstones tend to occur with embryos that begin on the upshear (flanking line) side of a large supercell updraft and are then able to experience the longest residence times in the hail growth zone by traversing the full length of the updraft's long dimension.

Student Notes:

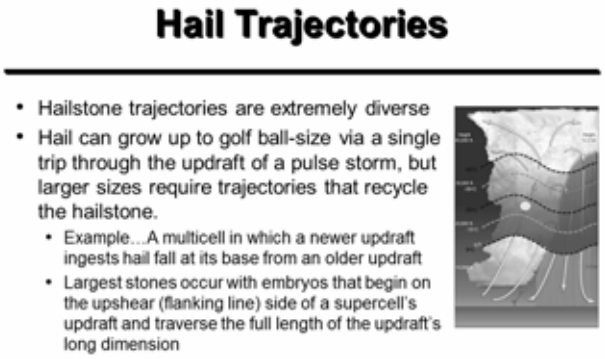

14. Hail Trajectories (Cont'd)

Instructor Notes: Let's graphically explain what we mean by residence time. In this first image, the color filled isopleths represent updraft velocities in meters per second, the gray dotted isopleths are radar reflectivities in dBZ, and the thick, blue, horizontal, dashed lines are isotherms in degrees Celsius. Let's begin with a forward-sheared updraft and a graupel particle which originates from the back-sheared anvil. In this highly simplified two-dimensional model there is horizontal flow across the updraft within which the graupel particle is being advected. As the graupel particle enters the updraft, its terminal velocity is less than that of the updraft velocities it encounters and so it is lofted into the updraft. When the graupel particle enters the region of supercooled water it grows into a hailstone. This growth is most efficient in the hail growth zone between -10° to -30°C. Eventually, the stone's terminal velocity exceeds updraft velocity and the hailstone falls to the surface.

Student Notes:

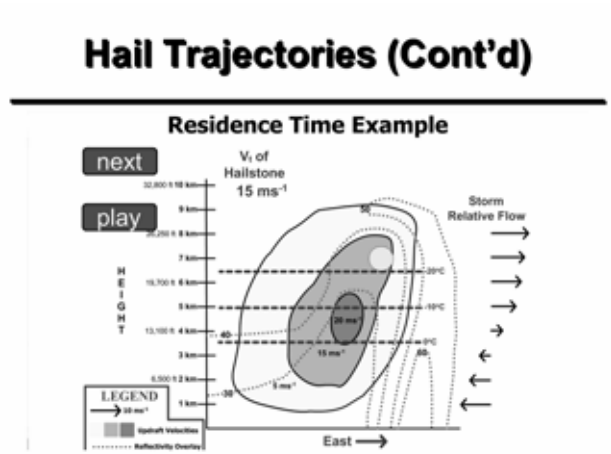

15. Hail Trajectories (Cont'd)

Instructor Notes: This is another view of the previous recycling example. The color filled isopleths represent updraft velocities in meters per second and the gray dotted isopleths are radar reflectivities in dBZ. Notice the particle never rises through the core of the updraft because that is typically precipitation-free as we see in the weak echo region (WER).

Student Notes:

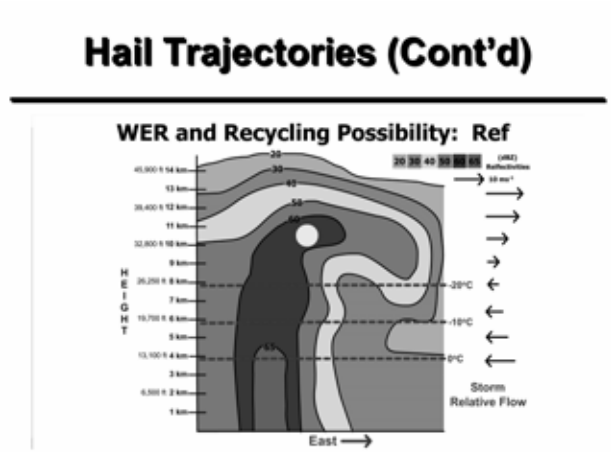

16. Hail Melting Factors - Size

Instructor Notes: Many factors influence the amount of melting a hailstone undergoes once it falls below the freezing level and into the melting layer, the most important of which is hailstone size. All other factors being equal, a smaller hailstone melts proportionately more than a larger hailstone for two reasons: A smaller hailstone has a slower terminal velocity and spends more time in the melting layer before reaching the surface. For example, a 3-inch hailstone may only take 2 minutes or less to reach the surface, while a smaller stone may take at least twice as long. Surface area versus volume ratio. Surface area identifies how much of a hailstone is exposed to melting, while volume identifies how much of its potential water can be melted. A hailstone's surface area is proportional its radius, squared, while its volume is proportional to its radius, cubed. Thus, a smaller hailstone has a proportionately larger surface area exposed to air and, proportionately, melts faster. For example, a 3-inch hailstone has a surface area of 28.3 in2 and a volume of 14.1 in3 while a 1 inch hailstone has a surface area of 3.1 in2 and a volume of 0.52 in3. The ratio is 2:1 for the 3-inch hailstone, but 6:1 for the 1-inch hailstone, and thus, proportionately it melts much more.

Student Notes:

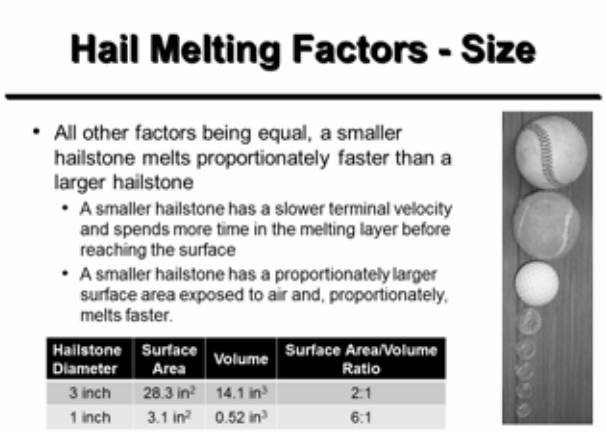

17. Hail Melting Factors – Density, RH, and Temperature

Instructor Notes: Hailstone density is an important factor that affects how a hailstone melts. Lower density hail (common on the high plains), typically with graupel cores, melts much more effectively than higher density hail Relative humidity is directly related to hailstone melting. Lower relative humidity decreases hailstone melting because it delays the onset of melting by providing favorable conditions for the hailstone surface to remain dry. In melting layers with 50% or less relative humidity, melting has been found to proceed when the stone reaches air with a temperature of +5 oC, obviously diminishing the amount of time the hail falls through the melting layer. Additionally, lower relative humidity hinders melting even if the stone is coated in water, since the layer of water is more likely to evaporate off the surface, cooling both the hailstone and the surrounding environment via the latent heat of vaporization, further slowing the melting process. Temperature is directly related to hailstone melting. A lower freezing level with colder temperatures below it intuitively favors less melting as heat transfer from the atmosphere to the hailstone is smaller in a colder environment. Conversely, a higher freezing level with warmer temperatures below it enhances melting. Finally, microphysical differences between the makeup of all the stones in a hail fall can also influence melting, although these differences have not been studied nor can they be measured at this time. Some of these differences are shape of the hailstone, hailstone size spectrum within a particular hail fall, and direct influences of surface hailstone heat transfer, among others.

Student Notes:

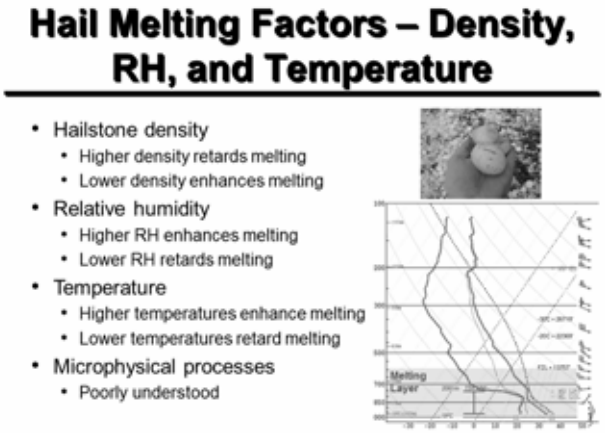

18. Hail Melting Factors - Examples

Instructor Notes: Now it's your turn to investigate the various melting parameters we've discussed. This Flash animation is based on a AMS Journal Article by Rasmussen and Heymsfield from 1987. You're going to find that lower hailstone density, higher relative humidity, and warmer temperature favor melting, but larger hailstones don't proportionately melt much regardless of these factors. However, remember back to the hailstone size versus kinetic energy chart at the beginning of this lesson. Melting a large hailstone even by a little can noticeably reduce its destructive power.

Student Notes:

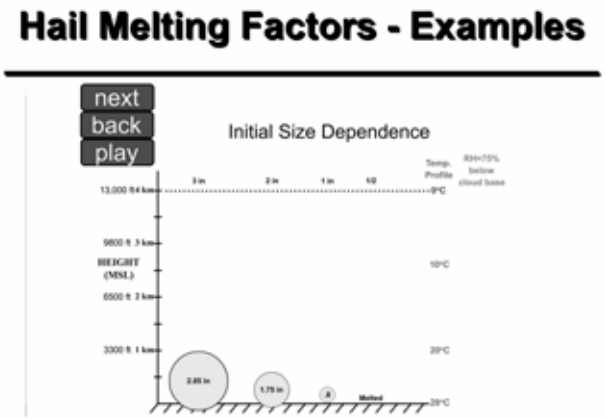

19. High Precipitation (HP) Supercell with a Deep Convergence Zone (DCZ)

Instructor Notes: A high precipitation (HP) supercell with a deep convergence zone (DCZ) is a large, rare, persistent, potentially catastrophic thunderstorm which produces large amounts of significant (> 2-inch diameter) and sometimes giant (> 4-inch diameter), wind driven hail over an extraordinarily large swath. It typically produces only a few, weak, brief tornadoes or none at all. The storm chaser slang term for this storm is “hurricane hailer.”

Student Notes:

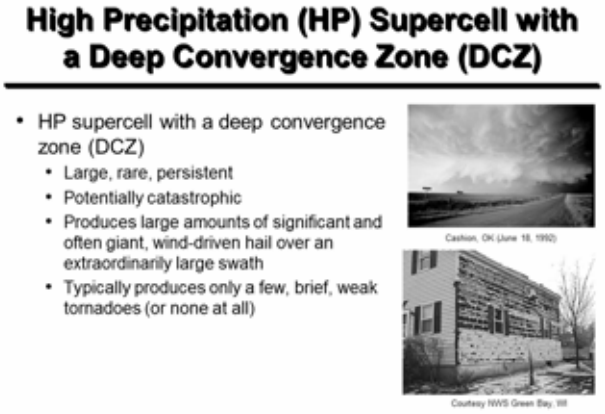

20. Deep Convergence Zone (DCZ) - Illustration

Instructor Notes: This HP supercell's most prominent characteristic is a deep zone of convergence (DCZ) which is a narrow zone of high shear and turbulence found along the leading edge of both the rear and forward flank gust fronts and sloping vertically though midlevels of the storm (~10 km/ 33 kft). The DCZ behaves like a "fluid wall" separating the major storm drafts; dry, potentially cold mid-level inflow feeding downdraft on one side and very warm, moist, low-level inflow feeding the updraft on the other side. Air stream mixing is effectively confined to this narrow zone which shields the supercell updraft from destructive mixing effects and allows the undiluted updraft to approach parcel theory values supportive of significant and often giant hail. The storm contains a very wide region of updraft; not necessarily one single updraft, but many updrafts which collectively form an extensive hail growth zone. The DCZ accounts for the sheer size of the hail cores as revealed by high reflectivities along both the rear and forward flanks. This illustration of the deep convergence zone (shaded region) associated with the Lahoma HP supercell of August 17, 1991, is adapted and updated from an image first published in Lemon and Parker (1996). Arrows indicate storm relative flow while dashed arrows indicate, in perspective, flow behind the deep convergence zone surface. The orange "X" marks the approximate location of the photographer in the following image. Storm motion is out of the illustration, directly towards you. The supercell updraft with a bounded weak echo region (BWER) is located from B to C and the storm summit is in the vicinity of B. The most intense and deep portions of the deep convergence zone are found nearly coincident with the strong reflectivity gradients bordering the weak echo region (WER) and BWER. In the Lahoma supercell, the deep convergence zone passage signaled the greatest wind threat and within 2-5 minutes, the greatest hail threat.

Student Notes:

Deep Convergence Zone (DCZ) - Illustration

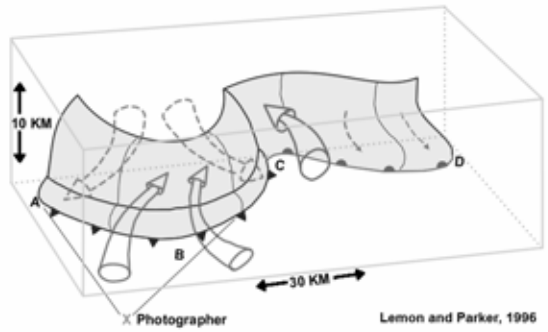

21. High Precipitation (HP) Supercell with a Deep Convergence Zone (DCZ) – Radar Example

Instructor Notes: Here is a radar example of an HP supercell with a DCZ on April 10, 2001, as seen from the Kanas City/Pleasant Hill, MO (EAX) WSR-88D. The 0.5 degree base Reflectivity is on the left and the corresponding base velocity is on the right. In reflectivity, we can see a giant core of extreme 70 to 80 dBZ reflectivity within both the forward and rear flank downdrafts. In velocity, we see extreme convergence along the supercell's rear flank which extended upward as a deep convergence zone. This storm tracked all the way eastward across Missouri along I-70 from Kansas City to Columbia to St. Louis. It produced several weak tornadoes and large amounts of golfball to baseball size hail driven by winds of 60 to 70 mph. It was the costliest hailstorm in U.S. history at the time. In the St. Louis area alone, more than 40,000 insurance claims for vehicles were taken. In Florissant, a suburb with more than 50,000 people, it was estimated that almost every home suffered some type of hail damage.

Student Notes:

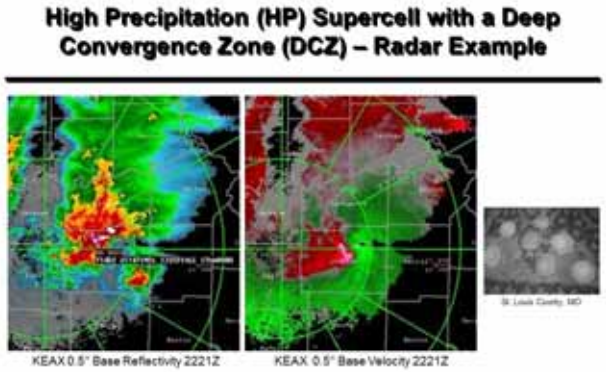

22. HP Supercell with a Deep Convergence Zone (DCZ) – Reflectivity Example

Instructor Notes: This is a Base Reflectivity cross section taken through an HP supercell with a DCZ near Cashion, OK. This image is quite similar to the hail trajectory recycling Flash animation shown earlier. Note the bounded weak echo region and extreme reflectivity hail core suspended above it.

Student Notes:

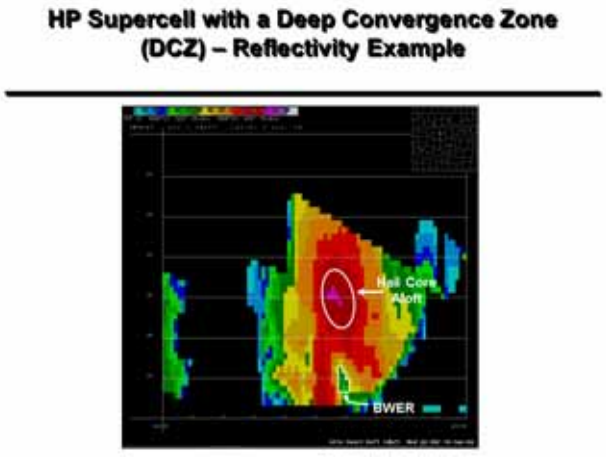

23. HP Supercell with a Deep Convergence Zone (DCZ) – Velocity Example

Instructor Notes: Here is the corresponding Base Velocity cross section of the Cashion HP supercell. Notice the deep convergence zone (DCZ) extends through a considerable fraction of the supercell's depth.

Student Notes:

HP Supercell with a Deep Convergence Zone (DCZ) – Velocity Example

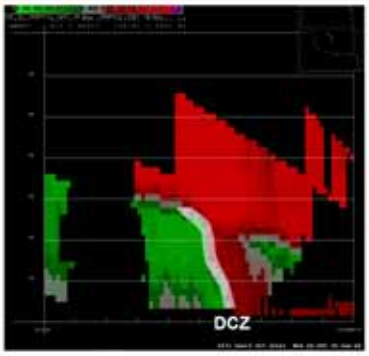

24. Hail Ingredients Summary

Instructor Notes: Here are summaries of microphysical and kinematic ingredients favorable for larger hailstone sizes and larger amounts of hail. The problem with many of these ingredients is they cannot be forecasted or measured operationally. This helps to explain why hail forecasting is so difficult. Fortunately, radar detection of hail is somewhat easier, especially with the advent of dual-polarization radar. Be sure to review WDTB's DLOC Topic 7 "Severe Hail Detection" lesson for refresher training on this.

Student Notes:

Hail Ingredients Summary

Ingredients Favorable for Larger Hailstone Sizes	
Microphysics	Kinematics
High supercooled liquid water content	Light storm-relative flow though updraft
Wet growth in mixed phase region	Large contiguous updraft of 20-40 m/s (39-78 kt)
Low density growth	Optimal trajectories
Large embryos	Favorable horizontal updraft gradients

Ingredients Favorable for Larger Amounts of Hail	
Microphysics	Kinematics
High embryo concentration	Large contiguous updraft of 20-40 m/s (39-78 kt)
Ample supercooled liquid water content	Flow that injects embryos across a broad updraft front

25. Significant Hail Parameter (SHIP)

Instructor Notes: As previously stated, hail forecasting is an immature science, ripe for further research. Many hail forecast predictors commonly used in the past have later been proven to have little or no skill. However, one parameter which has shown operational utility is the Significant Hail Parameter (SHIP). SHIP was developed at the Storm Prediction Center using a large database of surface-modified, observed severe hail proximity soundings. It is based on 5 parameters and is meant to delineate between significant (> 2" diameter) and non-significant (< 2" diameter) hail environments. It is important to emphasize that SHIP is not a forecast of a specific hail size. Values greater than 1 indicate a favorable environment for significant hail. Values greater than 4 are considered very high. In practice, values 1.5-2.0 or higher will typically be present when significant hail is going to be reported. Recall that supercells produce a high percentage of significant hail events. Thus, it's not surprising that most unstable CAPE and 0-6 km bulk shear are two of the ingredients. Note: The 10th, 25th, 75th, and 90th percentiles are shown for each box and whiskers subset.

Student Notes:

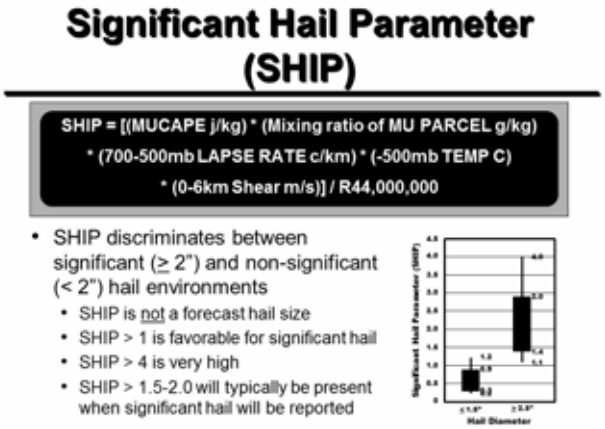

26. References

Instructor Notes: Click this link for a list of references used in this lesson.

Student Notes:

References

- Our website has a full list available:
- CLICK HERE FOR HAIL REFERENCES

1. Conceptual Models for Origins and Evolutions of Convective Storms

Instructor Notes: Welcome to Lesson 3 of IC Severe 1, which will focus on conceptual models related to heavy rainfall and flash floods events. This lesson should take you about 40 minutes to complete.

Student Notes:

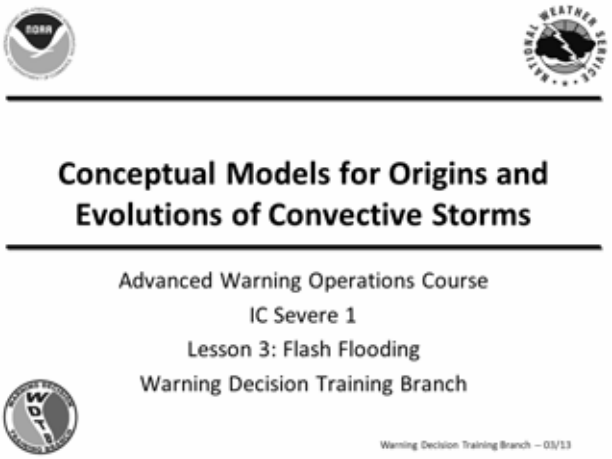

2. Learning Objectives

Instructor Notes: There are three primary learning objectives for this lesson. Most of this module will concentrate on research that identified synoptic scale patterns and meteorological ingredients that are associate with heavy rainfall and flash flood events. Later in the module, we will discuss other events and features that provide heavy rainfall and flash flooding, such as tropical cyclones, predecessor rain events, and atmospheric rivers.

Student Notes:

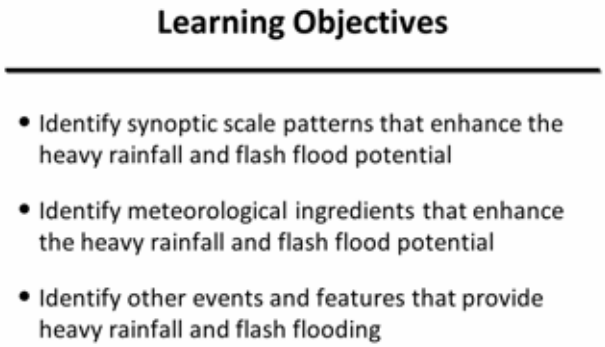

3. Pattern Recognition of Heavy Rainfall Events - Maddox et al.

Instructor Notes: In January of 2011, the National Weather Service released a service assessment on the record floods of middle Tennessee and western Kentucky that occurred from May 1-4, 2010. This lesson will help address Finding #12 of that assessment, which discusses forecaster experience in pattern recognition of heavy rainfall events. We will begin with the work by Maddox et al. from 1979. In their research, they analyzed 151 flood events from 1973 to 1977. Using these events, they were able to define some basic synoptic scale patterns. It should be noted that 139 of these events had precipitation totals greater than or equal to 4 inches (10 centimeters). All the storms were convective in nature and exhibited similar basic atmospheric characteristics, such as high surface dew points, large moisture content, and weak to moderate vertical wind shear.

Student Notes:

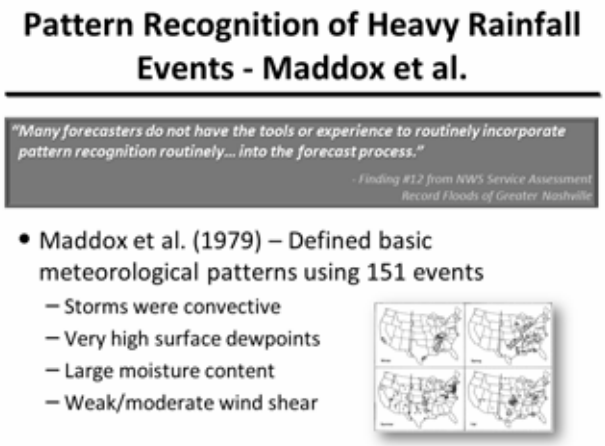

4. Maddox Synoptic Pattern

Instructor Notes: The first pattern we will look at is the synoptic pattern. The heavy rainfall event with this pattern is defined by its association with an intense synoptic scale cyclone or frontal system. Using a top-down approach, Maddox et al. noted a major trough at the 500 mb level that would move slowly to the east or northeast. The atmosphere ahead of the 500 mb trough axis would be considerably moist, defined here by the region of dew point depressions less than 6°C. The 850 mb level is characterized by a strong southerly low-level flow and abundant moisture transport, highlighted here with dew point temperatures greater than 10°C. There is also little speed or directional shear in the 850-300 mb level. The average wind difference observed was about 25 kts with 40 degrees of veering, depending upon the orientation of the synoptic scale system and surface fronts. And speaking of the surface fronts, they were often found to be quasi-stationary and generally oriented SSW to NNE. Development of the heaviest rain, highlighted by the shaded boxes, is located on the warm side of both the quasi-stationary front and a warm front. The warm front limits the northern extent of the development of the heaviest rainfall, but it also aides in triggering new development farther eastward.

Student Notes:

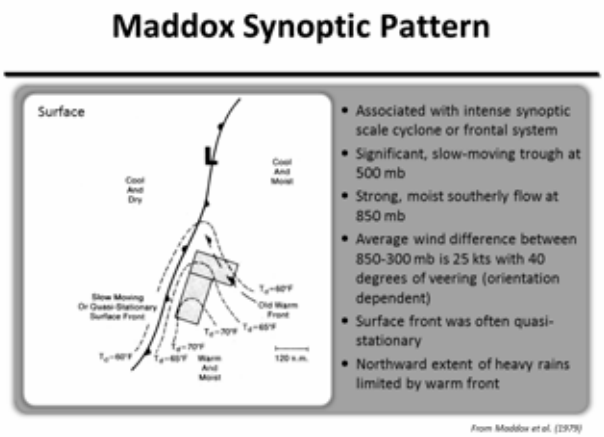

5. Maddox Frontal Pattern

Instructor Notes: The frontal pattern is defined by a stationary or slow moving zonally oriented synoptic scale frontal boundary. Starting again with the top-down approach, the 500 mb pattern shows a large ridge to the southeast with the area of heaviest rainfall occurring within a region of dew point depressions less than 6°C near the large-scale ridge axis. Most events had some weak meso-α scale trough or a mesolow along the frontal boundary, which can assist in frontal overrunning and small-scale convergence. Just like the synoptic pattern, the 850 mb level shows a strong low-level jet feeding very moist air into the area of interest. There is little speed shear in the 850-300 mb level, but there is a significant amount of veering in the wind profile. At the surface, Maddox et al. noted that the heaviest rainfall fell on the cool side of the E-W oriented front as warm unstable air flowed over the frontal zone. Since the winds aloft (i.e., the 700-200 mb level) paralleled the front, the greatest rainfall totals were a result of repeated convective development and training.

Student Notes:

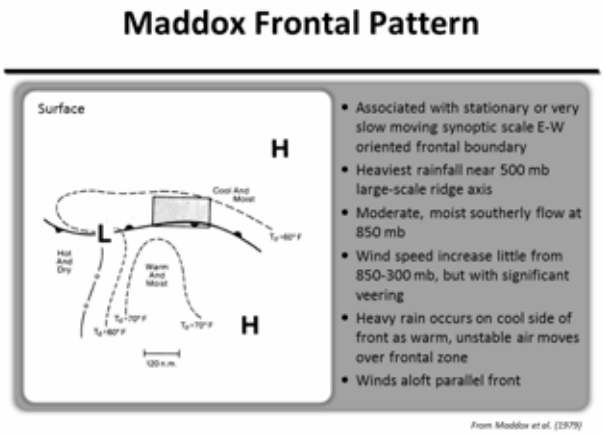

6. Maddox Mesohigh Pattern

Instructor Notes: The mesohigh pattern was the most common event sampled during the work of Maddox et al. (34% of events). Mesohigh events are the result of quasi-stationary thunderstorm outflow boundaries (generated from previous convection), and they usually occurred during the summer months. The 500 mb and 850 mb patterns are similar to that of the frontal pattern, where the greatest rainfall totals occurred in an area of low dew point depressions near the large-scale ridge axis, the presence of a weak trough to the west, and moderate southerly flow in the low-levels. Again, there is little speed shear but significant veering in the 850-300 mb level. The details regarding the mesohigh pattern reside in the surface features. Maddox et al. noted that half of their events occurred to the east of a large-scale frontal system, while the other half were not located near any notable surface fronts. The diagram here shows the previously generated quasi-stationary outflow boundary and associated mesohigh. The greatest rainfall would occur along the cool side of the boundary usually to the south or southwest of the mesohigh. Convection would repeatedly develop and train over the same area since the winds aloft were near parallel to the outflow boundary.

Student Notes:

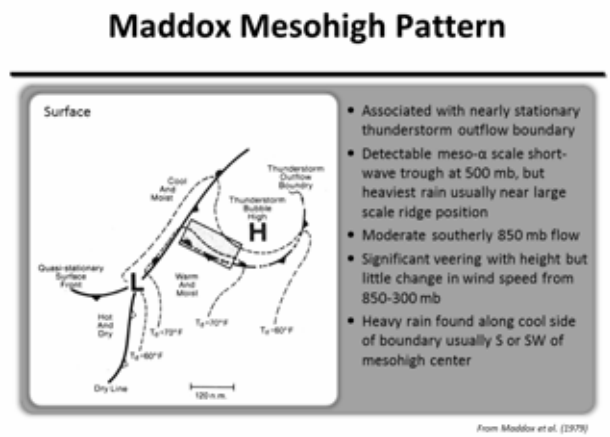

7. Maddox Western Pattern

Instructor Notes: The final type of event that Maddox et al. observed were those in the western U.S. In their work, typical surface and upper-air maps were not developed due to weak large-scale patterns without well-defined surface features. A lack of surface observations also hindered their ability to define any pattern(s) from these events. However, they noted that the heaviest rainfall from western events occurred near old frontal boundaries, thunderstorm outflow boundaries, or induced by orographic features. Maddox et al. also noted that the atmosphere was quite moist and had large conditional instability, generally in the area ahead of a mid-tropospheric meso-α scale trough.

Student Notes:

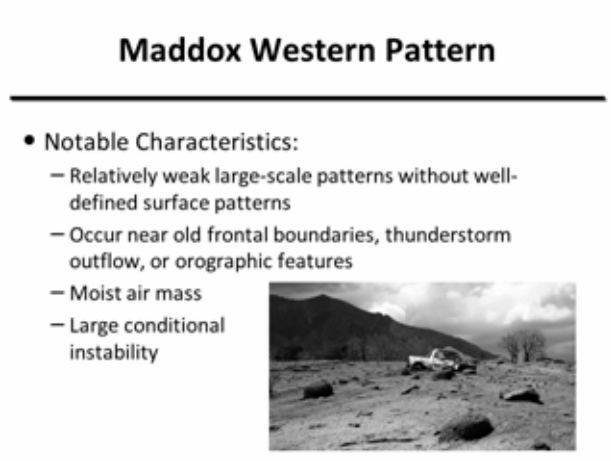

8. Ingredients Based Methodology – Doswell et al.

Instructor Notes: The work by Doswell et al. in 1996 focused on an ingredients based methodology, rather than a pattern-based approach, to forecasting heavy rainfall events. In their work, they noted that heavy rainfall and flood events from a variety of meteorological situations all contained similar atmospheric ingredients. Thus, the ability of a forecaster to identify such critical ingredients can be used in the recognition of heavy precipitation potential. Doswell et al. stated that "In order for a flash flood to occur, heavy precipitation must fall in a region that has appropriate hydrological ingredients in place." From there, the heavy precipitation factor was separated into two key ingredients: high rainfall rates and long rainfall duration. The rainfall rates were found to be influenced by rapid ascension of moist air and occurring with deep moist convection. Rainfall durations were characterized by storm motion and size. The hydrologic ingredients were not addressed in their work.

Student Notes:

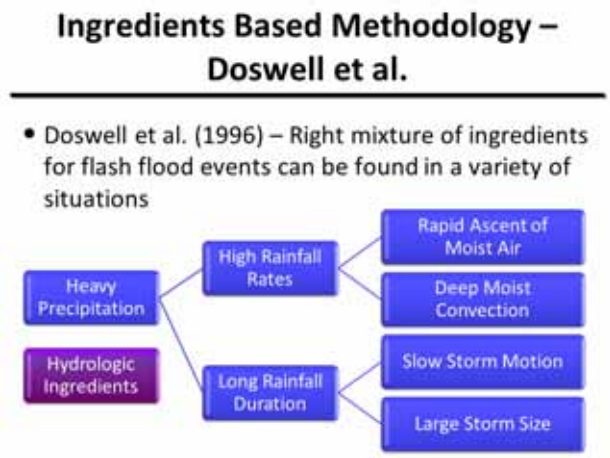

9. Heavy Precipitation and Precipitation Efficiency

Instructor Notes: Using an analogy attributable to Charles Chappell, “The heaviest precipitation occurs where the rainfall rate is highest for the longest time.” Doswell et al. stated that is an “almost absurdly simple concept,” but in its simplicity brings forth the very fundamentals behind heavy rainfall events. Starting with rainfall rate, the total precipitation for a given point is reduced to the equation, P=(R bar)D, where the total precipitation (P) is the combination of the average rainfall rate (R bar) and the duration of rainfall (D). The instantaneous rainfall rate (R) is assumed to be proportional to the vertical moisture flux, which is the combination of the ascent rate (w) and mixing ratio of the rising air (q). Rapidly ascending water vapor then condenses and falls as precipitation. However, not all water vapor falls as precipitation. This leads to the coefficient of proportionality relating the rainfall rate to input water vapor flux, otherwise know as the average precipitation efficiency (E). Doswell et al. states that the precipitation efficiency is a function of space and time (as seen in the diagram on the slide), and the key is to “anticipate the efficiency in a general sense” over the average of the life-time of the event.

Student Notes:

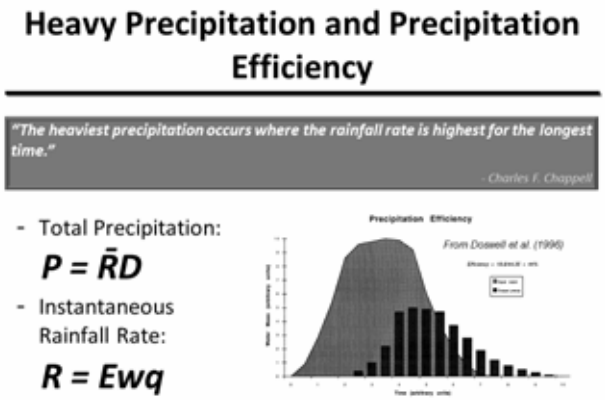

10. Storm Motion and Duration

Instructor Notes: Moving on from rate to duration, Chappell (1986) stated that "Quasi-stationary or slow moving MCSs pose the greatest threat for excessive rains and flash floods." Individual convective cells have lifetimes that are too short to produce heavy rainfall, so a system of multiple convective cells does provide the desired duration to produce flash flooding. Doswell et al. expanded upon this by stating that duration of high precipitation rates for a given location is related to system movement, system size, and within-system rainfall rate variability. The equation for the duration of rainfall for a given point is the combination of the length of the system (Ls) and the inverse of the system motion vector (Cs). In the diagram shown here, a N-S oriented MCS with the motion vector, C, will not produce long-lasting high rainfall rates at a given point. If the motion vector is more parallel to the precipitation orientation, then high rainfall rates will occur at a given point for a much longer duration, resulting in more rainfall. Although Doswell et al. did not quantify any of the aforementioned features, they found that these conceptual models of rainfall rate and duration can be useful in providing a framework for forecasters to analyze model and/or observed data for heavy rainfall events.

Student Notes:

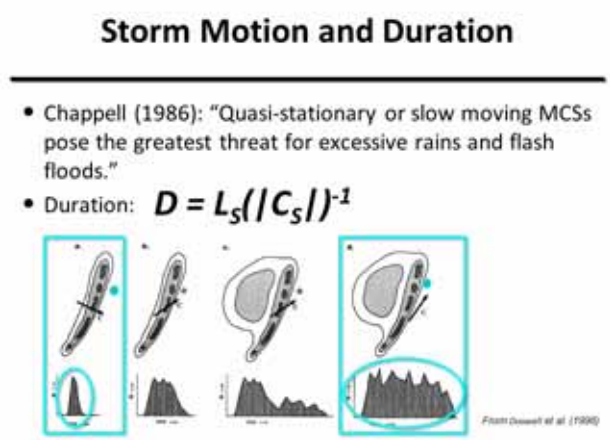

11. Moisture Flux Convergence and Mean Flow – Junker et al.

Instructor Notes: The work by Junker et al. in 1999 followed the Doswell et al. ingredients-based approach and applied it to the heavy rainfall events that resulted in the Great Midwest Flood of 1993. Their work identified 85 heavy rainfall events, and the events were categorized by the areal size of the three inch isohyet. They noted that the heavy rainfall events occurred north (downwind) of the axis of greatest 850 mb winds and greatest moisture flux in an area of 850 mb temperature and equivalent potential temperature advection. Junker et al. evaluated a variety of meteorological fields to determine what fields were related to the scale and intensity of the heavy rainfall events. The scale and intensity of these events were then found to be influenced by the magnitude of the warm air advection, the 1000-500 mb mean relative humidity, the breadth of the moisture transport axis, and the strength and orientation of the moisture flux convergence. We will start by discussing the moisture flux convergence.

Student Notes:

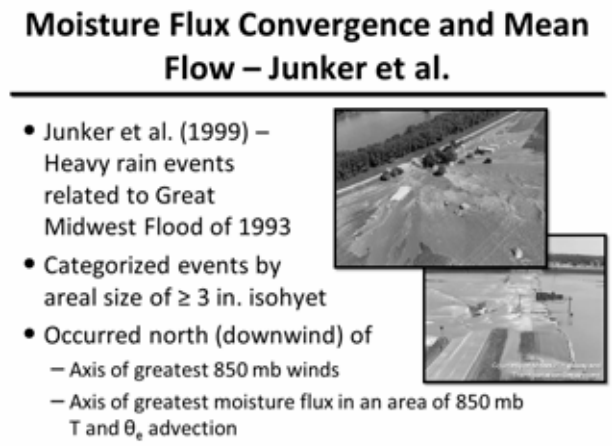

12. Moisture Flux Convergence and Mean Flow

Instructor Notes: We will begin with a quasi-stationary E-W oriented surface boundary with a broad, southerly 850 mb flow. Junker et al. noted that the breadth, location, and movement of the moisture flux appears to attribute to altering the rainfall in the area. They found that a broad axis of low-level moisture flux into the boundary created a large area of moderate-to-strong moisture flux convergence, which can assist in convective development. In the more extreme cases, the axis of strongest low-level winds and moisture flux translated downstream more slowly than in more moderate heavy rainfall cases. Another critical element of this is the orientation of the mean flow with respect to the surface boundary and the axis of low-level moisture flux convergence. The more extreme events were characterized by having a mean flow that is roughly parallel to the surface boundary (and consequently, parallel to the axis of low-level moisture flux convergence). This allows for the increased opportunity for continuous cell generation and training, including backward propagating MCSs.

Student Notes:

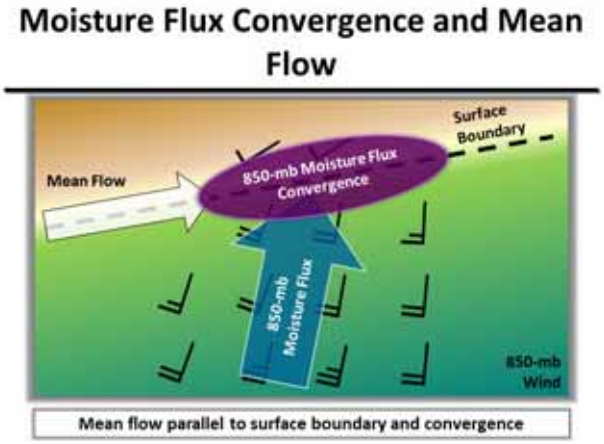

13. Available Moisture and Mean Relative Humidity

Instructor Notes: The other major factor that Junker et al. found was the magnitude of available moisture in the atmosphere. Recall that the heavy rainfall events were categorized by the areal size of the three inch isohyet. Events that were designated as “Category 0” had an areal extent of less than 36 nm2. Events that were designated as “Category 4” had an areal extent of greater than 3600 nm2. In the chart shown here, Junker et al. plotted each event again the average 1000-500 mb thickness and precipitable water (PW) value, which was based on the work by Funk (1991) and Lowry (1972). The 70% saturated thickness line was defined by Funk (1991) based on work by HPC stating that heavy rainfall events were typically associated with a 70% or greater mean relative humidity (assuming a standard atmosphere). Higher mean relative humidity values lie along and to the right of the line. Using this methodology, it was shown that most extreme heavy rainfall events (Category 3 and 4 type events) occurred to the right of the line. It was also noted that the core of the heaviest rainfall fell within the axis of the greatest relative humidity values.

Student Notes:

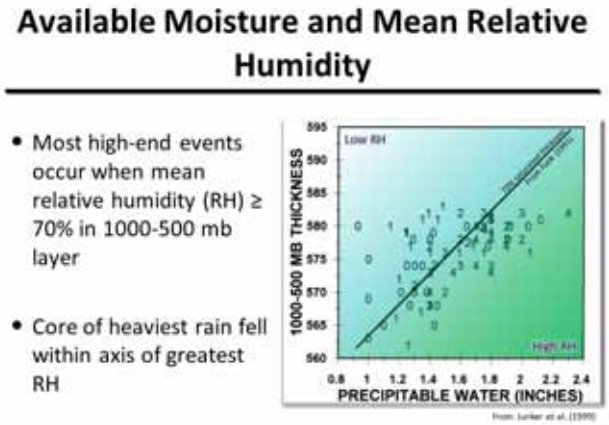

14. Recognition of a Heavy Rainfall Event: Patterns (500 mb)

Instructor Notes: Now, let's take the concepts from Maddox, Doswell, and Junker and apply them to a real-world event. The first AWIPS image here displays the GFS 500 mb wind, height, and dew point depressions less than 6°C (shown in color fill). There is a large ridge off the southeastern U.S. coast with predominantly zonal flow across the northern two-thirds of the country. The dew point depression analysis shows a region of moist mid-level air extending from the Rockies across the central U.S. to the mid-Atlantic region. So, on our map to the right, we will highlight the location of the ridge and the moist 500 mb region based on the low dewpoint depressions.

Student Notes:

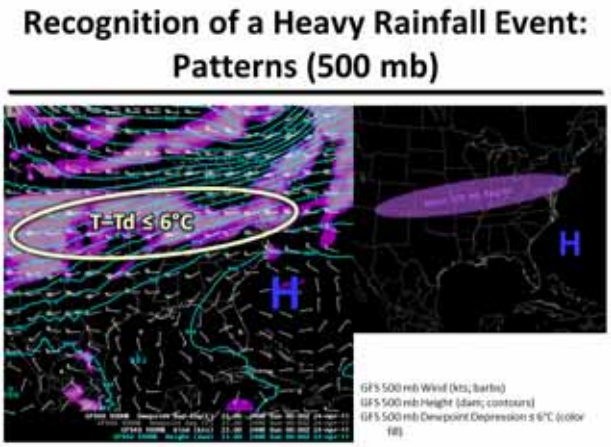

15. Recognition of a Heavy Rainfall Event: Patterns (850 mb)

Instructor Notes: Moving on, here is the 850 mb level with the height, wind, and dew-point temperatures ≥ 10°C in color fill on display. The first thing that stands out is the plume of high dew point temperatures. This low-level moisture originates from the inter-tropical convergence zone (ITCZ) and streams northward through the southern Plains into the Ohio River valley. The moisture transport in this event is aided by south to south-westerly winds forecasted to be 30-35 kts. On our map to the right, we will highlight the region of 850 mb dewpoint temperatures ≥ 10°C and the 850 mb axis of maximum winds. There is now a region from the southern Plains to the mid-Atlantic coast where the moist 500 mb region overlaps with the 850 mb moisture transport.

Student Notes:

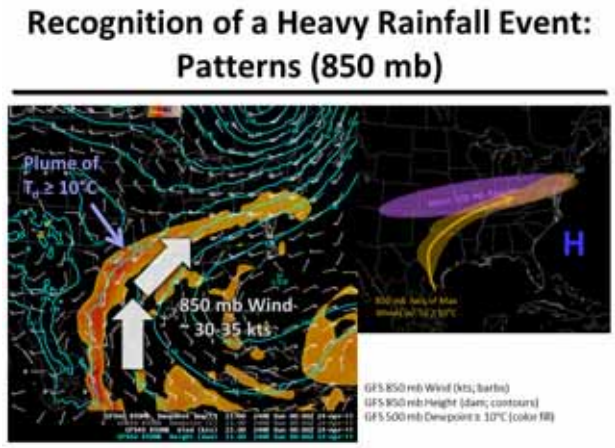

16. Recognition of a Heavy Rainfall Event: Patterns (SFC)

Instructor Notes: Now looking at the surface features, here is the GFS surface winds, temperature, and dew points temperatures ≥ 60°F in color fill. Starting with the wind and temperature analysis, there is a WSW-ENE oriented boundary located from the TX/OK border towards PA and the mid-Atlantic region. To the south of the boundary is a large pool of ≥ 60°F dew point temperatures with southerly winds at 5-10 kts. In our map to the right, let's first overlay the surface boundary and the southerly wind field. Now let's add the areas of ≥ 60°F dew point temperatures. You can see the analysis at the 500 mb level, the 850 mb level, and the surface all come together in a region from eastern OK extending up to OH. Based on the patterns we have seen described by Maddox et al., the setup appears similar to that of the frontal pattern. The region of highest heavy rainfall potential is located north of the boundary within the area denoted by the white box.

Student Notes:

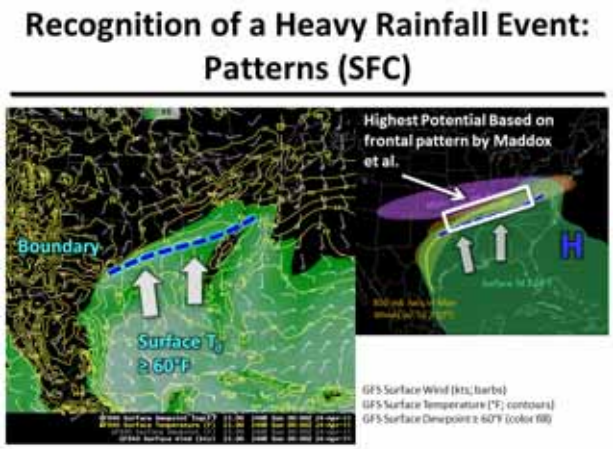

17. Recognition of a Heavy Rainfall Event: Ingredients

Instructor Notes: We will take the same event and apply a more ingredients-based approach from that of Junker et al. and Doswell et al. Here, we are looking at the 850-300 mb winds and the 850 mb moisture transport magnitude shown in color fill overlaid with the boundary location based on our previous surface analysis. The first thing you notice is that the moisture transport is focused in the area of the boundary. This is where you would expect the greatest low-level moisture convergence (not shown). Looking at the mean wind over the region, it is generally from the WSW around 40-45 kts. The individual storm motion over this region would be rather quick, but it is important to note that mean will is near parallel to the surface boundary and moisture convergence. Therefore, this region is primed for continuous convective generation and training over the same area if the boundary and axis of moisture flux transport moves slowly.

Student Notes:

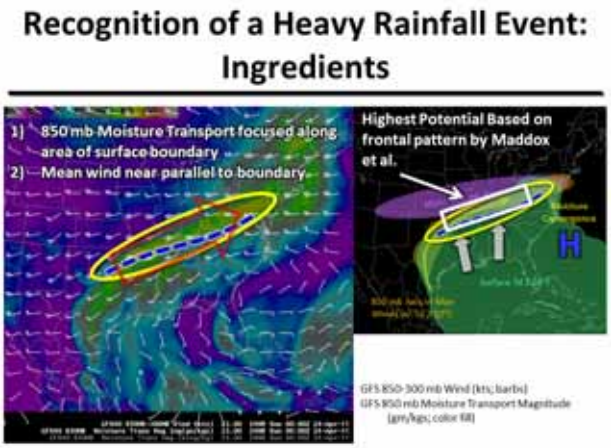

18. Recognition of a Heavy Rainfall Event: Ingredients

Instructor Notes: Finally, we will assess the moisture content of the atmosphere. Here is the GFS precipitable water (PW) plotted in contours and in color fill for values greater than one inch along with the 1000-500 mb thickness. Values of PW above 1.50 inches exist in the region of the surface boundary. Areas of very moist air in a region of forcing is one of the factors Doswell et al. described in the production of high rainfall rates. When comparing the 1000-500 mb thickness and the PW values against the 70% saturation thickness rule (as done in Junker et al.), the maximum PW value of 1.65 inches with a thickness of 565 dam would be located here on the graph. This is well to the right of the 70% saturation thickness line, meaning that the atmosphere in this layer is very moist. To graphically show this, here is the GFS 1000-500 mb relative humidity (RH) with it color filled for values of 70% and above. Note how the greater RH values are co-located with the region of highest heavy rainfall potential based on the pattern analysis and area of moisture convergence. Now that we have completed our analysis of this event, let's see how it verifies.

Student Notes:

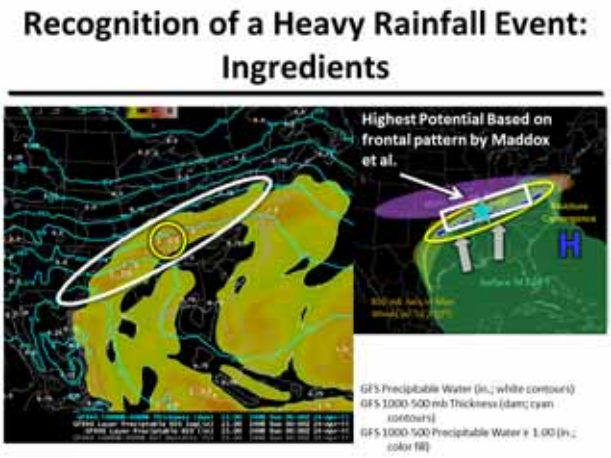

19. Recognition of a Heavy Rainfall Event: Resulting QPE

Instructor Notes: We defined our area of interest along and north of a WSW-ENE oriented surface boundary from eastern OK to southern OH, and we have a fairly high confidence that this region could see significant rainfall totals. The 24-hour multisensor precipitation estimator (MPE) totals depict a large area of rainfall of over 1.50 inches in our area of interest, with precipitation totals of 3-6 inches from northwest AR to southern IN. Continuous heavy rainfall over consecutive days in this area led to significant flash flooding with numerous evacuations and water rescues.

Student Notes:

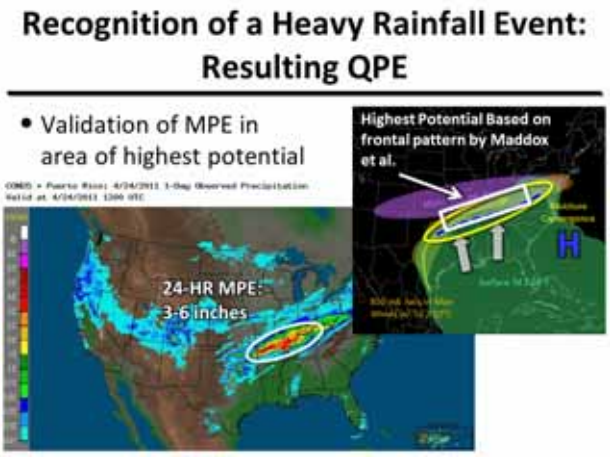

20. Heavy Rainfall with Tropical Cyclones

Instructor Notes: Now that we have discussed basic meteorological patterns and ingredients associated with flash flood forecasting, let's take a look at other scenarios that also result in heavy rainfall and flash flooding. Let's start with the very obvious tropical cyclones. We know that these systems are very efficient precipitation producers with modest CAPE values, a very deep warm cloud layer, and extremely high precipitable water (PW) content. Rainfall with tropical cyclones can also be enhanced by interactions with boundaries and topography. Unfortunately, the copious amounts of rainfall that induce flash flooding are the most lethal part of a landfalling tropical cyclone. Almost 60% of tropical cyclone fatalities are associated with freshwater flooding.

Student Notes:

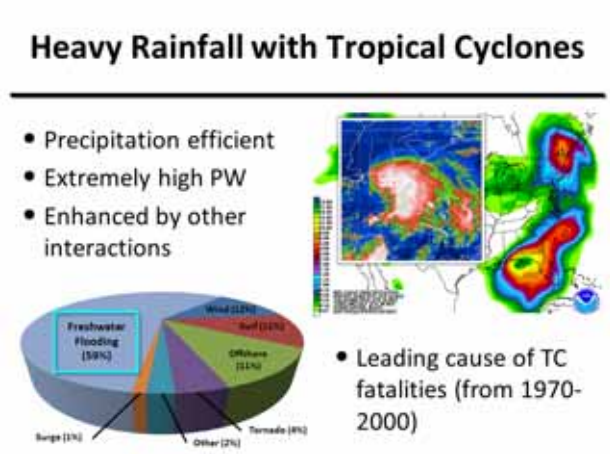

21. Precipitation During Extratropical Transition (ET) – Jones et al.

Instructor Notes: As tropical cyclones move toward the midlatitudes, they often decay and undergo a process that is referred to as extratropical transition (ET). During ET, tropical cyclones lose their symmetric appearance and deep convection and evolve into a broad “comma-shaped” extratropical cyclone. This module will only address the evolution of ET related to precipitation impacts. The work by Jones et al. in 2003 discussed the challenges of forecasting the different meteorological variables and their impacts with ET. In their precipitation analysis, a poleward expansion of the precipitation field began during the onset of ET and continues to generally bias left-of-track during the ET process. Research has shown that the interaction between a tropical cyclone and a baroclinic midlatitude environment during ET can lead to the development of midlatitude cylcone features, such as defined regions of warm and cold air advection and frontogenesis.

Student Notes:

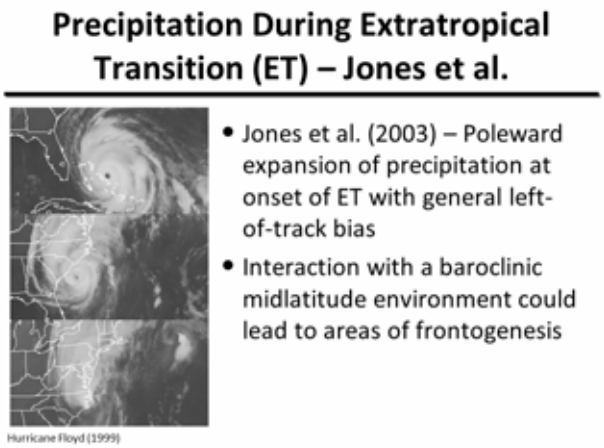

22. ET and Frontogenesis with Tropical Storm Hermine (2010)

Instructor Notes: We will use the remnants of Tropical Storm Hermine from September 2010 to show the impacts of frontogenesis after the completion of extratropical transition (ET). Hermine was located near the tail end of a cold frontal boundary that originated from a midlatitide cyclone over eastern Canada. Surface analysis near the time of this combination satellite/radar image shows the extension of that cold front into the southern Plains while the remnants of Hermine develop a warm frontal boundary near the center of the surface low. A secondary boundary begins to develop farther south and east as Hermine exhibits more trough-like characteristics. The heaviest precipitation occurred along and north of the E-W oriented front and along the developing N-S oriented boundary. Regions in eastern TX accumulated over six inches of rain in a 12 hour period due to the slow movement of the system. So, the key to heavy precipitation forecasting with ET is understanding the asymmetric transition of the storm and the rainfall with respect to the track. Remember that precipitation is enhanced along areas of frontogenetic forcing and large-scale ascent, and note that heavy rainfall can occur over land even without the tropical cyclone center ever making landfall.

Student Notes:

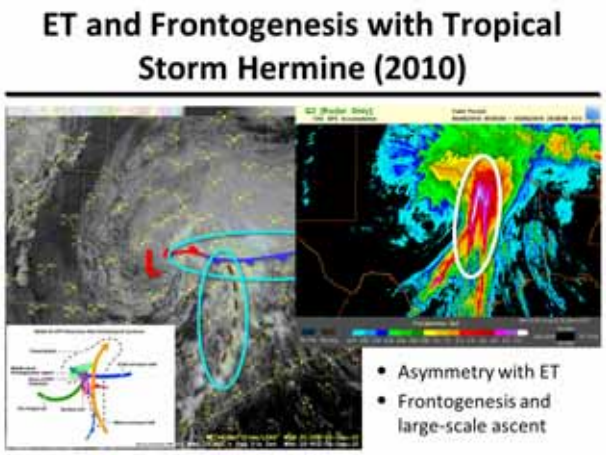

23. Predecessor Rain Events (PREs)

Instructor Notes: Another type of heavy rainfall event that is influence by tropical cyclones (TCs) are predecessor rain events (PREs). Predecessor rain events are defined by Galarneau et al. in 2010 as coherent areas of rain persisting for at least six hours with radar reflectivity values ≥ 35 dBZ that are displaced poleward within a region of moisture transport from the tropical cyclone. A PRE has to have clear separation on radar between its coherent area of rainfall and the precipitation field directly related to the TC. The work by Galarneau et al. noted that the average distance between a PRE and the TC is approximately 1000 km and have an average time lag of 36 hours between the PRE and TC passage for a given location. The average longevity of a PRE is approximately 15 hours and can contain maximum rainfall rates that are greater than 100 mm in a 24 hour period. The challenge with PREs is the ability to forecast these events, since they are dependent upon mesoscale features, such as surface boundaries and moisture plumes. These mesoscale features can be under-analyzed and/or improperly forecasted by operational models.

Student Notes:

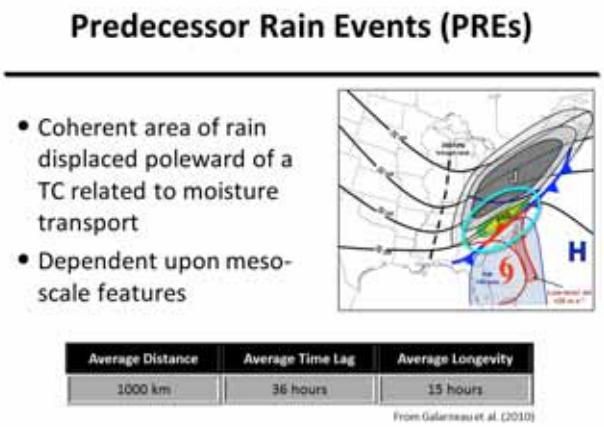

24. General PRE Patterns

Instructor Notes: In the work by Galarneau et al., predecessor rain event (PRE) patterns were defined by their location with respect to the forecast track (left-of-track, right-of-track, and along-track) and by the curvature of the 200 mb jet. The majority of PRE events occur left-of-track and within the presence of an anti-cyclonically curved 200 mb jet. The graphics shown here are the conceptual models of the synoptic-scale environment for a left-of-track PRE event. Starting with the broader view on the left, this conceptual model places a tropical cyclone (TC) and its associated precipitation area over the Carolinas. There is a clear separation between the precipitation directly related to the TC and the defined PRE locations. Representative TC tracks are highlighted here, showing that the PRE locations are occurring left of the representative track. This conceptual model shows the PREs occurring in the right-entrance region of the upper-level jet and on the western flank of a low-level theta-e ridge near a midlatitude trough. On the mesoscale level, heavy rainfall with PREs can be focused along features such as frontogenetic forcing or orographic upsloping.

Student Notes:

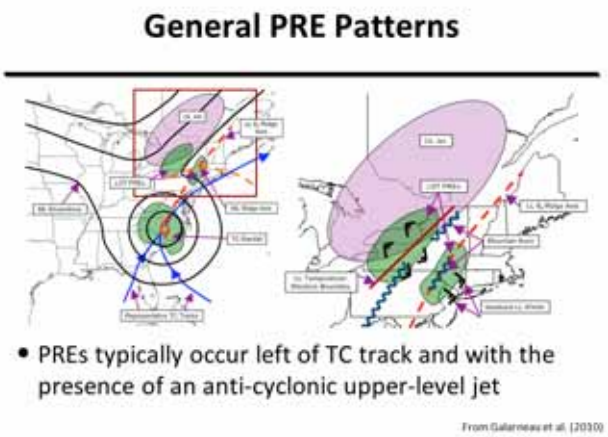

25. Tropical Storm Erin (2007) PRE Analysis

Instructor Notes: A well documented PRE was associated with the remnants of Tropical Storm Erin in August of 2007. In this event, a localized area of 5-15 inches of rain fell within a 24-48 hour period in southern MN and WI. As the remnants of Erin were located over OK, there was a significant poleward moisture flux associated with southerly 30-35 kt 850 mb winds. A slow moving warm front was located within a region of 850 mb vorticity and 700 mb quasi-geostrophic (QG) forcing in the presence of an anti-cyclonically curved 200 mb jet. Precipitation developed in this area of low-level voriticy and frontogenetic/QG forcing and evolved into a quasi-stationary MCS. Like the majority of PRE events, this event was poleward of the tropical system, occurred left-of-track, and was influenced by an anti-cyclonically curving upper-level jet. While the basic synoptic setup was present, and one could make the argument that it resembled that of the Maddox frontal pattern, it was the mesoscale features that influenced the heavy rainfall and flash flood potential.

Student Notes:

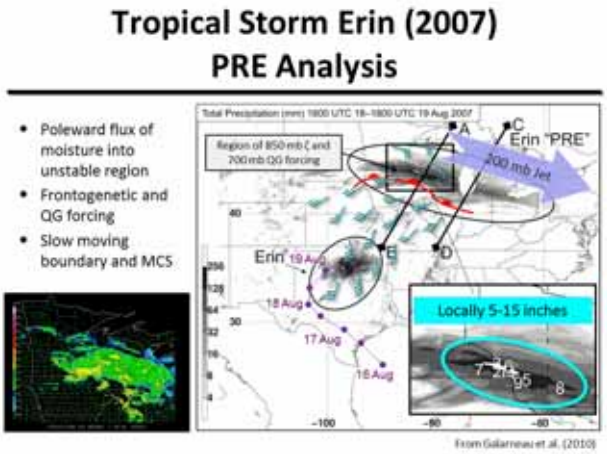

26. Atmospheric Rivers

Instructor Notes: Another scenario that typically results in heavy rainfall and enhanced flash flood potential is an atmospheric river. Atmospheric rivers were first defined by Zhu and Newell in 1998 as narrow plumes of water vapor flux that are typically situated near the leading edge of polar fronts. Their research determined that 95% of meridional water vapor flux occurs within these atmospheric rivers and that there are typically 3-5 of these plumes within a hemisphere at any one moment. The CALJET and PACJET experiments utilized various sensing techniques, including aircraft and dropsonde observations, to study the characteristics of atmospheric rivers. Their results showed that these long, narrow plumes have integrated water vapor (IWV) values of greater than 2 cm (0.8 inches), are generally narrow in size [around 400 km (250 mi.) in width], and occur in the vicinity of a low-level jet.

Student Notes:

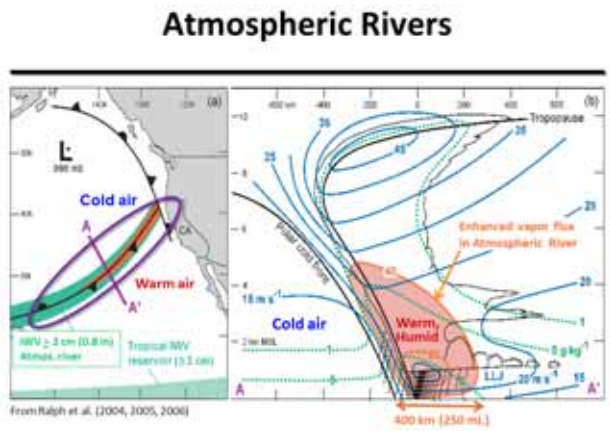

27. Role of Atmospheric Rivers in Western U.S. Extreme Rain Events

Instructor Notes: Atmospheric rivers can result in heavy rainfall events on both coasts. However, they are one the predominant methods for heavy rainfall in the western United States due to the characteristics of an atmospheric river combined with topographic features of the west coast. The moisture associated with an atmospheric river is shallow in depth, where research has shown that approximately 75% of the water vapor flux occurs in the lowest 2.5 km MSL. The CALJET and PACJET experiments also observed that the atmosphere below 3 km is in moist neutral stratification, meaning that the atmospheric profile follows the moist adiabat, and thus, has no resistance to any form of uplift. With the pre-cold frontal low-level jet (LLJ) maximized at 1 km MSL and the shallow moisture flux directed toward the coast, orographic rain enhancements occur along the coastal mountains.

Student Notes:

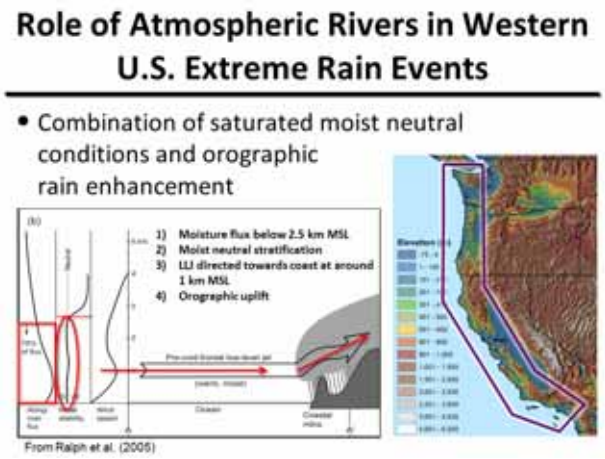

28. Northern/Central California Atmospheric River: October 2009

Instructor Notes: This heavy rainfall event in northern and central CA on October 13-14, 2009 is a classic example of an atmospheric river impacting the western United States. Starting with the SSMI water vapor content, you can clearly identify the atmospheric river originating from the tropical air in the western Pacific Ocean and advecting towards a low pressure system off the U.S. west coast. Low-level analysis shows a strong 850 mb jet (40-50 kts), with moisture flux values on the order of six standard deviations above normal. The Oakland, CA (OAK) sounding during the event shows a moist neutral profile that parallels the moist adiabat and is nearly saturated throughout the entire vertical column. Precipitable water values approached and even exceeded 1.50 inches. When compared to climatology, these values are near record levels for the month of October and are greater than two standard deviations above normal. This event resulted in a large area of 2-4 inches of rain with maximum 24-hour totals exceeding 10 inches in numerous locations (highlighted on map), including a maximum rainfall total of nearly 19 inches of rain along the CA coast.

Student Notes:

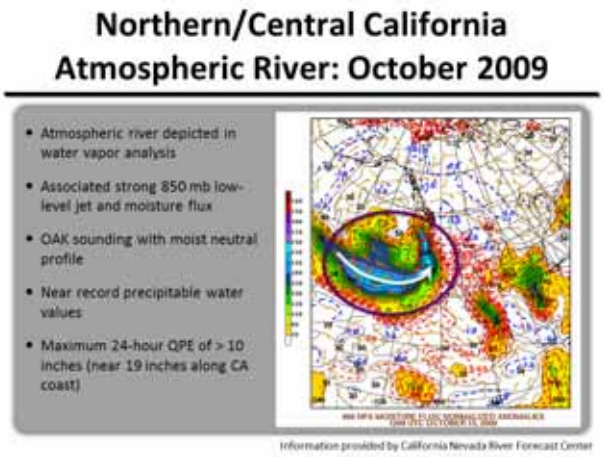

29. Determining the Significance of Events Through Anomalies

Instructor Notes: One thing we saw in the atmospheric river example was the use of anomaly data to describe how strong the 850 mb moisture flux was towards the California coast. We have spent the majority of this module examining the different patterns and ingredients that influence the flash flood and heavy rainfall potential. The use of standardized anomalies puts the strength of the pattern and ingredients into context. This four-panel display shows a SREF analysis of 250 mb height, 250 mb wind, 850 mb wind, and precipitable water (PW) values. You can easily recognize the amplified trough-ridge pattern in the upper-levels with an associated 140 kt (70 ms-1) jet across the Mississippi and Ohio River valleys. There is also a very strong southerly 850 mb low-level jet with winds exceeding 54 kts (28 ms-1), and PW values at or above 2 inches (50 mm) ahead of a SSW-NNE oriented surface front (surface analysis not shown). My attention is drawn to the southeastern U.S. with the strong low-level jet and high PW values near the surface front while being co-located under the right-entrance region of the upper-level jet. So, without knowing anything else, there appears to be a favorable setup that resembles the Maddox synoptic pattern. But the question is how strong is this pattern? With the use of standardized anomalies, you can see that all of the features here exceed three standard deviations of their normal climatology, and the 850 mb winds over TN and KY are between four and five standard deviations above normal. Using standardized anomalies allows you to distinguish ordinary rainfall events from significant, high-impact events, and thus, increasing your confidence in predicting a high-end hydrometeorological event. The anomalies shown here were from the record flood event in middle TN and western KY in May of 2010. This image of 48-hour MPE totals show a large area of > 6 inches of precipitation (yellow) with areas of central TN having received more than 12 inches of rain (light purple).

Student Notes:

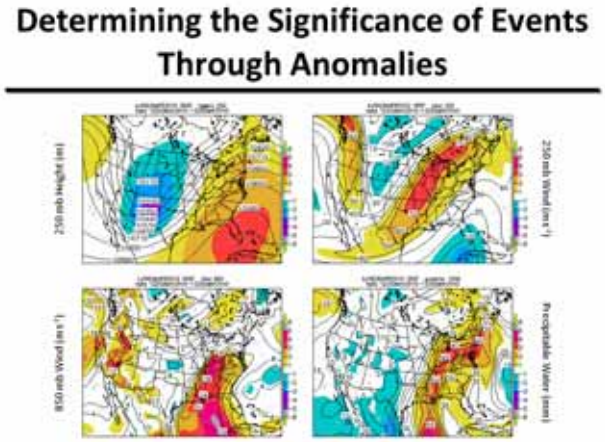

30. Not All Events are Identifiable on the Synoptic Scale

Instructor Notes: Be aware that not all events are identifiable on the synoptic scale. This example here shows the sea level pressure, precipitable water (PW), and 850 mb U- and V-wind component anomalies. We will focus our attention to the southern OH and northern KY region. Note that all but the PW values are within one standard deviation of normal climatology. Although other pressure levels and meteorological parameters are not shown here, there was no significant evidence of a synoptic-scale heavy rainfall potential. However, mesoscale features that are not easily distinguishable in the models played a factor in having a localized region of heavy rainfall and major flash flooding for this area. Short-term mesoscale forecasting becomes critical in identifying localized events and even determining the areas of greatest impact in large-scale events.

Student Notes:

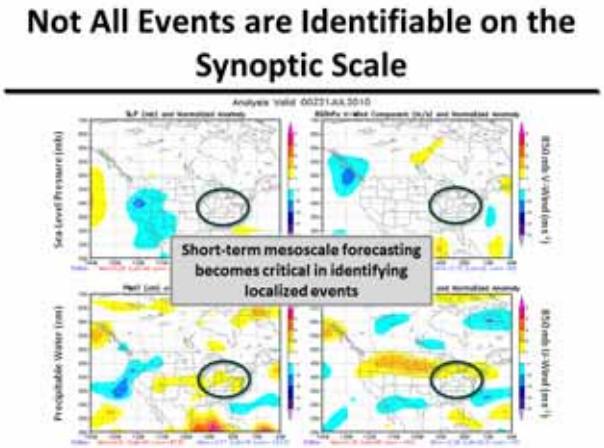

31. Summary

Instructor Notes: From this lesson, you should now be able to identify meteorological patterns and ingredients that are relevant to increasing the potential for heavy rainfall and flash flooding. We reviewed both pattern-based and ingredients-based methodologies for flash flood forecasting and applied them to a model forecast. We also identified other patterns and situations that enhance the flash flood potential, including tropical cyclones, predecessor rain events, and atmospheric rivers. There was also a brief discussion on applying standardized anomalies to increase confidence in forecasting high-end events. The ability to recognize synoptic-scale patterns and ingredients conducive to significant rainfall and flash flood events can provide forecasters the opportunity to better prepare for warning operations and decision support services.

Student Notes:

Summary

- Identify synoptic scale patterns that enhance the heavy rainfall and flash flood potential
- Identify meteorological ingredients that enhance the heavy rainfall and flash flood potential
- Identify other events and features that provide heavy rainfall and flash flooding

32. Don’t Forget About Your Hydrologic Factors

Instructor Notes: Identifying the flash flood potential for an event is more than just recognizing patterns and meteorological ingredients. Recall the following statement shown here from Doswell et al. (1996). Even though this module addressed the meteorological components of flash floods, it is only half of the equation. Other training modules are available that focus on the hydrologic-based factors that impact the flash flood potential.

Student Notes:

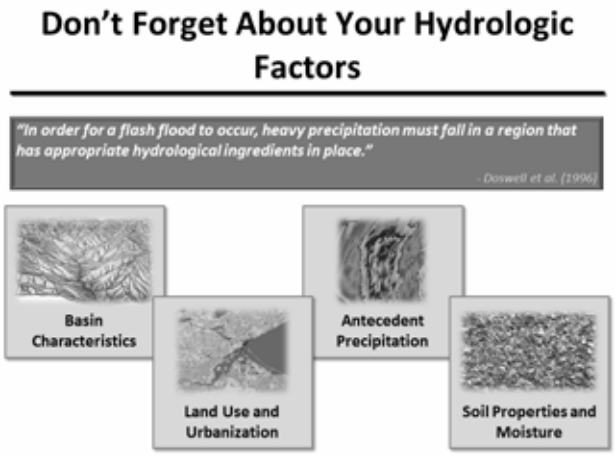

33. Contact Information

Instructor Notes: If you have any questions or issues regarding this module or the AWOC course, you can contact us at the AWOC Severe List email address. You can also contact me directly at Steven.Martinaitis@noaa.gov.

Student Notes:

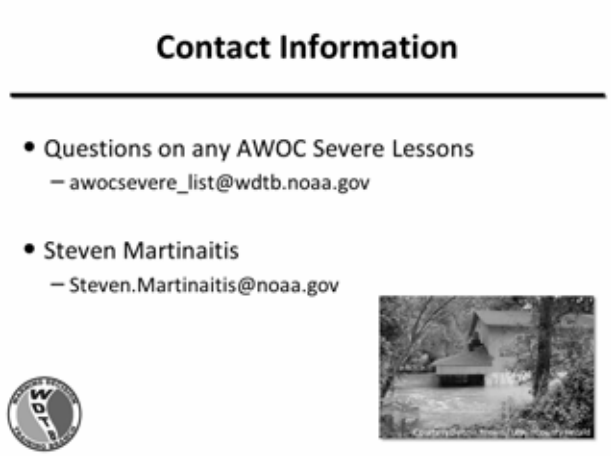

1. Threat Assessment

Instructor Notes: The title for this instructional component is “Threat Assessment.” This is the 2nd instructional component for the AWOC Severe Track. This is lesson 1 on lifting mechanisms.

Student Notes:

2. AWOC Severe Track Training Components

Instructor Notes: This IC (one of 3 in Severe Track) is devoted to environmental threat assessment. There are 3 lessons in this IC. The IC will highlight important factors in evaluating the threat for severe weather hazards.

Student Notes:

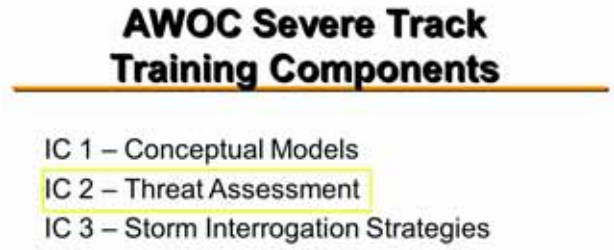

3. IC2 Outline

Instructor Notes: There are 3 lessons in this IC. This Lesson is on lifting mechanisms, Lesson 2 on outlook and short-term assessment, and Lesson 3 on threat assessment of Quasi-Linear Convective Systems (QLCS).

Student Notes:

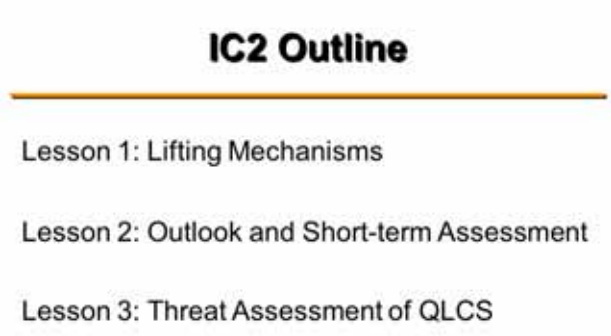

4. Lesson 1 Learning Objectives

Instructor Notes: The detection and analysis of lifting mechanisms and instability are crucial components in short-term threat assessment. Your learning objectives for this lesson are: be able to identify regions of potential convective instability, types of lifting mechanisms, how to evaluate lift, and to identify the effects of orientation of the line of forcing and boundary-relative steering-layer flow on convective evolution.

Student Notes:

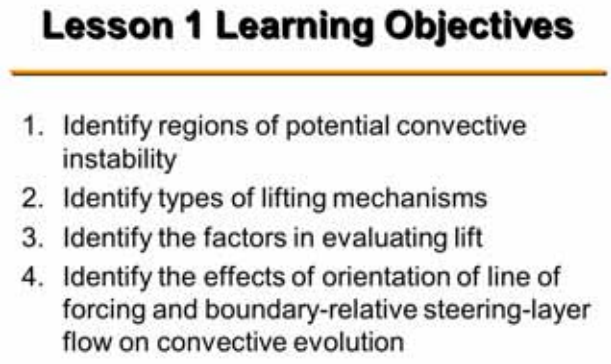

5. Why do we forecast convective coverage first?

Instructor Notes: So why is it important to look for lifting mechanisms and expected storm coverage first? Because a wide variety of storm types can occur in very similar synoptic settings and it's important to diagnose the types of lifting mechanisms which trigger initiation and lead to the resultant evolutions of convective modes.

Student Notes:

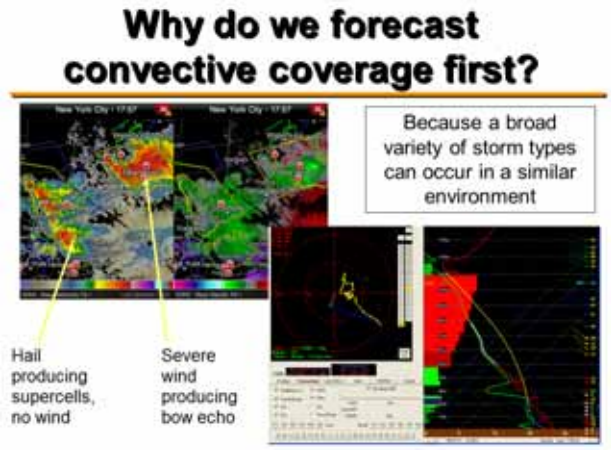

6. Ingredients for deep, moist convection

Instructor Notes: The ingredients needed for deep moist convection include both instability and some kind of lifting mechanism. Instability can come from steep lapse rates, moisture and heating. The lifting mechanism can come from either the upper levels of the atmosphere (such as a trough) or from a lower level source (such as a front).

Student Notes:

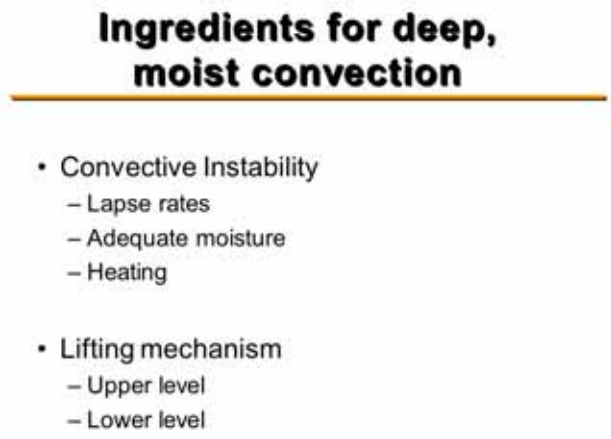

7. Ingredients-based convective coverage forecasting

Instructor Notes: Here are the steps to take when forecasting convective coverage: first we look for regions of instability, then we look for forcing mechanisms that can destabilize the atmosphere, finally we look for low-level triggering mechanisms.

Student Notes:

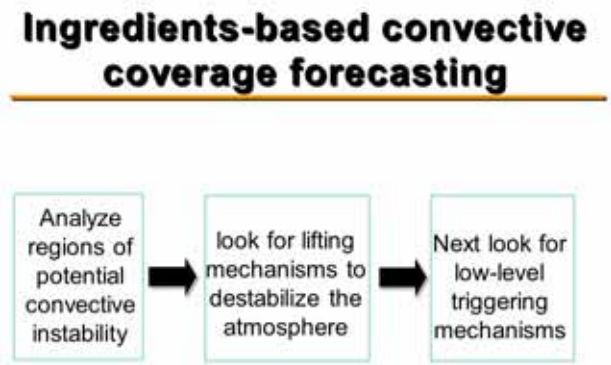

8. Ingredients-based convective coverage forecasting

Instructor Notes: In analyzing regions of potential convective instability it is important to note that the nature of the instability is a key factor in determining how much destabilization and forcing is required to result in convection. Let's take a look at several different scenarios and see if they will lead to convection or not.

Student Notes:

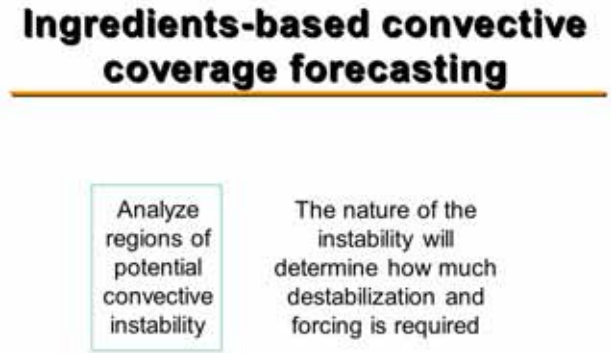

9. Instability: Case 2

Instructor Notes: This case is similar to case 1 but this time we have increased moisture aloft which allows for the parcel to remain buoyant for longer despite only weak forcing. This allows for initiation to occur.

Student Notes:

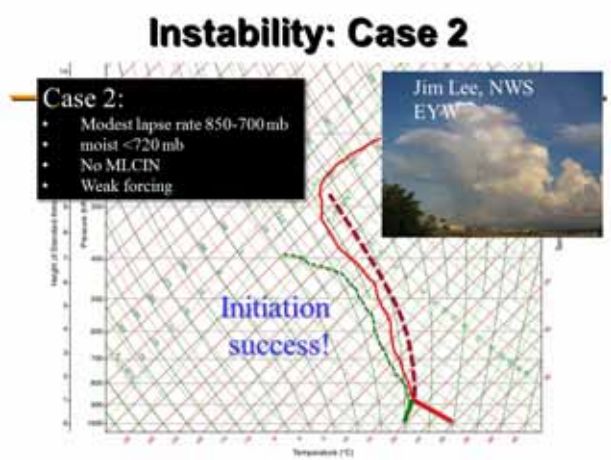

10. Instability: Case 1

Instructor Notes: In Case 1 with a modest low-level lapse rate, dry air above the surface, no CIN and weak forcing. We note that this will lead to failed storm initiation due to the lack of moisture aloft allowing entrainment to cool the parcel down and lose its buoyancy before reaching an adequate height for heavy precipitation production. This is why the parcel ascent doesn't follow the moist adiabat all the way up.

Student Notes:

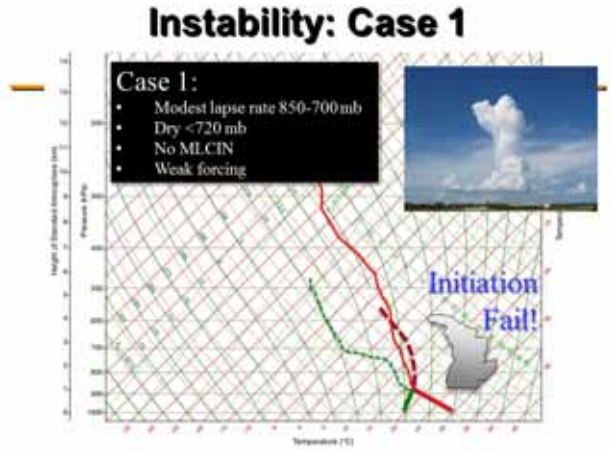

11. Instability: Case 3

Instructor Notes: In case 3 we have steep lapse rates in the low levels, dry air aloft, no CIN and weak forcing. Despite having less moisture than in the previous case, we note that the strong lapse rates increase the instability and allow for a parcel to remain buoyant and a storm to initiate.

Student Notes:

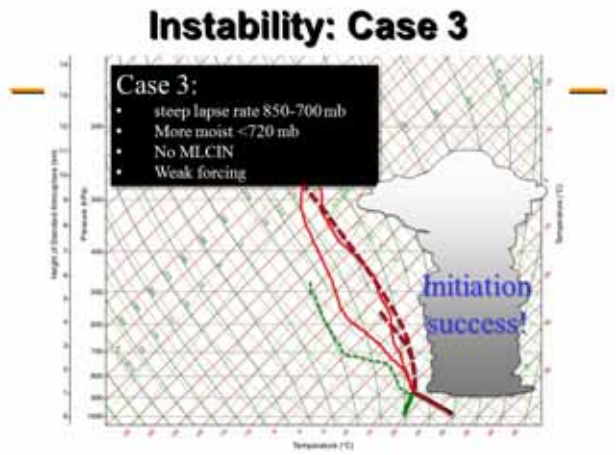

12. Instability: Case 4

Instructor Notes: In case 4, we see steep lapse rates again with the same dry air aloft and weak forcing, but this time warm air aloft has allowed for strong MLCIN. We see that, in this case, the strong MLCIN will inhibit any convection from occurring.

Student Notes:

13. Instability: Case 5

Instructor Notes: In our last case, we see what happens when a strongly capped atmosphere is met with strong lifting, the lift steepens the lapse rates and removes the cap which leads to convective initiation.

Student Notes:

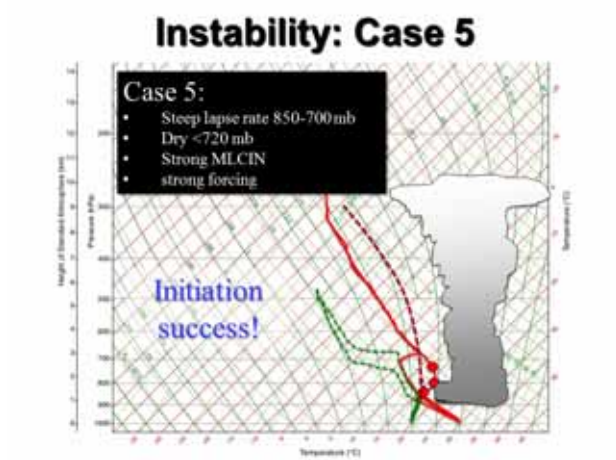

14. Ability for a towering CU to become a thunderstorm

Instructor Notes: Summarizing the cases above, the ability for a towering cumulus cloud to become a thunderstorm depends on: The amount of convective inhibition (CIN), steepness of the lapse rates in the convective layer, the strength of the cap, the amount of dry air entrainment and the amount of mesoscale destablization.

Student Notes:

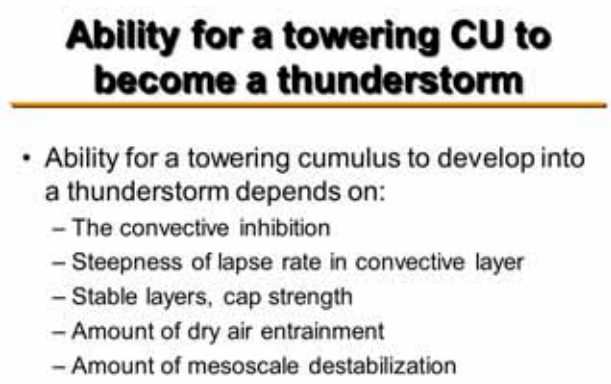

15. How much destabilization depends on the initial conditions

Instructor Notes: The amount of destabilization depends on the strength of the forcing and the strength of the inhibition as shown in this figure. Strong forcing with weak inhibition will lead to widespread convection, weak forcing with strong inhibition will result in no convection and moderate forcing with moderate inhibition will lead to isolated modes of convection.

Student Notes:

16. Ingredients-based convective coverage forecasting

Instructor Notes: So now that we've analyzed regions of potential instability, the next step is to look for lifting mechanisms that can destablize the atmosphere. Let's evaluate lift and what those lifting mechanisms are.

Student Notes:

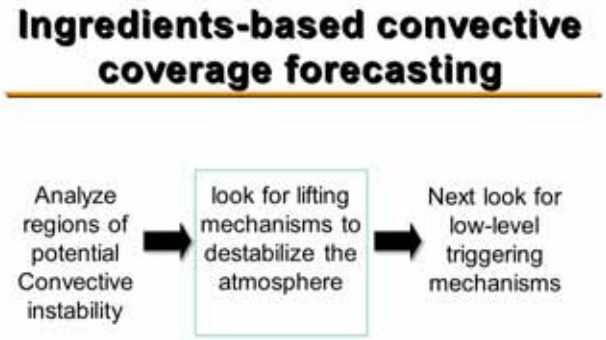

17. Lifting Mechanisms

Instructor Notes: The evaluation of lift involves 5 factors: Type, scale, duration, the details of the lift and the orientation of lift. All lifting mechanisms are not created equal. Boundaries with the greatest persistent convergence would have the highest potential for initiating convection given all other parameters being equal. But it is difficult to define persistence based on our limitations of the observing network. Often what may seem to be convergence could be a bad wind observation, or minor fluctuations in the reported winds. Persistence adds credibility that something is really there. So here are some cautions to evaluating the strength of boundaries WRT convergence: Most boundaries converge air on scales too small for even mesonetworks to resolve (Crook 1996). Strength of convergence doesn't always mean deep convergence. A boundary may have strong convergence down low and be capped well below the LFC. This is a problem especially when the LFC is high and/or if there's a significant capping layer below it. Drylines are notorious for exhibiting strong surface convergence and yet shallow circulations. One thing to remember is that when looking at the vertical continuity equation, the vertical velocity at some level depends on the integrated values of convergence/divergence below. Vertical velocity is highest at the level of non-divergence where convergence resides below and divergence above. In most cases, the deeper the convergence, the higher the level of maximum vertical velocity will occur.

Student Notes:

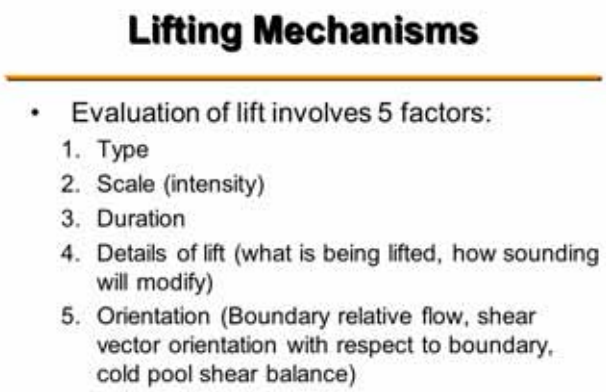

18. Types of Lift

Instructor Notes: There are many types of lifting mechanisms, low-level boundaries being the most common. Depending on the scale, observable boundary attributes are: Location, density gradients, low-level convergence and ascending air. Density gradients produce direct mesoscale ascent, so that's why we analyze direct observables such as T, Td, q, P, and θ (actually θv is the best for density). Convergence can be estimated by calculating delta velocity across the width of the boundary. Ascending air, W, can be estimated by integrating values of convergence with height. It's also important to note you get the strongest lift along a boundary that is coupled with a low level and/or upper level jet.

Student Notes:

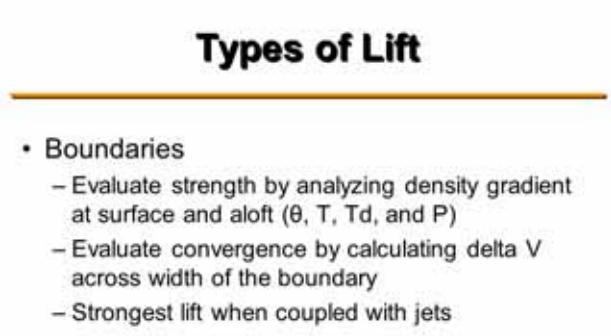

19. Estimating Convergence

Instructor Notes: Estimating one-dimensional convergence assumes a uniform airflow on either side. In other words, a front with no undulations or intersections with other boundaries. Convergence will be higher at intersections, mergers and collisions with other sources of ascent. Convergence is scale dependent. Data from METARs and mesonets will underestimate convergence in boundaries by 2 to 3 orders of magnitude. Model analysis will underestimate convergence similarly. All operational model resolutions are too poor to capture the true width of a boundary. Also, stormscale boundaries are typically unobserved by models. Typical boundaries are 3-10 km wide. Actual convergence will be occuring on these scales. Convergence will be higher at boundary intersections with other boundaries, circulations and rolls. Two dimensional convergence with boundary intersections becomes important since winds vary both along and normal to the boundary axis. Surface convergence may not always mean deep convergence/ ascent . A capped atmosphere may limit the depth of even strong surface convergence. Therefore, the deeper the convergence zone relative to the LFC, the more likely initiation will occur.

Student Notes:

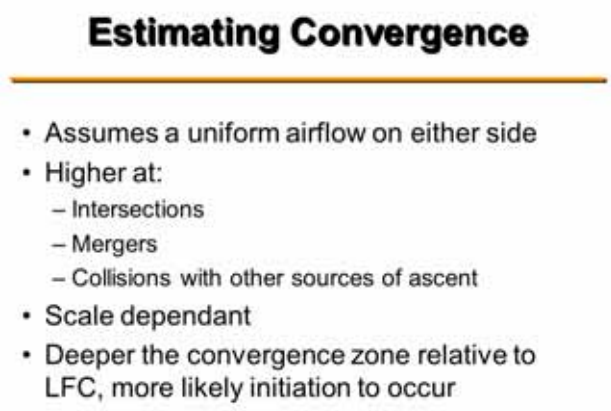

20. Observable Boundary Attributes

Instructor Notes: When analyzing boundaries as a potential lifting mechanism, try to evaluate the following: Location and movement Density gradients (which create a thermally direct circulation and ascent on the least dense side of a boundary) Low-level convergence (typically strongest near the surface) Ascending air, (note: even if you have convergence at the surface, it doesn't necessarily imply ascent). It has to be integrated values of convergence with height (decreasing convergence with height for example). Visual manifestation of moist ascent is cumulus clouds. All of these are important when assessing lift.

Student Notes:

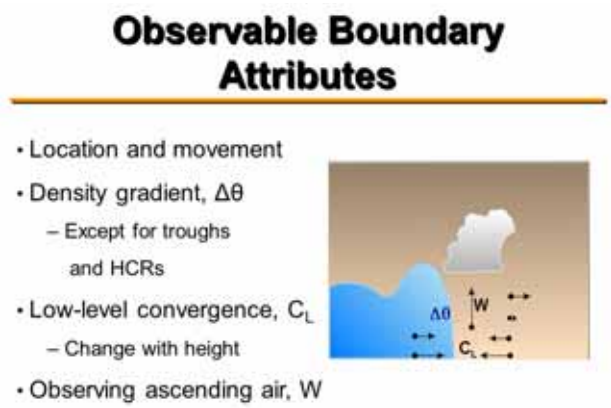

21. Lifting Along the Dryline

Instructor Notes: Here's a schematic from Ziegler and Rasmussen showing lifting along the dryline. Moist boundary layer air parcels must be lifted to their LCL and LFC prior to leaving the mesoscale updraft to form deep convection. Cloud formation is predicted when the vertical mesoscale moisture flux predominates below the LCL, and deep convection is predicted if strong mesoscale lifting is deeper than the LFC.

Student Notes:

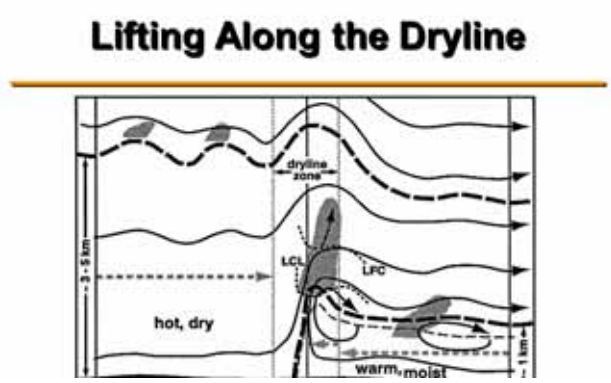

22. Types of Lift

Instructor Notes: In addition to boundaries, there are other lifting mechanisms like these shown here, which produce synoptic scale ascent. Most of these types of lifting can also support the development of convection via large scale destabilization.

Student Notes:

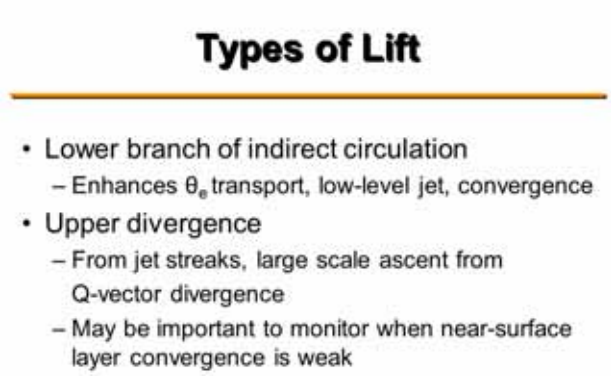

23. Upper-tropospheric Waves

Instructor Notes: It's important to note the difference between a lifting mechanism and a trigger. A lifting mechanism is an atmospheric process that forces the air to rise. A trigger mechanism is any process that initiates precipitation or storm development. Continuing to look at different lifting mechanisms, we'll examine a few more processes that can provide lift. Upper-tropospheric waves are important in synoptic scale dynamics and often induce surface cyclogenesis upstream (see the shaded area).

Student Notes:

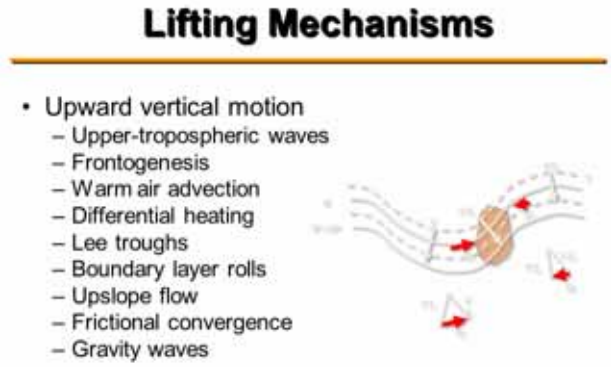

24. Frontogensis

Instructor Notes: Frontogenesis occurs when warm air converges onto colder air and the horizontal temperature gradient is amplified. The tightening thermal gradient initiates a circulation where the ascending branch can help provide a convective trigger, or at least destabilization.

Student Notes:

25. Frontogenesis

Instructor Notes: The diagnosis of frontogenesis will result in a diagnosis of the forcing for vertical motion on the frontal scale. Analyze incremental layers from the surface to 700 mb determined from AWIPS cross sections drawn perpendicular to the temperature gradient. Ascent occurs on the warm side of a maximum of frontogenesis and on the cold side of a region of frontolysis (Schultz, 2001)

Student Notes:

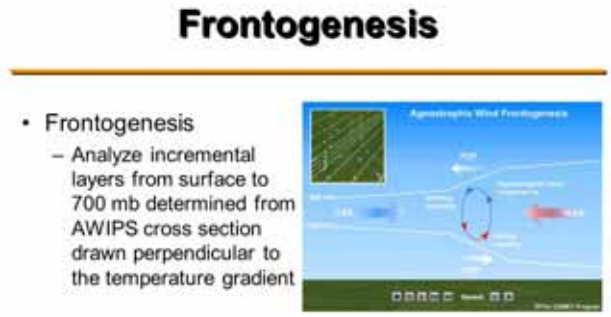

26. Elevated Convection and Frontogenesis

Instructor Notes: This is an example of elevated convection and the effects of frontogenesis. The graphic on the left shows a circulation within the plane of cross section, such as in a frontal circulation. Vertical motion is shaded and theta-E lines are solid. The graphic on the right shows circulation normal to the plane of a cross section, that is a synoptic-scale circulation. Vertical motion is shaded and lines of potential temperature are solid. If sufficient instability is available aloft, severe elevated convection can result from these types of circulations

Student Notes:

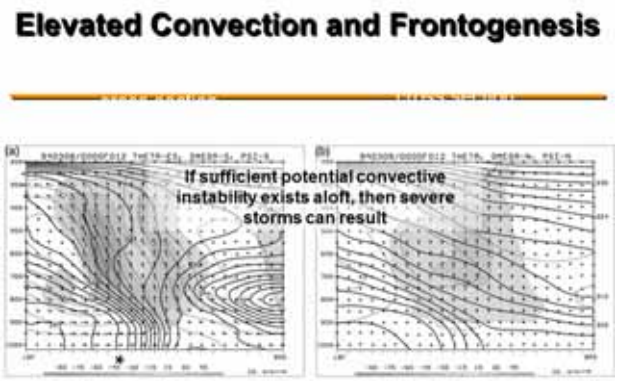

27. Warm Air Advection

Instructor Notes: Warm air advection is another mechanism which causes upward motion and can destabilize the atmosphere. With warm air advection, temperatures in the 500-1000 mb layer increase with time and the surface pressures decrease. The surface winds then accelerate in response and converge into a developing low.

Student Notes:

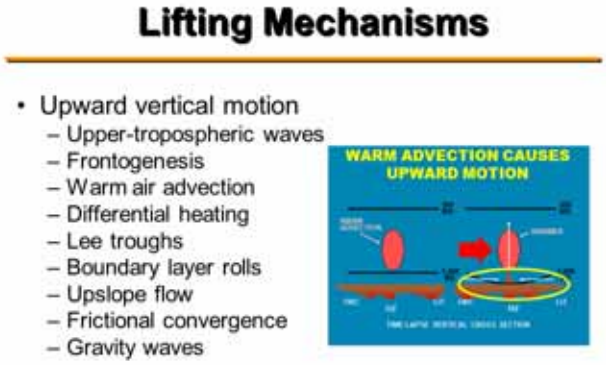

28. Differential Heating

Instructor Notes: Differential heating can also lead to rising motions, the image at right shows how differential heating acts to produce a sea or lake breeze. The next slide will go into more detail on the effects of differential heating.

Student Notes:

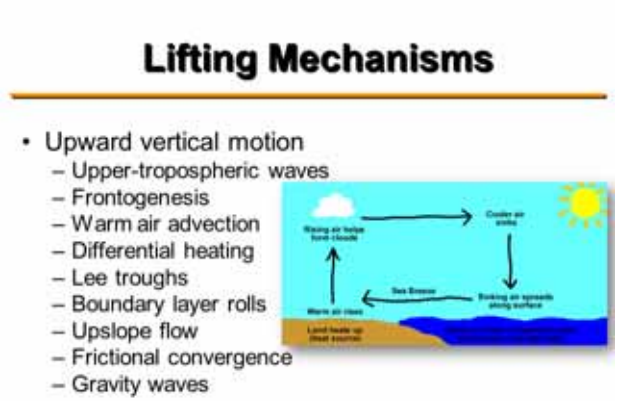

29. Differential Heating

Instructor Notes: With differential heating, pressure rises near the top of the boundary layer over the warmer air mass. This leads to divergence aloft and surface pressure falls near the surface. The adjacent cooler air subsequently flows toward the area of lowered pressure, and a direct circulation (warm air rising, cold air sinking) results. The increased gradient produces a solenoidal circulation, which, depending on amount of CAPE/CIN and external lifting mechanisms, can initiate severe convection. The thermal gradient can also act to back low-level flow and locally increase near-ground storm-relative helicity. An image will pop up which shows a situation in which differential heating lead to the development of severe thunderstorms from southern MO northeastward into OH and PA. These storms produced damaging winds and large hail on July 26, 2012 You may play and pause this loop manually. When you're done, advance to the next slide.

Student Notes:

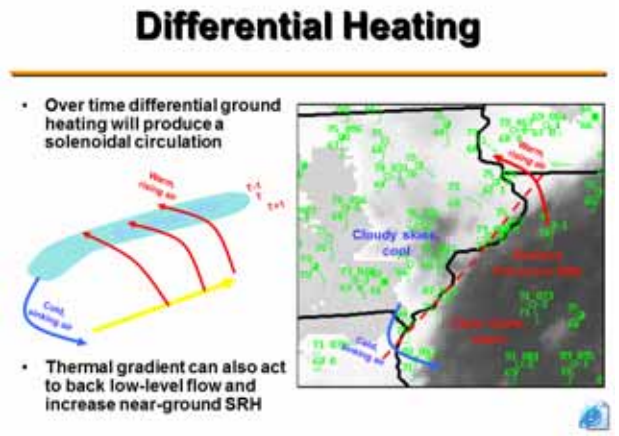

30. Lee Troughs

Instructor Notes: Lee troughs or areas of low pressure are another method of lifting, albeit on the synoptic scale.

Student Notes:

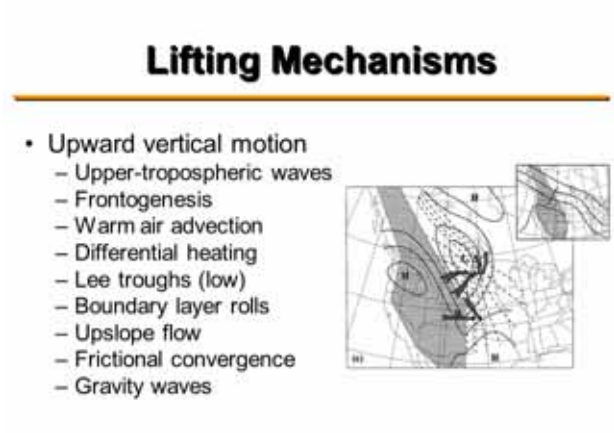

31. Boundary Layer Rolls

Instructor Notes: Boundary layer rolls are counter-rotating horizontal vortices within the boundary layer that arise from a combination of shearing instability and daytime heating. These rolls have ascending and descending branches that can locally destabilize a portion of the atmosphere and lead to locally enhanced lifting that can lead to convective initiation.

Student Notes:

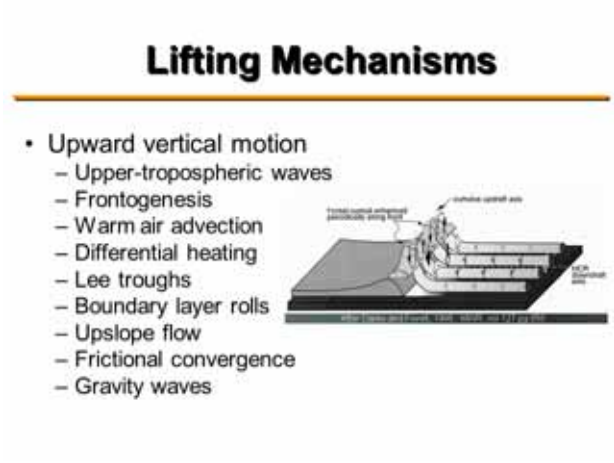

32. Upslope Flow

Instructor Notes: Upslope flow is obviously an important consideration where there are significant changes in topography and wind flow. Terrain effects can influence boundary layer low-level jet characteristics and also flow effects due to topography. The ascent occurring with upslope flow over the higher terrain and upslope transport of water vapor can lead to convective initiation over mountainous terrain often earlier than over adjacent, more flat, terrain.

Student Notes:

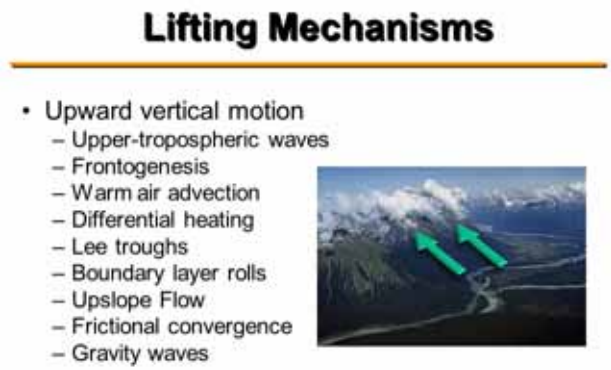

33. Frictional Convergence

Instructor Notes: Frictional convergence can also provide upward vertical motion. There is less friction over a body of water than over land, so as air moves from a water (or ice) surface to land, it slows down due to friction and the air upstream catches up to and converges with the air that is moving over the land.

Student Notes:

34. Gravity Waves

Instructor Notes: Gravity waves and their associated vertical motion can also produce lift. In a gravity wave, the parcel of air will try to remain at a location in the atmosphere where there are no forces causing it to rise or sink. Once a force moves the parcel from its natural state of equilibrium, the parcel will try to regain its equilibrium. But in the process, it will overshoot and undershoot that natural position each time it is rising or sinking because of its own momentum. The upward moving region of a gravity wave is the most favorable region for cloud development with clear skies likely in the sinking region.

Student Notes:

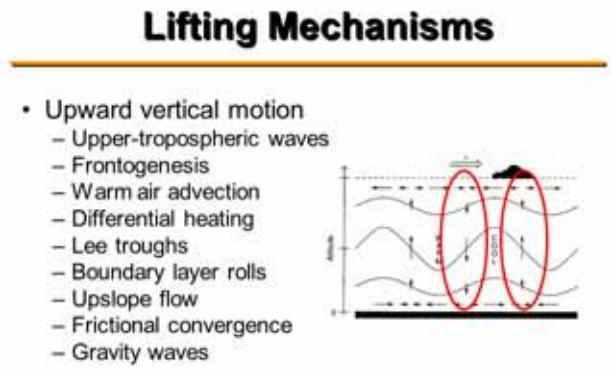

35. Orientation of Lift

Instructor Notes: There are some additional factors to consider when evaluating how strong (and deep) the lift will be: These are Boundary-relative flow (low-levels and steering layer) and Boundary-orthogonal shear (RKW Theory) In addition to evaluating the individual details of parcels for lifting, we should look at the characteristics of lift associated with boundaries in terms of how strong and deep the lifting will be.

Student Notes:

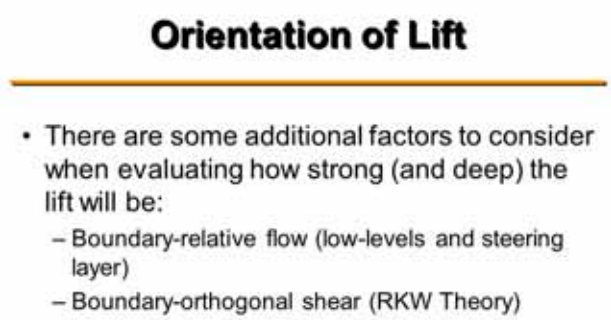

36. Interim summary

Instructor Notes: So to summarize what we've learned thus far: In order for convection to form, it must overcome the cap and dry air entrainment. Destabilization is a result of synoptic scale vertical motion. Mesoscale upward forcing acts as a trigger which can come from a variety of sources. Finally, an increase in storm coverage is a result of either stronger or deeper forcing. But that's not all, there's more, next we'll consider Boundary Relative Flow…..

Student Notes:

37. Boundary-Relative Flow Considerations

Instructor Notes: Now we'll take a look at some boundary-relative flow considerations. Based on observations by Wilson and Megenhardt, boundaries in Florida were most active if the convective steering flow minus the boundary motion was less than or equal to 5 m/s. Boundary relative flows greater than 5 m/s exhibited less storm activity and those storms that did form on the boundary would quickly be left behind in less stable air and they would dissipate. The orientation of the line of forcing can also be as important as CAPE and shear in determining the type of outbreak. We'll discuss more about this in lesson 2.

Student Notes:

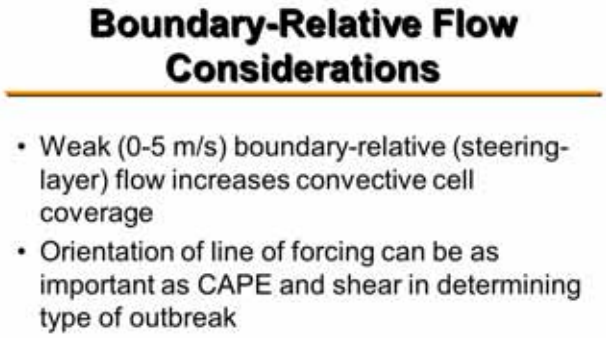

38. Boundary-Relative Flow Parameters

Instructor Notes: This is a schematic of some of the boundary-relative flow parameters. Some of these theories apply to density current boundaries. A boundary-relative headwind increases the depth of the ascending air column. Conversely, a boundary-relative tail wind decreases the depth of the ascending air column. Based on numerical modeling of an outflow boundary, the boundary height increases when the boundary moves into a headwind. Boundaries with a headwind move more slowly then those with a tailwind. From these theoretical and numerical experiments, an ascending air column will be deeper for boundaries experiencing a significant headwind than those which fall into a tailwind. It also stands to reason that low level convergence with a headwind boundary is much higher.

Student Notes:

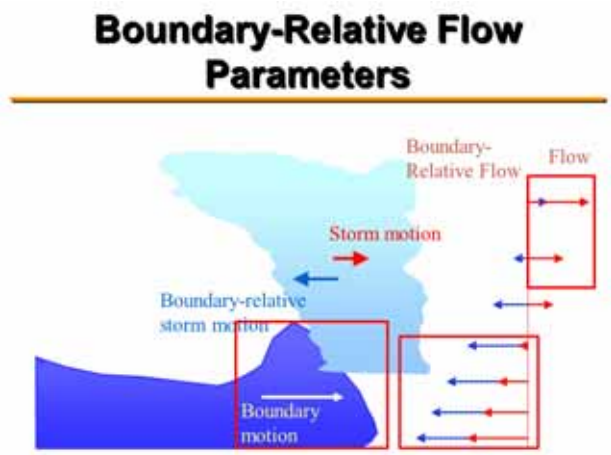

39. Residence time – boundary-relative steering flow

Instructor Notes: One way to increase residence time is to match the storm and boundary motion. Here we present three scenarios with respect to towering cumulus along a boundary moving to the east. In the top, the steering flow is parallel to the orientation of the boundary. The tower moves to the northeast while the boundary moves east taking the mesoscale lifting zone away from the cumulus. Quickly, the cumulus is subjected to an atmosphere devoid of support and subsequently the tower dies. The middle towering cumulus has a steering flow that carries it northeast but with a small component normal to the boundary orientation. Since the boundary is moving east, the steering flow allows the cumulus to remain in the lifting zone of the boundary and is thus allowed to grow in a destabilized atmosphere. In the bottom scenario, the towering cumulus has a large component of motion normal to the boundary orientation and thus it leaves the lifting zone behind and is forced to endure a capped atmosphere. Matching boundary and cell motion is what Wilson and Megenhardt found to be an important factor in determining the coverage of convection along Florida seabreezes and outflow boundaries. We would like to see what is called boundary-relative cell motion to be less than +- 5 m/s to ensure a long residence time.

Student Notes:

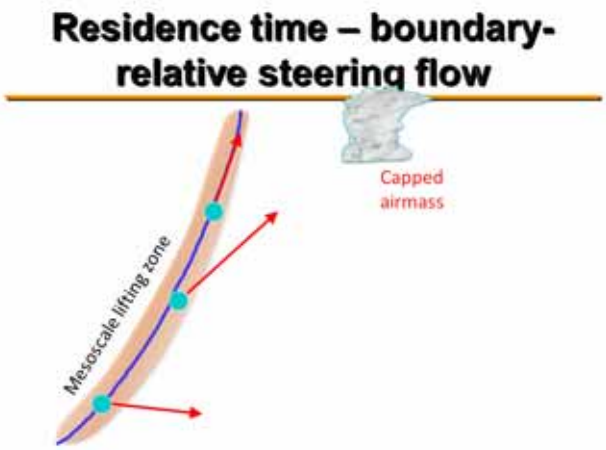

40. Residence time – width of lifting zone

Instructor Notes: In the second scenario, we retain the concept of the boundary-relative steering flow but now the width of the lifting zone is varied. In this case, even a cell that falls behind the boundary will maintain a favorable environment of lifting. Only in this case, the cell becomes elevated.

Student Notes:

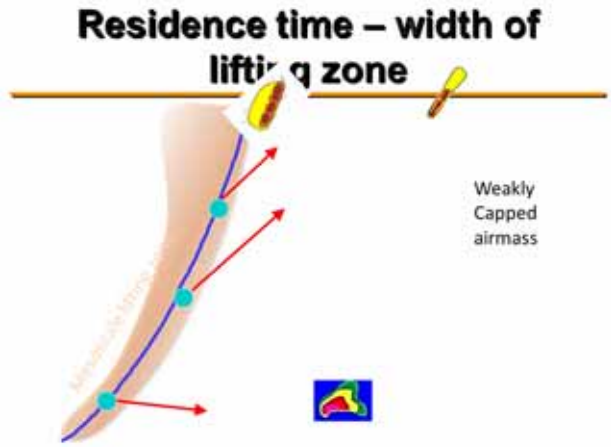

41. Depth of Ascent Zone

Instructor Notes: Finally we discuss evaluating the depth of the ascent zone. This is another important consideration when evaluating the details of lift. This theory is based on Rotunno, Klemp, and Weisman (RKW) numerical simulation studies from the 80s and early 90s. It is based on horizontal vorticity arguments. The key to RKW is maximizing residence time of a parcel in the ascent zone to ensure it reaches the LFC. (See http://meted.ucar.edu/mesoprim/shear/frameset.htm). These theories apply to density current boundaries. Density current boundaries include strong fronts, including seaband outflow boundaries. Deepest ascent occurs when boundary orthogonal environmental shear balances cold pool vorticity (Rotunno et al. 1988), or when the boundary speed (C) cancels out positive shear magnitude (UL). C/ UL ~ 1. When the boundary-normal (or orthogonal) component of the shear is oriented forward away from the cold side of the boundary (positive shear) and it has the same magnitude as the forward speed of the boundary, the conditions are optimal for the strongest, most vertically oriented ascent zone. That is C/ Delta UL ~ 1. This is graphically shown in the right side schematic. What often occurs is shown in the left side figure where the shear vector is directed front to rear of the boundary (negative shear). In that case, no balance occurs in C/ UL and the ascent zone becomes much shallower.

Student Notes:

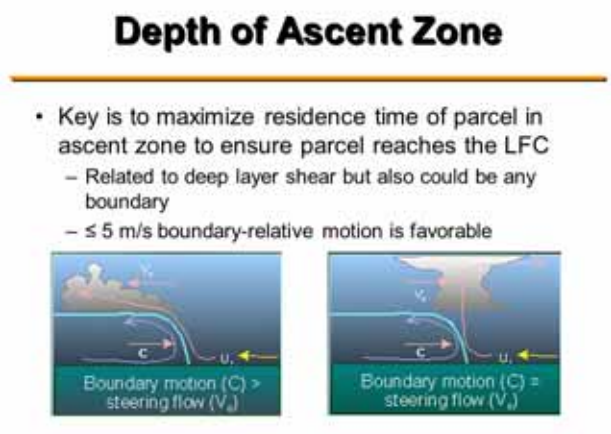

42. Lifting Mechanisms Case Study

Instructor Notes: Let's take a look at an actual event and examine the forcing and lifting mechanisms involved. Here is an event from November 7, 2011 in Oklahoma. The 300 mb level shows one weak jet entrance region in the Central Plains. Otherwise the large trough to the west is likely creating a wide area of weak ascent, but acting over the air for a day lapse rates likely increased.

Student Notes:

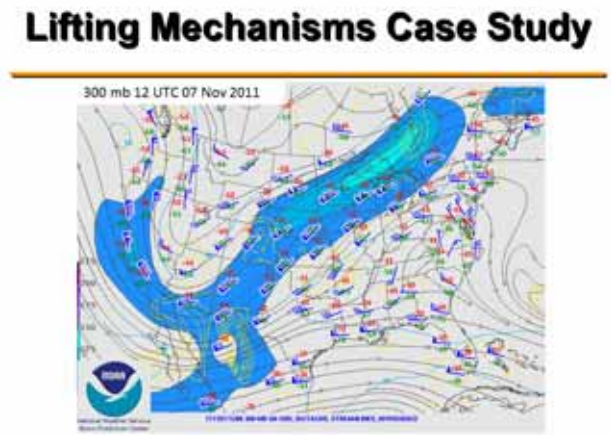

43. Lifting Mechanisms Case Study

Instructor Notes: The trough shows up at 500 mb with a more pronounced inflection point in the flow as it moves east. But notice the 500 mb temperatures in OK actually increased somewhat. Was that increase too much?

Student Notes:

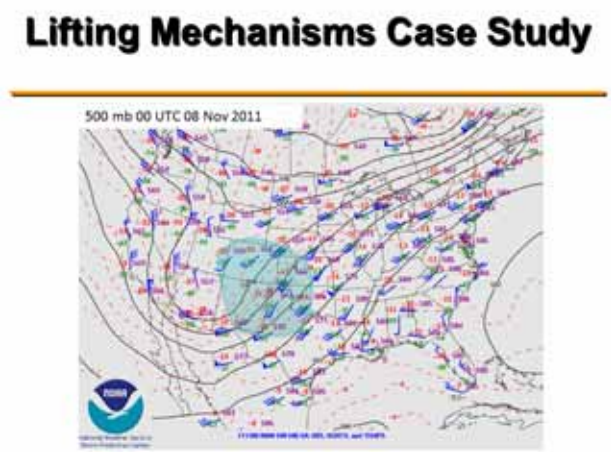

44. Lifting Mechanisms Case Study

Instructor Notes: The 700 mb temp also increased by 7 degrees in Oklahoma City (indicated by the black circle) and so overall the lapse rate might've decreased between 700 and 500 mb.

Student Notes:

45. Lifting Mechanisms Case Study

Instructor Notes: At 850 mb, the temps remained the same at Oklahoma City (black circle) but warmed dramatically in Midland (yellow circle) due to diurnal heating. Air moving northeast from Midland likely induced warm air advection and ascent and destabilization. There's one more major forcing function but we'll zoom in to see.

Student Notes:

46. OUN Soundings

Instructor Notes: The morning sounding started out relatively free of CIN. In the afternoon, warming aloft was matched by diurnal heating. This is even relatively far from the initiation point which was to the southwest.

Student Notes:

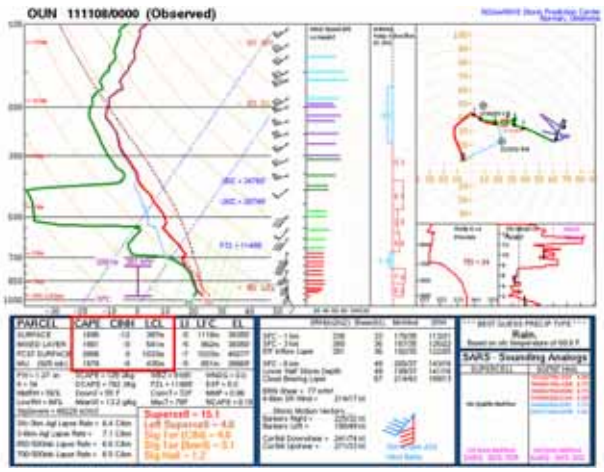

47. Model forecast for FDR

Instructor Notes: Here's a forecast sounding for Frederick which is located in southwest OK. The 12z forecast sounding shows a weak CAP, however most of this is removed by 22Z mostly by diurnal heating…

Student Notes:

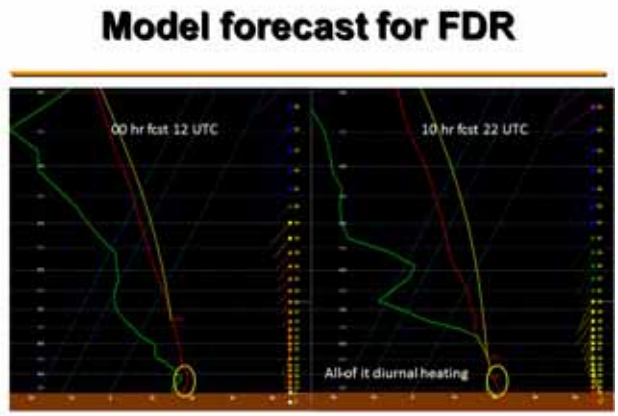

48. 1743 UTC sfc map

Instructor Notes: So what did a weakly capped atmosphere with broad WAA do? It depended ultimately on the nature of the boundaries near the surface. At 1743 UTC the cold front was the primary driver. But there was also a weak outflow boundary, a dryline and a subtle boundary that we're not quite sure of its nature.

Student Notes:

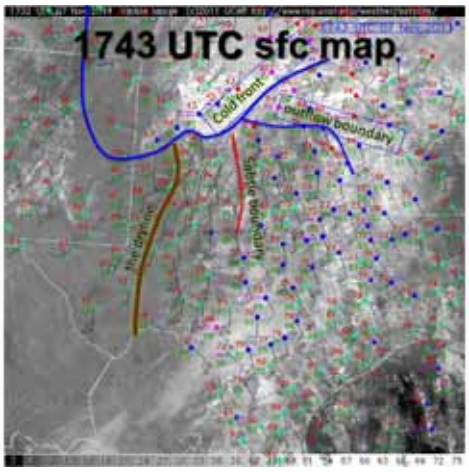

49. 1943 UTC sfc map

Instructor Notes: Two hours later we find that the subtle boundary was apparently a secondary dryline demarcating the western edge of the deeper moisture. It's subtle and yet pivotal in organizing convection. Drylines have been found to be frontogenetic in nature. So certainly it should show up in a frontogenetical analysis. Maybe the outflow boundary would too.

Student Notes:

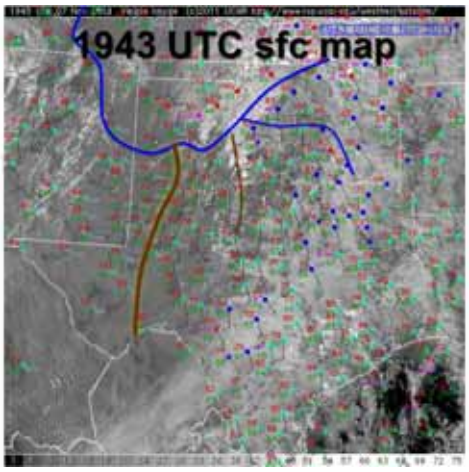

50. Main front has frontogenesis up to 850 mb deep

Instructor Notes: So we look at the 19Z SPC Mesoanalysis of frontogenesis at 850mb but no other boundaries show frontogenesis up to this depth.

Student Notes:

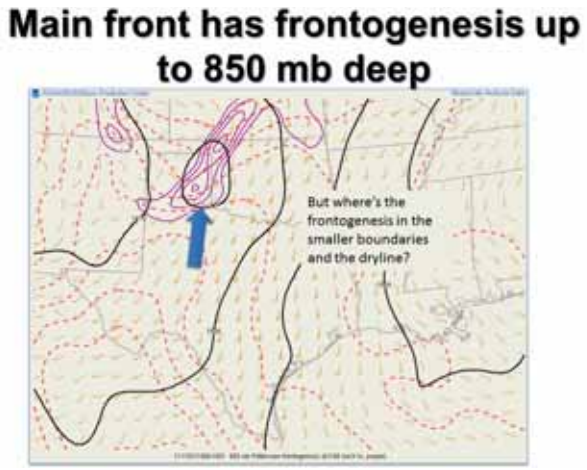

51. Main front shows strong surfce frontogenesis

Instructor Notes: At the surface, there's no real evidence of dryline frontogenesis or that of the outflow boundary either.

Student Notes:

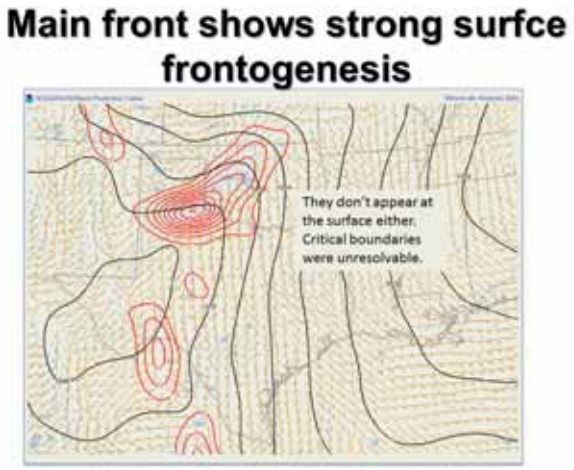

52. 1950 UTC Boundary Locations

Instructor Notes: Yet there is significant vertical motion along the dryline, as evidenced by developing convection. However it is perhaps not as significant as with the front. The stars shown on the map mark the location of 2 separate hodographs that we will examine on the next slide.

Student Notes:

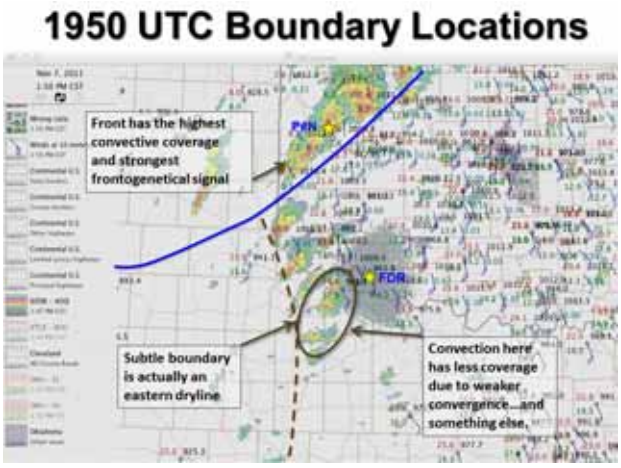

53. Boundary-relative steering flow

Instructor Notes: Using BUFKIT here are two different locations in OK. The white lines on each hodograph show the orientation and motion of the boundary. The orange circle shows the storm motion and the M the mean wind. The first, P#N, located in northwest OK shows that storms that develop will fall behind the front and likely become elevated or dissipate altogether. The second location, Frederick, shows that storms that develop should stay ahead of the boundary and likely remain surface-based.

Student Notes:

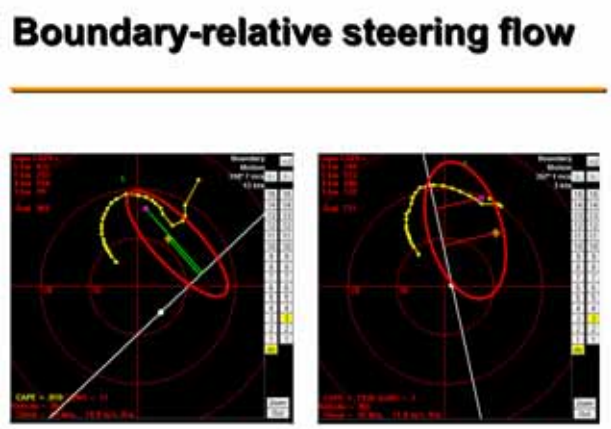

54. Boundary-relative motion vs storm coverage

Instructor Notes: Let's take a look at where the boundary relative motions compare to the general theory. All these figures are from Dial et al, 2010; The figure in the upper left contains their data set where the black squares represent storms that evolved into lines and the white circles indicate storms that remained discrete. Note that the front has a negative motion, as we overlay the boundary motions on the findings from Dial et. al, we find that the dry line storms should be cellular in nature. In contrast the boundary motion of the cold front is on the lower-bounds of the box and whiskers, indicating that if storms form, they are more likely to form into a more linear mode. So What happened with this event? (Data from Dial, Greg L., Jonathan P. Racy, Richard L. Thompson, 2010: Short-Term Convective Mode Evolution along Synoptic Boundaries. Wea. Forecasting, 25, 1430–1446.)

Student Notes:

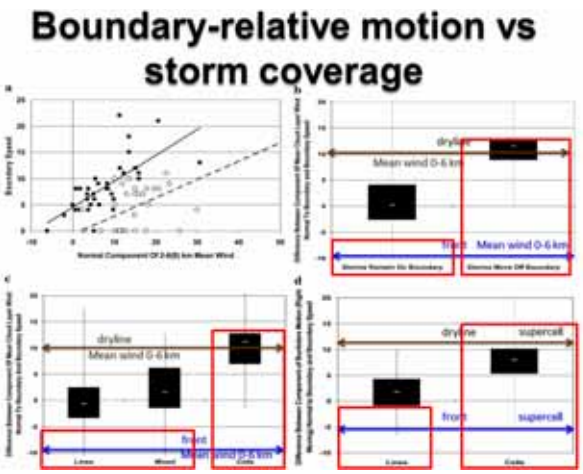

55. 11/7/11 Storm Reports

Instructor Notes: Here's a map of the storm reports from this event (wind reports are blue, hail reports are green and tornado reports are red), this was a rare event for Oklahoma in November and was the second largest November tornado outbreak since records began. 10 tornadoes were surveyed, with 1 being an EF-4. You can see that the storms that formed along the dry line and were able to stay ahead of the cold front were the storms that produced tornadoes while those that crossed over or were undercut by the front either produced no severe weather or mostly hail with a isolated wind damage.

Student Notes:

56. Photos

Instructor Notes: And here are a couple of pictures of one of the tornadoes courtesy of Chris Spannagle.

Student Notes:

57. SummaryLesson 1

Instructor Notes: In summary, storm coverage is impacted by the amount of CIN and dry air entrainment. There are several factors to account for in assessing lift, including boundary-relative flow and shear/cold pool relationships. Lifting can occur on both the synoptic and meso-scale and can be created by many different processes. Finally we note that the intensity and longevity of storms can be affected by the orientation of lines of forcing. This completes lesson 1, you are now ready to complete the test. Advance to the next slide to complete the exam, after passing the exam you are ready to advance to lesson 2 of the course which is on outlook and short-term threat assessment.

Student Notes:

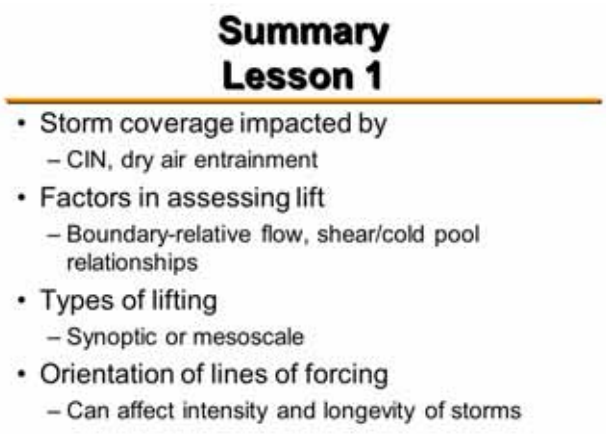

58. AWOC Severe IC 2 Lesson 1 Test

Instructor Notes:

Student Notes:

59. Questions?

Instructor Notes: Have a question? Feel free to contact us at awocsevere_list@wdtb.noaa.gov.

Student Notes:

1. Threat Assessment

Instructor Notes: The title for this Instructional Component (IC) is “Threat Assessment.” This is the 2nd instructional component for the AWOC Severe Track. Lesson 2 in this IC is on outlook and short-term assessment of hazards.

Student Notes:

2. IC2 Performance Objective

Instructor Notes: The performance objective (the desired trainee behavior from training) for this IC is to demonstrate processes for continuous evaluation of hazardous weather threats to support effective warning methodologies. Some examples of this performance would include: Demonstrating ability to coordinate with SPC and adjacent FOs on watch decisions (for ex. watch extensions and cancellations) Demonstrate the ability to utilize the full suite of products to issue short-term forecasts of convection. Demonstrate the ability to monitor mesoscale conditions (including near-storm environment) and provide input to warning decisions based on that data.

Student Notes:

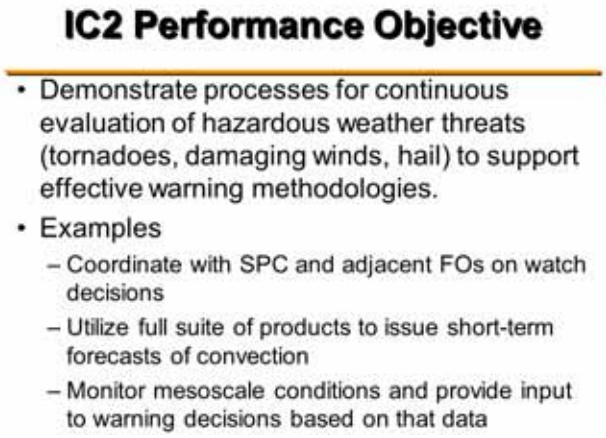

3. Lesson 2 Learning Objectives

Instructor Notes: The learning objectives for this lesson are: Identify the purposes of threat assessment Identify 3 key job tasks for threat assessment in the 0 to 6 hour time period Identify the conditions favorable for severe weather in the 0-6 hour time period

Student Notes:

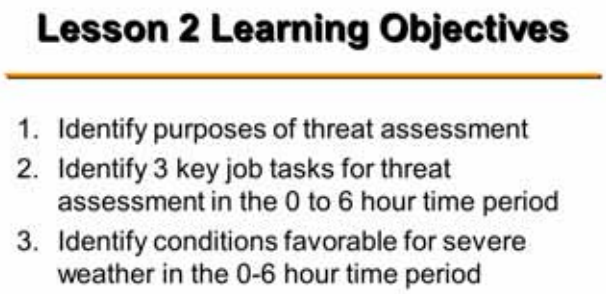

4. Purpose for Threat Assessment

Instructor Notes: Threat assessment (TA) is an important part of an effective warning methodology. It is important in determining the tone of awareness for the subsequent event. This step enables the severe weather warning team to begin to focus on specific threat areas and specific storms within the CWA (how to initially sectorize the CWA for severe weather operations). By assessing the spatial and temporal evolution of the mesoscale convective environment, forecasters can improve their decision making skills because they can acquire an increasing knowledge of the perceived level of threat for each storm. Threat assessment is a continuous process, not a one-time action. Thus, many of the key job task skills presented here are applicable throughout the entire severe weather event, especially during warning mode, because forecasters often lose their situational awareness of the environment once warnings commence.

Student Notes:

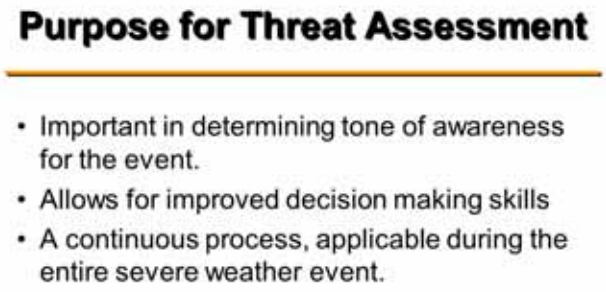

5. Threat Assessment Flow Chart

Instructor Notes: Environmental threat assessment influences subsequent actions in a warning methodology. There is an initial assessment of convective storm mode shown in the first square (Individual cells, Multicells) then an evaluation of specific hazards. These threats for each storm help determine radar interrogation procedures. Note that staffing strategies are determined to a large degree based on the initial forecasts of convective mode. This might be from the Day 1 or 2 Hazardous Weather Outlook.

Student Notes:

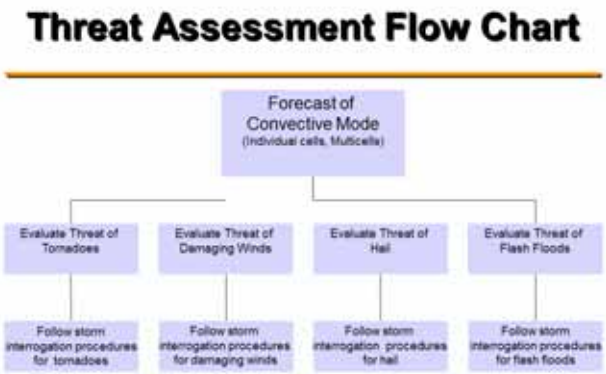

6. Short-Term Threat Assessment Key Tasks

Instructor Notes: Here are some tasks in short-term threat assessment, a few of these have been discussed in the previous lesson. The tasks are: First, to examine the synoptic setting for any recognizable patterns; then evaluate the environment to determine: The expected location and timing of severe development, the expected convective mode, the likelihood and intensity of specific threats, and finally the expected evolution of the threat(s).

Student Notes:

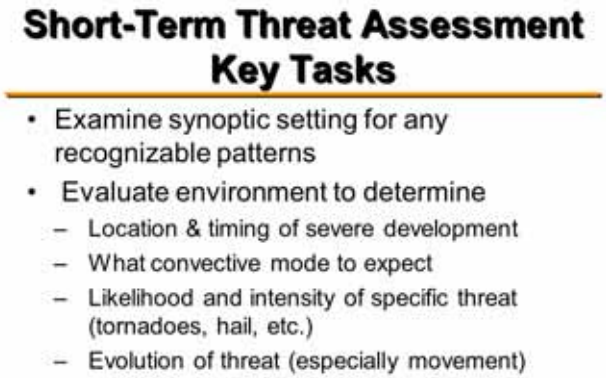

7. Pattern Recognition Ex. 1

Instructor Notes: Let's take a look at a few common severe weather synoptic patterns. This is pattern recognition example 1. This is a hand-analyzed composite chart of synoptic features at 00Z on May 5th, 2003. It is important to compare synoptic patterns to analog events. This is part of the pattern recognition process.

Student Notes:

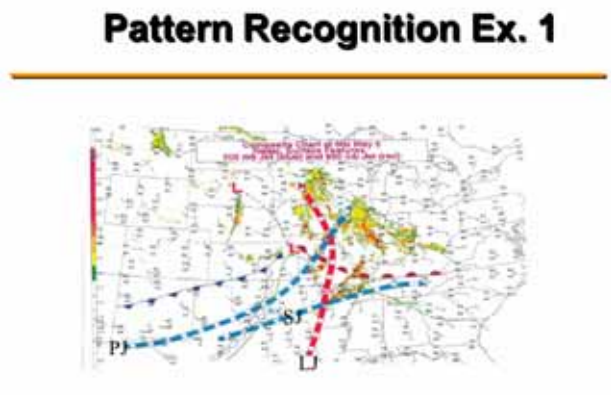

8. Pattern Recognition Ex. 1

Instructor Notes: Does the previous composite chart look like this? Well if it does, you're going to have problems if your CWA is in the hatched area. This is a pattern well-known to severe storm forecasters; a classic tornado outbreak pattern from Barnes and Newton. It shows a prominent crossing of the polar and lower-level jets in the warm sector of a developing low pressure system. Newton found most tornado outbreaks occurred north of the subtropical jet.

Student Notes:

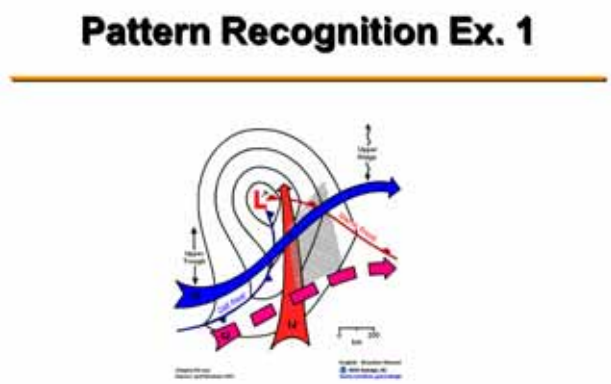

9. Pattern Recognition Ex. 1

Instructor Notes: This composite chart previously shown was from the May 4th, 2003 tornado outbreak, which was a well forecast event. This graphic was taken from the NOAA/NWS Service Assessment of the May 4-10, 2003 tornado outbreak. The website listed in the speaker notes provides more details. For more details on the May 4, 2003 tornado outbreak, which was a well forecasted event, see http://journals.ametsoc.org/doi/pdf/10.1175/BAMS-86-4-531.

Student Notes:

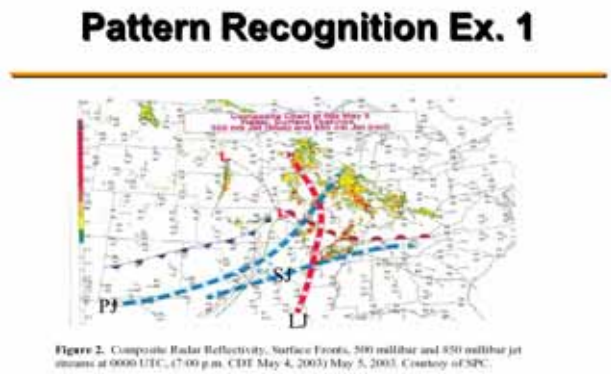

10. Pattern Recognition Ex. 2

Instructor Notes: Here's another common synoptic pattern from Johns 1993, this time for long-lived bow echoes and derechos. It depicts a classic strongly forced synoptic situation usually found in advance of a mid-latitude cyclone. This pattern can be found with a varied amount of CAPE depending on the season. These systems are also typically characterized by dry air in the midlevels. Note that this pattern is similar to that shown previously for tornado outbreaks but the LLJ is oriented more parallel to the polar jet resulting in less curvature of the hodograph.

Student Notes:

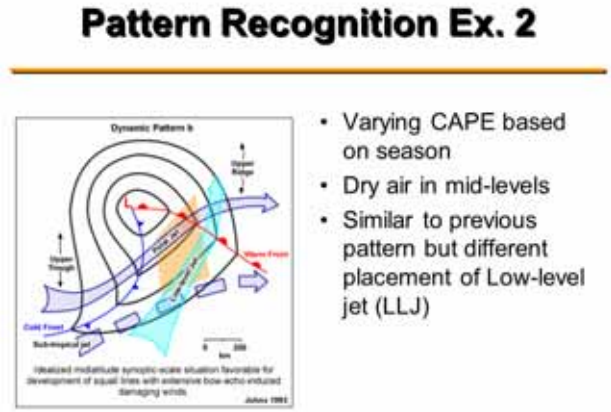

11. Pattern Recognition Ex. 3

Instructor Notes: This pattern is also favorable for bow-echoes and derechos and taken from Johns 1993. This is a warm-season, weakly forced situation almost always associated with high CAPE and a boundary with strong vertical vorticity. As in the previous situation, this pattern is also characterized by dry air in the mid-levels. This serves to enhance evaporational cooling in downdrafts which results in stronger outflows and damaging surface winds. It's important to note that a number of bow echo systems occur with elements of both this and the previous pattern.

Student Notes:

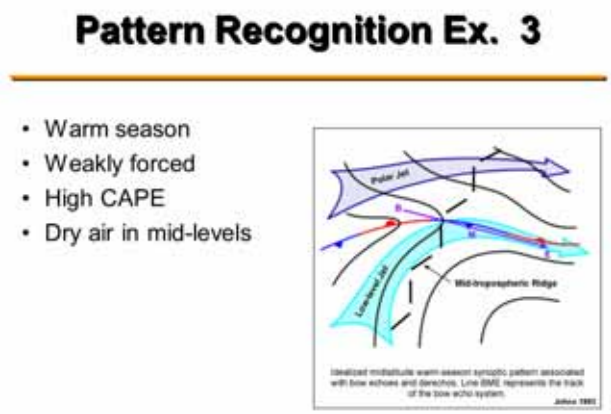

12. Pattern Recognition Ex. 4

Instructor Notes: This is an idealized pattern that supports non-mesocyclonic tornadoes. It consists of a stationary front or boundary possessing steep, low-level lapse rates, enhanced 0-3 km CAPE, little or no CIN, weak deep-layer shear, and large cyclonic surface vorticity. An example of this pattern will be shown later on in the lesson.

Student Notes:

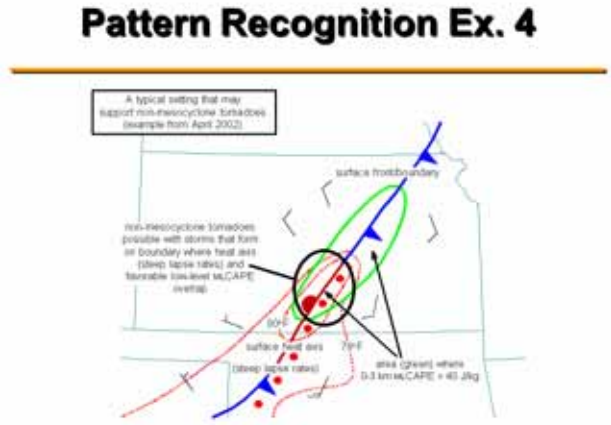

13. Pattern Recognition

Instructor Notes: It's important to note that these are only a few of the best documented patterns, not an exhaustive list. Severe weather can and frequently does occur outside of these patterns. Pattern recognition can only supplement, not replace, an ingredients-based methodology to severe weather forecasting.

Student Notes:

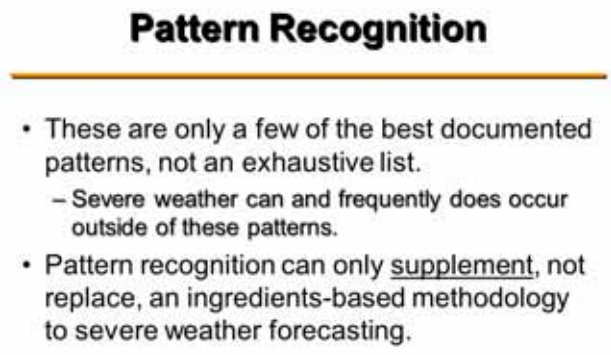

14. Relationship Between Line of Forcing and Deep-Shear Vector

Instructor Notes: Bluestein and Weisman performed a set of numerical model experiments to demonstrate that the evolution of supercells in a homogeneous environment depends upon the orientation of the vertical-shear profile with respect to the orientation of the line along which the convection is initiated (the “line of forcing”). This work was motivated by the observations that the nature and consequences of the interaction of neighboring cells depend upon differential cell motion, which in turn is a function of the characteristics and orientation of the vertical-shear profile and its impact on the behavior of outflow boundaries. Their first set of simulations was for strong, deep-layer, vertical wind shear profiles with straight (unidirectional) hodographs supportive of supercells. Their results suggested that if the shear vector is oriented at a 90 degree angle (normal) to the boundary (left example), then it is expected that a series of left-moving and right-moving storms will be generated; the right-moving storms will collide with the left-moving storms to their south; only the southernmost right-moving and northernmost left-moving storms will likely not interact with their neighbors. If, however, the shear is oriented at a 45 degree angle to the boundary (center example), then, with the exception of the northernmost storm, the left-moving members will move across the outflow boundary generated by their right-moving neighbor to the north, and weaken, while the right-moving members will move away from the boundary and may not collide with their neighbors at all. Finally, if the shear is oriented parallel to the boundary (right example), then the left movers will move behind the boundary, while the right movers will slowly move ahead of the boundary (Fig. 2c). However, since there is also a component of storm motion parallel to the boundary, the right movers might catch up to the outflow boundaries generated by the adjacent right movers along the line, and weaken. Only the downshear-most storms would be able to evolve without interacting with their neighboring cells.

Student Notes:

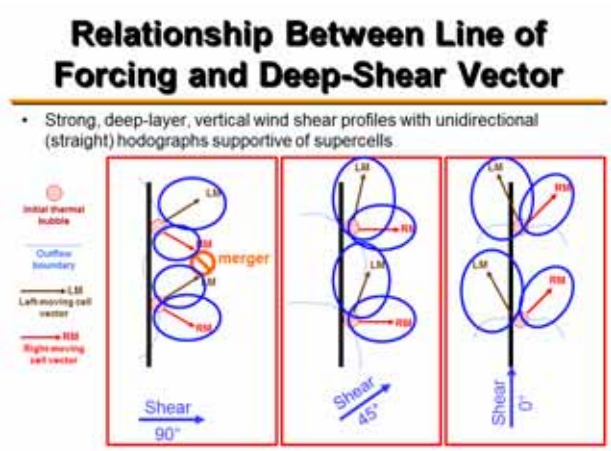

15. Relationship Between Line of Forcing and Deep-Shear Vector: α= 90°

Instructor Notes: The following four slides show the results of Bluestein and Weisman's (2000) numerical model simulations of line segments of cells, each with identical clockwise-curved hodograph shapes clearly supportive of supercells, but with a unique orientation of the deep-layer vertical wind shear vector relative to the line of forcing (α=90 degrees, 45 degrees, 0 degrees, and 135 degrees). The left image contains the ground-relative tracks of each cell, characterizing their propagation characteristics, longevity, and degree of interactions with neighboring cells. Supercells tracks are indicated by the thick, solid lines, while non-supercell tracks are indicated by the thinner, dotted lines. The right image contains simulated fields of rainwater (solid contours), updraft (shaded region), and gust front (thin dashed line) at Time=1 hours, 1.5 hours, and 2 hours into the simulation. When the deep-layer vertical wind shear vector is normal (α=90 degreees) to the line of forcing, an isolated, cyclonically-rotating, right-moving supercell develops at the end of the line to the right of the deep-layer shear, while an isolated anticyclonically rotating, left-moving supercell develops at the end of the line to the left of the deep-layer shear. A squall line having embedded, but distinct, intense cells develops in between. The squall line develops after neighboring right- and left-moving cells collide. The cells in the squall line have some supercellular characteristics, but the updrafts at midlevels are not very well correlated with vertical vorticity.

Student Notes:

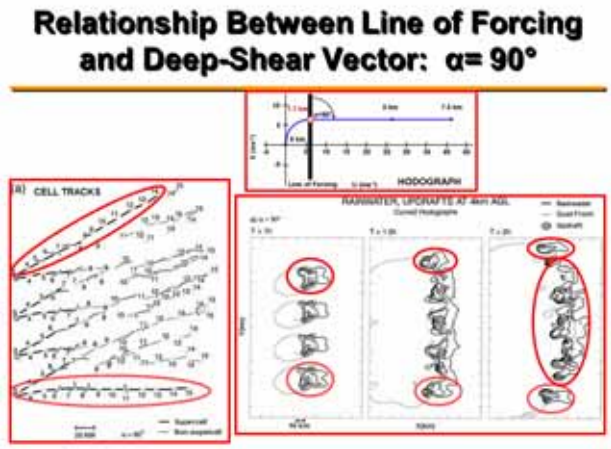

16. Relationship Between Line of Forcing and Deep-Shear Vector: α=45°

Instructor Notes: When the deep-layer vertical wind shear vector is 45 degrees from the line of forcing, a line of cyclonic supercells can be maintained for long periods of time (e.g., more than 2 h). In addition, an isolated, anticyclonically rotating, left-moving supercell is prominent at the downshear end of the line. It is noteworthy that, owing to neighboring storm interactions, this prominent anticyclonically rotating supercell persists, even when the low-level curvature in the hodograph favors right-moving supercells.

Student Notes:

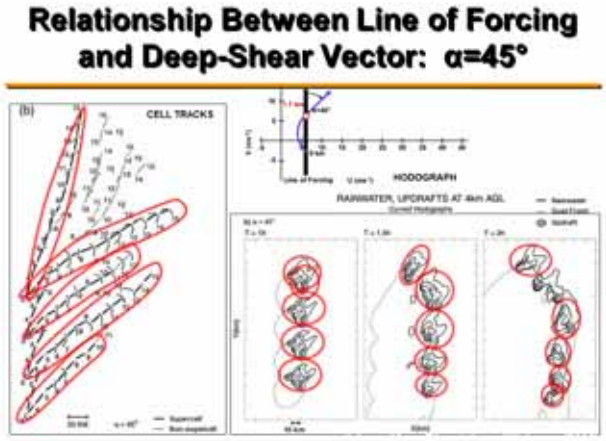

17. Relationship Between Line of Forcing and Deep-Shear Vector: α=0°

Instructor Notes: When the deep-layer vertical wind shear vector is parallel (α=0 degrees) to the line of forcing, the initial storms again split; however, in this case the anti-cyclonic left movers survive longer than the cyclonic right movers because the left movers are better able to keep up with the westward expanding cold pool, owing to the low-level hodograph curvature. The exception is the original isolated, cyclonically rotating, right-moving supercell which forms on the downshear side of the line of forcing. The strongest cells remaining after 2 hours are along the downshear (northern) side of the surface cold pool, including the original right and left movers from the initial splitting of the northernmost cell in the line, along with some newly developed ordinary cells in between.

Student Notes:

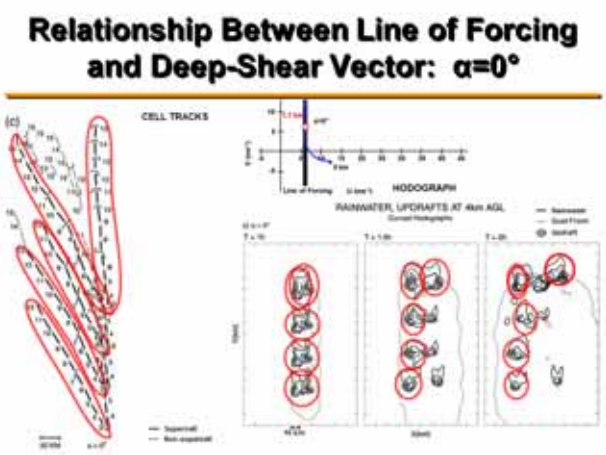

18. Relationship Between Line of Forcing and Deep-Shear Vector: α=135°

Instructor Notes: Finally, when the deep-layer vertical wind shear vector is 135 degrees from the line of forcing, the early evolution is similar to that for the case when the vector is 45 degrees (α=45 degrees), but rotated about the axis normal to the line of forcing. Neighboring left- and right-moving cells interact after 1 h, except at the ends of the line. However, after this time the system evolves into a multicellular squall line between the end cells. The southernmost cyclonic supercell is the strongest produced in any of the presented cases, with a quintessential hook and forward flank notch apparent by 1.5 h. This cell becomes increasingly separated from the rest of the convective system, remaining well defined past 2.5 h.

Student Notes:

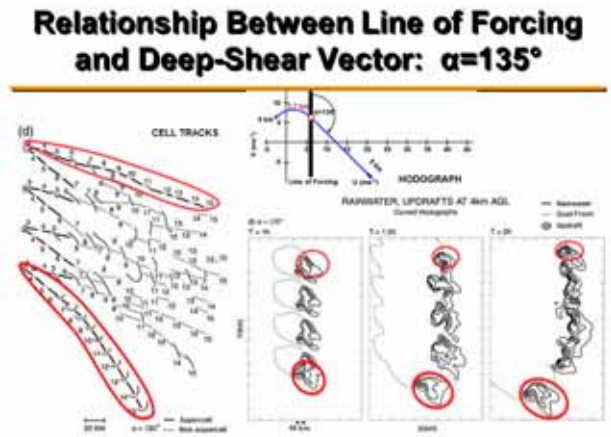

19. Short-Term Assessment (0-6 hr) “Nowcasting”

Instructor Notes: It is important to QC environmental data because using “bad” data can be an impediment to effective warning methodologies. Misinterpreted or inappropriate data can mislead the warning team. Most staffing strategies recommend a dedicated threat assessment forecaster, for this reason.

Student Notes:

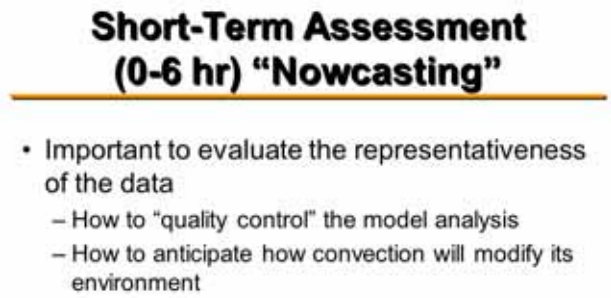

20. QC-ing Model Forecast HRRR April 30, 2012

Instructor Notes: Convection allowing forecast models tend to perform best when they have sufficient data to resolve critical features including boundaries, low-level moisture, and cap strength. The most useful and accurate forecast runs typically occur during and shortly after the mid-morning diurnal convective minimum, when 12z radiosonde and morning aircraft observations have been ingested, outflow boundaries have become quiescent, and diurnally-induced boundary layer mixing has revealed the true quantity and distribution of the low-level moisture. It's also important to note convection allowing model forecast accuracy tends to increase after about 3 hours into the run. COMET has created a module on the use of high-resolution models. For more information see the link included at the bottom of this slide.

Student Notes:

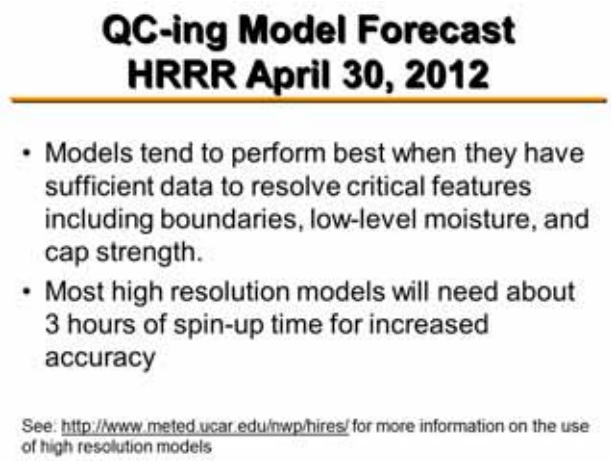

21. QC-ing Model Forecast HRRR April 30, 2012

Instructor Notes: Here are two High-Resolution Rapid Refresh (HRRR) model composite reflectivity forecasts for 02 UTC on April 30, 2012. The left image is the 15 hour forecast from the 11Z run, while the right image is the 12 hour forecast from the 14Z run. You can see that the 11Z run predicts relatively discrete cells from central Oklahoma into central and eastern Kansas and essentially no storms over north TX. However, the 14Z run predicts a line of storms along the OK/KS border with a few discrete cells ahead of it, along with another area of storms in north TX.

Student Notes:

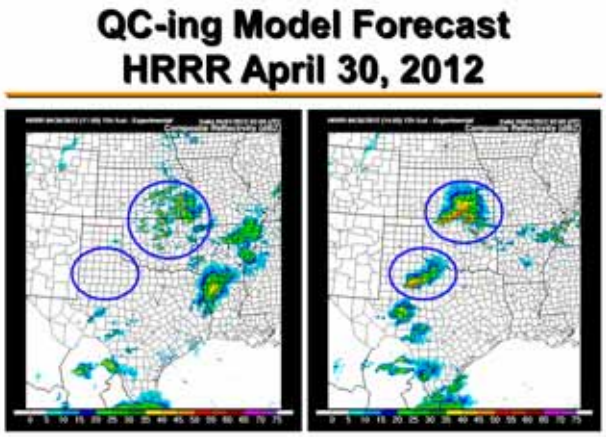

22. QC-ing Model Forecast HRRR April 30, 2012

Instructor Notes: Here is a loop of what actually happened on April 30, 2012. Note that the 14Z run, was able to pick up on several boundaries that affected convection in the southern TX panhandle as well as along the OK/KS border. Note also that BOTH model runs missed the squall line that moved across OK. This illustrates the point that model forecast reflectivity can give a good idea of storm timing and type, but should not be used to forecast the exact location of where convection will occur.

Student Notes:

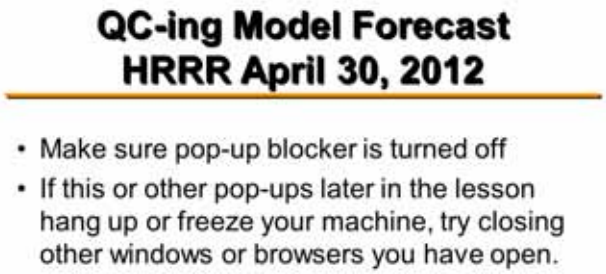

23. May 19, 2012 - Environment

Instructor Notes: Let's take a look at an example of short-term threat assessment. Note that this setup consisted of a cold front moving across central KS that arced to the west across the TX panhandle. Ahead of the front a corridor of 60+F dew points and CAPE of 2500-3000 J/Kg could be found.

Student Notes:

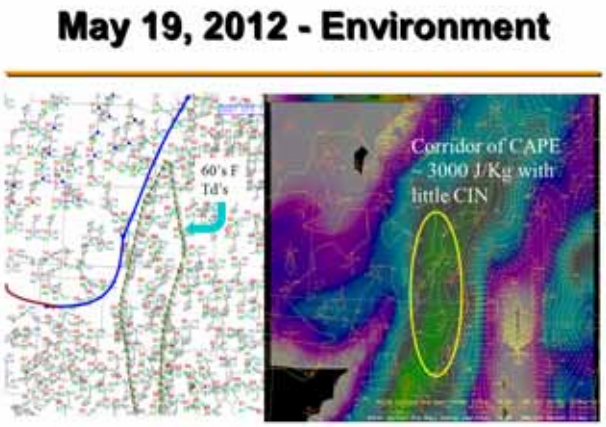

24. May 19, 2012 – Environment (Cont'd)

Instructor Notes: SPC meso-analysis suggested that storm-relative helicity (SRH) values were not favorable for supercells or tornadoes. However, strong surface vorticity was associated with the frontal boundary.

Student Notes:

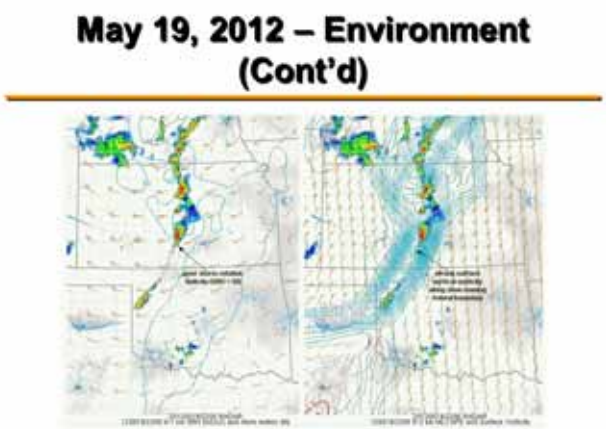

25. May 19, 2012 – Visible Satellite

Instructor Notes: The 1945Z visible satellite image indicated clouds associated with the front across west-central KS. By 2015Z, thunderstorms could be seen developing along the front.

Student Notes:

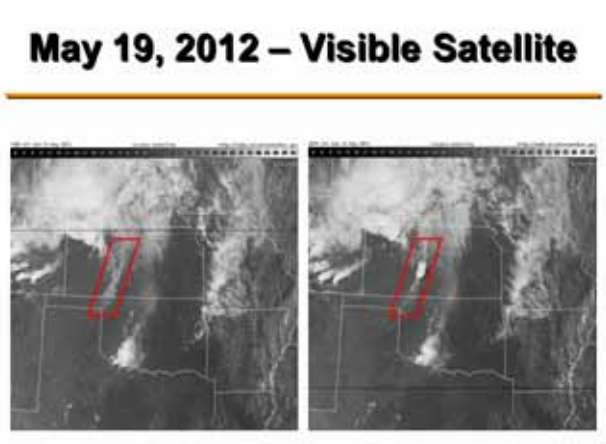

26. May 19, 2012 – Radar

Instructor Notes: Radar indicated the storms produced a south-southwestward moving outflow boundary that would play an important role in subsequent storms.

Student Notes:

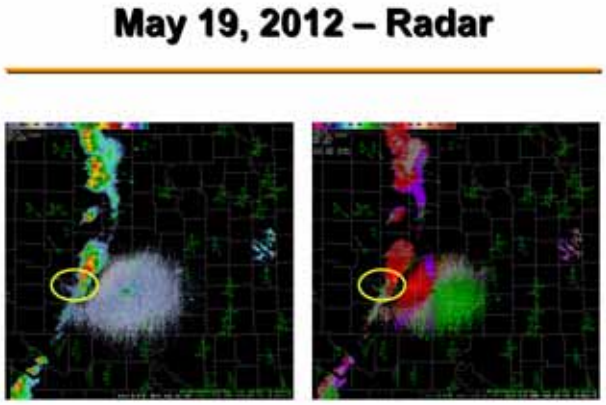

27. May 19, 2012 - KICT 0.5° Reflectivity Loop 2022-0059Z

Instructor Notes: Here's a 0.5 degree reflectivity/velocity loop of the event. Note each new storm which forms in the area of lift at the front-outflow boundary intersection quickly produces a small, tight-rotational couplet indicative of a tornado. A total of eight tornadoes were later surveyed. This event illustrates the importance of closely monitoring the mesoscale environment. You may play and pause this loop manually and advance to the next slide when ready.

Student Notes:

May 19, 2012 - KICT 0.5° Reflectivity Loop 2022-0059Z

28. Short-Term Threat Assessment Key Tasks

Instructor Notes: So now that we've discussed some of the things to look for in environmental threat assessment. Let's go through the short-term threat assessment process to put everything together. We'll examine a case from May 25, 2012. The first step is to examine the synoptic setting to see if there are any recognizable patterns.

Student Notes:

Short-Term Threat Assessment Key Tasks

- Examine synoptic setting for any recognizable patterns
- Evaluate environment to determine:

1. Location & timing of severe development
2. What convective mode to expect
3. Likelihood and intensity of specific threat (tornadoes, hail, etc.)
4. Evolution of threat (especially movement)

29. Threat Assessment Case Study

Instructor Notes: In this case study, we will play the role of a mesoscale analyst in the Dodge City, KS forecast office. An approximate outline of the CWA is noted on the images. Let's take a look at the large scale pattern to look for any easily recognizable synoptic patterns and sources of lift. At 21Z, at 300mb we note a strong jet stream stretching from Nevada, northeastward into northern Nebraska and the Dakotas with southwest flow aloft over the CWA. At 500mb we see a trough located out to the west of the CWA with southwest flow over the CWA. At 700mb, we see indications of an elevated-mixed layer capping inversion over the southern and central plains, including the CWA. At 850mb we see a warm front and dryline with southerly winds bringing warm, moist air into eastern portions of the CWA. The HPC Surface Analysis Chart confirms the existence of the boundaries with the east-to-west oriented warm front extending along the northern portions of the CWA and a dryline extending south-southwestward from the warm front into west Texas. This event doesn't really match any of our previously discussed severe weather patterns.

Student Notes:

30. Short-Term Threat Assessment Key Tasks

Instructor Notes: Our next step is to evaluate the environment to determine the expected location and timing of any severe storm development.

Student Notes:

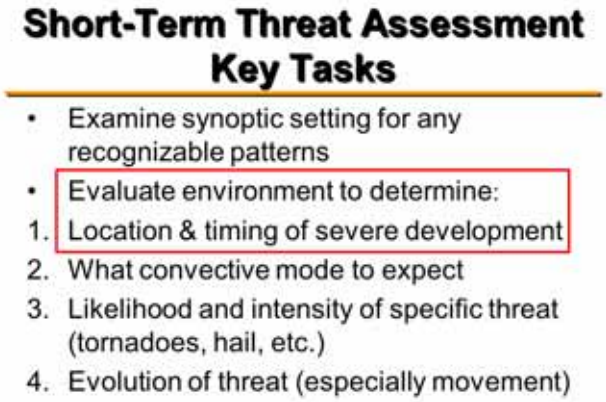

31. Surface Analysis

Instructor Notes: The HPC Surface Analysis Chart only provides synoptic-scale resolution and is insufficient for evaluating the mesoscale storm environment. The best way to evaluate the pre-storm environment is to hand analyze a current WFO-scale surface plot, making sure to include all synoptic and mesonet observations, cross-referenced with high-resolution satellite and radar data. A short example (minus surface pressure) is shown here. The warm front is located across the northern 1/3rd of the CWA and the dry-line extends south-southwestward from the warm front, dividing the CWA in half.

Student Notes:

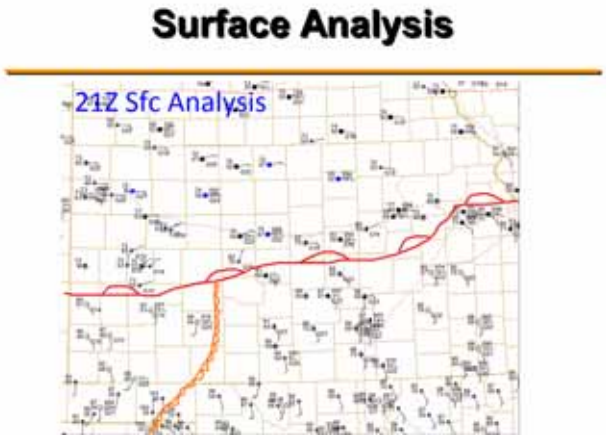

32. Satellite

Instructor Notes: High-resolution visible satellite imagery indicates the warm front/dry-line triple point is located in northeast Hodgeman County as denoted by the intersection of towering cumulus lines. The towering cumulus extends east-northeast in the zone of lift along the warm front into northern Barton County. The remainder of the warm fronts' position is well-demarcated by stable, stratus clouds north of the warm front versus capped, cumulus cloud streets south of it (ahead of the dryline). The high-based cumulus and towering cumulus demarcates the dryline extending from northeast Hodgeman County southwestward into eastern Ford County, but further southwest we must resort to surface obs and/or a radar fine line to denote its position. A subtle boundary denoted by enhanced cumulus clouds on satellite extended from southeast Ness County south-southeastward to eastern Comanche County and into Oklahoma. This boundary appeared to be a secondary (eastern) dryline, denoting the western edge of the deeper low-level moisture. This analysis presents us with three potential sources of lift for storm initiation: Area 1 along the dryline; area 2 along the secondary (eastern) dryline; and area 3 along the warm front near and east of the dryline triple point.

Student Notes:

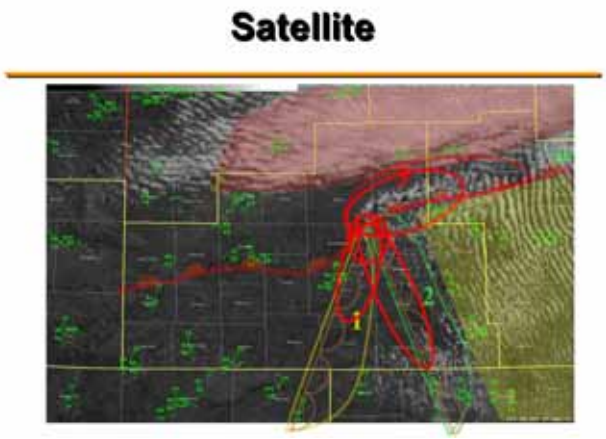

33. Radar

Instructor Notes: WSR-88D Reflectivity allows us to locate the boundary positions more precisely via fine lines, particularly the warm front. It's important to monitor the evolution of the boundaries for clues as to when and were convection will occur and what influence their position relative to the deep-layer shear vector will have on convective mode.

Student Notes:

Radar

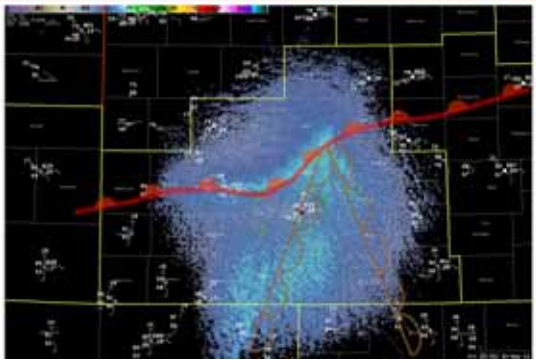

34. High-Resolution Models

Instructor Notes: It's also important at this point to evaluate short-term convective models and their trends to anticipate convective timing, location, storm type, and mode. Here is the 17Z HRRR forecast which was the latest version available as of 21Z. The model has the warm front a county or two too far south, but it forecasts a band of storms (some of which have supercell characteristics) to fire along the warm front from the dryline triple point eastward starting around 21-22Z.

Student Notes:

High-Resolution Models

- Convective models help to anticipate
  - Timing of convection
  - Location
  - Storm type
  - Mode

35. Location and Timing Summary

Instructor Notes: Combining the surface, satellite, and radar observations with the short-term model runs, it appears that area 1 has a chance of storms within the next 1 to 3 hours before diurnal cooling commences, but only if high-based updrafts don't wither due to entrainment issues in the hot, deeply-mixed airmass and shallow low-level moisture. Moisture is deeper along the secondary (eastern) dryline, and storms are possible, but only if lift is strong and deep enough to overcome the cap. This is unlikely due to satellite trends which reveal flat, capped, low-level cloud streets and a limited window for further diurnal heating. The most likely area for storms is area 3 from the secondary (eastern) dryline triple point eastward due to moderately-strong, sustained lift of a deep, moist airmass along the along the warm front. A band of enhanced towering cumulus eroding the cap gives us confidence that storms will eventually form, probably within the next 1-3 hours. The HRRR model adds confidence in this scenario.

Student Notes:

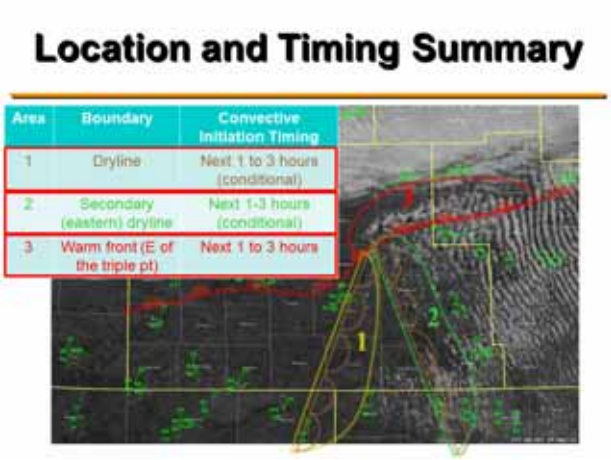

36. Short-Term Threat Assessment Key Tasks

Instructor Notes: The next step in the threat assessment process is to look for what convective mode to expect.

Student Notes:

Short-Term Threat Assessment Key Tasks

- Examine synoptic setting for any recognizable patterns
- Evaluate environment to determine:

1. Location & timing of severe development
2. What convective mode to expect
3. Likelihood and intensity of specific threat (tornadoes, hail, etc.)
4. Evolution of threat (especially movement)

37. Convective Mode

Instructor Notes: Next, we'll evaluate a RAP model analysis sounding that represents the convective environment in each of our three areas: Dodge City (DDC) for the dryline (area 1), Haviland (P#E) for the secondary (eastern) dryline (area 2), and Hays (HYS) for the warm front (area 3).

Student Notes:

Convective Mode

38. RAP DDC (1) Point Sounding

Instructor Notes: Here's the 21Z RAP analysis sounding for Dodge City (DDC). We can see that it is essentially along the dry line due to southerly low level winds, large temperature-dew point spreads, and a hot, deeply mixed airmass. MLCAPE is only 395 J/Kg with SBCAPE at 653 J/kg. Meanwhile, MLCIN is 97 J/Kg with SBCIN at 26 J/Kg. This suggests marginal, high-based storms are at least possible with a bit more surface heating. Effective bulk shear (EBS) is 38kts while the Supercell Composite Parameter (SCP) is only 0.4. 38kts of EBS is within the upper bounds for marginal supercell and the lower bounds for non-tornadic and weakly tornadic supercell. SCP is on the lower-bound potential for marginal supercells. Thus, from this environment we would expect any storms that develop to be ordinary (non-supercell) or marginal supercells.

Student Notes:

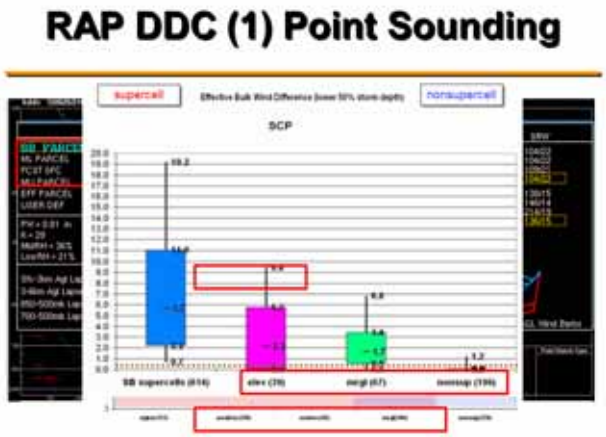

39. RAP P#E (2) Point Sounding

Instructor Notes: Here's the 21Z RAP analysis sounding for Haviland (P#E). Low-level moisture is richer and deeper here, but temperature-dew point spreads are still quite high at 31 degrees F. MLCAPE is 3444 J/Kg and SBCAPE is 3750 J/Kg; much higher than that at Dodge City. However, some CIN still remains with MLCIN at 42 J/Kg and SBCIN at 15 J/Kg. Effective bulk shear (EBS) is 37kts and the Supercell Composite Parameter (SCP) is 2.8. 37kts of EBS falls within the upper bounds for marginal supercells and the lower bounds for non-tornadic and weakly tornadic supercells. SCP of 2.8 fall within the upper bounds of marginal supercells and at the lower bounds of surface-based supercells. Thus, this environment suggests marginal supercell or supercell potential.

Student Notes:

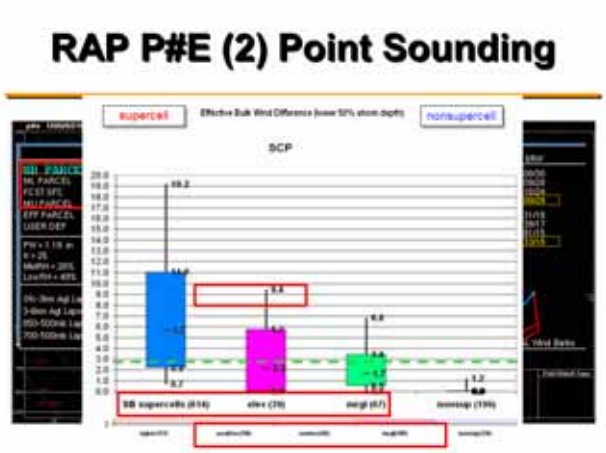

40. RAP HYS (3) Point Sounding

Instructor Notes: Here's the 21Z RAP analysis sounding for Hays (HYS). It's quite impressive for severe storms. MLCAPE is 3322 J/Kg with SBCAPE at 2927 J/Kg. MLCIN is still substantial at 32 J/Kg with SBCIN 75 J/Kg, but the saturated layer between 870-780mb suggests warm frontal lift is working to erode the cap. Recall that visible satellite imagery indicated a zone of clearing skies on the cool-side of the warm front which would allow continued diurnal heating and destabilization to occur. Effective Bulk shear (EBS) is 72 kts and the Supercell Composite Parameter is 35.3. 72kts of EBS is well above the upper bounds of the box and whiskers plot for tornadic supercell storms and a SCP of 35.3 is off the chart for surface-based supercells. A long, clock-wise curved hodograph lends confidence to this evaluation. Thus, tornadic supercells appear likely assuming the cap can be broken and surface-based storms occur. Recall that current satellite indications of a band of enhanced towering cumulus suggest convective initiation is likely.

Student Notes:

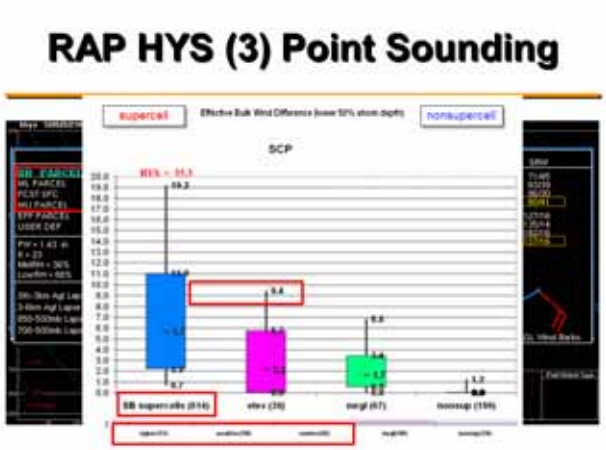

41. Convective Mode Summary

Instructor Notes: After examining the data, area 1 suggests ordinary or marginal supercell storm modes, area 2 suggests marginal supercell or supercells, while area 3 supports supercell storm modes.

Student Notes:

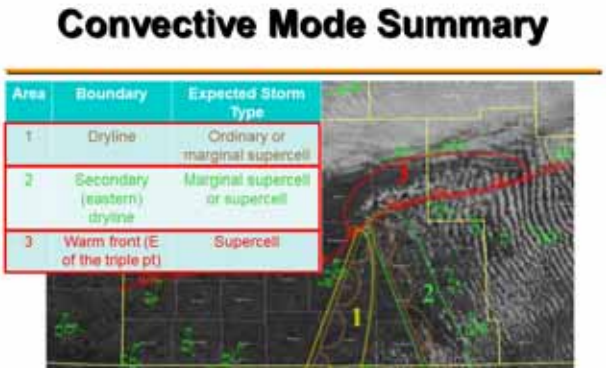

42. Short-Term Threat Assessment Key Tasks

Instructor Notes: The next step in threat assessment is to determine the likelihood and expected intensity of each specific threat.

Student Notes:

Short-Term Threat Assessment Key Tasks

- Examine synoptic setting for any recognizable patterns
- Evaluate environment to determine:

1. Location & timing of severe development
2. What convective mode to expect
3. Likelihood and intensity of specific threat (tornadoes, hail, etc.)
4. Evolution of threat (especially movement)

43. Tornado Threat Assessment

Instructor Notes: Here is a list of the most important tornado forecast parameters. These are: Mixed Layer CAPE (MLCAPE), Mixed Layer CIN (MLCIN), LCL Heights, 0-1km Bulk Shear, Effective Storm Relative Helicity (ESRH), Effective Bulk Shear (EBS), The Non-Supercell Tornado Parameter (NST, if you're not expecting supercells) and the Effective Significant Tornado Parameter (ESTP). For more information on any of these parameters, you may click on the parameter of interest.

Student Notes:

Tornado Threat Assessment

- MLCAPE
- MLCIN
- LCL Heights
- 0-1km Bulk Shear
- Effective SRH (ESRH)
- Effective Bulk Shear (EBS)
- Non-Supercell Tornado Paramter (NST)
- Effective Significant Tornado Parameter (ESTP)

44. Hail Threat Assessment

Instructor Notes: Hail forecasting is an immature science, ripe for further research. However, when assessing the threat for severe (greater than or equal to 1” in diameter) hail, three parameters are thought to have some operational utility: Steep mid-level lapse rates, CAPE in the Hail Growth Zone, and the Significant Hail Parameter (SHIP). By “steep,” we mean severe hail potential increases as mid-level lapse rates approach dry adiabatic (approximately 9.8 C/km). The ingredients for calculating SHIP are: Most Unstable CAPE, the mixing ratio of the most unstable parcel, the 700-500mb lapse rate, the 500 mb temperature, and the 0-6km effective bulk shear. SHIP values greater than one indicate a favorable environment for significant (greater than or equal to 2” diameter) hail. For more information on any of these parameters, you may click on the parameter of interest.

Student Notes:

Hail Threat Assessment

- Steep, mid-level Lapse Rates
- CAPE in the -10 to -30C layer (Hail Growth Zone)
- Significant Hail Parameter (SHIP)

SHIP = [(MUCAPE j/kg) * (Mixing Ratio of MU PARCEL g/kg) * (700-500mb LAPSE RATE c/km) * (-500mb TEMP C) * (0-6km Effective Shear m/s)] / 44,000,000

45. Wind Threat Assessment

Instructor Notes: Here's a list of the most important parameters to evaluate when assessing the severe wind threat: Steep Lapse Rates below the LCL, minimal surface based CIN (SBCIN), large amounts of DCAPE, sufficient CAPE to support a storm, and strong vertical shear (enough that a supercell may produce a low level mesocyclone). For more information you may click on the particular parameter of interest.

Student Notes:

46. Tornado Threat Assessment

Instructor Notes: Let's first assess the tornado threat. The box and whiskers diagrams on this slide and the next are from Thompson et. al 2012. The top left is MLCAPE, the top left is MLCIN, bottom left is MLLCL, and bottom right effective bulk shear. The values for each parameter at Dodge City (dotted yellow line labled "DDC"), Haviland (dashed green line labeled "P#E"), and Hays (solid red line labeled "HYS") have been overlaid. Notice Hays appears to have the highest tornado threat due to the combination of High MLCAPE, moderate but not insurmountable amount of CIN, low LCLs and High EBS.

Student Notes:

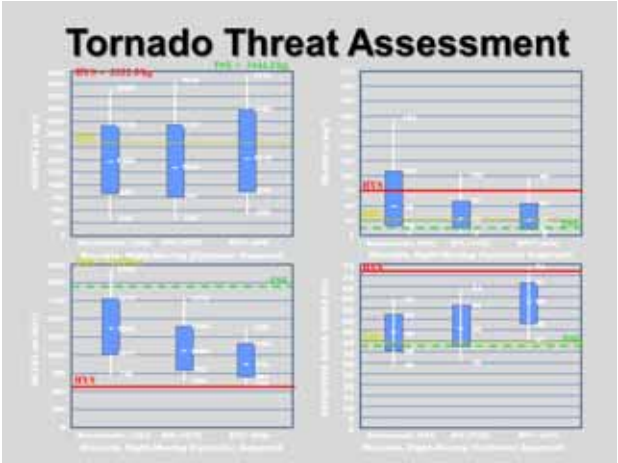

47. Tornado Threat Assessment

Instructor Notes: On this slide 0-1km bulk shear is on the top left, effective storm-relative helicity (SRH) is top right, and effective layer significant tornado parameter (STP) is in the bottom two figures. These parameters emphasize the enhanced tornado threat already present at Hays as of 21z. These parameters are likely to increase at Hays during the evening as the nocturnal low-level jet commences.

Student Notes:

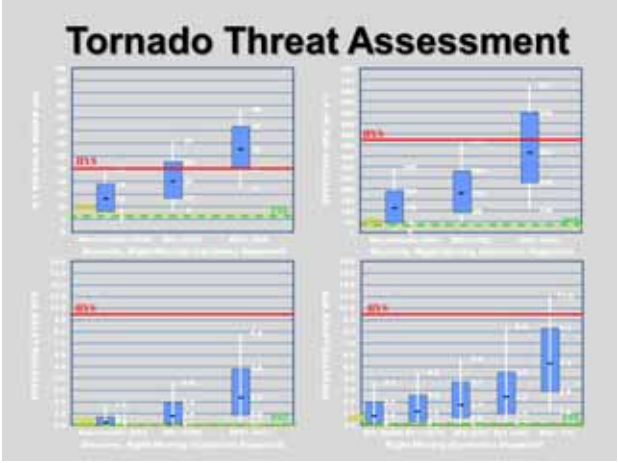

48. Hail Threat Assessment

Instructor Notes: An assessment of our hail forecast parameters suggest a threat of severe hail at both Hays (HYS) and Haviland (P#E) (given a storm). 700-500mb lapse rates are quite similar at all sounding locations; not quite dry adiabatic (~9.8 degrees C/km), but rather steep nonetheless. However, SHIP values are supportive of significant (greater than or equal to 2” diameter) hail at both Hays and Haviland, but near zero at Dodge City (DDC). CAPE in the -10° to -30°C layer (not show) was quite large at both Hays and Haviland, but rather small at Dodge City.

Student Notes:

49. Wind Threat Assessment

Instructor Notes: Finally, an assessment of the wind parameters indicates the environment is favorable for severe wind at all three sounding locations.

Student Notes:

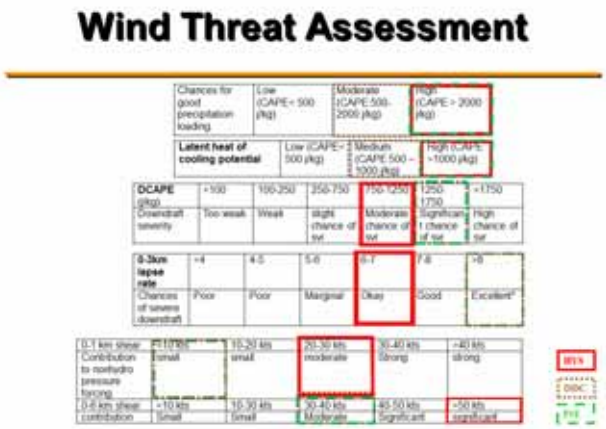

50. Hazard Assessment Summary

Instructor Notes: Our hazard assessment threat is summarized in these tables. Of course, these threats are conditional on storms developing.

Student Notes:

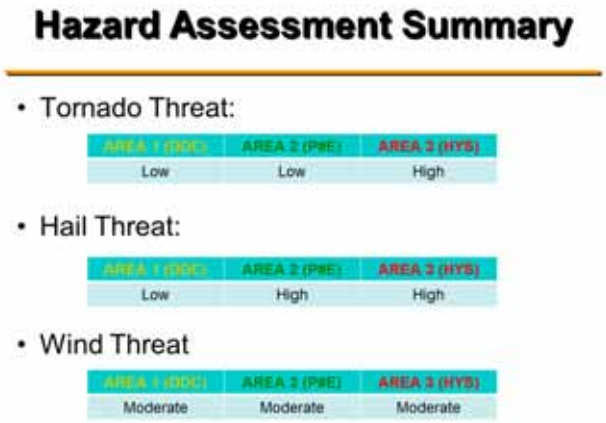

51. Short-Term Threat Assessment Key Tasks

Instructor Notes: The last step in the threat assessment process takes us to evaluating the expected evolution of the threat (including the expected storm motion).

Student Notes:

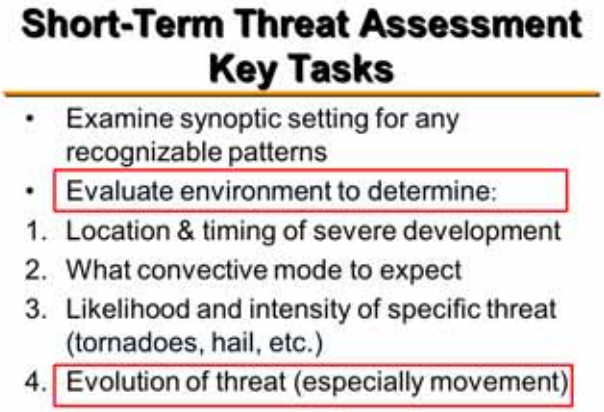

52. Expected Storm Motion DDC (1)

Instructor Notes: The 21Z RAP model analysis hodograph from Dodge City (DDC) indicates the mean wind (MW) is from 231 degrees at 45 knots, the right-moving (RM) supercell motion is expected to be from 241 degrees at 27 knots, and the left-moving (LM) supercell motion is expected to be from 193 degrees at 39 knots. The hodograph is mostly straight which would favor neither the right or left-movers. This information can also be found in the sounding analysis table, where the LCL-EL (Cloud Layer) provides the expected mean storm motion, shown here to be 230 degrees at 45 knots. The bunkers right and left-moving storm motions are also indicated. Eye-balling the hodograph, the effective bulk shear vector (denoted by a vector drawn from “0” to halfway up to the “EL”) is towards the northeast and the table indicates its magnitude (“Lower Half Storm Depth”) is 38 knots.

Student Notes:

53. Expected Storm Motion P#E (2)

Instructor Notes: The 21Z RAP model analysis hodograph from Haviland (P#E), indicates the mean wind (MW) is from 224 degrees at 40 knots, the right-moving (RM) supercell motion is expected to be from 236 degrees at 22 knots, and the left-moving (LM) supercell motion is expected to be from 191 degrees at 40 knots. The hodograph was roughly straight which appears to favor neither right or left-movers. This information can also be found in the sounding analysis table, where the LCL-EL (Cloud Layer) provides the expected mean storm motion, shown here to be 224 degrees at 38 knots. The bunkers right and left-moving storm motions are also indicated. The effective bulk shear vector is towards the east-northeast at 37 knots.

Student Notes:

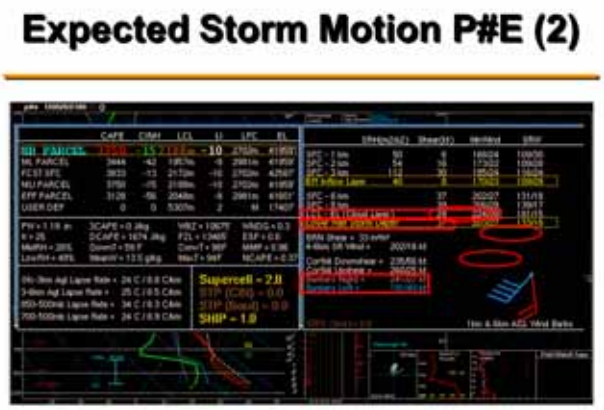

54. Expected Storm Motion HYS (3)

Instructor Notes: Finally, the 21Z RAP model analysis hodograph from Hays (HYS) indicates the mean wind (MW) is from 219 degrees at 37 knots, the right-moving (RM) supercell motion is expected to be from 241 degrees at 27 knots, and the left-moving (LM) supercell motion is expected to be from 192 degrees at 39 knots. The hodograph exhibits strong clock-wise curvature which would strongly favor right movers. This information can also be found in the sounding analysis table, where the LCL-EL (Cloud Layer) provides the expected mean storm motion, shown here to be 219 degrees at 38 knots. The bunkers right and left-moving storm motions are also indicated. The effective bulk shear vector is towards the northeast at 72 knots.

Student Notes:

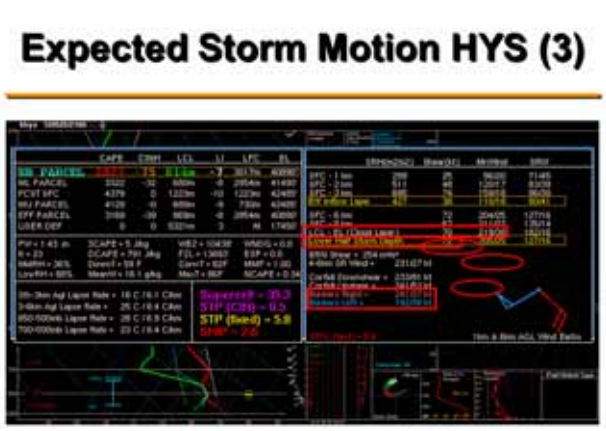

55. Storm Evolution

Instructor Notes: In this image we overlay the effective bulk shear vector from each sounding location on top of the boundaries. Recall from earlier in this lesson (and DLOC modules) that the deep layer shear vector orientation relative to the forcing mechanism (boundary) can help predict storm evolution (particularly when the shear is strong). The effective bulk shear vector at Dodge City (DDC) is at a 45 degree angle to the dryline and the hodograph was nearly straight which suggests that, with the exception of the northernmost storm, the left-moving members will move across the outflow boundary generated by their right-moving neighbor to the north, and weaken in the hot, deeply mixed air behind the dryline, while the right-moving members will move away from the boundary and may not collide with their neighbors. Meanwhile, the effective bulk shear vector at Haviland (P#E) is at a 90 degree angle relative to the secondary (eastern) dryline and the hodograph was mostly straight which suggests that a series of left-moving and right-moving storms would be generated; the right-moving storms would collide with the left-moving storms to their south; only the southernmost right-moving and northernmost left-moving storms would likely not interact with their neighbors. Finally, the effective bulk shear vector at Hays (HYS) is nearly parallel (a 0 degree angle) relative to the warm front, which suggests if we had a straight hodograph that the anticyclonic left movers would survive longer than the cyclonic right movers because the left movers would be better able to keep up with the expanding cold pool. The exception would be the original isolated, cyclonically rotating, right-moving supercell which forms on the downshear side of the line of forcing. If the storms develop into an MCS, the environment favors the difficult to maintain parallel stratiform (PS) subtype you learned about in DLOC. However, since the hodograph was strongly clockwise-curved we expect that left-moving storms would die off and any left-moving non-supercells will be facing an environment with increasing CIN the further they move into that environment and would also expect to die off.

Student Notes:

56. Threat Evolution

Instructor Notes: Now we look at some 21Z RAP40 model output to see how the environment is expected to change over the next 6 hours. SBCAPE is overlaid as an image with SBCIN contoured in black. The 0-1 shear is shown in yellow (south wind vector) and the 0-6 shear (the west and southwest wind vector) is shown in beige. At 21Z we see that the dry-line appears to be weakly capped with a somewhat stronger cap along the secondary (eastern) dryline. Along the warm front we see an area of weak SBCIN along Ness and Rush counties which when combined with the towering cumulus on satellite give us indications that the warm front may see development first. At 23Z the RAP40 predicts the warm front to move slightly northward with a general increase in SBCAPE, but stronger SBCIN. We also note that the 0-1 shear is predicted to increase along the warm front. With the dry lines starting to retreat, it's important to note that the forcing along it will be much weaker and we can expect reduced chances for storms to initiate along them. At 01Z, the RAP40 predicts the warm front to become stationary, the dry line to continue to retreat westward, and the secondary (eastern) dryline to have dissipated. With the loss of heating, SBCIN will continue to increase so any new surface-based initiation is unlikely. 0-1 km shear will continue to increase with values of 35-40 kts along the warm front very supportive of mesocyclonic tornadoes. Finally, at 03Z, the RAP40 predicts both the front and dryline to remain stationary. SBCIN will be quite strong suggesting only pre-existing supercells and/or elevated storms north of the warm front would be able to survive.

Student Notes:

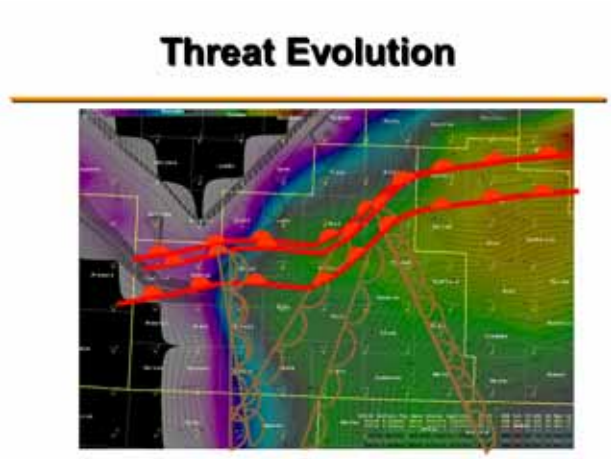

57. Event Summary

Instructor Notes: So what actually happened? Here's a loop of the reflectivity and velocity. We can see that storms fired along the warm front around 2230Z , then began to congeal and form a cold pool behind the initial northern supercell that developed over eastern Ellis county at 2330 and moved into Russell County in the Wichita CWA. This is what we expected based on the study by Blustein and Weisman, 2000. However, as CIN increased the multicellular storms were suppressed and we were left with a line of discrete supercells. A few high-based thunderstorms formed along the dryline between 23-00Z, but they eventually dissipated due to the hot, deeply-mixed airmass and shallow moisture ahead of the dryline. No storms formed along the secondary (eastern) dryline due to weak lift and strong capping.

Student Notes:

58. Event Summary

Instructor Notes: Here's a map showing the SPC storm reports received from this event. You can see that all the severe weather occurred along the warm front in the northern portions of the CWA. Zooming in, we can see a number of hail reports as well as a large number of tornado reports. According to Storm Data, there were 14 tornadoes surveyed with this event, a large number of them were brief but there were three EF-2 tornadoes including one that traveled almost 10 miles with a maximum width of about 10 football fields (950 yds). Additionally there were a number of large hail reports with the largest hail reported to be golf ball size. No severe wind reports were received. Here are a few pictures of the tornadoes that occurred with this event, the first was taken at around 2345Z in eastern Ellis County. The second picture was taken at 02Z from central Rush County.

Student Notes:

59. Lesson 2 Summary

Instructor Notes: In summary, it's important to perform threat assessment as a routine part of your warning methodology as it will help to determine what storm interrogation procedures to perform. It's important to analyze and monitor the mesoscale environment in which storms are expected to develop. Finally it's important to monitor the quality of the environmental data and be able to recognize observations and model data that doesn't make sense with the surrounding environment. You have now completed lesson 2, when you are ready, advance to the next slide to take the exam.

Student Notes:

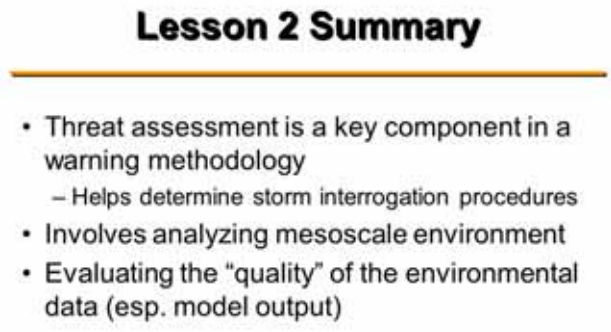

60. Quiz1

Instructor Notes:

Student Notes:

61. Questions?

Instructor Notes: Have a question? Feel free to contact us at awocsevere_list@wdtb.noaa.gov.

Student Notes:

1. Threat Assessment of Quasi-Linear Convective Systems

Instructor Notes: Welcome to a brand new lesson in the AWOC Severe Track. This lesson is on environmental threat assessment of Quasi-Linear Convective Systems (or QLCS). It is Lesson 3 of Instructional Component 2 in the AWOC Severe Track. My name is Brad Grant, Team Leader of the Warning Decision Training Branch. I will be narrating this lesson along with the other meteorologists listed on this slide, who have been the primary content collaborators for this lesson.

Student Notes:

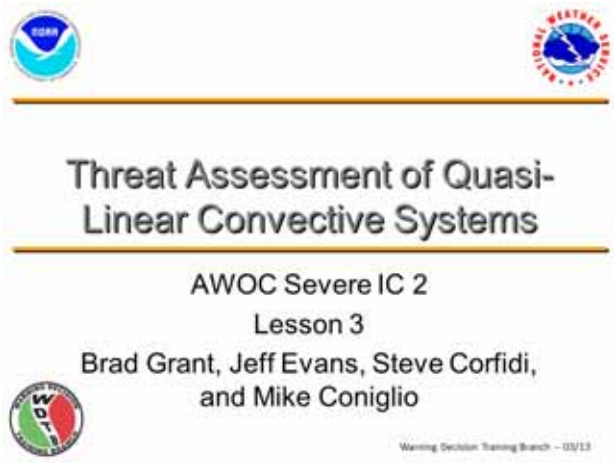

2. Rationale

Instructor Notes: So, why do we need to learn about QLCS Events? The answer is that many long-lived multicell convective systems have a propensity to take lives and damage property with high winds, hail, and tornadoes. Damage often occurs over a broad swath encompassing multiple county warning areas. Danger to public in these situation is obvious and often more extreme, impact-wise, than a single tornado storm. Challenges for a warning forecaster on the threat assessment level include: Recognition of the intensity of these type of events Determination of duration and movement, and Determination of all the threats associated with these type of events. In this lesson, which is a companion to the storm interrogation module in IC Severe 3 on recognition and detection of QLCS storm-scale features, we are going to treat many of these challenges associated with forecasting QLCS events.

Student Notes:

3. What is the Link to Warnings?

Instructor Notes: When individual forecasters analyze the root cause for missed tornado events, like this chart from AWOC Core (2004-05), one of the reasons frequently cited for missing events is the lack of a perceived threat. This can be a result of a number of things, including aspects of environmental analysis, or a failure of a conceptual model. In the case of QLCS events, the ability to use a correct conceptual model to recognize threats typically associated with the events is a big part of successful threat assessment.

Student Notes:

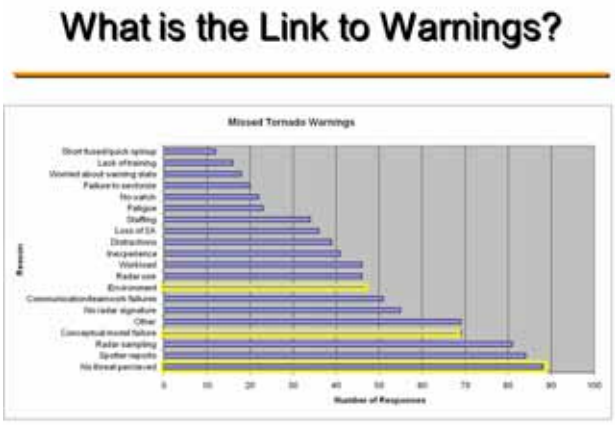

4. Learning Objectives

Instructor Notes: For this lesson on threat assessment of QLCS events, we have identified 6 learning objectives, as listed in the speaker notes: Identify some of the key features found in conceptual models of QLCS events. Identify the types of QLCS events that produce the most intense impacts. Identify parameters for evaluating the severity of QLCS events. Identify discrimination capabilities of parameters used in forecasting QLCS events. Identify patterns/parameters that affect longevity of a QLCS. Determine motion of a QLCS (both forward propagating and backward).

Student Notes:

5. What are the Recognizable Physical Features?

Instructor Notes: An understanding of the primary features and associated physical processes of some of the well-accepted conceptual models of long-lived multicell convective systems is essential to evaluating QLCS environmental threats. Most of the physical features listed here have been identified in various conceptual models. Well-known radar features like the Bow Echo and Rear Inflow Jet have been described in previous training lessons such as DLOC Topic 7 Lessons 12 and 13. If you haven't taken these modules in a while, it would be worth your time as these features are discussed in more detail.

Student Notes:

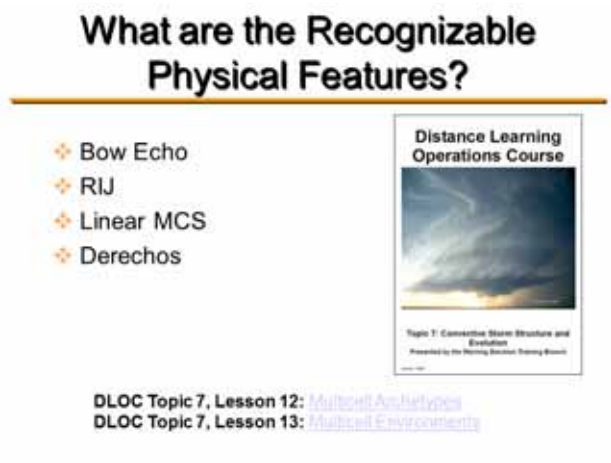

6. Conceptual Model #1

Instructor Notes: Conceptual models of quasi-linear convective systems span several years. One of the earliest models was Fujita (1978), who defined the evolutionary stages of convective development from conventional radar signatures as in the image shown on this slide. There was an initial large, strong echo which developed into a bow echo with cyclonic and anticyclonic rotation , and then into a comma shaped echo. The bulging portion of the line of echoes was termed a “bow echo” , which he said was produced by thunderstorm downburst winds. Fujita also noted cyclonic and anticyclonic circulations at the ends of the bowing segments. Later bow echo researchers such as Weisman (1993) referred to these counter rotating circulations as “bookend vortices.” This early conceptual model fit well with other models on squall line type bow echoes and presented that the bow echo bulge was associated with a strong rear-inflow jet. There was also important work conducted on discriminating the location of tornadoes with bow echoes (black dots in this figure).

Student Notes:

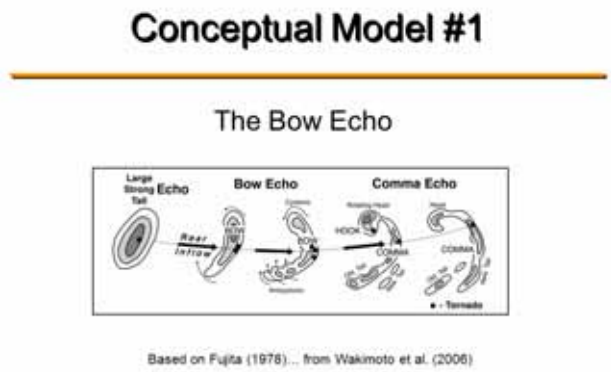

7. Conceptual Model #2

Instructor Notes: Smull and Houze, as well as other researchers, examined a number of squall lines using radar data and concluded that the bulge and associated concavity seen in Fujita's bow echo was directly related to the rear-inflow jet. How did the RIJ form the bow echo? By doing two things: 1) advecting part of the squall line forward and 2) entraining dry air into the rear flank which then erodes the back side of the echo through evaporation of hydrometeors. They developed a complex conceptual model of a mature squall line within a Mesoscale Convective System (or MCS) that included a large anvil and a cold pool that modulated the pressure field from the surface to upper levels. The development of the RIJ was attributed to midlevel, mesoscale areas of low pressure (labeled L3 & L4). The RIJ transported strong buoyant ambient air to the anvil. The mesolow "L3", formed immediately behind the leading line convection, was a hydrostatically-induced negative pressure perturbation that develops under up- shear tilted warm convective updrafts and above the attendant cooled downdrafts. Midlevel mesolow "L4" forms in the stratiform region in between the warm buoyant air which gets pulled rearward past the cool, dry descending air flow. Note that there are can be significant differences in the evolution of multicell systems based on the strength of the cold pool, ambient shear, and attendant RIJ. But one thing appeared to be clear, the RIJ could push descending air all the way to the front of the leading line in the most extreme, long lasting situations. As more details emerged from examining the thermodynamic structure within a mature mesoscale convective system containing a squall line, the focus in research switched to numerical simulations and the role of the cold pool and ambient shear.

Student Notes:

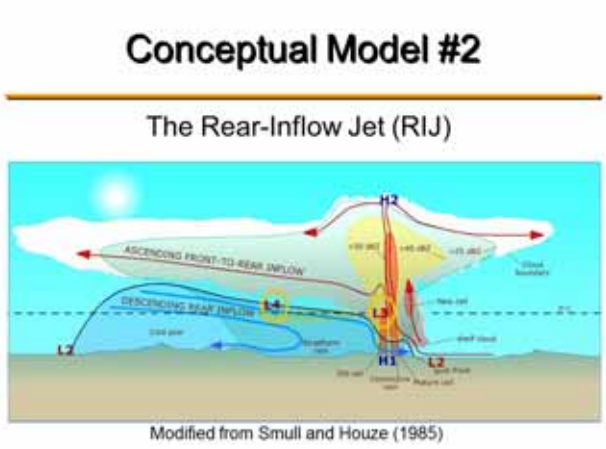

8. Conceptual Model #3

Instructor Notes: Modeling studies by Weisman suggested that shear in the lowest 2.5 km and the strength of the cold pool controlled the orientation of the rear-inflow jet . A typical transition shows ideally what takes from an initial surface based convective element to a multicell. Discrete multicellular convection initiates from forcing, and slowly generates a cold pool that builds in strength over time. Multicell forcing may be dominated by either external forcing or updraft induced dynamic pressure gradients. Eventually the cold pool may take control of the multicell including both the initial forcing and its embedded updraft forcing. How long it takes for the cold pool to dominate matters depends on how strong the cold pool becomes compared to the vertical wind shear and the strength and orientation of the initial forcing.

Student Notes:

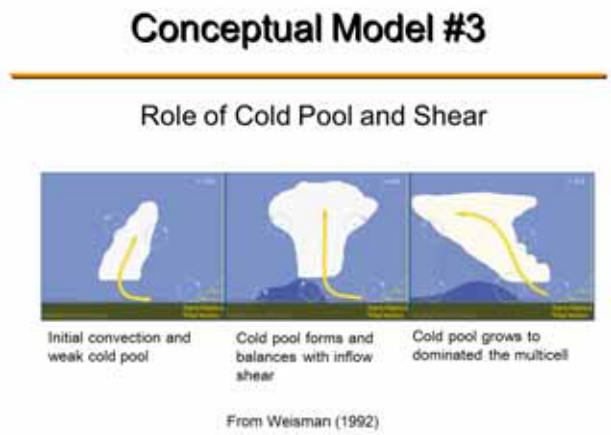

9. Conceptual Model #4

Instructor Notes: One of the most recent conceptual models of MCS and how they develop are from Parker and Johnson (2000). Although MCSs develop a number of ways, typical mature systems contain convective and stratiform precipitation regions. The eventual MCS type is determined to a large extent by the environmental conditions in which it develops and the strength of the system cold pool. Parker and Johnson studied numerous MCSs and determined the distribution of hydrometeors and stratiform precipitation shapes were largely a result of mean storm-relative winds. The speed and direction of the environmental mid- and upper-level winds relative to system motion affect the resulting evolution of the MCS. According to their studies, Parker and Johnson (2000) found MCS squall lines evolve into three major archetypes (shown in their modified figure from top to bottom): 1) Leading Stratiform, 2) Parallel Stratiform, and 3) Trailing Stratiform. The main distinction arose from storm-relative flow fields. For more details on these three multicell archetypes, please refer back to Lesson 12 of DLOC Topic 7. More recent conceptual models of QLCS events, especially on the storm scale, will be presented in parts of AWOC IC Severe 3: Storm Interrogations.

Student Notes:

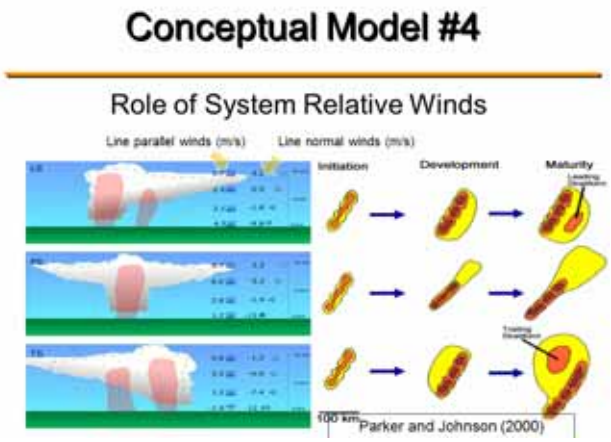

10. Linear MCS Archetypes Examples

Instructor Notes: This figure shows an example of all three archetypes occurring simultaneously ahead of an ejecting strong upper-level shortwave trough. Each MCS formed from a different boundary. The TS formed on a stationary front north of the surface low, the PS formed on a dryline, and the LS formed on what may have been a residual outflow boundary with the cooler air to the east (French and Parker, 2006).

Student Notes:

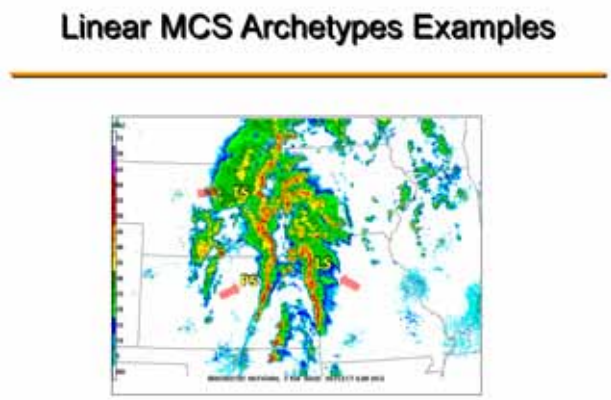

11. Threats from Various Types

Instructor Notes: While we can to some degree distinguish (after the fact) environments and radar morphologies of resulting QLCS events, an important point is that ALL types can produce severe weather . This graph from a study by Gallus et al. shows the percentage of storms with at least one severe report (not including flooding), organized by morphology. The morphology TS, LS, and PS are similar to Parker and Johnson's notation. BE is for Bow Echoes. The numbers of events of each type are shown beneath the morphology codes.

Student Notes:

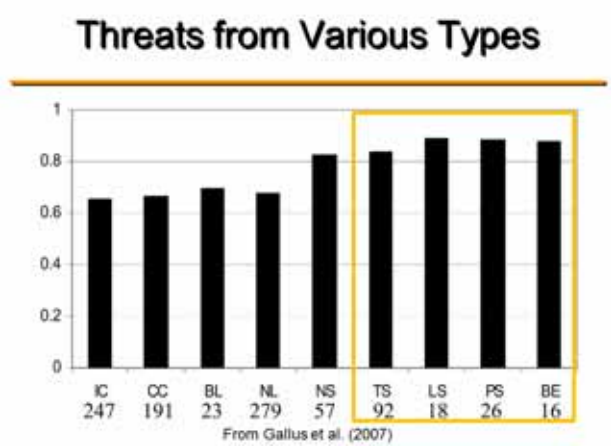

12. Can We Discriminate Intensity of QLCS Events?

Instructor Notes: To identify the types of QLCSs that produce the most intense impacts, you must evaluate forcing, shear (at low, mid- and upper-levels), CAPE, especially in the region supporting updraft parcels, and especially, the potential for downwind cell propagation.

Student Notes:

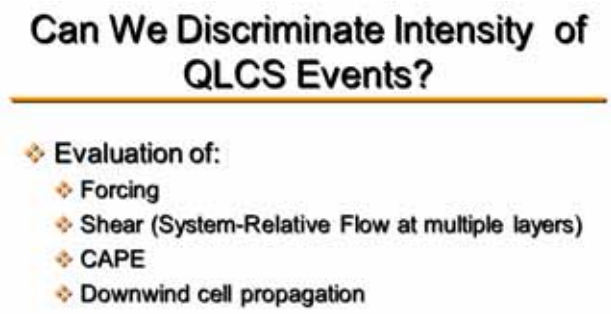

13. Role of Forcing and Orientation

Instructor Notes: Large multicells are more apt to exhibit a linear nature to them reflecting the elongated lifting that commonly occurs along external forcing mechanisms (e.g., fronts), and internally generated cold pool boundaries. Fronts offer a linear nature to forcing, however multicells may not merge into a long line if the forcing is weak. If the deep layer shear is largely boundary-parallel (such as the left-most evolutions) individual cold pools may more easily merge, reinforce the front, and enhance upscale growth into a long line. In terms of forcing, the next image is a similar depiction showing the initiation of storms in two different flow regimes relative to a boundary. The dark arrows represent the mean cloud-layer wind and shear vector orientations, the shading represents precipitation regions, the dotted lines are convective outflow and the hatched areas indicate where new development is likely as convective outflows merge (from Dial and Racy, 2009). Once again, the most intense QLCSs likely develop from the orientation shown on the left. Note that both of these results are most relevant in situations along well defined, linear boundaries and most appropriate during the developing stages of the QLCS.

Student Notes:

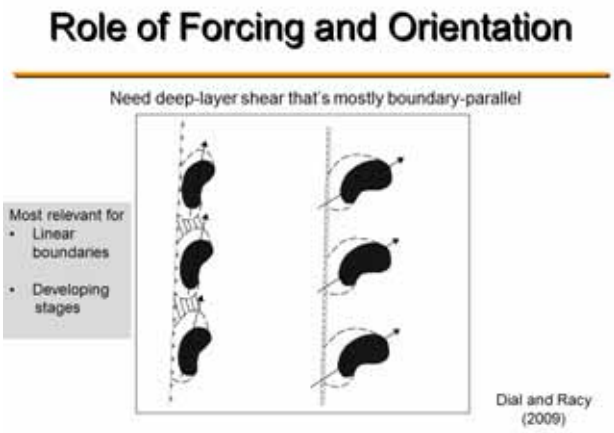

14. Role of Shear

Instructor Notes: This plot of composite hodographs from Evans and Doswell (2002) illustrates differences in mean wind profiles associated with derechos (dashed lines) and discrete supercells (solid lines). The hodographs were created from proximity soundings near 65 derechos, stratified by synoptic-scale forcing strength, and 100 supercells divided into: non-tornadic, F0-F1 tornadoes, and those producing F2 or greater tornadoes. The differences in these mean hodographs indicate that shear plays a very important role in helping determine the organization potential and any ensuing severe threats. The SF derechos (dark blue dashed line) occur in stronger flow and shear than the other derecho categories, while the WF Derechos (red dashed line) commonly occur in weaker shear environments. In addition, the mean WF derecho hodographs indicate weaker and more uniform nwly flow at mid and upper levels. In comparison, the significant tornadic supercells (lt. blue solid line) have much longer hodographs and more substantial low and deep layer shear. However, it important to note the similarities between the SF derecho and tornadic supercells mean wind profiles. In fact, the SF derecho average falls well within the range of shear magnitudes and hodograph structure associated with discrete supercells producing significant supercells! Shear, though a necessary ingredient, will not provide ample forecasting clues regarding the impending mode of expected thunderstorms. It is very important to consider the nature of initiation and storm motion/speed relative to the initiating boundary when dealing with events in strong synoptic-scale forcing.

Student Notes:

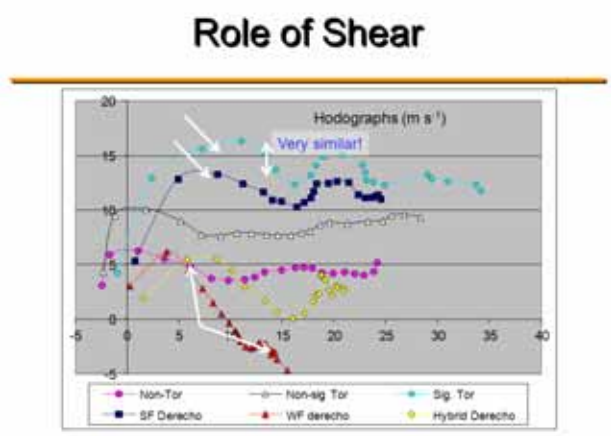

15. Can We Discriminate Intensity of Events?

Instructor Notes: To address the question of distinguishing run-of-the-mill MCSs from high-end events, the figure shown is a graphic of mean MCS-relative hodographs from a proximity sounding data set of 55 weak MCSs (shown in blue), 78 severe but non-derecho MCSs (show in red), and 51 derecho MCSs (shown in light green) that were taken in the downshear environment during the developing stages of the systems. This analysis is based on the data set described in Cohen et al. (2007) in W&F. The mean hodograph clearly shows that shear becomes more stretched and straight-line along the x-axis (MCS-motion) as you go from the weak MCSs to the derecho MCSs (the colored numbers along the hodographs are kilometers Above Ground Level (AGL)). You can also see the huge increase in low-level storm-relative inflow for the derecho MCSs.

Student Notes:

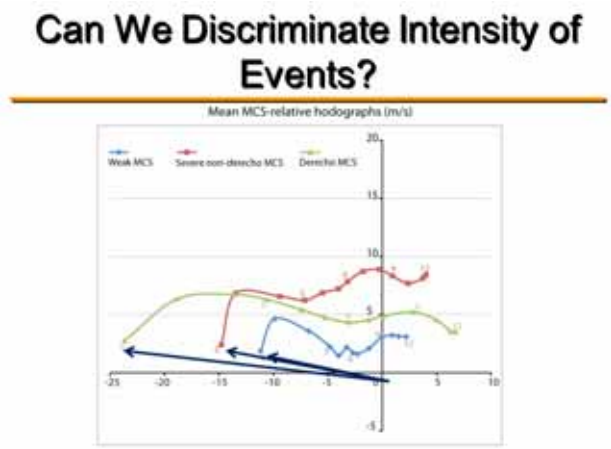

16. Role of CAPE

Instructor Notes: The role of convective instability is multifaceted. Not only is sufficient CAPE necessary to maintain intense updrafts along the leading edge of the cold pool, but the larger the CAPE the more intense the updrafts and resultant supply of moisture and energy to the overall MCS. This in turn increases the subsequent downdrafts and strengthens or at least maintains the cold pool momentum. If CAPE weakens or the outflow surges into an environment of little or no CAPE and/or significant convective inhibition, then the convective system would quickly lose its energy source and diminish-sometimes quite quickly.

Student Notes:

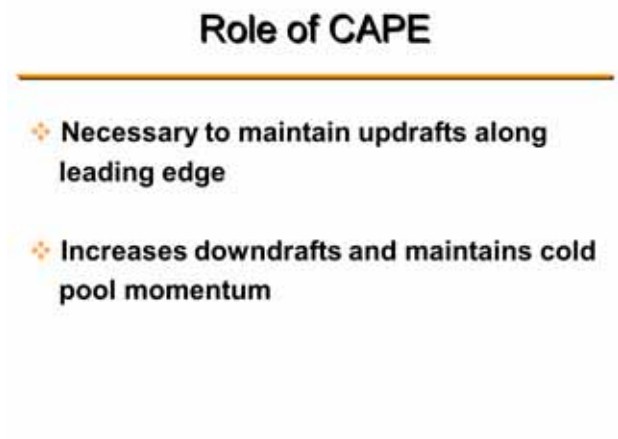

17. Limitations of CAPE

Instructor Notes: There are a couple of caveats of using CAPE. CAPE alone can be misleading, and is most relevant when used in combination with environmental lapse rates or lifted-indices. For instance, one can derive equal amounts of CAPE from a deep, moist sounding (shown on the left) and a more typical mid-latitude Spring-like sounding shown on the right. However, the steep lapse rates in the second sounding would be expected to support greater vertical motion within the ensuing updraft and stronger/colder downdrafts. In addition CAPE is very dependent on the lifted parcel choice. Craven et al. 2002 found that lifting a 100-mb mixed parcel was most representative of cloud heights near peak heating.

Student Notes:

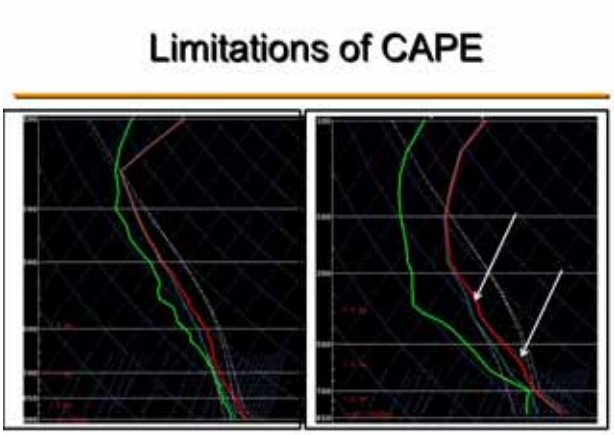

18. Other Factors Related to QLCS Maintenance

Instructor Notes: To anticipate high-end QLCS events, it is important to identify environments that are conducive to rapid, downwind cell propagation near an existing thunderstorm or a group of storms. "Downwind cell propagation" is simply the development of new thunderstorms on the downwind side of existing convection. Environments that foster rapid downwind propagation are those that allow incipient convective systems to continuously redevelop --- and potentially grow upscale. Such systems are more likely to produce large-scale bow echoes, MCVs, and severe weather. Although many factors ultimately govern the rate and location of new cell development relative to existing storms, downwind propagation is especially encouraged by the presence of the following:

Student Notes:

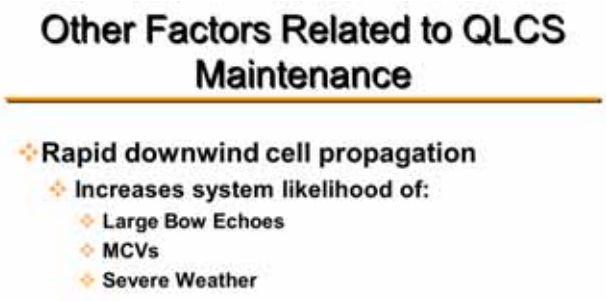

19. Other Factors Related to QLCS Maintenance

Instructor Notes: (1) Rich boundary layer moisture --- Moisture-rich air fosters new storm development by lowering the LCL and enhancing precipitation drag (2) Steep low-level lapse rates --- Steep lapse rates enhance both CAPE and downward momentum transfer (3) Minimal Convective Inhibition or CIN --- The potential for storm initiation is maximized when CIN is low (4) Fast cloud-layer flow --- Fast flow increases gust front speed by strengthening storm outflow; fast flow also fosters the development of embedded supercells and their associated severe threats (5) Deeply unidirectional flow --- Unidirectional flow encourages elongation of the system cold pool in a preferred direction, thereby enhancing storm-relative inflow in that direction (6) Slightly-backed near-surface winds relative to the mean flow --- Backed low-level winds enhance storm-relative inflow and the rate of downwind cell development

Student Notes:

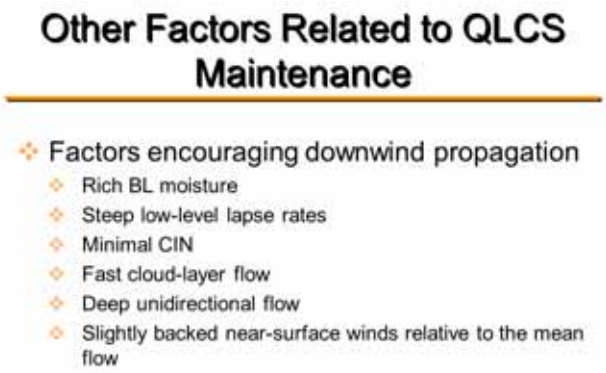

20. How to Anticipate Dominant Direction of QLCS Development?

Instructor Notes: The previous slide noted that unidirectional flow encourages elongation of convective system cold pools along the direction of the mean flow. As a cold pool elongates, a portion of its associated gust front necessarily becomes oriented perpendicular to the flow, while the other part comes to lie parallel to it. This process is shown schematically for unidirectional northwest flow in the plan view at the top of the slide. Recurring production of storm outflow along the part of a gust front oriented perpendicular to the mean wind --- and downward momentum transfer --- cause that part of the gust front to move steadily downwind with time. This is shown on the right side of the plan view in the slide. In contrast, the flow-parallel portion of the boundary moves very slowly or not at all, as shown on left side of the plan view. The orientation of the gust front relative to the mean flow is important in determining the direction of cell propagation and, therefore, the type of MCS that will be most favored along it.

Student Notes:

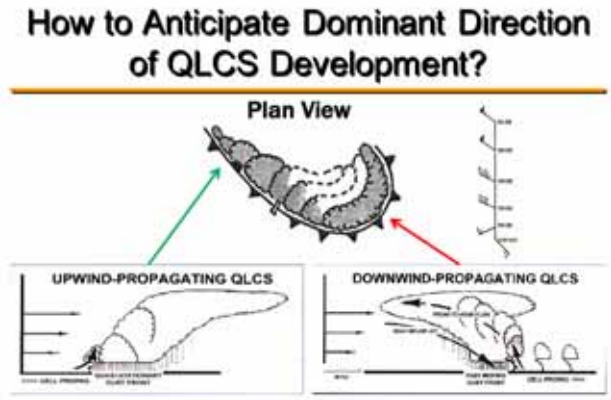

Corfidi (2005)

21. How to Anticipate Dominant Direction of QLCS Development?

Instructor Notes: If low-level convergence and the thermodynamic environment are favorable for new cell development along the flow-parallel portion of the gust front, a back-building or regenerative MCS is likely to develop, as shown in the lower left inset of the slide. Such convective systems are best known for their ability to produce excessive rainfall as storms "train" or move repeatedly along the stationary boundary. But if sufficient cloud-layer shear is present, embedded supercells and LEWPs (line echo wave patterns) may yield damaging winds and tornadoes, especially when the moisture content is great. If convergence and instability are favorable for storm development along the flow-perpendicular part of the gust front, a downwind-developing or "forward-propagating" MCS is likely to form, as seen in the lower right inset. Because new storm development occurs in the direction of the mean wind, the convective system can move faster than the mean flow. Such systems may evolve into a bow echo or derecho-producing MCS if the rate of forward propagation is great --- and this condition persists.

Student Notes:

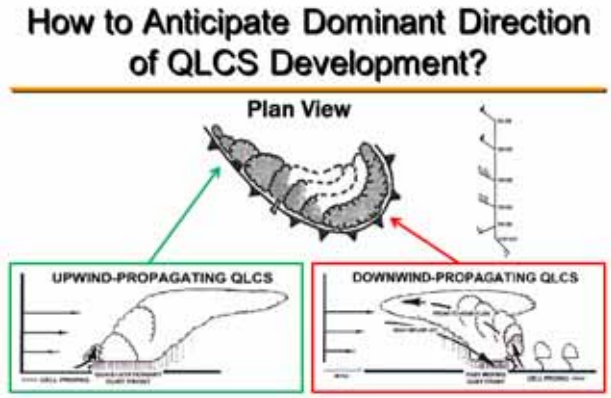

22. Derecho Composite Parameter

Instructor Notes: As forecasters attempt to differentiate between typical warm season, non-severe MCS development versus a forward-propagating/accelerating-Derecho MCS, SPC developed a parameter that is based on 113 Derecho soundings from ED01. This parameter examines four primary mechanisms discussed previously for MCS forward propagation development: 1) DCAPE, used as a proxy for cold pool strength and/or strong downdraft production, 2) MUCAPE- was used as a proxy for the ability to sustain strong storms along the leading edge of the gust front, 3) Surface to 6 km shear, used to account for potential of organization , and 4) Surface to 6 km mean wind to account for favorable ambient flow to elongate the cold pool in a favored downshear direction. Similar to other composite indices developed at the SPC, a value of 1 or greater becomes favorable for a weak forcing Derecho development. Each of these parameters was 'normalized' by mean values developed from the ED01 proximity sounding dataset. DCP = (DCAPE/980)*(MUCAPE/2000)*(sfc-6 shear/20 kt)*(sfc-6 km mean wind/16 kt)

Student Notes:

23. Limitations in Discrimination Process

Instructor Notes: As mentioned in earlier slides, there are many limitations to discriminating what mode storms will develop and evolve into, and what specific severe threats will ensue. This is especially true when dealing with very dynamic events associated with strong large scale ascent and pronounced low and deep layer shear- which are typical from Fall into late Spring. Despite very favorable wind profiles for discrete tornadic supercells, limited thermodynamic support and/or the nature of initiation may force storms to evolve in the form of a fast moving QLCS. For instance in cases where capping remains strong in the warm sector, development may remain tied to a fast moving surface boundary. Also, many times the mean storm motion vector is not sufficient in magnitude and/or direction to move updrafts away from the initiating feature. The images shown here are an example of how similar environments can produce distinctly different thunderstorm modes and severe weather. These are two proximity soundings: 1) near the F4 tornado which struck Tuscaloosa, AL on Dec. 16th, 2000 (in purple), and 2) near the long-lived derecho MCS which produced widespread wind damage and one fatality (but no tornadoes) as it swept across central AL on Feb 16th, 2001 (red/green and yellow wind barbs).

Student Notes:

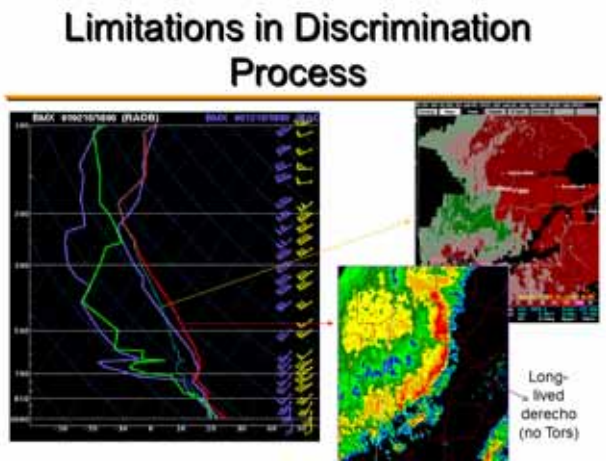

24. Operational Uses

Instructor Notes: The mesoscale analysis page from the Storm Prediction Center can be found at the URL shown above, and has been developed to aid forecasters assess the severe threats evolving over the next 0-3 hrs. The SPC runs a 2-pass Barnes surface objective analysis around 5 min after each hour, using the latest RUC forecast as a first guess. Next, the surface data is merged with the latest RUC forecast upper-air data to represent a 3-dimensional current objective analysis. Finally, each grid point is post-processed with a sounding analysis routine called NSHARP to calculate many technical fields related to severe storms. The parameters are organized under their primary uses on the left hand of the page under the yellow headers. In the case displayed here, the 'Composite indices' sub-menu is expanded to display the available fields. A description of each field is available near the top center of each page for each of the parameters.

Student Notes:

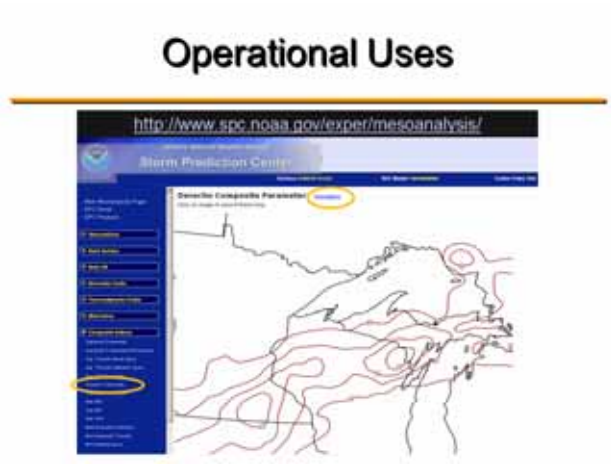

25. Revisiting the Key Points

Instructor Notes: To revisit some of the key points made in the lesson: QLCS events can be described as intense, multi-hazard events that are based on many conceptual models with recognizable features such as rear-inflow jets, bow echoes, linear MCSs, and derecho producing windstorms. The recognition of these features are typically made by evaluating the following parameters , which have been shown to play important roles in helping determine severity and duration: Forcing - look for deep layer shear that's mostly boundary-parallel, Shear - longer straighter hodographs favor the QLCS derecho producing windstorm types, but, the pattern can be similar to supercells. You need to carefully consider the nature of the convective initiation and the storm motion relative to the forcing to help evaluate the role of this factor for each event.

Student Notes:

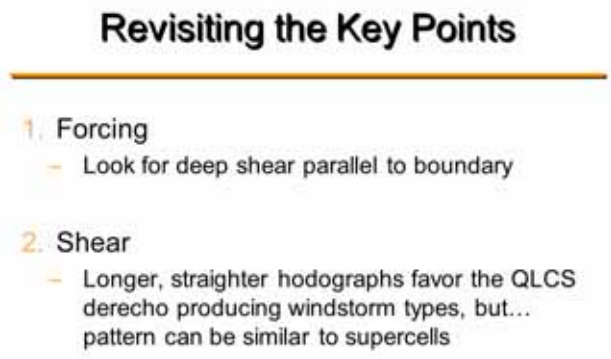

26. Revisiting the Key Points

Instructor Notes: Key Point 3) CAPE- A multifaceted, necessary parameter related to strength of updrafts along the leading edge of the cold pool and strength of subsequent downdrafts. CAPE helps quantify intensity of updraft, and how the system is provided a supply of moisture and energy . Note that computed amounts of CAPE can be misleading when trying to use this variable as a discrimination variable for convective mode.

Student Notes:

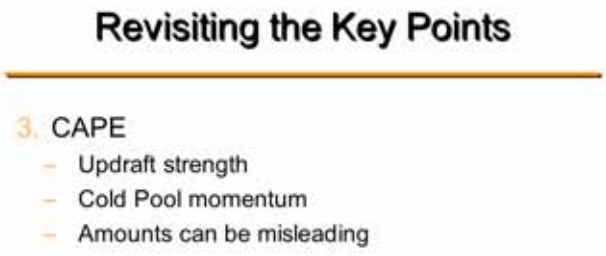

27. Revisiting the Key Points

Instructor Notes: And finally, the 4th Key point: Downwind propagating MCS. Remember that the development of rapid, downwind cell propagation is tantamount to estimating QLCS intensity. Factors such as rich, boundary-level moisture, steep, low-level lapse rates, minimal CIN, fast, cloud-layer flow, deep, unidirectional flow, and slightly backed near-surface winds relative to the mean flow are ALL factors that favor the development of this situation. The example shown is from forward propagating MCS from May 28, 2001 in Oklahoma.

Student Notes:

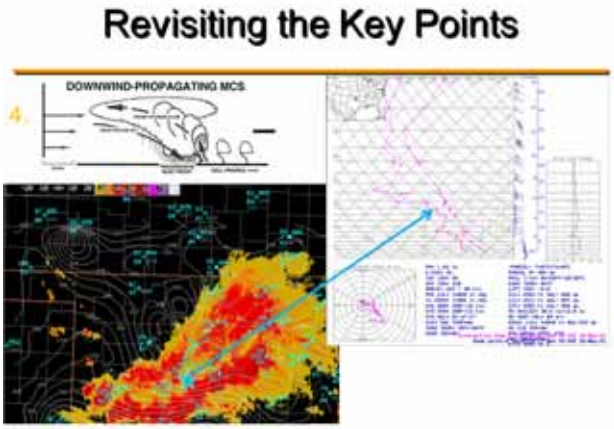

28. Revisiting the Key Points

Instructor Notes: Finally, the SPC has several parameters to help you discriminate if QLCS –type of events are the most intense and long-lasting. You should use these to help assess threats associated with QLCS events. And remember, there are limitations in our science of forecasting convective mode and eventual evolution, as well as determining specific threats due the fact that these parameters don't always tell the full story. Use of the SPC Mesoanalysis Page (http://www.spc.noaa.gov/exper/mesoanalysis/) as well as Model Forecast Sounding applications like BUFKIT are some of our best forecasting tools to assess subtle changes in the mesoscale environment which can influence modality changes.

Student Notes:

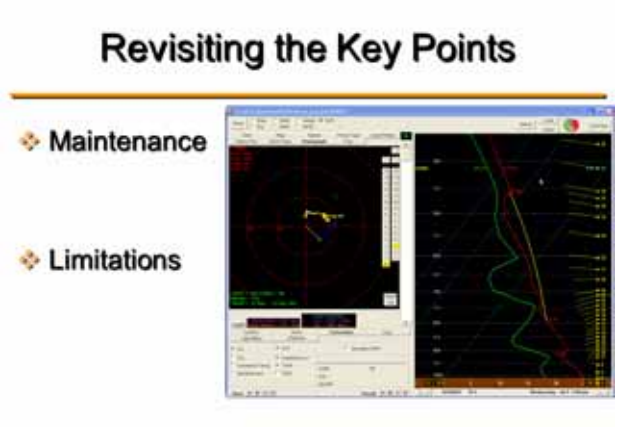

29. Contact Information

Instructor Notes:

Student Notes:

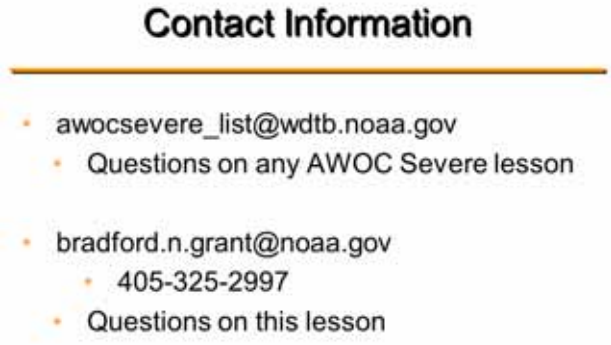

1. Storm Interrogation

Instructor Notes: Storm Interrogation, Updraft location of a sheared cell by satellite This lesson is 17 slides long and should take 20 minutes to complete.

Student Notes:

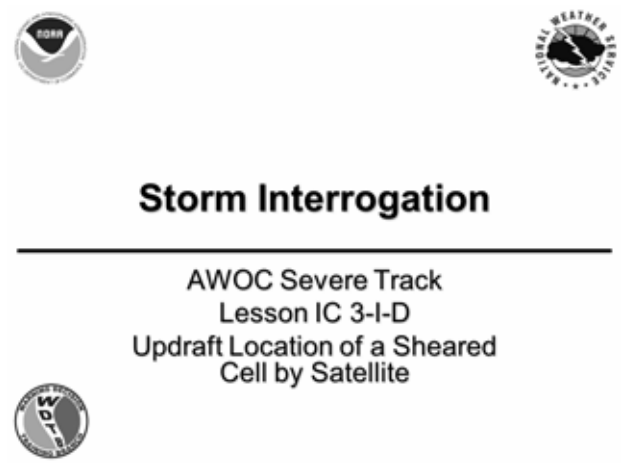

2. Objective

Instructor Notes: This lesson looks at how to interpret storm top brightness temperature information from GOES to locate the storm top in an environment with significant vertical wind shear. This process may seem straightforward if there is a unique relationship between storm height and brightness temperature. However, that is often not the case. We will look at how you can locate a storm top even if cloud height and brightness temperature are not co-located.

Student Notes:

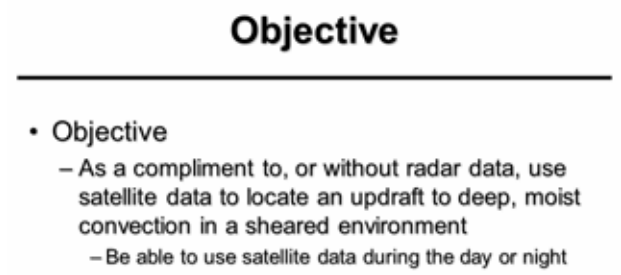

3. Motivation

Instructor Notes: Why do you want to use satellite to locate a storm top? Satellite data can compliment radar in cases where the radar data are poor in quality or you just need some confirming piece of evidence as to the location of a storm. More likely than not, poor radar data, or even lack of radar data provides a strong incentive to use satellite data as a backup.

Student Notes:

Motivation

- Motivation
  - Uncertain radar presentation of storm structure requires interpretation from independent sources
  - No radar data available
  - No spotters
  - No web cams

4. Sheared Storm Updraft Location via Satellite

Instructor Notes: In this lesson, we will assume that the upper-level updraft is near the location of an overshooting top that is depicted well in visible imagery. As we mentioned before, the cloud top summit and the brightness temperature minimum can be occasionally displaced from each other, especially in sheared storm environments.

Student Notes:

Sheared Storm Updraft Location via Satellite

- Locating updraft summits with GOES 0.6 and 10.7 μm data
  - Assume that the updraft location is at the summit of an overshooting storm top
  - Most of the time, cloud height and brightness temperature are related
  - However, not always, and this complicates locating the updraft summit

5. Brightness Temperature in Relation to Storm Top Height

Instructor Notes: Research has theorized three possible contributions for why brightness temperature and storm top summits may be uncorrelated. There could be a plume of elevated cirrus over and downwind of the storm top. If the temperature at the elevated cirrus is warmer than the storm top summit, as may be the case in an inversion, then the storm top may appear warm. The storm top summit may be too small to be adequately resolved. The most likely scenario is that the storm summit cloud boundary contains strong mixing resulting in the cloud edge taking on the properties of the environment around it, including its temperature. Let's examine the bottom two possibilities in more detail

Student Notes:

Brightness Temperature in Relation to Storm Top Height

- Brightness temperature can be uncorrelated from storm top height because
  - Elevated cirrus over storm top
  - **Resolution of IR imagery**
  - **Mixing warm air above the tropopause**

6. IR Resolution Issues

Instructor Notes: Most overshooting storm tops are large enough to be resolved even by the GOES IR imager. But a significant minority of storm tops may be too small for detection compared to the surrounding anvil brightness temperature. The result is that the anvil brightness temperature may be lower than the storm summit, since the anvil is a large, relatively flat expanse much larger than the Instantaneous Field Of View or IFOV from the GOES satellite. In order to properly resolve any overshooting top, the GOES IR imagery will need to decrease this size of its IFOV to about 1 km. This requirement will be met by the time GOES-R is launched within the next several years. The 2X4 km IFOV at nadir refers to the point directly below the satellite. If you want to figure out the resolution for any area of your choice, consider reviewing the lesson on satellite data quality in the section on data quality in AWOC. We show you a simple method to determine the satellite resolution anywhere within view of a GOES satellite.

Student Notes:

IR Resolution Issues

- IR Resolution
  - 2 X 4 km Instantaneous Field of View (IFOV) at nadir is too large to resolve small overshooting tops.
  - Downwind anvil T_b may be lower than at updraft summit.

7. Updraft Dome Mixing

Instructor Notes: The most likely explanation for decorrelating storm top height and brightness temperature involves mixing the edges of the overshooting top with the relatively warm environmental air. Note that the 10.7 ?m radiation is emitted mostly right at the cloud top edge in the region of thermal gradient between the extremely cold undiluted updraft air and the environment. The stronger the mixing along this edge, the more diluted the temperature gradient, and the more likely the thermal IR emissions are closer to that of the environment. Now imagine that the overshooting top is penetrating into a thermal inversion. It is quite conceivable that the mixing may cause the cloud edge to actually warm with height. Let's go on and explore the thermal inversion some more.

Student Notes:

Updraft Dome Mixing

- Mixing along the top of the updraft dome mixes environmental air with cloud air

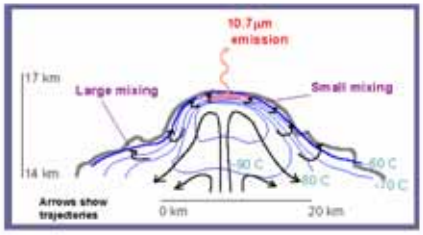

8. Temperature Profiles Above the EL

Instructor Notes: The figure to the right shows the temperature vs. height track of a theoretical air parcel marked as a blue curve as it passes above its equilibrium level, reaches its maximum altitude and descends. In this case, the temperature lapse rate is still positive (temperature decreasing with height) across the equilibrium level as shown by the cyan line. Therefore, as the parcel continues its slowed ascent, the parcel cools. The rate of cooling decreases as mixing commences with the environment but temperature still cools with height until it reaches its maximum altitude located at “C”. This is the case where the overshooting top and brightness temperature minimum are co-located.

Student Notes:

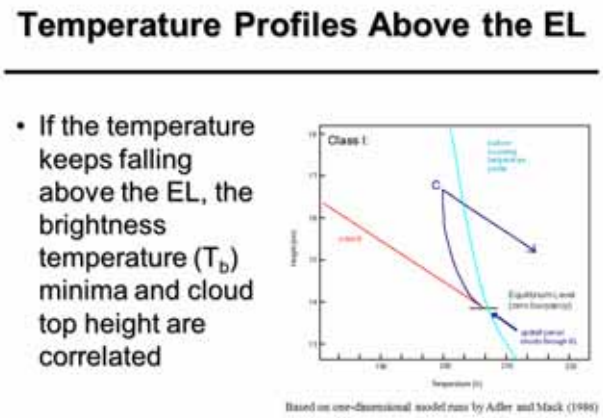

9. Example of EL Below Tropopause

Instructor Notes: Here is a case from South Texas from a cool season severe weather event with supercells. The nearby Corpus Christi sounding showed that the equilibrium level is below the tropopause and positive lapse rates exist above it. This environment suggests that we stand a good chance of picking out the storm top location at its cold point “C”. Any warm wakes “W” may lie downwind of the storm top.

Student Notes:

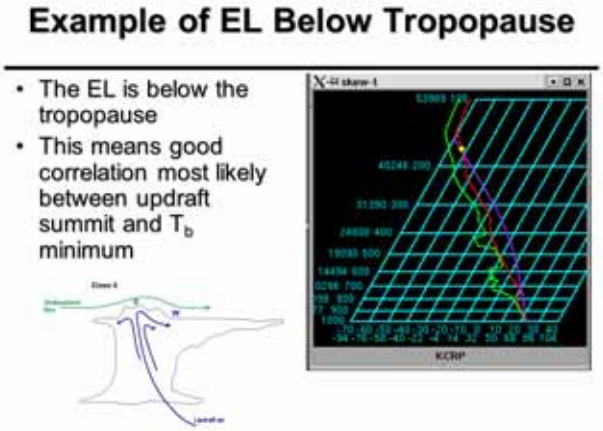

10. Vis vs. IR Satellite for Updraft Summit

Instructor Notes: Comparing the visible imagery with the IR, we see that the brightness temperature minima just northwest of the black arrow is right where the brightest cumuliform cloud top shows up in the visible imagery.

Student Notes:

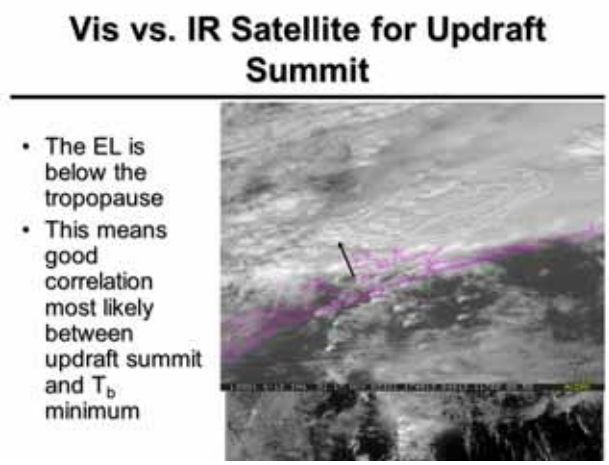

11. EL in an Inversion

Instructor Notes: When the EL is in an inversion, mixing causes the cloud top to actually start warming with height. This causes a displacement between the highest cloud and the coldest temperature. The cold spot is displaced upwind of the highest point. The cloud sinks downwind of the highest point warming nearly adiabatically until it settles to a level closer to the environmental EL.

Student Notes:

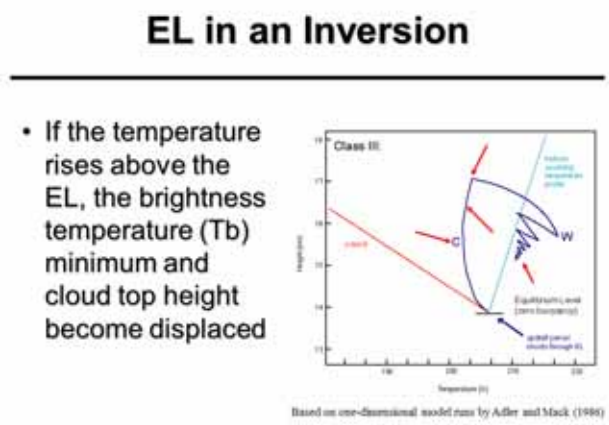

12. Displaced Cold Top Example

Instructor Notes: The Spencer, SD tornadic storm on 31 May 1998 exhibited a typical upwind displacement of the coldest tops. In fact, the overshooting top was warmer than the rest of the anvil. The coldest top visible here is actually a collision of two anvils between two storms and has nothing to do with updraft.

Student Notes:

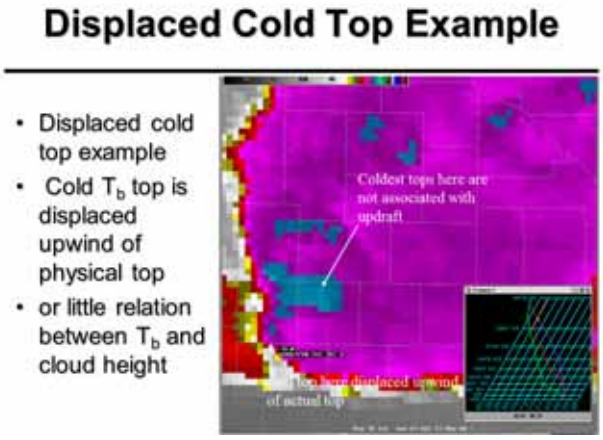

13. Test Your Knowledge

Instructor Notes:

Student Notes:

14. Interim Summary

Instructor Notes: To summarize, if the EL is in a positive lapse rate, the Tb minimum is well correlated with cloud height. Once the EL becomes embedded in a neutral or inverted lapse rate, the cloud actually begins to warm with height creating features such as the warm wake, the enhanced-V, and decorrelating the relationship between Tb and cloud height.

Student Notes:

Interim Summary

- If the EL is in a positive or neutral lapse rate, the T_b minimum is located over the updraft summit
- If the EL is in an inversion, the updraft summit may lie between the T_b minimum and the warm wake
- You may compare to visible imagery during the day

15. Updraft Summit in Small Storms

Instructor Notes: Small overshooting tops from small storms may be completely unresolved by GOES. Or a storm struggling in high wind shear will have no overshooting top. The result is an anvil whose lowest Tb is in the flat anvil well downwind from the updraft. In these cases, the updraft will be at the extreme upwind location of the cold anvil.

Student Notes:

Updraft Summit in Small Storms

- For small storms, the updraft summit will be at upwind edge or point

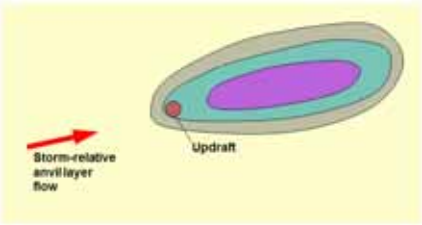

16. Example of Unresolved Overshooting Top

Instructor Notes: On 28 April 2003, a supercell southwest of Pocatello, ID exhibited a very small overshooting top that was unresolved by the GOES satellite. However, there is a warm wake since the EL is in a near isothermal layer. Both of these factors contribute to difficulty in finding the updraft summit by satellite. Two things help to make an educated guess as to where the updraft is located: Look to the upwind wide of the anvil with respect to the storm-relative anvil-layer flow. Upwind of the warm wake.

Student Notes:

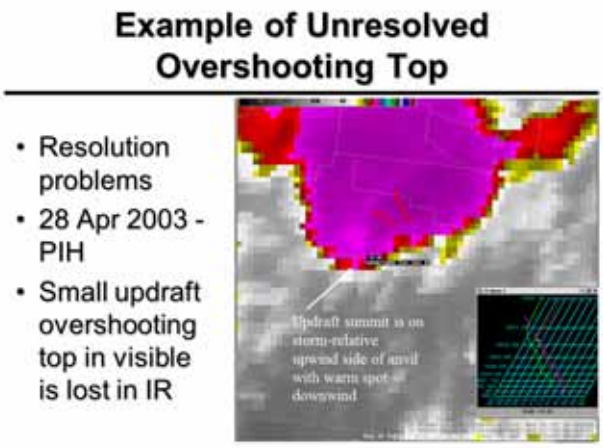

17. Radar/Satellite Overlay

Instructor Notes: Overlaying the high level reflectivity core shows good agreement between satellite educated guess and the radar observed location of the upper-level updraft. Note the parallax correction.

Student Notes:

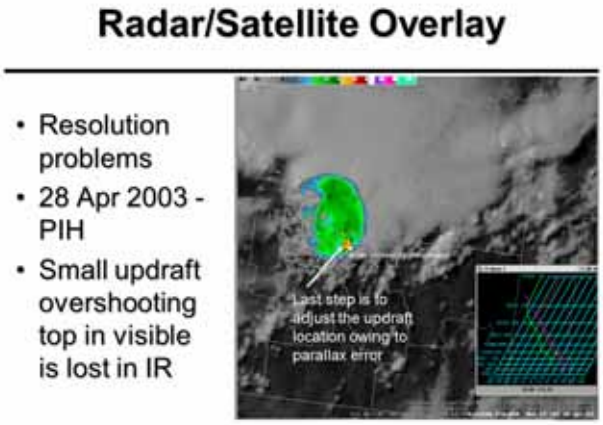

18. Summary: Sheared Updraft Detection by Satellite

Instructor Notes: When there are positive lapse rates above the EL, there is good agreement between updraft summit height and IR Tb. When the lapse rates become negative (inversion), the Tb minimum gets displaced upwind. In some cases, there might not be a Tb minimum. Small overshooting tops are likely to be unresolved by satellite and therefore, you need to look at the upwind side of the anvil relative to the storm-relative anvil layer flow.

Student Notes:

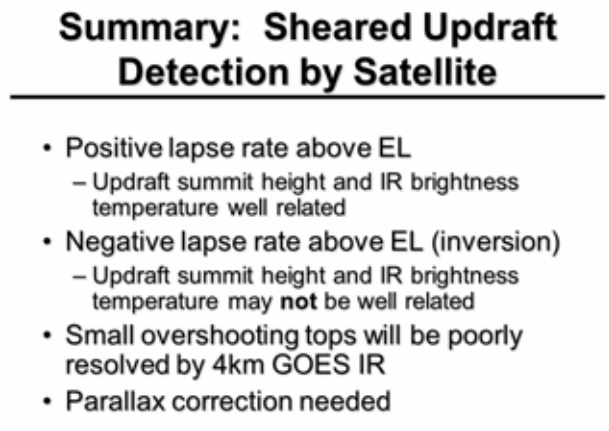

1. Storm Interrogation

Instructor Notes: Slide 1: Storm Interrogation - Estimating updraft intensity by satellite - part 1 This presentation is 23 slides long and should take 20 minutes to complete.

Student Notes:

Storm Interrogation

AWOC Severe Track
IC3-II-D
Estimating updraft intensity with satellite: part 1

2. Estimating updraft intensity with satellite: part 1

Instructor Notes: As a motivation for this lesson, there have been times when offices are stripped of radar data for various reasons. Satellite data can provide a useful backup, or as a tool of confirmation. The objective of this lesson is to qualitatively estimate updraft strength from satellite based on two major parameters that you have the capability to evaluate The cloud top growth rate in terms of time trends of cloud top temperature and height. Temperature and height of the storm Equilibrium Level (EL) Both of these parameters, you can evaluate for yourself using the D2D cloud height estimation tool. We will discuss this more later in this lesson.

Student Notes:

Estimating updraft intensity with satellite: part 1

- Objective
  - Use satellite data to qualitatively estimate updraft strength in the absence of radar data based on
    - Cloud top growth rates determined from temperature and the D2D cloud height estimation tool
    - Temperature and height of the storm equilibrium level

3. Estimating updraft intensity with satellite: part 1

Instructor Notes: There are many methods for evaluating storm intensity from satellite: Cloud top cooling rates prior to anvilgenesis. Cloud top cooling rates after anvilgenesis. Now we are talking about the cooling rate of the overshooting top Cloud top growth rate using the cloud height tool in AWIPS. This technique simply converts cloud top temperature to height. Otherwise, the physical basis remains the same as 1 and 2. Anvil equilibrium level temperature and/or height. In many ways, this technique is better to use than cloud top growth rates

Student Notes:

Estimating updraft intensity with satellite: part 1

- Possible methods
  - Cloud Top Temp (CTT) cooling rates pre-anvilgenesis
  - CTT cooling rates post-anvilgenesis
  - Cloud top growth rate using the cloud height tool in AWIPS
  - Anvil equilibrium level temperature/height

4. Estimating updraft intensity with satellite: part 1

Instructor Notes: I mentioned that the D2D cloud top height tool is used in evaluating some of these techniques. This tool was developed by the Aviation Weather Center to help forecasters write convective sigmets around the world. Now that this technique is available to all, this tool should help you out in convective forecasting. The VISIT program has developed a training session for the general use of this tool at http://www.cira.colostate.edu/ramm/visit/cldhgt.html. The session is generic in the use of this tool. Here we provide some specific potential applications.

Student Notes:

Estimating updraft intensity with satellite: part 1

- Recommended Prerequisite
  - Be familiar with the Interactive cloud height algorithm in D2D
  - Training is available at
    - http://www.cira.colostate.edu/ramm/visit/cldhgt.html

5. CTT cooling rate pre-anvil

Instructor Notes: Satellite-based severe thunderstorm analysis research peaked in the mid 1980's prior to the advent of the WSR-88D because of the incentive to provide more information than the old radar system could provide. Some of the results from that time are still relevant today but there are caveats since we are now talking about higher resolution satellite imagery. Nevertheless, I present some of the techniques devised then in our current framework. Adler et al 1985 approached discriminating severe from nonsevere storms using the cloud top cooling rate determined from rapid scan GOES imagery. After several severe storm outbreaks, they found a fairly good relationship between cooling rate and eventual severe weather reports. This bar chart shows the maximum cooling rate found in a storm before it had a chance to produce an anvil. Note that the storms that went on to produce severe weather (gray shaded bars) tend to dominate when the cooling rates exceeded 2 degrees/minute. This only corresponds to a 4 m/s updraft. Poor resolution was blamed for the low values. GOES IR imagers before the advent of GOES 8 had a 4X8 km field of view at nadir (below the satellite). Now we have routine 2X4km imagery. Today's cooling rates are higher as a result and so this graph's purpose is to highlight the relationship, rather than specific thresholds.

Student Notes:

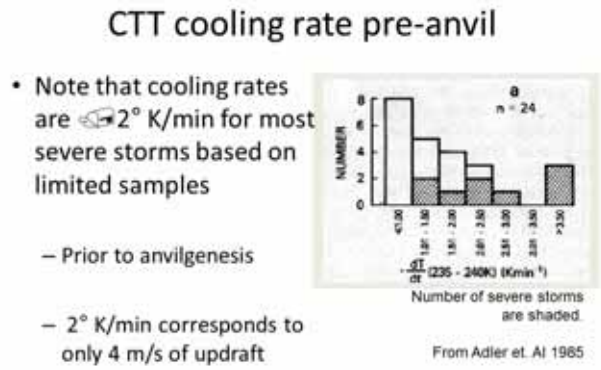

6. CTT cooling rate post-anvil

Instructor Notes: As the storm creates an anvil, and the overshooting top begins to extend above it, the cooling rate typically slows down. Following updraft surges also have slower cooling rates. The reason is that the overshooting top growth is in a region of negative buoyancy. Adler et al 1985 reflects this with much smaller cooling rates. Instead of 2 deg/min, now we are talking 0.4 deg/min as a strong severe/nonsevere thunderstorm discriminator. Again, these cooling rates reflect the maximum cooling rate found in the overshooting top prior to the severe report. Another word of caution, their database was limited to major spring severe storm outbreaks with strong vertical windshear. We will look at multiple events as examples later.

Student Notes:

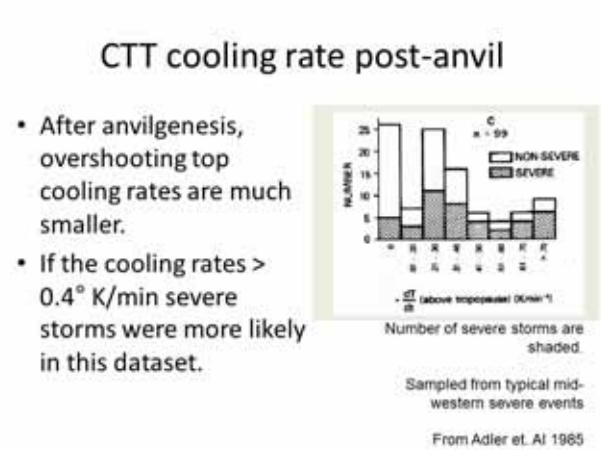

7. Cloud top cooling rates example Storm A

Instructor Notes: This storm is embedded in a monsoon environment with a shortwave trough moving northwest through AZ. It is generating off some high terrain north of LAS. GOES-10 is in normal scan mode and the D2D cloud height algorithm is basing the cloud top height on the KDRA sounding at 12 UTC. It may be a bit on the dry side but should be fairly relevant when trending the cloud height and temperature. Right away, notice the 6 deg temperature drop in the overshooting top in 15 minutes. This is the pre-anvil growth stage of this storm. See http://www.cira.colostate.edu/ramm/visit/cldhgt.html for the training on the AWIPS cloud height algorithm.

Student Notes:

Cloud top cooling rates example Storm A

- Initiation in pre-anvil stage north of LSV (Storm A)
- Use the cloud height algorithm to track cooling rate and cloud top growth

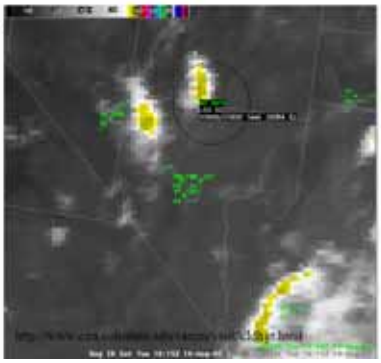

8. Cloud top cooling rates example Storm A

Instructor Notes: In these three frames of this loop, this storm is now creating an anvil and any growth rate during this part of the storm growth can only be compared to the growth rates of storms after their respective anvils have formed.

Student Notes:

Cloud top cooling rates example Storm A

- post-anvil stage north of LSV (Storm A)
- Use the cloud height algorithm to track cooling rate and cloud top growth

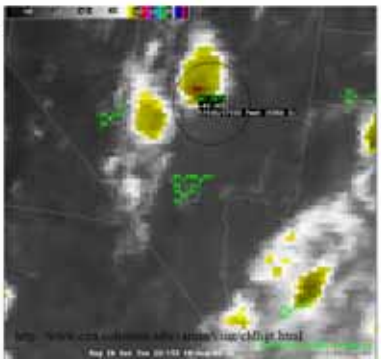

9. Cloud top cooling rates example Storm A

Instructor Notes: Time trends of temperature were taken of this storm from first cumulus to reveal this graph. Note there are large temporal gaps in the imagery which tend to overlook rapid growth spurts (see between 1000 and 2500 seconds). Still, the maximum temperature rate of –0.9 K/sec occurs in the first stages of the towering cumulus. After anvilgenesis the peak cooling occurs as a followup updraft surge cools the overshooting top by 0.4 K/sec at 7200 seconds after initiation. These rates are small compared to Adler's work. Adler et. al 1985 used 5 minute data, and if we had access to such, we would get higher rates. However, our higher resolution imagery should produce higher rates than Adler et. al 1985. Do the competing differences cancel each other? We don't know.

Student Notes:

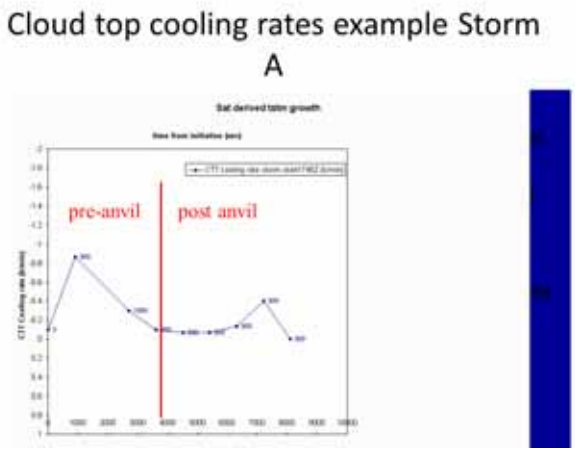

10. Cloud top vertical velocity example Storm A

Instructor Notes: Converting temperature rate to growth rate of storm top height gives us maximum vertical motions of 5 (2) mph for the pre- (post) anvil stage respectively. To create this graph, I simply read off the maximum cloud height found nearby the cursor using the D2D cloud height algorithm (see the altitude on the right in the cursor readout) These results agree with Adler's results very nicely. We'll compare this storm with another one that formed closer to Las Vegas.

Student Notes:

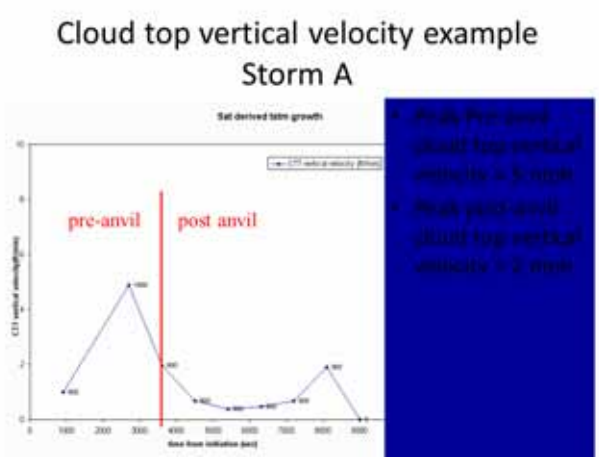

11. Cloud top cooling rates example Storm B

Instructor Notes: Storm B initiates on the high terrain northwest of the city's northern Suburbs near an implied outflow boundary (inside the white circle). Now we have RSO operations going on GOES-10. I cannot emphasize enough the importance of having RSO imagery should you try any of these techniques. Note the cloud tops are taller with this storm. There are two separate updraft surges within this multicell. This loop shows only the first surge, mostly prior to anvil production. See http://www.cira.colostate.edu/ramm/visit/cldhgt.html for training on the AWIPS cloud height algorithm

Student Notes:

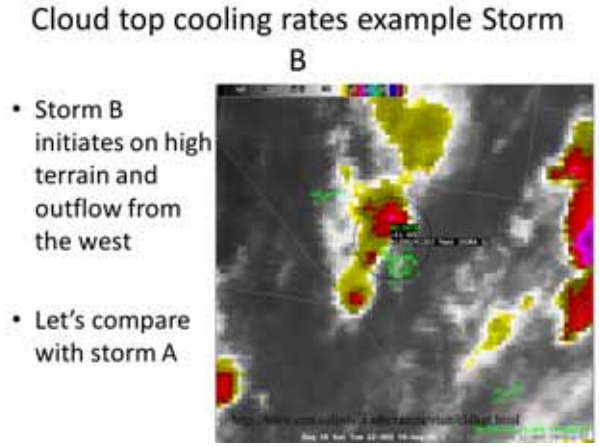

12. Cloud top cooling rates example Storm A

Instructor Notes: This graph compares storm A and storm B, where the storm A profile is set in a grey background. Both have also been set so that the timeline is time from initiation for both storms. Note that both of them exhibit a rapid growth but that storm B is a little more rapid than storm A, given the same image frequency. Storm B continues to show the same or more rapid cooling through its pre-anvil stage. During the post-anvil stage, the overshooting top is also more rapid than storm A. A second updraft surge, shown in purple, exhibits wild fluctuations in cooling rate but that the highest values are higher than with storm A.

Student Notes:

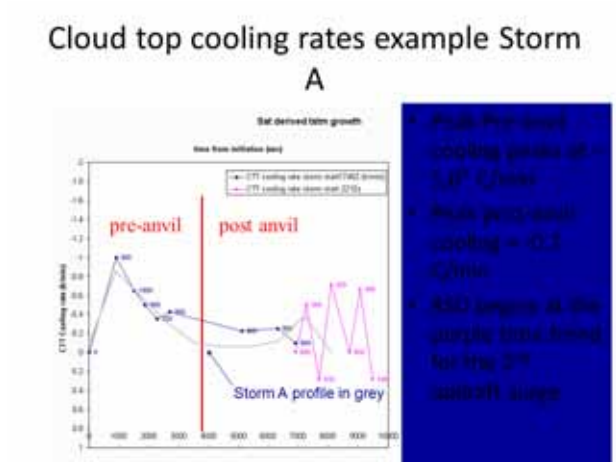

13. Cloud top vertical velocity example Storm B

Instructor Notes: Similarly, using the AWIPS cloud height estimator, peak updraft speeds are up to 5.7 (4) mph prior (after) to anvilgenesis. Actual updrafts are much higher given: that the satellite field of view is larger than individual updraft pulses, that the IR imager only senses cloud edge in the zone of mixing, and not parcel core temperature After anvilgenesis, updraft strength converts mainly to anvil-level divergence owing to adverse buoyancy gradients Therefore 5.7 mph, or 501 ft/min is a significant number in the towering cumulus stage, and 4 mph or 352 ft/min is quite big.

Student Notes:

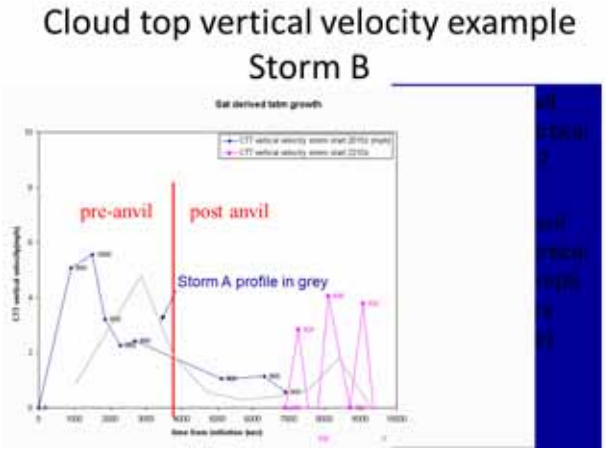

14. Interim summary: cloud top cooling rates

Instructor Notes: Storm B went on to produce 70 mph winds and 1” hail. No reports came in for Storm A, although I caution that storm A originated over relatively unpopulated territory and there may have been unreported severe weather at the surface. Note that we used the peak cooling rates prior and after anvilgenesis for the lifetime of a particular single or multicell event. Remember that cooling rates pre- and post-anvil are distinct and should be treated separately.

Student Notes:

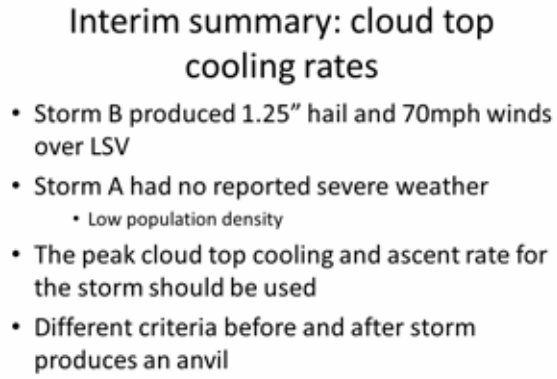

15. Interim summary: cloud top cooling rates (contd)

Instructor Notes: There are real problems using this technique, the worst of them is the uncertain image time interval. Cooling rates can be more a function of image frequency than anything real. A good check The optimal frequency should be 30 seconds, which the GOES satellites have done under research operations. Probably the best way to assess cooling rate is to compare cooling rates between storms in a similar environment. The next satellite-based updraft intensity technique may help a bit to account for image frequency problems.

Student Notes:

Interim summary: cloud top cooling rates (contd)

- Cooling rates are dependent on image temporal frequency
  - Faster scans usually result in higher growth rates
  - Really need 30 second scanning to capture individual updraft growth spurts
- Best to make relative comparisons
- Another technique next

16. Anvil equilibrium temperatures

Instructor Notes: When a thunderstorm updraft does reach its own equilibrium level (EL), anvil material spreads out to form a relatively flat region around the updraft over-shooting top. This flat region is relatively large, larger than the field of view of the GOES imagery, and therefore, its temperature is easily resolved by the imager. Quantitatively, the mode of the brightness temperature reveals the flat region of the anvil.

Student Notes:

Anvil equilibrium temperatures

- Each convective cell has its own equilibrium level height which is visualized on satellite data as relatively flat areas of anvil.
- Represented by the mode of the brightness temp

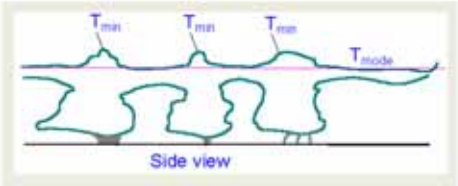

17. Anvil equilibrium temperatures

Instructor Notes: Every convective cell has its own equilibrium level, quite distinct from what your RAOB or model sounding may tell you. There are a million reasons for this to happen, the most frequent may have to do with dry air entrainment with updraft parcels. Another reason may be that the parcel originated at a level or incorporated air at different levels than the chosen method of deriving the theoretical parcel. As a forecaster, you can sample the brightness temperature of areas that appear flat around the overshooting domes. The equilibrium level brightness temperature can be theoretically converted to the updraft parcel ?e for the storm by looking on the sounding to where the EL . Then comparing ?e based off the satellite EL to that of a representative sounding should provide an impression as to how close to the sounding ?e the storm in question realized. A storm that is utilizing all of the potential ?e shown in the sounding should have an EL brightness temperature close to the EL temperature in the sounding (purple curve with yellow EL). Storms experiencing loss of updraft ?e through dry air entrainment, or a different level or parcel origin should show a warmer EL brightness temperature than the sounding suggests (yellow curve with red EL). In theory, this technique appears straightforward but there are complications as follows: 1. The comparison environmental sounding is wrong 2. Storm anvils modify the upper-level temperature environment and change your sounding. Anvils warm the environment at their bottoms and cool the environment at the top. Large contiguous anvils push the tropopause upward and cool it down so that subsequent updrafts are able to reach cooler brightness temperatures without necessarily being more intense. 3. An inversion at the EL may complicate the relationship between cloud height and brightness temperature. As stronger updraft pulses create a higher EL, the brightness temperature may not change or even show warmer values. Overall, this technique should be better than attempting to find the height of an overshooting top and comparing that to the sounding. The reason is that resolution, and cloud edge mixing prevents one from deriving an accurate, or even close to accurate, storm top height based on satellite. Even 1 km imager data will not solve the cloud edge mixing problem to get a picture of the parcel core temperature. This technique works best for: isolated convection growing in an undisturbed environment, that is an environment without prior anvil, Good environmental data, EL lapse rate still positive (no isothermal layers or inversions)

Student Notes:

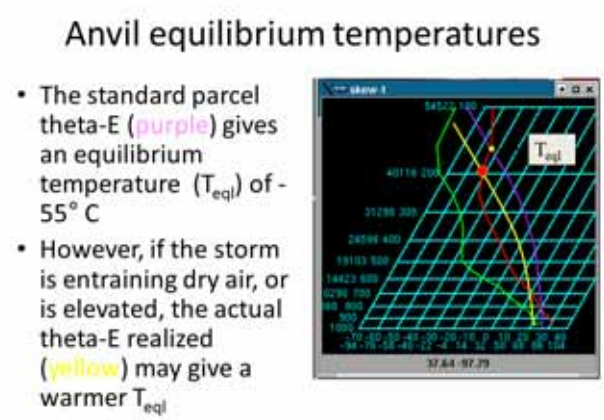

18. Teql example

Instructor Notes: A good example of the application of this technique is to examine storm behavior in a comparitive sense. On 12 June 2004, two storms in Kansas formed along a dryline. Given similar surface dewpoints, storm B looks relatively anemic vs. Storm A. Investigating the areas of relatively flat brightness temperature around the overshooting gives me an idea that the two storms have highly different EL temperatures. Storm A appears to be realizing all the SBCAPE found in the RUC model data in its proximity (see “RUC” in the AWIPS cloud height cursor readout). Storm B appears to be grossly underutilizing the SBCAPE available to it, and therefore realizes a much smaller ?e . Storm B eventually dissipated while A went on to produce all sorts of severe weather.

Student Notes:

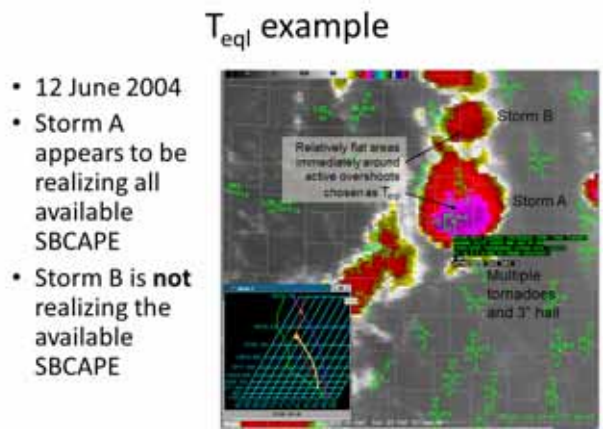

19. Teql example 2

Instructor Notes: Going back to the LSV example, storm B is the storm that struck LSV with hail, strong winds, and flooding. Note that Storm A has a much lower EL temperature than Storm B. It is likely that Storm B is accessing higher ?e air from the Colorado River Valley than Storm A. Or Storm A never realized the low-level ?e air available to it. Either way, storm A likely has a weaker updraft than B. http://www.cira.colostate.edu/ramm/visit/cldhgt.html

Student Notes:

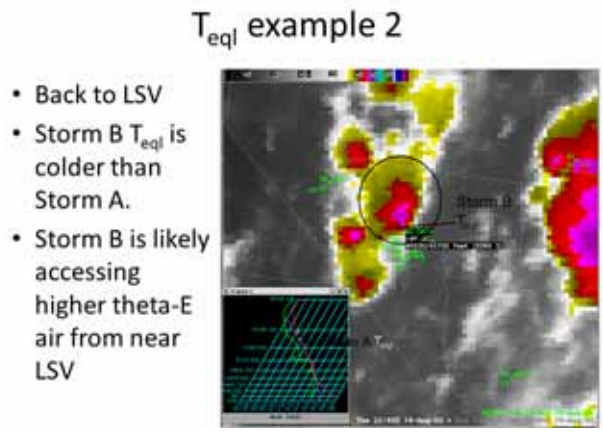

20. Teql example 2

Instructor Notes: We can add evidence to the conclusion by noting that Storm B (right column) has a much stronger core with higher reflectivities.

Student Notes:

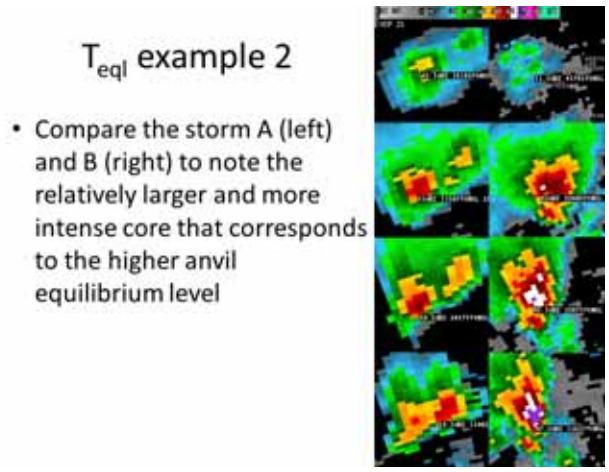

21. Choices

Instructor Notes:

Student Notes:

22. Interim summary: Anvil Teql

Instructor Notes: To summarize, assessing the satellite based EL temperature can give you clues as to the ?e in the updraft column, and therefore how well the storm is utilizing the ?e found in its environment. Use this technique to assess relative updraft strengths between adjacent storms. But be careful. The storm anvil should be exposed to undisturbed environment free of pre-existing anvils. Equilibrium temperatures may also lose their relation to anvil height where isothermal layers or inversions exist across the EL.

Student Notes:

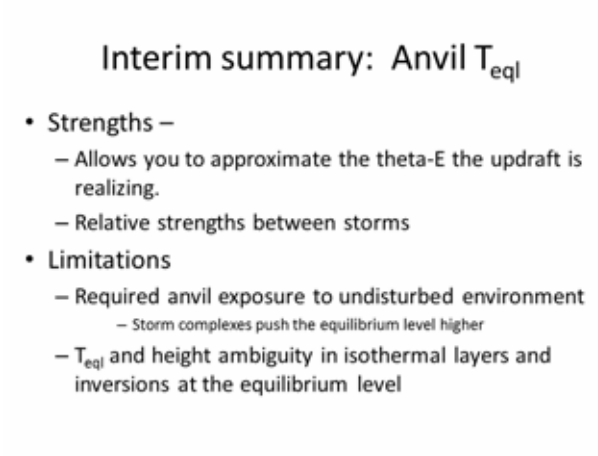

23. Interim summary contd: Anvil Teql

Instructor Notes: This is an example of the EL temperature and height ambiguity in an isothermal layer. All three parcel ?e profiles give out the same EL temperature. I'm sure the updraft strengths would not be the same, however.

Student Notes:

Interim summary contd:
Anvil T_{eql}

- Limitations: T_{eql} and height ambiguity contd.
  - Isothermal layer on right may result in ambiguity of equilibrium level height

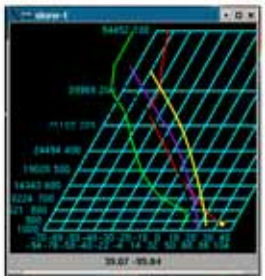

24. Other satellite-based severe convection training materials

Instructor Notes: Here are some extra satellite-based training sessions that address severe storms detection. There is another session centered on a case that illustrates the supporting role of satellite data while interrogating storm structure.

Student Notes:

Other satellite-based severe convection training materials

- Enhanced-V's and what they mean
  - http://www.cira.colostate.edu/ramm/visit/ev.html
- More on how Enhanced-Vs are formed:
  http://www.nssl.noaa.gov/istpds/icu624/
- Interpreting Rapid Scan Operations data
  - http://www.cira.colostate.edu/ramm/visit/rso3.html
  - http://www.cira.colostate.edu/ramm/visit/newrso.html

25. Contact info

Instructor Notes:

Student Notes:

Contact info

- If you have questions write to this group e-mail to ensure a quick response
  - awocsevere_list@wdtb.noaa.gov

1. Storm Interrogation

Instructor Notes: Storm Interrogation: Estimating Updraft Intensity with Satellite – Part 2 This session is a follow up to part 1 of estimating updraft intensity with satellite data. It is short with 11 slides and should take 15 minutes to complete. There is no “Test Your Knowledge” quiz with this lesson.

Student Notes:

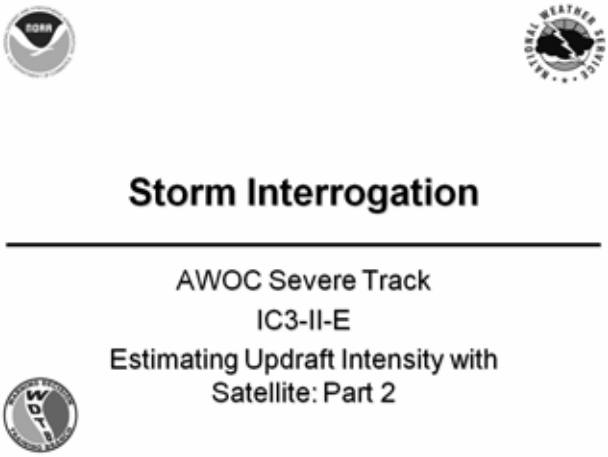

2. Objective

Instructor Notes: This objective uses a case to highlight how the following signatures can be used to assist radar in estimating updraft strength and severe storm potential. We will mention: Overshooting top characteristics, enhanced-V signatures, anvil shape vs. storm-relative anvil-layer flow, and Anvil top temperatures. We will also look at the radar presentation of this storm and some near storm environmental information.

Student Notes:

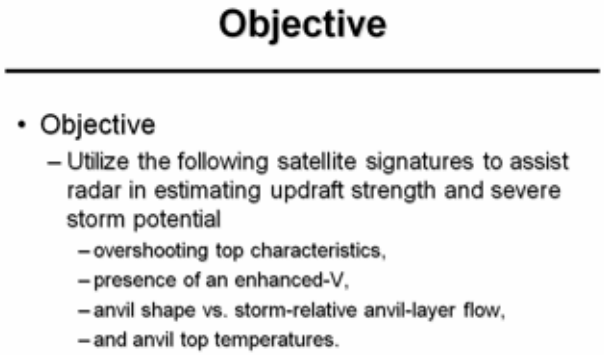

3. Prerequisite

Instructor Notes: This is a follow up to part 1 of estimating satellite updraft intensity. Because of this, many satellite-based signatures will be mentioned but not explained in any detail. If there is anything that confuses you, refer to part 1 of this session.

Student Notes:

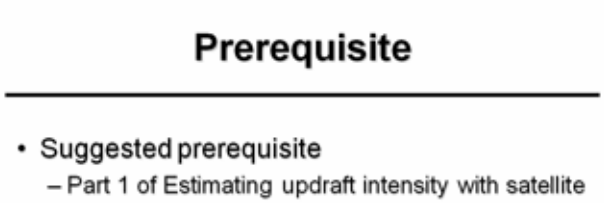

4. Example Case

Instructor Notes: This is a developing storm in northern Nebraska on 09 June 2003. It just recently formed ahead of a dryline bulge near or just south of a warm front. A fairly significant 500mb short-wave trough is coming in from the west and SPC has a MDT risk out for the area. The three frames of this loop show what appears to be a supercell structure with a low-level sharp concave reflectivity gradient, and what appears to be a BWER at 2.4° and 3.4° in elevation, or 21 to 25 kft AGL. However, the surrounding reflectivity is extremely weak at high altitudes. The only reflectivities > 60 dBZ are located at the lowest slice, well below the freezing level. Is this echo hole a true BWER, one with intense updraft or is it a gap between two cells? What is this cell capable of doing? Would you issue a warning based on this data alone? Let's take a look at some more information.

Student Notes:

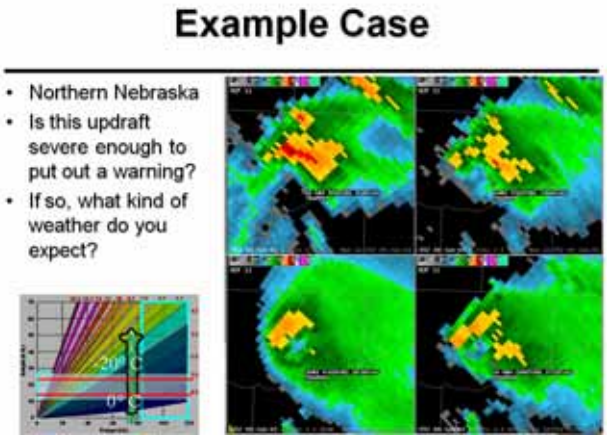

5. ETA Proximity Sounding

Instructor Notes: Since this storm is not near any RAOB sounding, I chose to pick an ETA analysis sounding at 00 UTC. During the actual event, this would've been impossible but a RUC or LAPS sounding showed a similar sounding profile to this one. This sounding shows strong 0-6 km shear of 30 m/s, more than enough for supercells. Steep lapse rates and high CAPE means any storm could go severe quickly and be supercellular in nature. The environment supports the radar structure to be more supercellular than two components of a multicell. But how to explain the low reflectivities?

Student Notes:

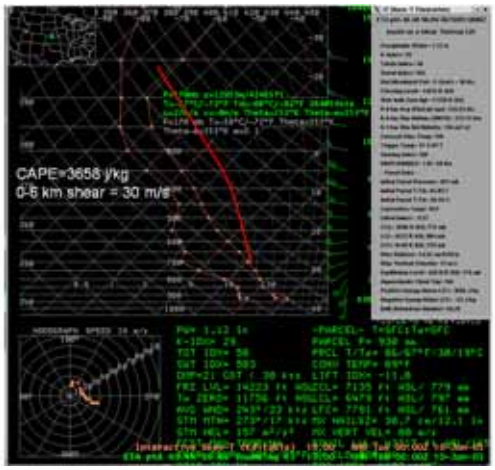

6. Reflectivity Based Vertical Profiles: 2245 UTC

Instructor Notes: If I take the vertical reflectivity profile for this event, and apply the HDA/VIL tool discussed in the lesson on updraft intensity and reflectivity core heights, I see a slowly decreasing profile of reflectivities, especially where it is needed to increase the Severe Hail Index (SHI). VIL reaches only 33 kg/m2, VIL density is only 2.39 g/m3, and SHI is far less than what's needed for a Probability Of Severe Hail (POSH) of 90% (it is only 41%). The Maximum Expected Hail Size (MEHS) seems a bit high given this pro-

file but it is barely over severe limits. Both VIL and VIL Density are far below any minimum threshold discussed in the literature for a warning. The reflectivity profile does not support any warning, and hasn't in all three volume scans.

Student Notes:

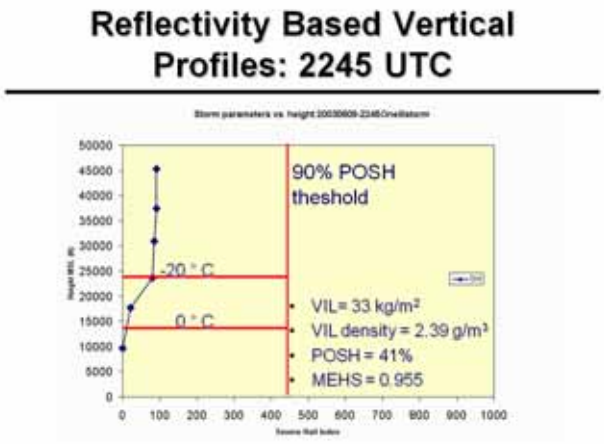

7. Visible Satellite Imagery: 2245 & 2300 UTC

Instructor Notes: The GOES-12 visible imagery shows a well defined overshooting top with a long anvil downwind and yet, significant upwind anvil growth. The Storm Relative anvil layer flow is about 20 m/s which is in the range to support classic supercells according to Rasmussen and Blanchard (1998). The presence of upwind anvil growth and the classic oval shaped anvil in the face of 20 m/s SR anvil layer flow supports the shape and morphology of the radar structure implying a severe updraft.

Student Notes:

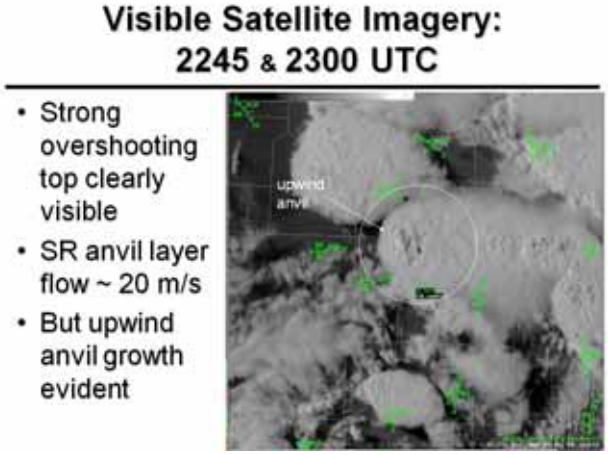

8. IR Satellite Imagery: 2245 & 2300 UTC

Instructor Notes: The GOES-12 IR imagery indicates that the brightness temperature EL based on the AWIPS cloud height tool is about where the ETA analysis expects it to be. However, note that there is an isothermal lapse rate across the EL. This means that a

fairly broad range anvil EL heights may give similar brightness temperatures. We will not use the EL method here. However, the presence of a weak Enhanced-V and a cold overshooting top supports the visible imagery and the radar reflectivity shape that this storm is a supercell.

Student Notes:

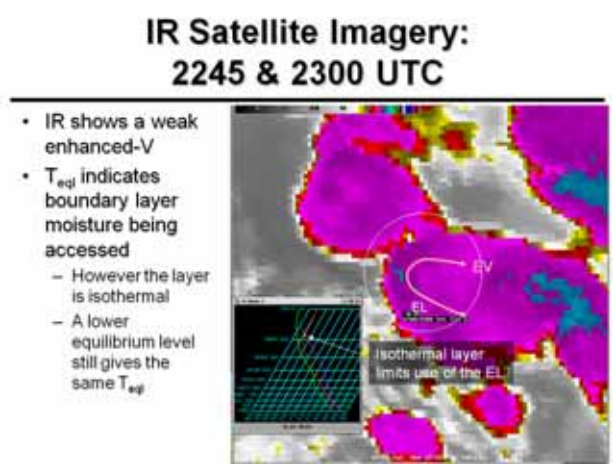

9. Summary of Available Data for a Warning Decision

Instructor Notes: To summarize, the radar showed weak overall reflectivities. The HDA and techniques using the vertical reflectivity profile of this storm fail to indicate the potential for severe weather. The presence of a WER is suggested but the classic definition of a WER is one that is overlaid by an intense echo overhang. This is not a classic WER and the same logic applies to the BWER presented here. The GOES 12 IR/VIS data support the argument that the WER and BWER are legitimate indicators of a severe updraft, even if they are not surrounded by high reflectivities aloft. The enhanced-V indicates the presence of a strong, persistent updraft in a sheared environment. Evidence of an overshooting top and upwind anvil growth against 40 kts of SR anvil layer flow both add additional support for a severe updraft. The storm appears to be a supercell with a strong updraft. This is not a high end updraft capable of creating baseball hail but it appears at least strong enough to support golfball hail. The lack of intense reflectivities suggest an LP supercell in appearance and probably has difficulty in developing any kind of severe downdraft. I will go for golfballs in this storm and they are likely to be widely scattered otherwise high reflectivities would show up throughout the storm.

Student Notes:

Summary of Available Data for a Warning Decision

- Radar
  - Weak reflectivities
  - Evidence of BWER and WER but no marginal echo overhang reflectivities
- Satellite
  - Evidence of Enhanced-V
  - Strong overshooting top
  - Upwind anvil growth against 20 m/s SR anvil layer flow
- Decision?

10. SRM Velocity Data for this Event

Instructor Notes: I purposely kept the velocity from entering into our analysis until now. But upon showing it, this storm clearly has a classic midlevel mesocyclone and intense updraft summit divergence of nearly 160 kts. This only adds evidence and confidence that this updraft is significantly strong. At 2300 UTC, golfball hail was observed by storm chasers from a supercell with visually LP appearance.

Student Notes:

SRM Velocity Data for this Event

- This velocity all-tilts scan should help
- What is your decision?

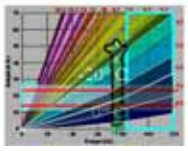

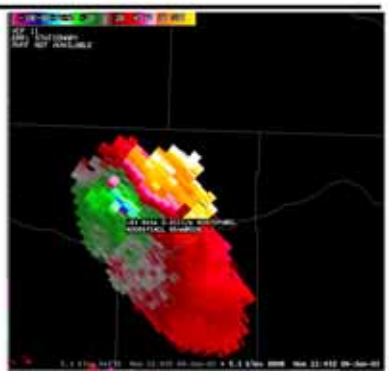

11. Summary

Instructor Notes: This is a low precipitation supercell that has a higher severe hail potential than any VIL or HDA products can estimate. There is a BWER and the proper shape of a supercell but the criteria that the BWER must be surrounded and capped by high reflectivities not being met might cast a bit of doubt about the structure indicating a severe updraft. However, the presence of an enhanced-V, large overshooting top, and the velocity structure showing a strong mesocyclone and storm top divergence adds credibility to the fact that this storm's updraft is very strong.

Student Notes:

Summary

- Low Precipitation supercell
- Severe hail potential higher than weak reflectivities suggest
- Structure analysis along with impressive satellite appearance suggests greater severe potential than the hail algorithm suggests

1. Storm interrogation

Instructor Notes: Welcome to the AWOC Severe Track Part 1: Near range tornadogenesis signatures viewed by the WSR-88D This lesson is 18 slides long and should take 20-25 minutes to complete. Part 2 of this duo examines near range tornadogenesis by the TDWR

Student Notes:

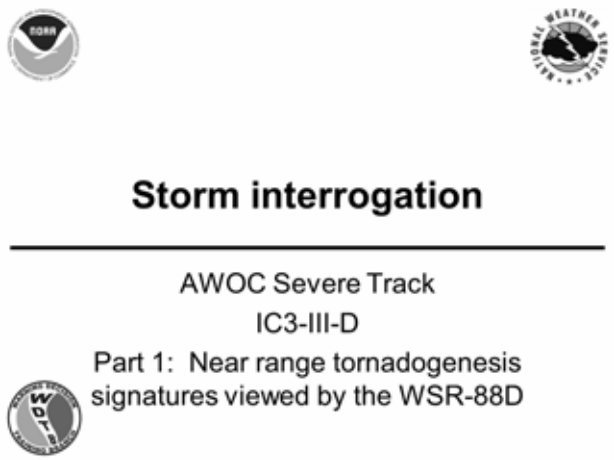

2. Part 1: Near range tornadogenesis signatures

Instructor Notes: The appearances of the classic mesocyclone and TVS are quite different when these features become large relative to the beam width. As we will see, the TVS may not represent the entire tornado cyclone, but perhaps an increasingly small part of it. The mesocyclone may not even look like a coherent rotational structure when smaller velocity structures within can be resolved. On the other hand, it is these close ranges where radar data becomes by far the most useful tool because of the extreme detail it can portray. There are two objectives in Part 1: Recognize how tornado precursor signatures such as the mesocyclone and TVS appear in ranges less than 50 km Interpret tornado signatures that can only be detected at close ranges.

Student Notes:

Part 1: Near range tornadogenesis signatures

- Objectives
  - Recognize how tornado precursor signatures such as the mesocyclone and TVS appear in ranges less than 50 km
  - Interpret favorable signatures indicating a likely tornado that can only be detected at close ranges

3. Part 1: Near range tornado signatures

Instructor Notes: This lesson, using two cases that represent a growing number of documented close range tornadic events to radars, will show the appearances of a TVS and mesocyclone at close range, low-level convergence signatures, the finescale appearance of hook echoes, and debris signatures.

Student Notes:

Part 1: Near range tornado signatures

- TVS and mesocyclone appearance at close range
- Low-level convergence
- Hook echoes
- Debris

4. Mesocyclone comparison: distant vs. nearby radar

Instructor Notes: This case on May 8, 2003 resulted in an F4 tornado that struck Moore, OK and was observed at close ranges by KTLX WSR-88D, a nearby TDWR, and the experimental radars at NSSL and the ROC. All the radars observed the entire lifecycle of the tornado less than 15 miles in range. To start off, we show the appearance of this mesocyclone at approximately 10 kft AGL from two radars of different viewing angles but 90 nm away to that of KTLX, only 17 nm away just before the start of the tornado at 2205 UTC. To the northwest, KVNX lucks out and manages to sample the tornado cyclone with an almost 0.5° offset angle (See IC3-III-A) resulting in a gate to gate signature that easily is strong enough to be called a TVS if it has vertical continuity. None of

the strong flow around the storms right flank can be detected because of weak returned energy. KFDR, 90 nm southwest, suffers from range folding problems in the area of the mesocyclone for the same reason. Other volume scan times show better resolved strong outbounds on the right flank of the storm and KFDR is well positioned to see the flow around the right side of the mesocyclone; some gates show > 100 kts of outbounds. KFDR is barely able to resolve the gate to gate tornado cyclone signature. KTLX, 17 miles away, and with an elevation in the center of the 0.5° slices of the other radars, is close enough to resolve the low reflectivity, high velocity signature on the storms right flank. This is often visualized as rapid horizontal motion in the cloud bands to the right of the visual storm updraft at midlevels and comprises part of the mesocyclone as viewed from more distant radars. These high inbounds are nearly completely separate from the occluded portion of the mesocyclone (or tornado cyclone) within the hook echo and inside the rear flank downdraft. Note that the tornado cyclone does not show the maximum velocities in this circulation in adjacent gates at this elevation angle. There is a 90 kt gate to gate velocity difference, but higher velocities exist at greater ranges from the tornado cyclone center. Sometimes a circulation may not even show up as a TVS at these ranges and yet be very tornadic.

Student Notes:

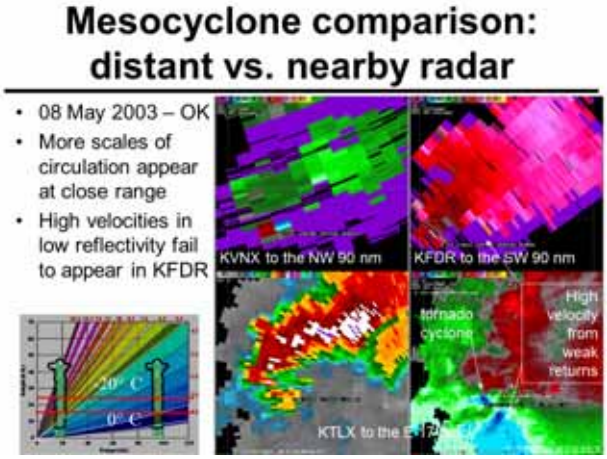

5. Near range tornadogenesis signatures: 08 May 2003

Instructor Notes: The environment on this day was very supportive of tornadoes, low LCLs, 0-1 km wind shear exceeding 25 kts, CAPE on the order of 4000 j/kg, no CIN and a strong dryline west. A PDS tornado watch is in effect and any supercell in the stage of development shown above is likely to have high tornado potential. We'll take a walk through of common signatures at near range leading up to the tornado. We'll start at 2145 UTC, about 20 minutes before tornado time. Two slices are displayed, the lowest slice at 1 kft AGL, and the other at 11 kft AGL. As the storm approaches the radar, I will change elevations to keep sampling the storm between 8 and 11 kft for the upper slice. Several precursor signals are coming together for tornadogenesis. The higher reflectivity slice shows evidence of a strong midlevel updraft signified by a BWER. Strong velocities appear on the right flank of the storm updraft comprise a well developed mesocyclone, more evidence that air is accelerating strongly upward between the surface and 10 kft.

Also at 10 kft, there are areas of separate inbounds and convergence which may indicate an RFD. Near surface velocities show almost pure speed convergence. But that convergence is under a mesocyclone further indicating some stretching potential is there for any near surface vorticity in the vicinity. At this time, there is no significant RFD outflow surge and low-level convergence is fairly weak. Given the elevated convergence, an RFD outflow surge may seem likely.

Student Notes:

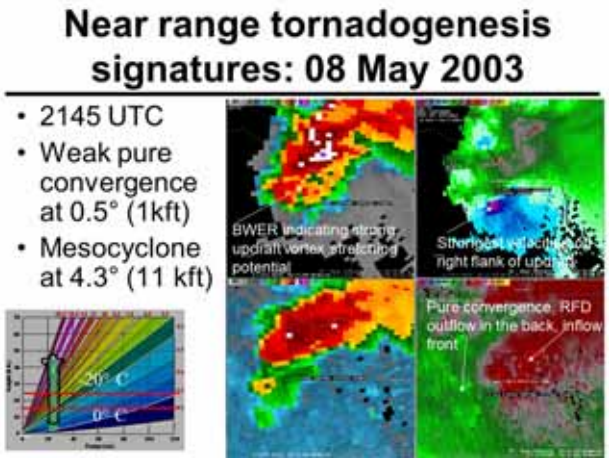

6. Near range tornadogenesis signatures

Instructor Notes: At 2155 UTC, 5 minutes later, the low-level velocity shows the RFD outflow surge may indeed be underway. Convergence at its nose ramps up considerably. But note there is no rotation. Above the RFD surge, note the inbounds and midlevel convergence increases a little behind the low-level convergence (accounting for system motion before the radar scans at 10 kft AGL) and is marked by the dotted white boundary. An area of precipitation forming above and behind the low-level RFD surge a feature that has been observed before prior to tornadogenesis and may have some relationship that has not been identified yet. We often call this a Descending Reflectivity Core (DRC).

Student Notes:

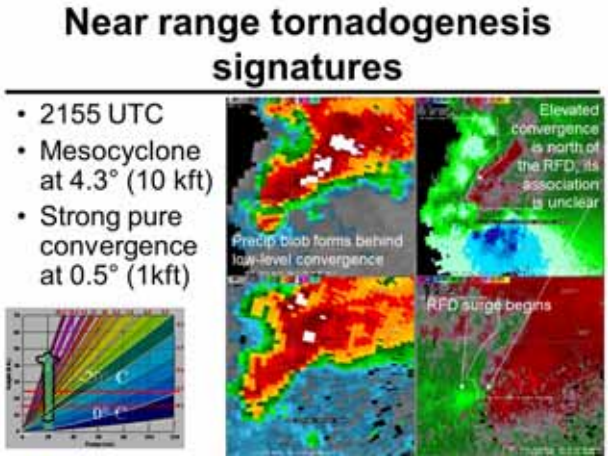

7. Near range tornadogenesis signatures

Instructor Notes: At 2200 UTC, the elevated precipitation blob connects with the low-levels to form the beginning of a hook echo. The part of the hook about to curl to the east lies in the middle to south part of the RFD surge. Strong convergence begins to broaden north to south just ahead of the hook echo. Note that the inflow into this convergence (visualized as outbound low-level velocities) increases too. At 8.7 kft AGL, small scale circulations begin to develop, nearly overhead of the low-level convergence. Developing rotation above strengthening low-level convergence, all underneath a strong echo overhang (not shown) signifies stronger and more immediate mesocyclonic tornado precursor signals.

Student Notes:

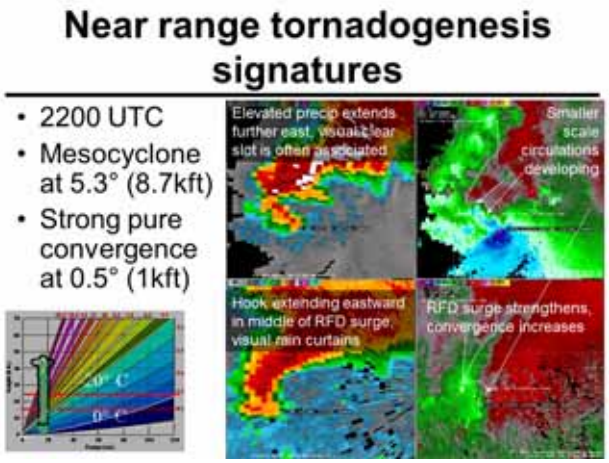

8. Near range tornadogenesis signatures

Instructor Notes: At 2205 UTC, the southern of the two circulations at 8.7 kft AGL consolidates and links with the rapid onset of circulation at the lowest level. This is tornadogenesis underway. The hook echo extends further east embedded on the strengthening RFD surge, now right of the circulation, now a tornado cyclone. Note that the radar must complete many scans before adequately sampling the low- and midlevels of this storm. Meanwhile the circulation is progressing eastward causing an artificial tilt of all features in the direction of storm motion.

Student Notes:

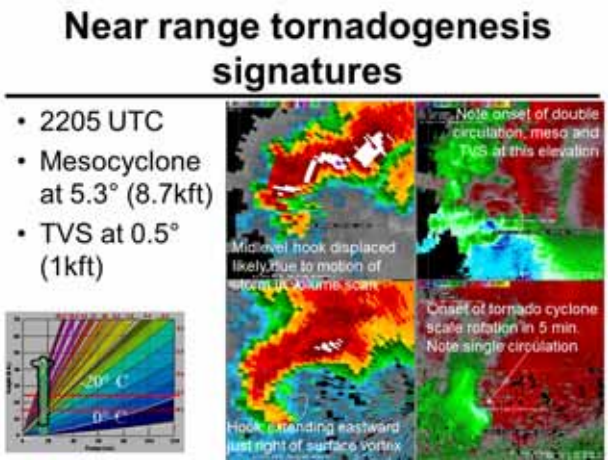

9. Near range tornadogenesis signatures

Instructor Notes: The tornado cyclone is still dominated by an RFD jet on its right side. At 8.7 kft AGL, note that the tornado cyclone (inner circle) still has the maximum inbound/outbound velocities away from the center. A TVS is present after noting the gate-to-gate shear of adequate magnitude. Some tornado cyclones at this range fail to show a TVS. The larger mesocyclone is still evident at 8.7 kft as a separate circulation from the tornado cyclone. Visually, the tornado cyclone is mostly RFD outflow swirling toward the cyclone center. The RFD air contains the hook echo. Part of that hook may be falling out of a deep dry slot carved out of the updraft (white shaded comma shaped region), which in turn, conforms roughly to the RFD gust front boundary. Thus the updraft becomes more horse shoe shaped. Not all updrafts will undergo this shape transformation to a horse shoe, but most will while low-level mesocyclogenesis commences. One other interesting effect of the RFD surge is that an area of anticyclonic vorticity can accumulate on the right side of the surge. If the radar is close enough and the anticyclonic circulation is large enough, you may see it visualized in the reflectivity data as an anticyclonic flare echo. What you are seeing is likely a reflection of baroclinic vorticity forming at the nose of the RFD in the form of arches, the south side of the vortex arch is anticyclonic, the north side, cyclonic. Sometimes this sheet of anticyclonic vorticity coincides with the tail part of the updraft over the trailing gust front and anticyclonic tornadogenesis may be the result

Student Notes:

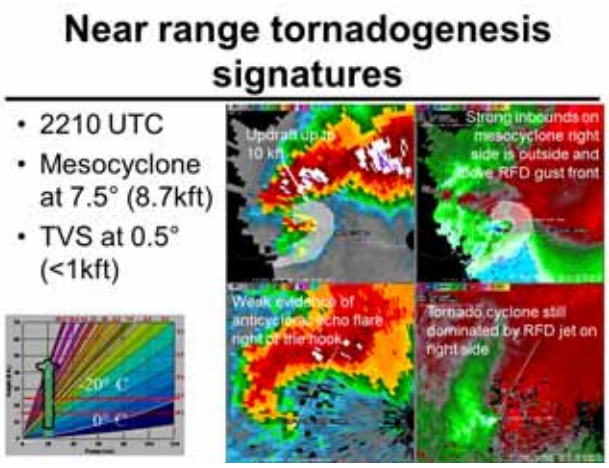

10. Near range tornadogenesis signatures

Instructor Notes: The RFD surge in combination with increasing storm-relative low-level inflow increases convergence rapidly just before tornadogenesis. Low-level convergence values rise above .01 s-1 across a one km baseline. There is perhaps a 1 to 10 minute leadtime before tornadogenesis in this case.

Student Notes:

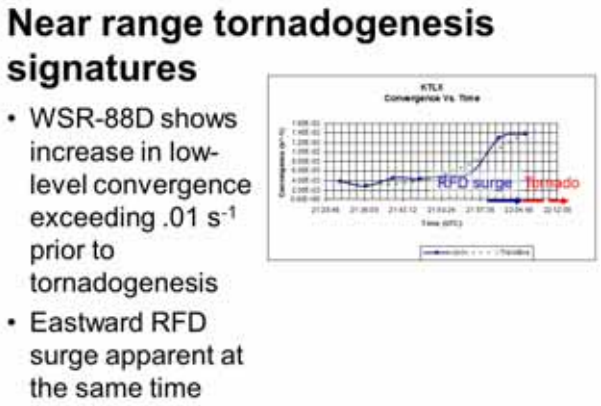

11. Another example of low-level convergence

Instructor Notes: A close range tornadogenesis event occurred just south of Pocatello, ID on 28 April 2003. This time, the radar was left of the storm track, whereas on 08 May 2003, the radar was to its right. The different viewing angle precludes viewing the full strength of the RFD surge; it is directed more to the east instead of straight at the radar. At 2256 UTC, the RFD gust front is evident as a horse shoe shaped region of convergence turning to shear on the left side. Given the ground clutter on the lowest slice, the convergence appears a little better at the 1.5° slice. The larger mesocyclone appears best at 10 kft AGL at 2256 UTC with more pure convergence below in the lowest two slices. A tornado cyclone also forms at 10 kft AGL over the left side of the RFD horse-

shoe shaped gust front. The next scan at 2301 UTC shows the tornado cyclone extending to ground level and tornadogenesis commenced.

Student Notes:

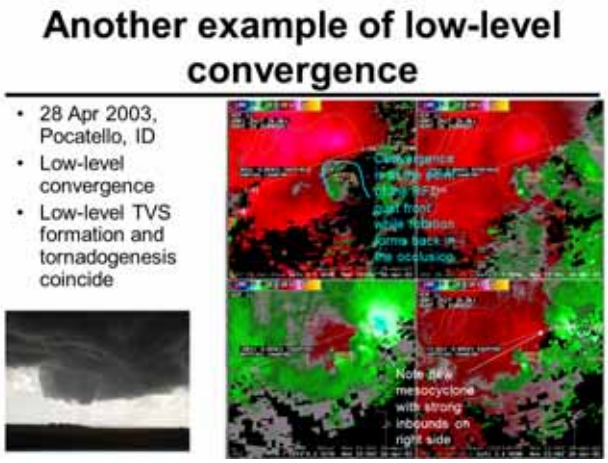

12. Near range mature tornado signatures

Instructor Notes: Going back to the 08 May 2003 tornado, we now look at some mature tornado signatures that show up only at near ranges. The lowest velocity scan now shows a more symmetrical tornado cyclone, although the RFD inbounds still provide some asymmetry to the circulation. The RFD shows strong connection to the downdraft and outflow from the forward flank region of the storm's core. The tornado cyclone and larger mesocyclone still appear as separate circulations at 10 kft AGL. Note, however that on the right flank of the midlevel mesocyclone, a separate area of enhanced inbounds increase in strength that indicates the development of localized updraft rotation and the beginnings of a new separate mesocyclone. Perhaps the most notable signature is the existence of a small area of strong reflectivities at the tip of the hook echo in the lowest scan. This small area of reflectivity appears just as the tornado destroys structures near I-35 in Moore. The reflectivity "ball" is the signature that the radar is detecting debris. The follow up session to this shows another region of even more intense reflectivities viewed by the TDWR.

Student Notes:

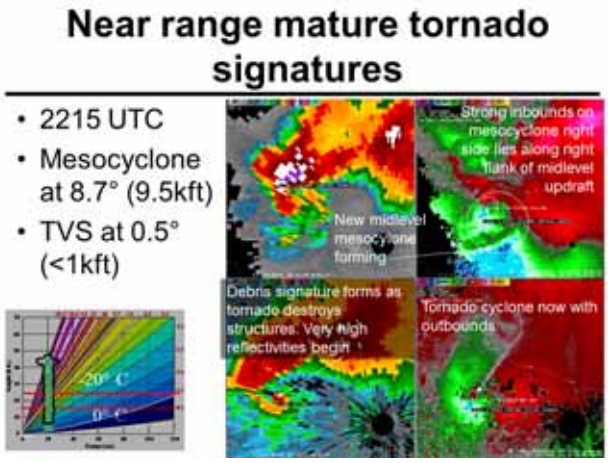

13. Near range mature tornado signatures

Instructor Notes: As observed from the ground to the northwest, and a couple minutes before the radar image, the tornado is beginning to loft debris several hundred feet into the air. At 16 miles range, large debris at this altitude is enough to be detected by the radar. Again, the debris needs to be large to present a significant radar cross-section. Dust particles alone are not enough to provide reflectivities that exceed normal reflectivities associated with the hook echo and other natural scatterers (e.g., insects).

Student Notes:

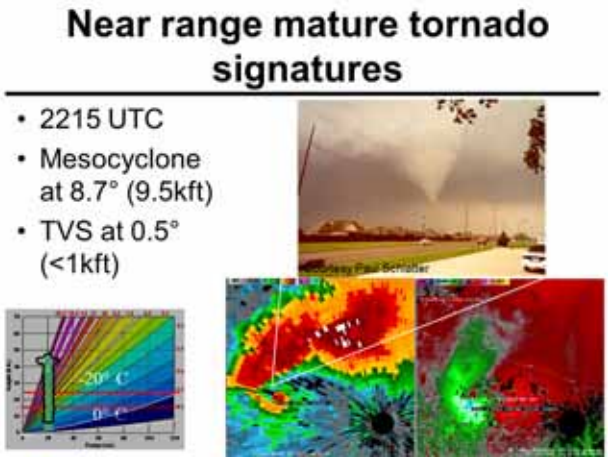

14. Near range mature tornado signatures - debris

Instructor Notes: At 2225 UTC, the tornado impacted the General Motors plant in Southeast Oklahoma City resulting in a significant upward surge in debris.

Student Notes:

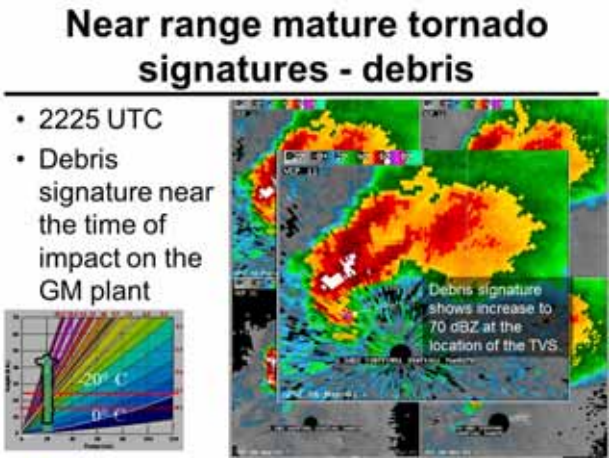

15. Is the close range TVS a tornado?

Instructor Notes: A question often arises as to whether the tornado core can be adequately sampled by the WSR-88D at close ranges. On May 3, 1999, the Doppler On Wheels (DOW) sampled a large tornado within a few km range. The small velocity couplet signature from the DOW that can be seen at two different times, 0013 UTC and 0027 was the tornado core. Its radius was chosen as the radius of maximum winds found around the tornado center. Superimposing the white circle at 0013 UTC, marking the tornado diameter on the WSR-88D from KTLX (20 miles range), and the test bed WSR-88D, KCRI (12 miles range), you can see that the tornado core is still far smaller than the individual gate sizes from both radars. Even when the radar was closer (16 miles from KTLX, 8 miles from KCRI) the tornado core diameter is still too small for the two radars to resolve it. Adequate tornado sampling requires about 4 azimuthal gates across the core. Other factors also hinder adequate velocity sampling of the tornado: The tornado offset angle from the beam centerline is too small, or a single range gate is sampling both sides of the tornado. Most of the returned power to the radar comes from relatively slow moving debris. You don't see the velocity spectra, only the velocity from which the radar detects the greatest returned power.

Student Notes:

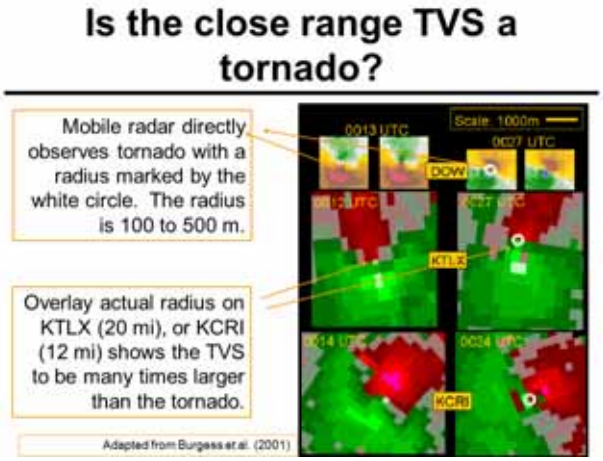

16. Extreme tornado size

Instructor Notes: So far in this lesson we've shown you that large tornadoes are not resolvable by the WSR-88D because of the gate to tornado size ratio is not large enough. However, since this lesson was first introduced, we've seen a couple events where the tornadoes were large enough to call our first assumption into question. Featured here is the Trousdale tornado from 0325 UTC, 05 May 2007. The inbound/outbound velocity maxima in this image are approximately 105 and 118 kts respectively. These velocities are certainly in the tornadic range, even with the limitations of the power weighting. The width of the damage track corresponds to a tornado width > 2.6 km though the core flow of this tornado was estimated to be close to 2.6 km. That's wide enough for the WSR-88D to sample this core with three azimuthally adjacent scans. We are very close to resolving the tornado here even at a range of 38 nm. See the paper by Lemon and Umscheid by clicking on the link in the lower right for a more detailed discussion on this event.

Student Notes:

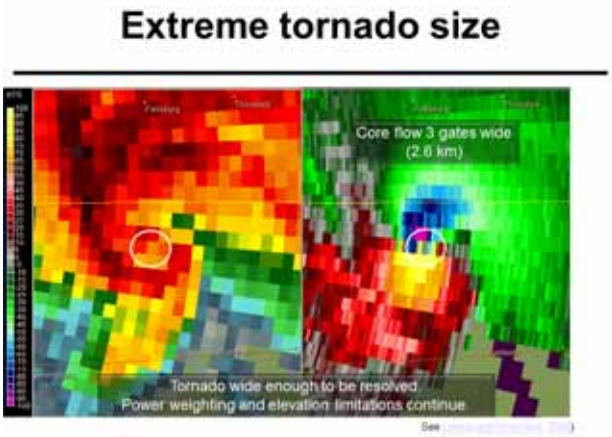

17. Superresolution impact on resolving tornado scale

Instructor Notes: The recent addition of super-resolution data adds the ability to detect features associated with tornadoes at greater ranges. This is especially true with reflectivity data where you're now able to view the individual 0.13 nm range gates. As a result, you are now more likely to see features associated with tornadoes such as vortex holes, and anticyclonic flares in hook echoes. The top reflectivity image shows an anticyclonically-shaped hook echo appendage much more clearly than the legacy resolution product on the bottom. While the main features in the SRM show up in both images, the velocity difference is a little larger in the SR product. Superresolution data is extremely useful in resolving features scanned by the radar such as tornado cyclones and vortex holes. However, you still have the range limitations of detecting certain features such as low-level convergence. For more information on super resolution data, I refer you to our training linkable in the lower right.

Student Notes:

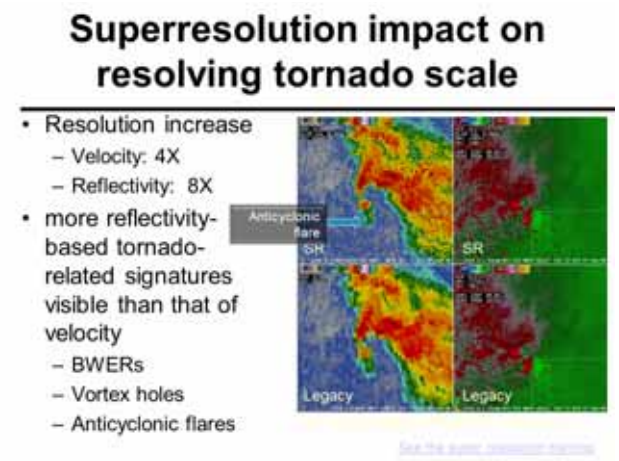

18. Choices

Instructor Notes:

Student Notes:

19. Summary: Close range rotation signatures

Instructor Notes: To summarize, close range rotation signatures are more complex in scales. At close ranges, the TVS is the manifestation of the tornado cyclone. The meso-cyclone does not appear as symmetric as before, with most of the strong velocities dis-placed to the right side of the updraft for cyclonically rotating storms. At low-levels, the mesocyclone may not appear at all.

Student Notes:

Summary: Close range rotation signatures

- More complexity of rotation
  - TVS is the detection of the tornado cyclone
  - Mesocyclone scale shows less symmetry
    - strongest velocities are located at midlevels on the right flank of the updraft for cyclonically rotating mesocyclones
    - Difficult to discern mesocyclone rotation at low-levels

20. Summary: Close range tornadogenesis signatures

Instructor Notes: Remember that these signatures apply best to mesocyclone induced tornadoes. Tornadogenesis signatures appear at low-levels as the RFD begins to develop. Convergence increases dramatically at low-levels and should appear under a midlevel mesocyclone and other strong updraft signatures. Only immediately before tornado formation is there any appearance of a tornado cyclone at low-levels. The convergence signature gives you on the order of 5 to 10 minutes of lead time. The onset of an intense tornado cyclone may only appear within a minute of tornadogenesis. The hook echo may appear to extend in length and definition as the RFD develops. More recent research work has suggested that a descending ‘blob’ of reflectivity on the back side of the storm may contribute to RFD genesis. As the RFD matures and begins to develop low-level rotation, an anticyclonic flare echo may be detected right of the main hook echo. Anticyclonic tornadoes are most likely if this anticyclonic flare coincides with the gust front underneath strong updraft.

Student Notes:

Summary: Close range tornadogenesis signatures

- Lowest level velocity signatures
  - RFD surge
  - strong convergence under higher level rotation and other updraft signatures
  - Increase in convergence with time
  - Rotation onset at tornado time
- hook echo
  - Rapid extension associated with RFD surge
  - Perhaps an elevated descent of reflectivity core into back side
  - Occasionally an anticyclonically shaped flare south of the hook

21. Summary: Close range mature tornado signatures

Instructor Notes: Close range radar signatures of a mature tornado include good sampling of the tornado cyclone. Sometimes, the sampling is such that no gate to gate TVS strength signature appears in the tornado cyclone. The RFD gust front appears well defined, and there may be other vortices appearing along its interface. If the tornado is ejecting large debris (e.g., tree branches, building parts), a reflectivity debris ball may appear as a small region of very high reflectivities extending upward several thousand feet or more.

Student Notes:

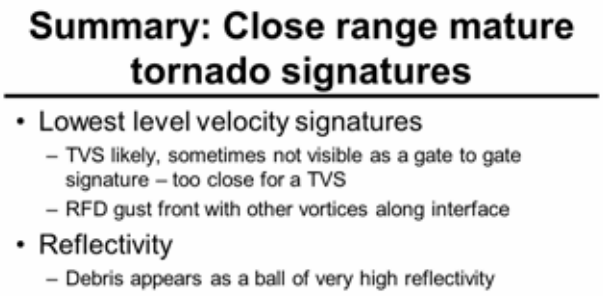

1. Storm interrogation

Instructor Notes: Welcome to the AWOC Severe Track IC svr3: Part 2, Near range tornadogenesis signatures viewed by the TDWR This part follows part 1 of near range tornadogenesis signatures by the WSR-88D. It is approximately 13 slides long and should take about 10 minutes to complete.

Student Notes:

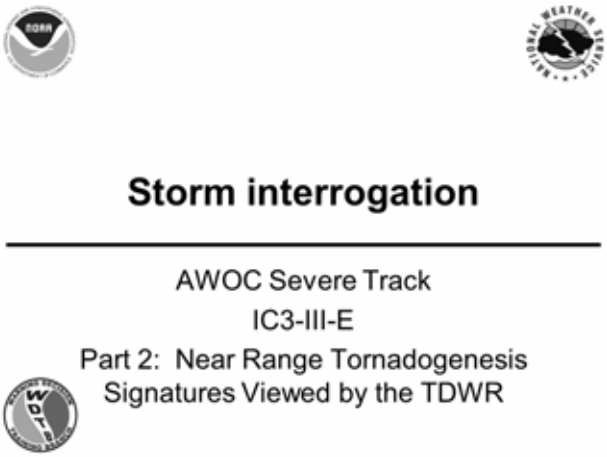

2. Objectives

Instructor Notes: As objectives, you should familiarize yourself with the applications and weaknesses of using the TDWR for analyzing close range tornadogenesis signatures. The same applications and weaknesses should apply to the interrogation of many meteorological features. This lesson will also help you become more familiar with the characteristics of the TDWR. At this point, development is underway to send TDWR data to WFOs on an operational basis. Thus for any site that has a TDWR in your CWA, this lesson will have more relevance to you.

Student Notes:

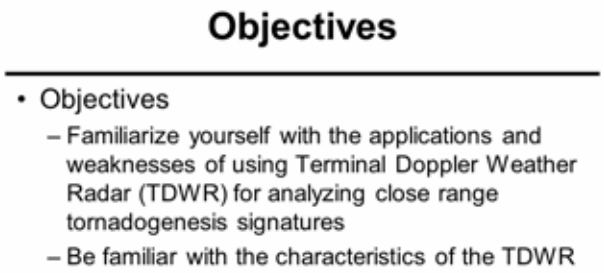

3. Part 2: Near Range TDWR Tornado Signatures

Instructor Notes: We will look at the similar events as with part 1, a close range mesocyclonic tornado formation case in Norman, OK, and a nonmesocyclonic case from Salt Lake City, UT. You will see how TVS signatures and mesocyclones appear in the TDWR, how low-level convergence signatures appear, how hook echoes become more complicated, and at the sensitivity of the TDWR to debris signatures.

Student Notes:

Part 2: Near Range TDWR Tornado Signatures

- TVS and mesocyclone appearance at close range
- Low-level convergence
- Hook echoes
- Debris

4. TDWR vs WSR-88D

Instructor Notes: The TDWR operates at 5 cm and is more susceptible to attenuation in heavy precipitation. However, this wavelength is more conducive to detecting most nonprecipitating echoes such as insects. One of the TDWR volume scan strategies allows for one minute sampling at the 0.5° angle while sampling other elevation angles on a 2.5 minute basis. The real advantage comes with the 1 minute sampling when a storm is undergoing tornadogenesis. The beam width of the TDWR is half that of the WSR-88D. Add a shorter range gate due to a faster PRF, and the TDWR delivers much higher resolution, 4 times more data than a single range gate from the WSR-88D. The tradeoff is that the maximum unambiguous velocity (from here on, Vmax) is a lot lower for the TDWR. Examples will show the effects on real information coming next.

Student Notes:

TDWR vs WSR-88D

	WSR-88D	TDWR
Wavelength	10 cm	5 cm
Volume Scan Time	4 minutes in VCP 12	1 minute 0.5°, 2.5 min for other angles
Beam Width	1.25°	0.5°
Range Gate	.13 nm for super resolution base data	.067 nm
Max Unambiguous Velocity	Up to 62 kts with a PRF = 1293.10 s^{-1}	20 - 30 kts

5. WSR-88D vs. TDWR (vel.)

Instructor Notes: Here are two views of a mature tornado cyclone at 8 miles the radar. The WSR-88D, left adequately samples the high velocities associated with the right flank of the tornado cyclone but washes out the tight velocity couplet that should be there given that the tornado is in its mature stage. The resolution of the TDWR produces a much tighter velocity couplet on the same order of size as the damage track being produced by the tornado (within the area bounded by the thin white perimeter). But notice that some aliased velocities exist near the circulation center, just on its left side. Much of the May 08, 2003 results are from a paper by Mike Charles (2003) while working with the NWS OUN as a summer student in the Research Experiences for Undergraduates (REU) program and with Dave Andra, Dan Miller, and Mike Foster serving as mentors.

Student Notes:

WSR-88D vs. TDWR (vel.)

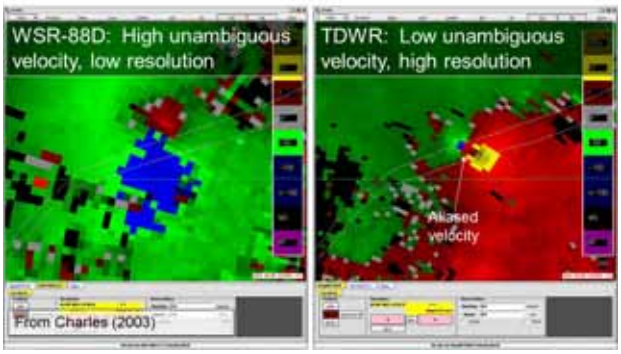

6. Near Range Tornadogenesis: TDWR - 08 May 2003

Instructor Notes: Displayed here is a 4 panel image of the 2.5°, and 5.1° velocity and reflectivity slices as the supercell is about to generate its first tornado. Each scan is roughly 3 minutes apart starting at 2141 UTC. The 2.5° slice ranges from 1.6 km AGL at

the beginning to 0.3km AGL at the end of the loop. The 5.1° slice starts from 2.8 km to 0.6 km in a similar way. The first few times show the strong inbounds south of the developing hook echo, and above 1.6 km AGL. The inbounds are folded once to outbounds and then again to inbounds again in the 5.1° slice from 2141 to 2148 UTC. At 2150 UTC, the 5.1° slice shows strong convergence on the back side of the hook echo. These velocities are folded over to outbounds. This is the elevated convergence of air flowing into the RFD, possibly visually manifesting itself as the “waterfall” of clouds on the back side of the updraft as long as the precipitation is not too dense. At 2156 UTC, the storm approaches enough that both slices samples well below cloud base where the RFD is mostly outflow. Again, the outflow winds exceed Vmax and are folded to outbounds. Convergence is much stronger along the nose of the gust front. At 2202 UTC, the RFD outflow is curling to the north ahead of the supercell updraft core causing an area of strong outbounds northwest of the radar. These outbounds exceed Vmax and are folded to appear as inbounds. Note at the same time in the 5.1° slice southwest of the hook echo, the strong inbounds of the midlevel mesocyclone. Also at the same time, the hook echo appears to gain some anticyclonic curvature just south of the strong RFD surge. At 2205 UTC and after, the strong tornado cyclone is apparent as a couplet of inbounds and outbounds, both sides with velocity folding. The tornado track begins at this time, visible on the map in a thin white perimeter. The hook echo has an inflection point, where it changes shape from cyclonic to anticyclonic at the tornado location. The shape of the hook echo deforms in this case as a result of the RFD surge. Anticyclonic vorticity is found to right of the tornado track. Sometimes, this deformation may appear as a small scale bow with a cyclonic, anticyclonic vortex pair.

Student Notes:

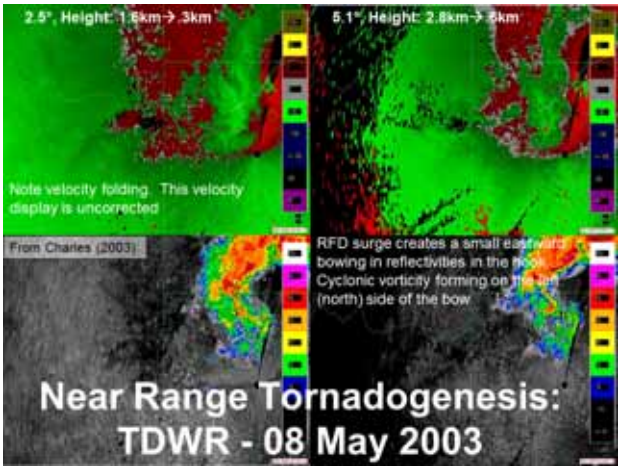

7. Convergence vs. Time Plots for Both Radars

Instructor Notes: An analysis of maximum convergence found at the lowest elevation from both radars show increasing values before first tornado. The improved TDWR temporal resolution results in more noise and sharper increases in the RFD convergence. Note that both show rapid increase in convergence less than 5 minutes before tornado time. Note that the trend line in the WSR-88D shows a false picture of slowly increasing convergence. Unfortunately, you only see the convergence represented by the data

points and thus the WSR-88D gives you less lead time to convergence increase than the TDWR. The TDWR maximum convergence exceeds .02 s-1, a third higher than that of the WSR-88D.

Student Notes:

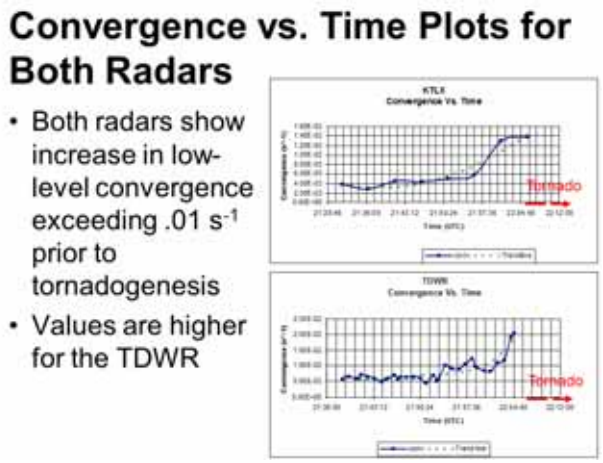

8. Near Range Tornadogenesis TDWR Reflectivity Signatures

Instructor Notes: The one minute resolution of the TDWR is just about enough to track individual reflectivity patterns northwest to southeast along the hook echo channel. As this loop proceeds, the onset of the debris signature in the TDWR occurs right as the damage track begins. The WSR-88D cannot detect it as early. During the event, forecasters, and ham radio operators were able to relay minute by minute positions of the tornado as it plowed through Moore and South Oklahoma city. This level of communication helped emergency responders at a level not done before.

Student Notes:

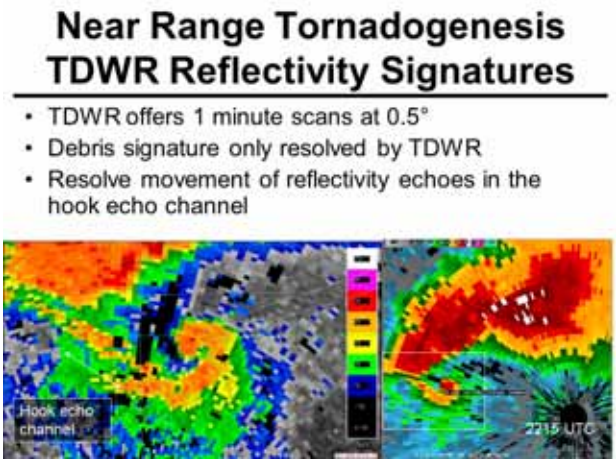

9. TVS Delta-V

Instructor Notes: The TDWR should provide stronger values of velocity difference in the TVS signature than the WSR-88D. Stronger may not be necessarily better when assessing tornado potential since just about all TVSs may appear stronger with finer resolution. However, the chance for early detection of a tornadic circulation is much greater with the TDWR. Given the better temporal resolution, the structure of the time/height trends show more detail. In either case, both KTLX and the TDWR clearly show the TVS signature strengthen during the mature stages of the tornado.

Student Notes:

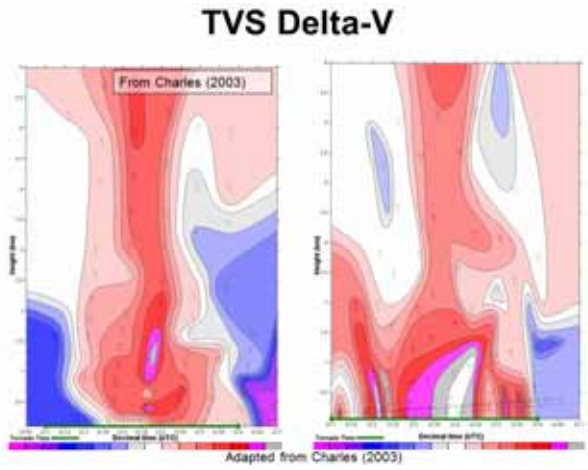

10. Accuracy of WSR-88D and TDWR TVS Track vs. Damage

Instructor Notes: Finer resolution does mean finer accuracy in positioning the tornado with the TDWR. Upon zooming in on the F-scale contour damage map, the lowest slice circulation center of the WSR-88D (black line) is a quarter mile off from the axis of worst damage. The TDWR track (red line) is just about dead center on the damage.

Student Notes:

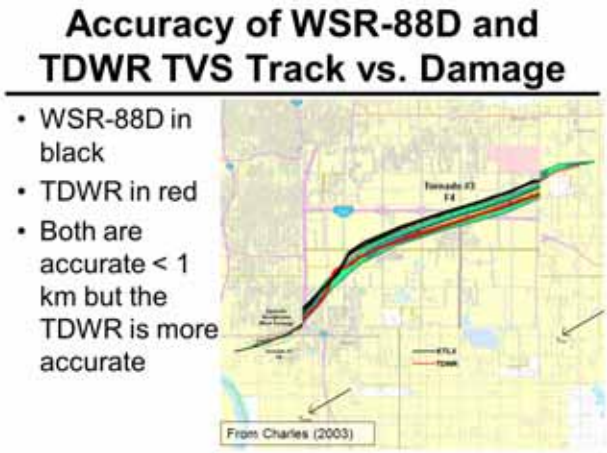

11. TDWR: Case #2

Instructor Notes: Another case has been published in Weather And Forecasting by Larry Dunn and Steve Vasiloff where the TDWR data were compared to the WSR-88D for the Salt Lake City tornado. The differences in distance between these two radars is much greater, with the TDWR in close proximity to the damage track. The fine resolution and number of beams below the 0.5° slice of the KMTX WSR-88D make the TDWR there indispensable for analyzing small features in the Salt Lake Valley. The tornadic storm here barely showed any gate to gate signature, labeled as “max GTG” with the storm as it scoured a damage path through downtown.

Student Notes:

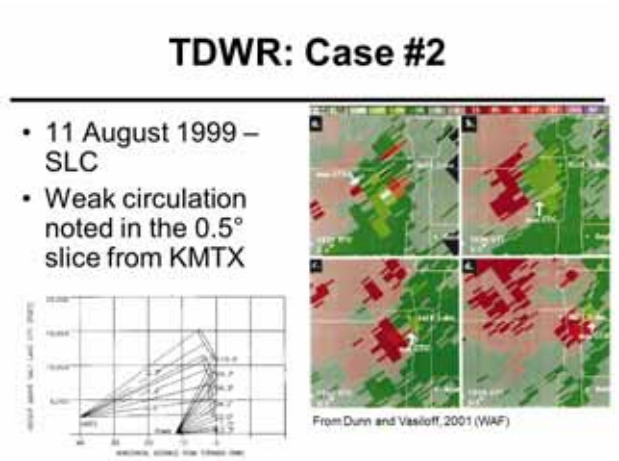

12. TDWR Data of SLC Tornado

Instructor Notes: The TDWR data, only 14 km (8nm) in range, and with numerous low slices below the lowest slice of KMTX, shows an accurate evolution of this tornado as a near surface-based vortex extending upward into the storm near 1840 UTC. A small hook echo feature and even a BWER forms around the vortex at the end of the loop. This TDWR did not have a one minute lowest slice sampling period but with its proximity, provided high quality information on the tornado vortex.

Student Notes:

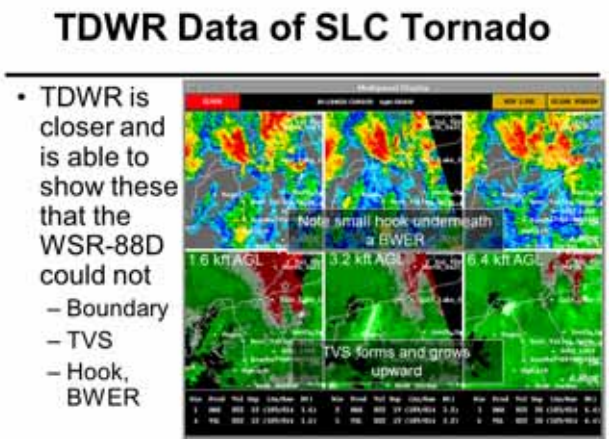

13. Summarizing: TDWR vs. WSR-88D in Near Range Tornadoes

Instructor Notes: The TDWR offers you excellent resolution and temporal frequency. However, given other factors favoring the WSR-88D, the TDWR will serve as an enhancement to the current network, and certainly not a replacement. Note the strengths of each radar are colored in yellow. The WSR-88D's advantages lie in its coverage, and high unambiguous velocities. Vmax, and it is under NWS control. The TDWR's strengths are its better spatial and temporal resolution.

Student Notes:

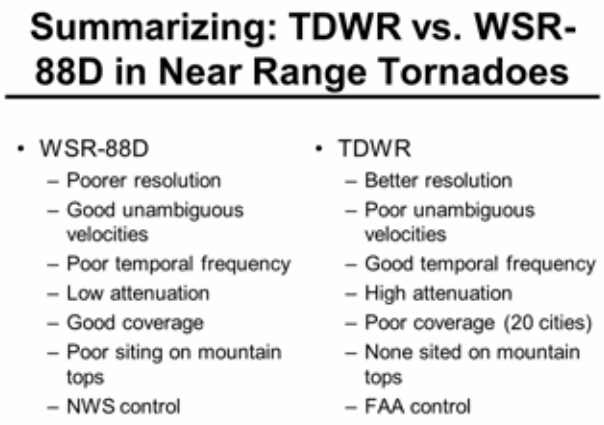

1. Supercell Collapse Phase

Instructor Notes: Hi, my name is Les Lemon and I would like to welcome you to this instructional training component dealing with the supercell storm collapse phase.

Student Notes:

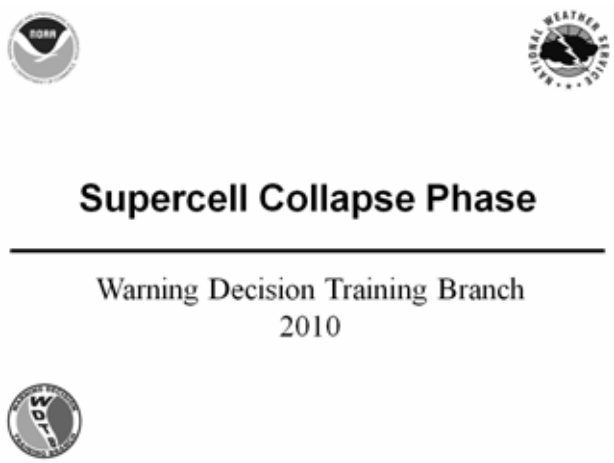

2. Training Objectives

Instructor Notes: At the conclusion of this module and without aids the student will be able to define the supercell collapse phase, identify its characteristics, identify the variations of the collapse phase, and to identify the significance of the supercell collapse. Finally, the student will be able to identify the importance of the supercell collapse to warning decision making and to the warning forecaster.

Student Notes:

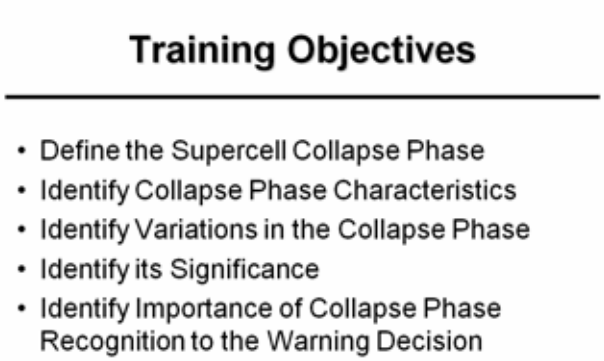

3. Supercell Collapse Phase

Instructor Notes: Here we will see that the supercell collapse phase, associated with mesocyclone occlusion, is characterized by a relatively ‘rapid’ reflectivity echo weaken-

ing and loss of the reflectivity supercell storm structure. We will see that during tornadogenesis all or part of the supercell updraft is disrupted and the storm can become multicellular and non-severe, reorganize as a mature supercell, or die. Sometimes the process affects only a portion of the updraft, at other times it disrupts the entire storm updraft. As the collapse proceeds the warning forecaster must pay careful attention to the velocity character or he/she can be mislead into thinking the storm is weakening and may no longer be a threat when, in fact, the tornado is just beginning or is ongoing. It is important to understand that not every tornadic supercell undergoes this collapse phase. But the purpose of this module is to alert the warning forecaster to this antithetical situation.

Student Notes:

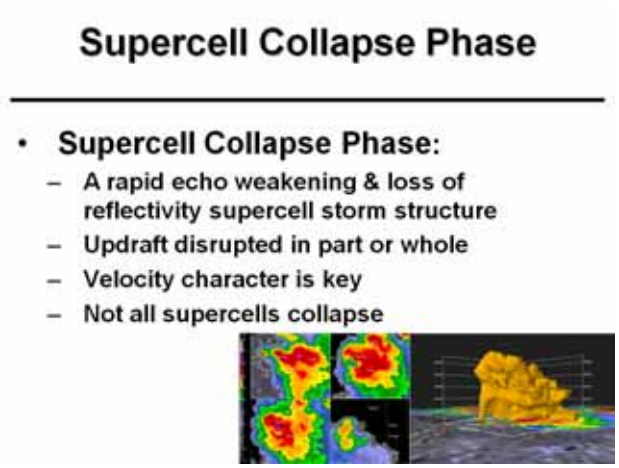

4. Early Work on Collapse

Instructor Notes: While Browning (1965) made the first observations hinting at the collapse phase (rapid hail size decrease, hook echo 'wrap up') it wasn't until Burgess (1974) that additional observations more strongly suggested a collapse phase. Here low-level (white) echo is seen as compared to mid-level echo overhang, (black). As a series of five tornadoes and a damaging wind swath began at 1700 CST the low-level hook echo was seen to "wrap-up" with echo top above (1700 – 1720). By the last damaging wind and tornado were occurring at 1740 the overhang had vanished; the Doppler radar mesocyclone was engulfed in strong echo (heavy rain and some hail) and the declining echo top above. The echo top and BWER collapse are illustrated here as the severe weather was occurring. Burgess termed this the collapse phase for obvious reasons. Following collapse, the storm was non-severe and a member of a squall line.

Student Notes:

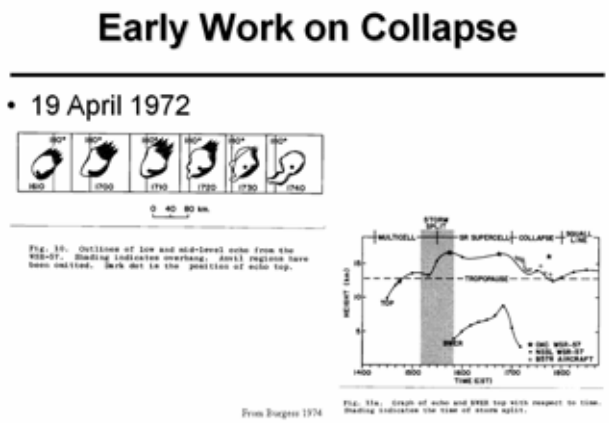

5. Early Work on Collapse

Instructor Notes: Arguably, the most thoroughly documented tornadic storm at the time, the Union City, OK storm inflicted F5 tornadic damage near the small hamlet on 24 May, 1973. In a comprehensive report it was shown that as the echo top and BWER B both collapsed surface tornadogenesis commenced (1536 CST). The tornado continued on as it enlarged and intensified. Simultaneously the echo overhang (dense stippling) descended around the occluding mesocyclone and tornado (star) as both migrated toward the rear of the storm. Doppler velocity data indicated that during the initial stages of reflectivity collapse the mesocyclone intensified and decreased in diameter and a TVS developed. The TVS developed aloft within the mesocyclone at 1517 CST and descended reaching the surface at 1536 CST. As the tornado weakened the mesocyclone broadened, decreased in vertical depth, and also weakened. Similar to the 19 April storm, at the conclusion of the collapse phase the Union City storm had again become a non-severe, multicellular storm and part of a squall line.

Student Notes:

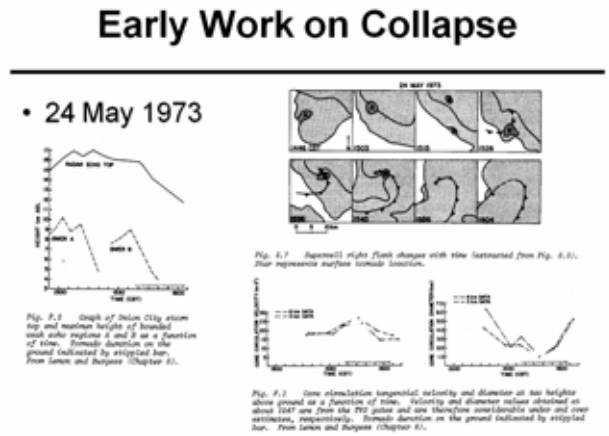

6. Early Work on Collapse

Instructor Notes: This 18 June storm was a very large supercell propagating slowly into the mean wind. Note that following BWER collapse and during tornado production the storm summit began a slow but fluctuating decline until the storm became a non-severe multicellular storm. The second study here again documented a general decline in reflectivity structure and weakening while the mesocyclone amplified and occluded while tornadoes occurred. Even though not shown here, the depth of the high reflectivity diminished and VIL declined. This storm also became multicellular and non-severe.

Student Notes:

Early Work on Collapse

- 18 June 1973 & 8 June 1974

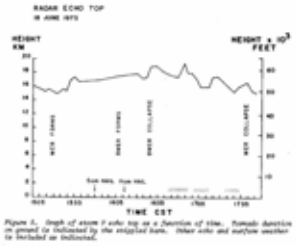

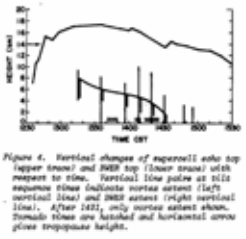

7. Supercell Collapse Phase: Reflectivity Characteristics

Instructor Notes: To summarize previous studies, during tornadogenesis and in some cases as the tornado increases in size and strength, the supercell collapse phase is revealed in reflectivity data by a rapid loss of supercell storm structure. In other words, the hook echo is seen to “wrap up” and disappear as the BWER and echo top descends and as the WER collapses downward. Overall, the echo top lowers, reflectivity weakens and the depth of the higher reflectivity diminishes as does VIL. These earlier studies found that this process is symptomatic of substantial updraft weakening leading to weakening of the entire storm. In fact, in the earlier studies, most of these collapsed storms became non-severe and multicellular as they were absorbed into squall lines. However, as we shall see later, only a portion of the supercell updraft may be affected.

Student Notes:

Supercell Collapse Phase: Reflectivity Characteristics

During Tornadogenesis & as tornado increased:

1. Rapid loss of reflectivity supercell storm structure –
   a. Hook Echo "wraps up", Bounded Weak Echo Region (BWER) fills with echo & disappears, Weak Echo Region (WER) disappears
2. Overall Storm Reflectivity Weakens
   b. Echo top lowers, reflectivity weakens, high reflectivity depth diminishes, VIL diminishes; all indicate updraft weakening
3. May involve entire storm updraft or only a portion

8. Supercell Collapse Phase: Velocity Characteristics

Instructor Notes: As the reflectivity structure of the collapsing supercell is diminishing the velocity characteristics are undergoing amplification. The mesocyclone shear/rotational velocity increases typically in lower levels. Contemporaneously the circulation may decrease in diameter and its depth increase. With the amplification of the mesocyclone, a TVS may develop and become detectable within the mesocyclone aloft and/or in low-levels. The overall reflectivity weakening may well be associated with RFD strengthening, surface gust front occlusions, and cutoff of low-level inflow.

Student Notes:

Supercell Collapse Phase: Velocity Characteristics

- As reflectivity structure weakens supercell velocity structures amplify
  a. Mesocyclone shear/rotational velocity increases near surface
  b. Mesocyclone diameter may decrease
  c. Mesocyclone depth often increase
  d. TVS often develops aloft and/or near surface
  e. RFD gust front occludes cutting off inflow

9. Supercell Collapse Phase: An Example – The Electra Storm

Instructor Notes: Here we will examine a supercell storm that occurred near Electra, TX on April 7th 2008. This photo was taken looking west toward the slowly rotating wall cloud from under the rain-free updraft base at about 21:50 CST. The wall cloud is the location of the updraft core and is tapping very moist contact layer air having originated in

the precipitation cascade and forward flank downdraft region. A few thousand feet above this cloud base a tornadic vortex was descending toward the surface.

Student Notes:

10. Supercell Collapse Phase: An Example – The Electra Storm

Instructor Notes: Just before the previous photo, the 0.5 degrees reflectivity echo of the mature isolated supercell is seen only 14 miles south of the KFDR radar as the storm moves east-southeast at 20 kts. It exhibits a well defined hook echo bounding the inflow notch to the west. The area where the wall cloud is located is in indicated here. The wall cloud itself is within but much smaller than this circle. Using GR2Analyst software we can see the large 3-dimensional 45 dBZ echo region surrounded the BWER. Because of the proximity of the storm to the radar, the upper surface of this echo is truncated by the cone of silence but very likely extends upward to a height greater than 45 kft. Using the GR2Analyst velocity processing algorithm we can also see the TVS aloft above the hook echo end and wall cloud. Note the TVS extend from a relatively short distance above the surface upward to near 30 kft.

Student Notes:

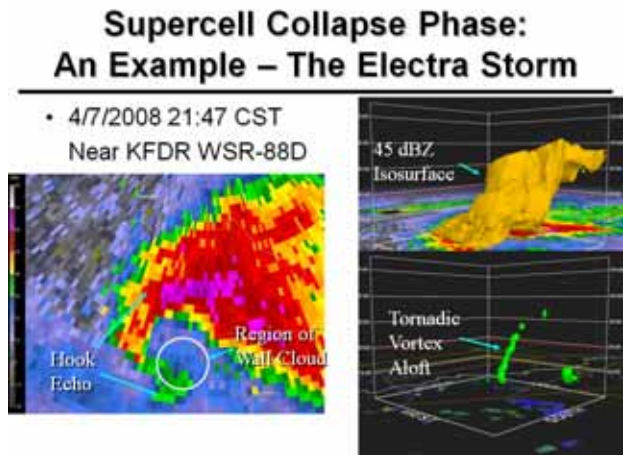

11. Supercell Collapse Phase: An Example – The Electra Storm

Instructor Notes: Again, looking west about 12 to 15 minutes later the dark, rain-free, cloud base of the primary supercell updraft is little changed but the wall cloud has now shifted back near the western edge of the primary updraft and the "clear slot" of the rear flank downdraft is seen rotating from the west and south around to east side of the wall cloud. And now, while the condensation funnel of the tornado is not in contract with the surface the vortex itself is and has been for about the last 4 minutes. Thus, the tornado is underway at this time.

Student Notes:

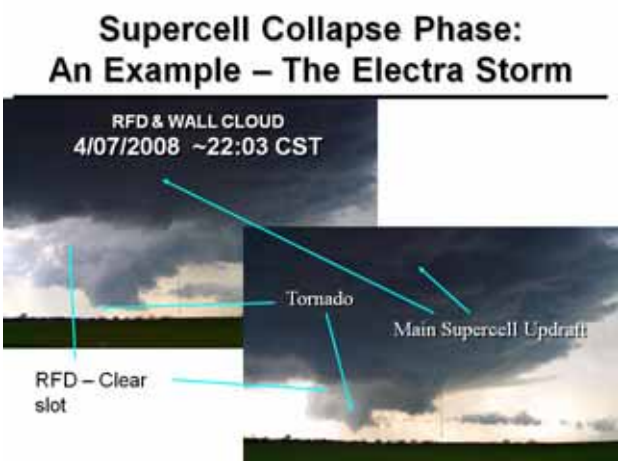

12. Supercell Collapse Phase: An Example – The Electra Storm

Instructor Notes: At the same time as the previous visual cloud appearance, the low-level reflectivity echo is seen here. The shank of the previous hook echo has pulled back northward and eastward from its previous storm-relative position. The wall cloud and tornado, just shown, is located within the encircled area and the wrapping clear-slot here. Aloft the old BWER has filled with echo while a new BWER is developing along with a new low-level hook echo here. There has occurred a substantial decrease in the hook and tornado associated 45 dBZ echo and the top of that portion of the supercell has fallen substantially to about 35 kft. We can see here that the surface tornado and TVS aloft still extends upward to about 30 kft as it moves northward at 15 kts.

Student Notes:

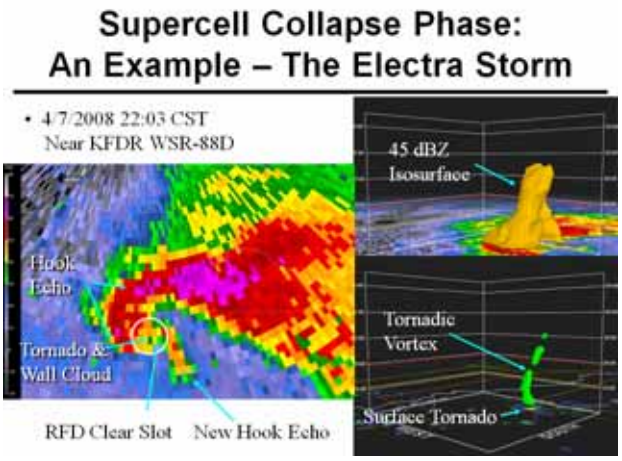

13. Supercell Collapse Phase: An Example – The Electra Storm

Instructor Notes: Just one volume scan later the 45 dBZ isosurface associated with the collapsing tornadic updraft is seen here. The TVS has also decreased in vertical depth to ~ 17 kft but the tornadic surface vortex is still present. Finally, by the 22:11 volume scan what is left of the original supercell updraft is shown here. It is a very small region of 45 dBZ extending upward to perhaps 12 kft! All that remains of the tornado is a rapidly weakening surface vortex with small vertical extension. Note the perspective has changed here so we can see to the rejuvenated primary supercell updraft and structure with overhang and BWER (just beneath storm summit). The supercell continued moving east-southeast with slow weakening for the next 40 minutes but without additional tornadoes.

Student Notes:

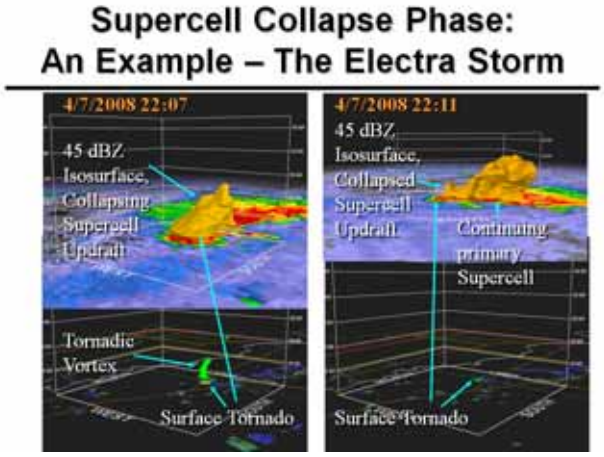

14. Electra Storm Summary

Instructor Notes: In this case study we began with an archetype large mature supercell storm, mesocyclone, hook echo, Weak Echo Region, and Bounded Weak Echo Region. A Tornadic Vortex Signature or TVS develops aloft within the mesocyclone as the collapse begins, signaled by a filling BWER and weakening portion of the supercell updraft. The hook echo, in a storm relative fashion, moves northward. As the collapse proceeds, visually a clear slot is seen to develop and encircle the developing tornado and wall cloud which has now shifted, storm relative, to the west and north of the primary supercell updraft cloud base. As this is occurring visually, on radar the TVS aloft lowers toward the surface as the updraft portion shrinks. That tornado persists at or very near the surface for 12 to 15 minutes before dissipating. A new hook echo has developed and the original but rejuvenated supercell updraft continues moving east-southeast but without further tornadoes.

Student Notes:

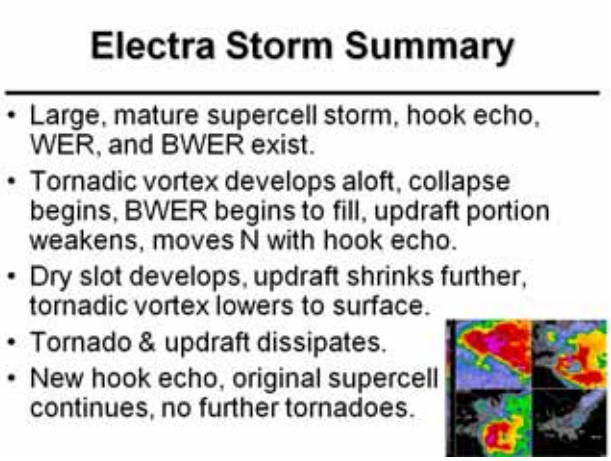

15. Supercell Collapse - Operational Impact?

Instructor Notes: What is the supercell collapse impact on operational applications? The warning forecaster must be careful not to be mislead by the supercell reflectivity structural weakening. During such, tornadogenesis may be taking place or an existing tornado may be continuing or even enlarge and strengthen. The warning forecaster must be vigilant to continue a tornado warning unless and until both reflectivity and the velocity storm characteristics weaken. The collapse may disrupt and weaken the entire storm updraft or it may affect only a portion of the updraft as with the Electra storm. During supercell updraft collapse, storm spotter reports are especially important. This is especially true because the mesocyclone and TVS (if detected) often have reduced vertical depth.

Student Notes:

Supercell Collapse - Operational Impact?

- Threat continues despite supercell reflectivity structural weakening.
- Tornadogenesis often as supercell weakens.
- Continue warning unless ***both reflectivity*** & ***velocity*** features disappear.
- Can affect entire or part of storm & updraft
- Spotter reports especially critical during weakening indicators.

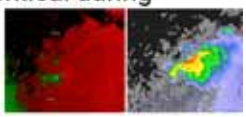

16. Supercell Collapse Phase

Instructor Notes: We have examined an aspect of some supercells called the collapse phase. The warning forecaster must be alert to the fact that not all supercells seem to exhibit this phase but some do and when it occurs the forecaster may me mislead. Should you have any questions, please contact Les Lemon at Les.Lemon@noaa.gov

Student Notes:

Supercell Collapse Phase

- We have examined an aspect of some supercells called the collapse phase. The warning forecaster must be alert to the fact that not all supercells seem to exhibit this phase but some do and when it happens the forecaster may me mislead.
- Should you have any questions, please contact Les Lemon at Les.Lemon@noaa.gov

17. REFERENCES

Instructor Notes: Here are a number of references should you wish to pursue the subject further.

Student Notes:

REFERENCES

- Brown, R. A., D. W. Burgess, and K. C. Crawford, 1973: Twin tornado cyclones within a severe thunderstorm: Single Doppler radar observations. **Weatherwise, 26**, 63-71.
- Browning K. A., 1965a: A family outbreak of severe local storms - A comprehensive study of the storms in Oklahoma on 26 May 1963. Part I: Air Force Cambridge Research Lab. Special Report No. 32, 346 pp.
- Burgess, D. W., 1974: Study of a right moving thunderstorm utilizing new single Doppler radar evidence. Masters Thesis, Dept. of Meteor., University of Oklahoma, Norman, OK, 77 pp.
- ———, D. W., and L. R. Lemon, 1976: Union City storm history. Chapter 5, The Union City, Oklahoma tornado of 24 May 1973. R. A. Brown, Editor. NOAA Tech. Memo. ERL NSSL-80, Norman, National Severe Thunderstorms Laboratory, 33-51.
- ———, D. W., R. A. Brown, L. R. Lemon, and C. R. Safford, 1977: Evolution of a tornadic thunderstorm. **Preprints**, 10th Conf. on Severe Local Storms, Boston, Amer. Meteor. Soc., 84-95.
- ———, D. W., 2004: High resolution analyses of the 8 May 2003 Oklahoma City storm. Part I: Storm structure and evolution from radar data. Preprints, 22nd Conf. Severe Local Storms, Hyannis, MA, Amer. Meteor. Soc.,
- Dowell, D. C., L.J. Wicker, and D. J. Stensrud, 2004: High resolution analysis of the 8 May 2003 Oklahoma City storm. Part II: EnKF data assimilation and forecast experiments. Preprints, 22nd Conf. Severe Local Storms, Hyannis, MA, AMS.,
- Lemon, L. R., D. W. Burgess, and R. A. Brown, 1976: Tornado production and storm sustenance. **Preprints**, 9th Conf. on Severe Local Storms, Boston, Amer. Meteor. Soc., 100-104.
- ———L. R., and D. W. Burgess, 1976: Tornadic storm airflow and morphology derived from single Doppler radar measurements. Chapter 8, The Union City, Oklahoma tornado of 24 May 1973. R. A. Brown, Editor. NOAA Tech. Memo. ERL NSSL-80, Norman, National Severe Thunderstorms Laboratory, 85-108.
- ———L. R., 1977: Severe thunderstorm evolution: its use in a new technique for radar warnings. **Preprints**, 10th Conf. on Severe Local Storms, Boston, Amer. Meteor. Soc., 77-80.
- ———L. R., 1979: Tornadic storm evolution: vortex value hypothesis. Appendix F, The Union City, Oklahoma tornado of 24 May 1973. R. A. Brown, Editor. NOAA Tech. Memo. ERL NSSL-86, Norman, National Severe Storms Laboratory, 228-234.
- ———L. R., 1977a: New severe thunderstorm radar identification techniques and warning criteria: a preliminary report. NOAA Tech. Memo. NWS NSSFC-1, Kansas City, National Severe Storms Forecast Center, 60 pp.
- ———L. R., D. W. Burgess, and R. A. Brown, 1978: Tornadic storm airflow and morphology derived from single Doppler radar measurements. **Mon. Wea. Rev., 106**, 40-61.
- ———, L. R., 1978b: Improved application of conventional radar data and satellite imaging to severe thunderstorm detection and prediction. **Preprints**, Conf. on Atmospheric Environment of Aerospace Systems and Applied Meteorology, Boston, Amer. Meteor. Soc., 154-158.
- ———L. R., 1980: Severe thunderstorm radar identification techniques and warning criteria. NOAA Tech. Memo. NWS NSSFC-3, Kansas City, National Severe Storms Forecast Center, 60 pp.

1. Storm Interrogation

Instructor Notes: AWOC Severe Track IC 3-VII-C, presented by Dan Miller, SOO at Duluth.

Student Notes:

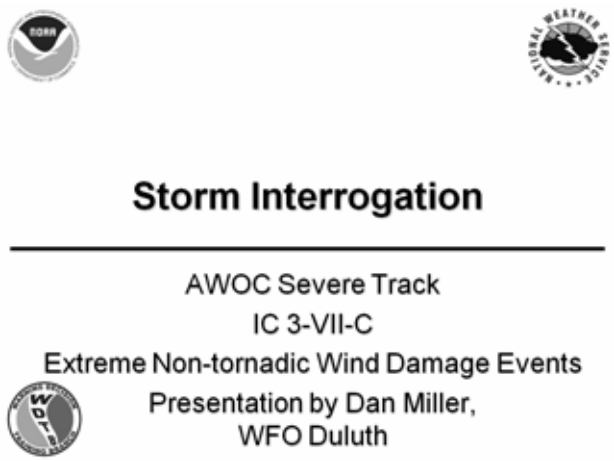

2. Extreme Non-Tornadic Wind Damage Events

Instructor Notes: Study of Extreme Non-Tornadic Wind Damage Events, or XDW events, began about 5 years ago and was motivated initially by a simple desire to document an event on 1 July 1997 in central Minnesota. After looking at that event in detail, and with level 2 WSR-88D data, it became apparent that the conceptual model of high-end non-tornadic wind events needed scrutiny, because many of these events do not fit well into the bow echo conceptual model very well when high resolution radar data is examined. The initial phase of the study was focused on derecho producing MCSs that resulted in exceptionally severe non-tornadic winds and/or wind damage. It should be emphasized that considerable effort was made to distinguish these events from “ordinary” derecho events, in that these events are a sub-set of derecho events, characterized by widespread forest blowdowns or wind damage areas that include observed damage of high-end F1 or greater intensity and/or peak measured wind gusts roughly 80 knots or greater. Two SLS conference papers has been published to date on this topic, and those publications are listed at the bottom of this slide.

Student Notes:

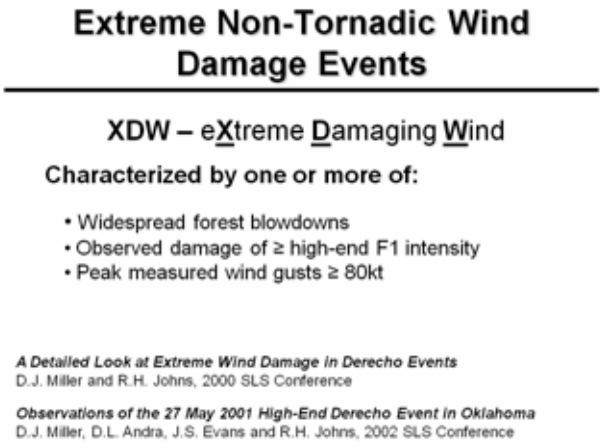

3. Objectives

Instructor Notes: Objectives Identify volumetric radar characteristics of extreme non-tornadic wind producing supercells within derecho producing MCSs. Understand storms-cale mechanisms for the production of extreme winds Understand suggested operational philosophies during warning operations

Student Notes:

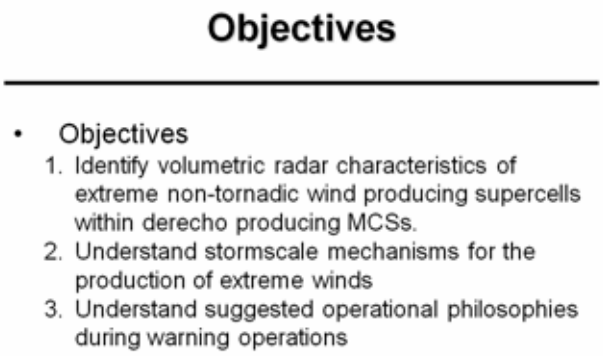

4. Motivation For Study

Instructor Notes: Additional motivations for further study are numerous. First, these events are the non-tornadic equivalent to tornado outbreaks, and although a qualitative study has not been done to date, it is quite likely that a disproportionate amount of the injuries, deaths, and damage from non-tornadic winds each year are due to XDW events. Second, many XDW events produce widespread damage areas that include consider-able areas of equivalent F1 damage, and some include quite sizeable areas of F2 equiv-alent damage. The figure at the top of this slide (from one of Dr. Fujita's publications) is an extreme example from 4 July 1977. The damage path is 166 miles long, and up to 17 miles wide, extending across parts of 6 counties in northern Wisconsin, and includes

widespread F1 damage (in the dark gray shading), and considerable areas of F2 damage (in the black shading.) Winds in this event were estimated at 100-120 mph winds with gusts up to 135 mph. One eyewitness account from this event stated that the intense wind continued for 20 minutes and was accompanied by large hail. Third, many XDW events produce just as much, if not more, dollars in damages than tornadoes, and injury/deaths can be comparable. For example, a major severe weather outbreak occurred on 30-31 May 1998 from the northern plains states eastward into much of the Great Lakes region. An F4 tornado struck the tiny town of Spencer, SD during the afternoon of the 30th, killing 6, injuring 150, causing $20 million in damage, and destroying over half of the town. Consequently, media converged on the town and provided several days of coverage. 6 years later, many remember the Spencer, SD tornado. However, what most DO NOT remember about this event is the very intense derecho event occurred during the overnight hours following the Spencer, SD tornado. This XDW event from the evening of the 30th, through the morning of the 31st, affected areas from central Minnesota, eastward across Wisconsin, Lake Michigan, Lower Michigan, extreme northern Ohio, Lake Erie, and far western New York State, resulting in 6 fatalities, 209 injuries, and $291 million in damage. The winds also resulted in a 4 foot seiche on Lake Michigan, that was the primary factor in the sinking of a ship in port on the eastern shore of the lake. It is only a matter of time before an event like this affects a major metro area, perhaps during rush hour, that could result in event greater loss of life and property. There is much improvement that can be done with respect to forecasting and warning for these events, and increased situation awareness to these events is the primary goal of this module.

Student Notes:

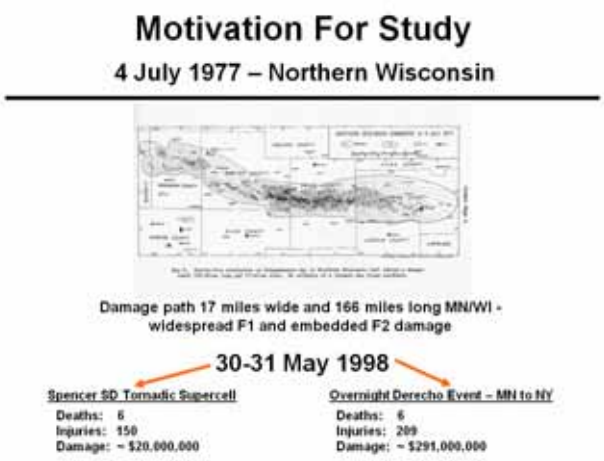

5. Extreme Non-Tornadic Wind Damage Events

Instructor Notes: To drive home the point, this slide shows a now somewhat-famous video taken during an XDW event in the Pakwash forest of northwest Ontario, Canada on 18 July 1991. Incidentally, this video was taken on the edge of a large forest blowdown area. Damage in the center of the blowdown path was described as considerably more severe than at the location where the video was taken. The entire video is about 15 minute long, and shows three separate pulses of extreme winds, within a period of sus-

tained winds ~50-60 mph. There was no hail in this video, but in some XDW events, particularly ones that involve supercells, the intense wind can be accompanied by golfball to baseball size hail. As an interesting aside, note the time stamp on the video (which is accurate) – 1051 AM CDT.

Student Notes:

6. What Convective Elements Are Associated with XDW Events?

Instructor Notes: In investigating XDW events, it quickly became obvious that the best way to look at them was to define an XDW event, and then work backward to the radar data and 4-D storm structure evolution. So, what storm-scale convective elements are associated with XDW events? Many (most?) of these events are produced by forward propagating MCSs, and therefore are, by definition, part of a derecho event. As one might expect according to the widely held conceptual model (from Johns and Hirt, 1987, and many other papers) some events are produced by serial or progressive bow echoes. However, some of the forward propagating MCSs involved exhibit very complex 4-D reflectivity/velocity structure evolution, and involve circulations on the storm-scale. For the purpose of this presentation, we will focus on the MCSs that contain embedded supercell storm structures. A summary of events that have been studied in full or in part are listed on the slide.

Student Notes:

What Convective Elements Are Associated with XDW Events?

Non-Supercell (Serial or Progressive Bow Echo)
15 July 1995 – Upstate New York
30-31 May 1998 – Minnesota to New York

Hybrid (Line Mesovortex/Supercell structure)
30-31 May 1998 – Minnesota to New York
4 July 1999 – Northern Minnesota
22 July 2003 – Western Tennessee (Memphis event)
4 March 2004 – Texas/Oklahoma

Supercell (MCS with embedded supercells)
3-4 May 1989 Texas/Oklahoma
1 July 1997 – Central Minnesota
29 June 1998 – Central Iowa
27 May 2001 – Oklahoma
26 August 2002 – Western Kansas

7. 27 May 2001 - Oklahoma

Instructor Notes: The first case example we will look at occurred on 27 May 2001 in Oklahoma. This slide and the next provide a brief overview of the larger-scale environment that supported this MCS. The thermodynamic profile was characterized by very strong instability (surface-based CAPE approaching 5000 j/kg), and rich tropical moisture in the low levels (surface dewpoints in the low 70s F.) Also of note is the relatively low LCL height at 858 mb, which is roughly 2,500 meters AGL.

Student Notes:

27 May 2001 - Oklahoma

SBCAPE 4874 j/kg
MLCAPE 3279 j/kg
CIN 0 j/kg
LI -11
WBZ 11653 ft
700-500 LR 7.6 deg/km
LCL 858 mb

8. 27 May 2001 - Oklahoma

Instructor Notes: The wind shear profile, when viewed in combination with the thermodynamic profile as seen on the previous slide, reveals an environment that would easily support supercell thunderstorms, with surface to 6 km wind shear of 60 kts (30 m/s), and BRN shear of 67 m2/s2.

Student Notes:

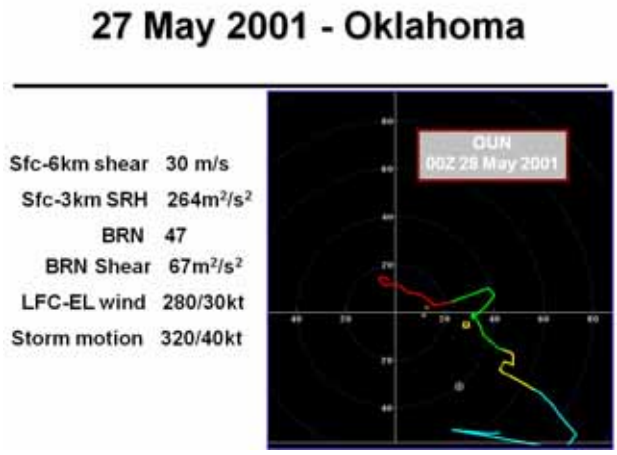

9. 27 May 2001 Radar Loop

Instructor Notes: This XDW event was produced by a forward propagating MCS that evolved from several discrete supercells over southwest Kansas. The annotated areas on the radar loop are corridors of XDW that were produced by this MCS (corridors were derived from a combination of Oklahoma mesonet peak winds, damage reports, and damage surveys conducted by local emergency managers.) Radar data viewed at this scale, suggests that this was a rapidly moving and large-scale bow echo. However, if one studies the loop carefully, individual storm elements can be identified, that coincide with the corridors of XDW. These elements are supercells embedded within the MCSs, and we will examine the storm structure in detail on the next several slides.

Student Notes:

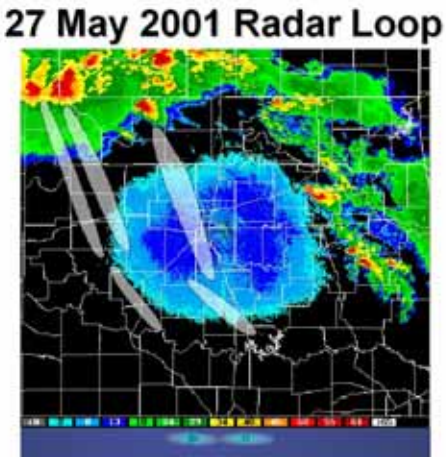

10. State-Scale Radar Data 0210 UTC

Instructor Notes: The image on this slide is a state-scale reflectivity image from the central Oklahoma Twin Lakes WSR-88D (KTLX) at 0210 UTC 28 May 2001. Again, viewed at this scale, the MCS at first glance appears to be a large-scale bow echo. However, on the next slide we will zoom in on the area within the white square.

Student Notes:

11. Volumetric Radar Data

Instructor Notes: Here is the volumetric reflectivity/velocity data from the white box on the previous slide at 0210 UTC. Reflectivity (top) and velocity (bottom) data are shown at roughly 4,000 ft agl (left), 20,000 ft agl (center) and 43,000 ft agl (right), which should provide a representative view of the storm at low, mid and high levels, respectively. The reflectivity core is strong and very deep, with 55+ dBz echo evident up to at least 43,000 ft, with significant mid and upper level overhang to the inflow (south) side of the storm. A rather large and high reflectivity hook echo is also evident in the low levels. Velocity data at low levels clearly indicates a cyclonically convergent mesocyclone that is displaced slightly to the lower reflectivities on the inflow flank. In the mid levels, a strong mesocyclone is evident (although there are velocity dealiasing errors in the radial inflow velocities), that is co-located with the high reflectivity core. At high levels, strong anti-cyclonic divergence is indicated near the storm summit. The combination of these reflectivity and velocity signatures is exceptionally consistent with the conceptual model of radar-observed supercell storm structure, and indicates a mature (likely Hp-type) supercell embedded within the MCS. The location just on the upshear flank of the low-level mesocyclone was directly associated with a long-tracked XDW corridor.

Student Notes:

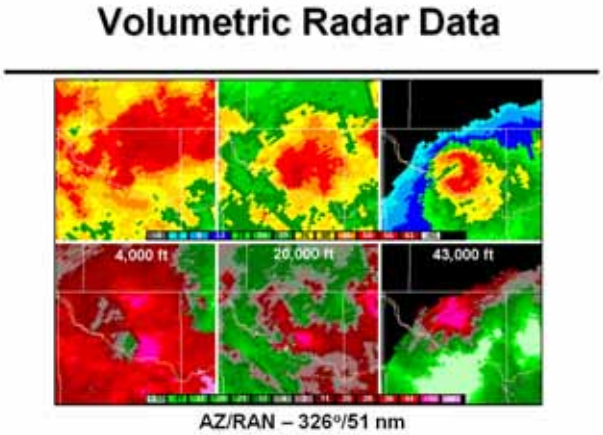

12. State-Scale Radar Data 0230 UTC

Instructor Notes: At 0230 UTC, we will zoom in and examine an area farther to the west in the quasi-linear MCS. On the next slide, we will look at volumetric reflectivity data from the area highlighted in the white box.

Student Notes:

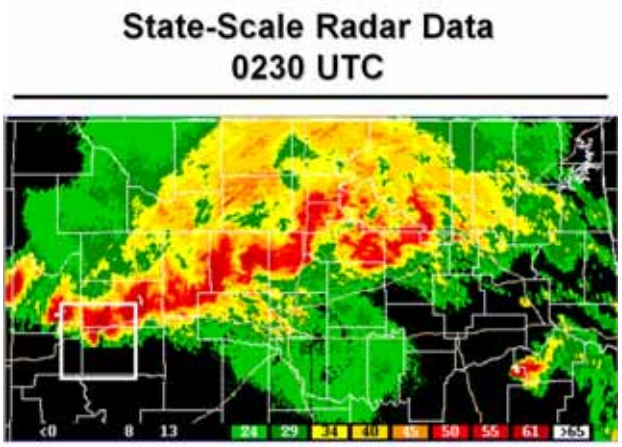

13. Volumetric Radar Data

Instructor Notes: Radial velocity data at this location was range-folded. However, the volumetric reflectivity data reveals a lot. We are somewhat limited in sampling the lower levels of the storm at a range of 93 miles, but at 10,000 ft agl, an notch on the inflow side and a well-defined hook echo are clearly evident. At 20,000 and 30,000 ft agl, a very well-defined bounded weak echo region is present, with the storm summit and highest reflectivities at 40,000 ft agl displaced to the inflow side, directly above the inflow notch at low levels. This feature was present for over 30 minutes, and again is clear evidence of a mature, intense and long-lived supercell updraft. This embedded supercell was responsible for another long corridor of XDW over western Oklahoma.

Student Notes:

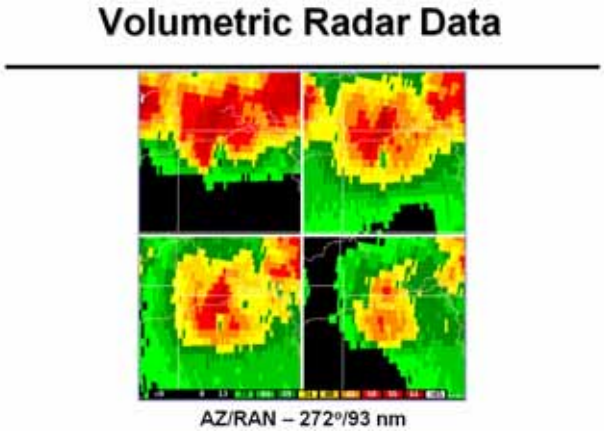

14. State-Scale Radar Data0249 UTC

Instructor Notes: Finally, at 0249 UTC, we will zoom in and examine a storm in the MCS immediately to the west of the storm we examined in slides 8 and 9. On the next slide, we will look at volumetric reflectivity data from the area highlighted in the white box.

Student Notes:

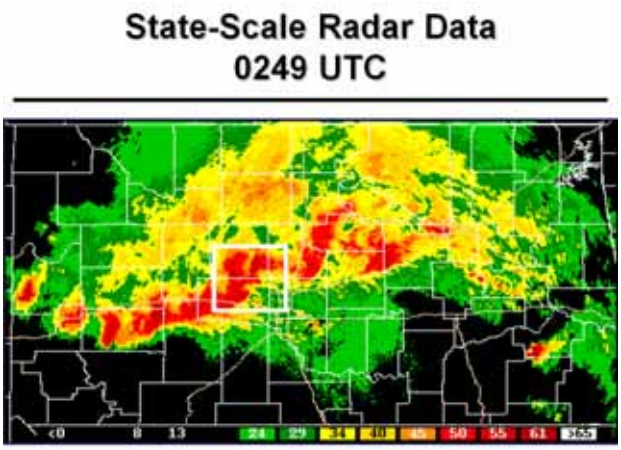

15. Volumetric Radar Data

Instructor Notes: This slide shows volumetric reflectivity/velocity data from the third storm embedded within the MCS at 0249 UTC. This storm was located immediately to the west of the storm that we looked at in slides 8 and 9 at 0210 UTC. Again, reflectivity (top) and velocity (bottom) data are shown at roughly 3,000 ft agl (left), 19,000 ft agl (center) and 42,000 ft agl (right). Very similar signatures are evident. The reflectivity core is strong and very deep, (although the highest reflectivities are a bit more shallow than the 0210 UTC storm we looked at) with 50+ dBz echo evident at 42,000 ft, with significant mid and upper level overhang to the inflow (southeast) side of the storm. A rather large and high reflectivity hook echo is once again clearly evident at 3,000 ft agl. Velocity data at low levels clearly indicates a strong and unbalanced cyclonically convergent mesocyclone coincident with the low level reflectivity hook. The velocity image at 3,000 ft agl above is radial base velocity, and raw data sampling revealed nearly 100 kt inbound velocities at 3,000 ft agl. In mid levels, a mesocyclone is evident, co-located with the high reflectivity core. At high levels, strong anti-cyclonic divergence is indicated near the storm summit. Again, clear indication of a mature (HP-type) supercell embedded within the MCS. As with the other two storms we have looked at, locations just on the upshear flank of the low-level mesocyclone (underneath the location of strong inbound radial velocities) experienced XDW. This storm was responsible for considerable F2 structural damage in the city of El Reno, including taking the roof off of a hospital and city hall.

Student Notes:

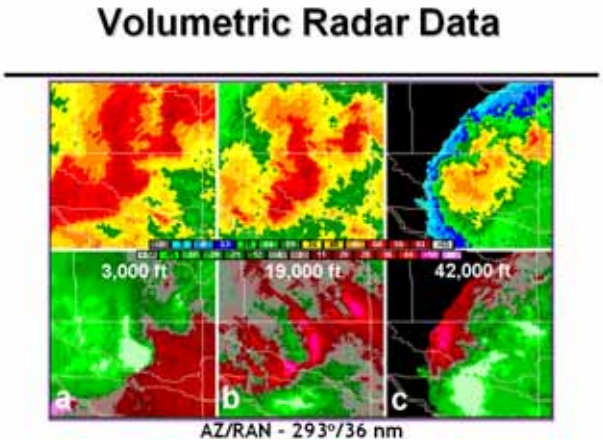

16. Relating Visual Appearance to Radar

Instructor Notes: Here is a photograph of the storm complex as it appeared in northwest Oklahoma, just before 730 PM local time (0030 UTC.) At this time, the MCS was still in the process of transitioning from discrete supercells, to a quasi-linear MCS with embedded supercells, but a common gust front and strong surface cold pool had already become established. The photo shows two distinct HP type supercell storms, linked by a common gust front. For comparison, the location of the photo is annotated on the lowest cut reflectivity image in the lower right, with the two arrows pointing to the two storms from their respective radar echoes.

Student Notes:

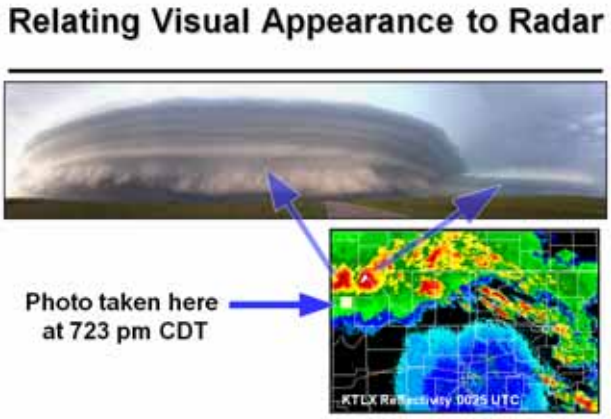

17. 1 July 1997 – Central Minnesota

Instructor Notes: It is also useful to provide an example from another part of the country. This is a 0.5 degree reflectivity loop of the 1 July 1997 MCS that produced an XDW event. The XDW areas are annotated in white on top of the radar loop. Much as in the Oklahoma case we just looked at, the MCS is quasi-linear, and at state-scale appears much as a large-scale bow echo.

Student Notes:

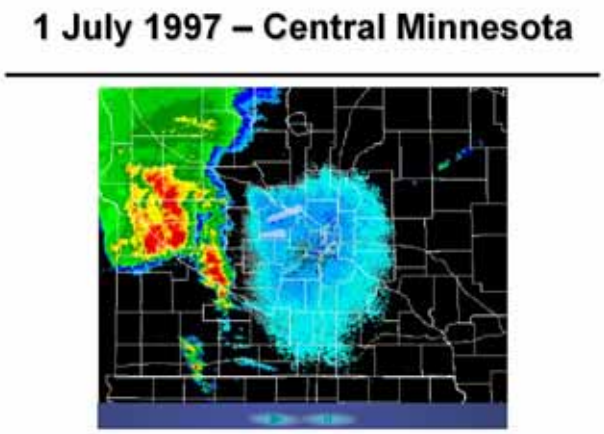

18. Volumetric Radar Data

Instructor Notes: This slide is an enlarged view of the volumetric radar data, zoomed in on Wright County, Minnesota at the time two corridors of XDW were in progress. Nearly identical volumetric reflectivity and velocity signatures are again clearly apparent, with the location of the XDW events placed just on the upshear flank of the low level mesocyclone, coincident with the precipitation filled rear-flank downdraft portion of the HP supercell.

Student Notes:

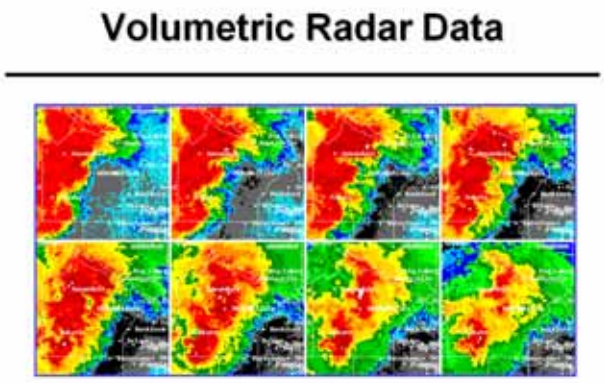

19. Ground-Relative Wind Production Mechanisms

Instructor Notes: So, why do XDW events seem to have a favored storm-relative location of occurrence? Primarily because of the juxtaposition of exceptionally strong storm-scale isallobaric wind accelerations near the surface, the ground relative winds in the near-surface mesocyclone circulation, and precipitation loading and column cooling from hail melt. The primary point is that these events appear to be much more complicated than a simple “downburst,” with a significant contribution to the extreme ground-relative wind speeds coming from storm-scale dynamic forcing.

Student Notes:

Ground-Relative Wind Production Mechanisms

Superposition of
1) Exceptionally strong storm-scale isallobaric accelerations
2) Maximum ground-relative winds within the mesocyclone circulation
3) Precipitation loading and
4) Column cooling due to melting hail

→ Overall message is that warning forecasters need to be keenly aware of an enhanced potential for wind damage (possibly high-end) when circulations are present

20. Pressure Perturbation Example

Instructor Notes: Meteograms from several XDW events indicate that a 5-10 mb pressure perturbation exists between the low under the updraft, and the high underneath the downdraft and cold precipitation core, and radar data suggests that separation of these storm-scale features was generally on the order of 5 to 10 miles. Most of the MCSs examined had forward propagation speeds of greater than 35 kts, and it follows that a very intense storm-scale isallobaric wind acceleration is likely a very strong contributor to the intense wind speeds.

Student Notes:

Pressure Perturbation Example

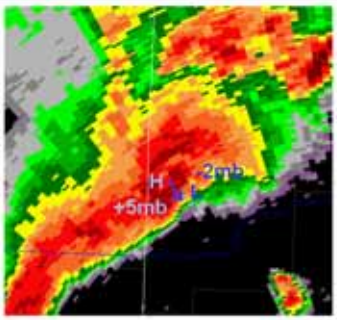

Much more than a simple 'downburst'

21. Location of XDW

Instructor Notes: This annotated velocity image simply shows where this area of the storm is located in the velocity imagery.

Student Notes:

Location of XDW

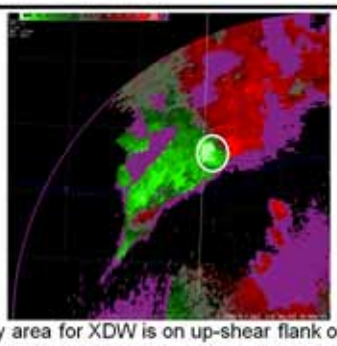

Most likely area for XDW is on up-shear flank of low-level mesocyclone and in the precip-filled RFD area

22. Unique? Characteristics of XDW Events

Instructor Notes: Much more research needs to be done, including obtaining data from new cases as they occur, to ascertain whether these XDW characteristics are generally the case with all XDW events. However, these characteristics were common in most cases examined thus far.

Student Notes:

Unique? Characteristics of XDW Events

1) Quite long in duration at any one location along the path (10-20 minutes - or longer in extreme supercell/mesovortex events vs. a few minutes or less for bow echoes)
2) Very tight damage gradients along the periphery of XDW area
3) Supercell events have a much higher probability of being accompanied by large hail (> 4cm)

23. Operational Considerations

Instructor Notes: The bullets presented here generally need little additional explanation. All are important things to remember when working an XDW event operationally. AWIPS and other operational procedures should be optimized to maintain maximum situation awareness during the event.

Student Notes:

Operational Considerations

- Supercells *within* a derecho producing MCS can be associated with an enhanced threat for XDW
- In *many* high-end derecho events - the most extreme damage is associated with supercells/mesovotices
- Supercell/Mesovortex XDW events *may* have somewhat different characteristics than "traditional" Bow Echo XDW events
- Events often move/evolve rapidly → timely flow of accurate information becomes *very* challenging
- Even high resolution surface mesonetwork observations may not be dense enough to completely capture storm-scale extreme wind events

24. Forecasting XDW 6-24 Hours Out

Instructor Notes: A few brief comments about forecasting these events. It should be emphasized that a qualitative study of environmental parameters has not been completed yet, primarily because the data set is still too small for results to be statistically significant. With addition of additional cases as they occur, hopefully the data set will reach a critical mass soon. With that said, there are a few general points about forecasting these events that can be stated from anecdotal and observational evidence. First, the fact that most of these events occur in tornado watches, and many in PDS tornado watches, seems to suggest that there is a significant overlap in the large-scale environmental conditions that support both XDW events and significant tornado events (strong instability, strong surface-6 km shear, strong surface-1 km shear, low LCL/LFC heights, etc.) It seems as though event type is highly dependent on convective mode (discrete supercells vs. MCS development.)

Student Notes:

Forecasting XDW 6-24 Hours Out

- Almost all of these events have tornado watches
  - → *many* have PDS tornado watches
- Significant overlap of atmospheric conditions between XDW events and tornado outbreak days
- Event type/evolution seems to be highly dependent on convective mode

25. Tips for AWIPS D2D Display

Instructor Notes: Here are a few tips for AWIPS procedures and conveying information to users in warnings, statements and graphical products.

Student Notes:

Tips for AWIPS D2D Display

- All tilts, in combination with judiciously constructed 4-panel displays from multiple radars, is exceptionally useful in seeing the 4-D storm structure evolution
- Remember to keep at least one radar panel paired with 8bit base velocity
- Possible to be fairly confident about specifics of enhanced wind damage area in warnings/statements and graphical products

1. QLCS storm-scale interrogation and warning considerations

Instructor Notes: Welcome to the AWOC Severe lesson on QLCS storm-scale interrogation and warning considerations. This lesson is 43 slides long and will probably take 45 minutes to take. Jim LaDue of WDTB and Ron Przybylinski, the SOO at NWS St. Louis, MO, will be your primary instructors.

Student Notes:

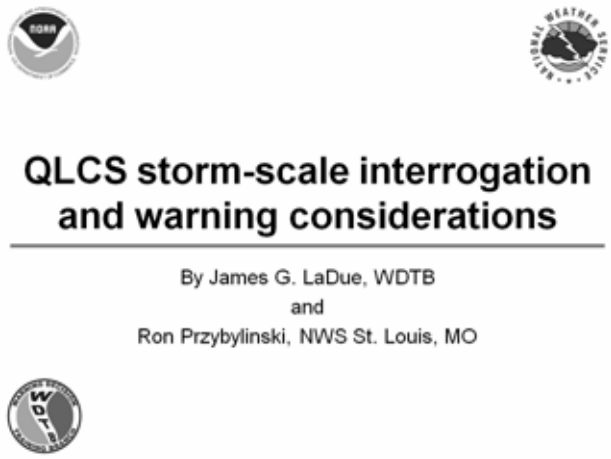

2. Objectives

Instructor Notes:

Student Notes:

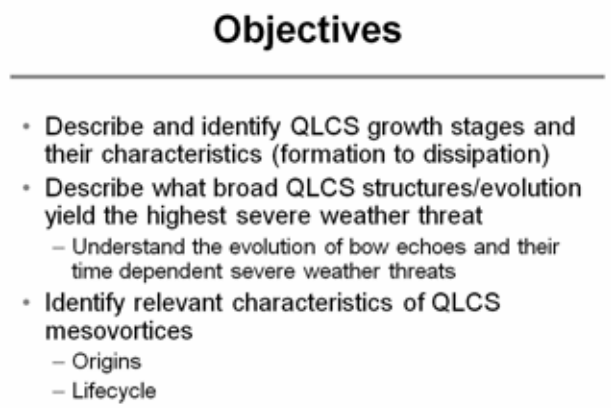

3. Objectives, contd

Instructor Notes:

Student Notes:

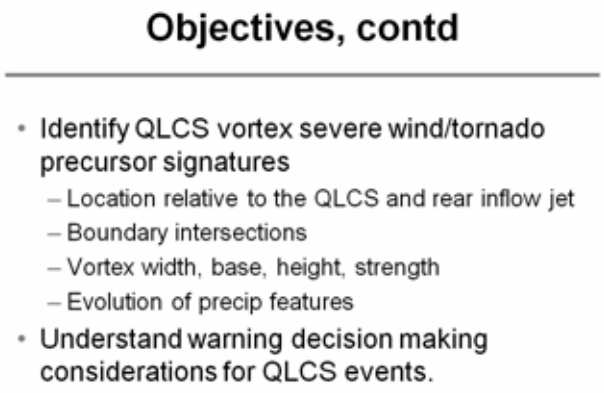

4. Generic Lifecycle of a QLCS

Instructor Notes: This is to answer what stage in a QLCS lifecycle is most likely to produce most severe wind (tornado) potential. We typically evolve convective systems from a point where the updraft is primarily the dominant feature and the cold pool is yet too immature to interact with a the sheared environment. If we were in an environment where deep-layer shear is capable of supporting supercells and severe QLCS events, we would most likely see supercells in this case because the shear dominates the cold pool and the shear would interact primarily with the updrafts. We wouldn't expect to see QLCS-based mesovortices or cold pool-induced severe winds in this stage. As the original small multicells, whether clusters, or a line segment, merge and begin producing an enhanced cold pool, you finally have a period in which it becomes a significant contributor to the morphology of the updrafts. The lifting on the cold pool becomes more aggressive allowing for more widespread updraft formation, and the updraft tilt becomes as much a function of the cold pool as the environmental shear. There's a period in time where the cold pool balances well with the environmental shear allowing for deep, upright updrafts along the gust front. Lifting along the gust front forms the base of the updraft and the balance between the cold pool vorticity and the environmental shear forces that updraft to stand upright. If the shear continues through the deeper layer in the atmosphere, the updraft maintains its upright character and eventually overturns in both forward and backward trajectories forming the anvil. This is the tall echo stage of an impending severe QLCS event where the strongest MARC signatures prevail. Sometimes when bows form, they remain in the tall echo stage if the cold pool and shear remain balanced and deep convective overturning continues in the upper-levels. More likely the updraft depth decreases as the bow forms as the cold pool begins to race ahead. The more severe bows still maintain a deep gustfront with strong slab-like updraft from near surface to 20 kft AGL but then the updraft quickly tilts rearward. When you recognize the tall echo phase, you'd maximize your odds of verifying on a warning with adequate lead time. If the cold pool becomes too dominant, it begins to outrun the deep updraft leading to the gust front outrunning the deep convection. The updrafts often lose their slab-like lifting appearance and begin to breakup into a more cellular appearance. This kind of structure can appear along the edges of a bowing echo because in those

areas, the cold pool dominates the shear. How is that possible? Well, it's really the component of the shear perpendicular to the gust front that's important and gust front bends back along the edges of a bow.

Student Notes:

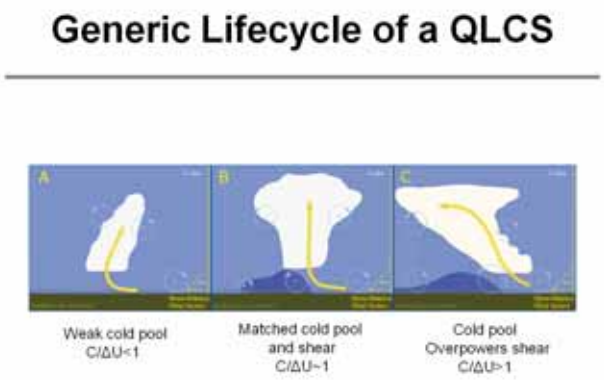

5. 3-D QLCS structure

Instructor Notes: The most severe QLCS events typically have and upright updraft with almost slab-like appearance along a deep gust front. The convection is able to remain attached to the gust front and so on radar, you may not actually see a separate fine line from the intense reflectivity cores. A deep convergent zone accompanies the gust front. On some occasions, and after accounting for system motion during volume scanning, you may see a strong echo overhang leading the reflectivity core. Rear inflow notches signify intense RIJ channels. The RIJ remains elevated to descend only immediately behind the convective line. Lightning often precedes the arrival of the line. Mesovortices are common with these structures as there is plenty of deep updraft over their formation regions. The less severe events exhibit more isolated convective cells often displaced well behind the gust front. A separate fineline is often visible ahead of the first reflectivity cores. The gust front is often severely sloped with a shallow leading edge. The RIJ often descends well behind the leading convective cores. Deep, severe mesovortices would be extremely rare with a sloped system like this.

Student Notes:

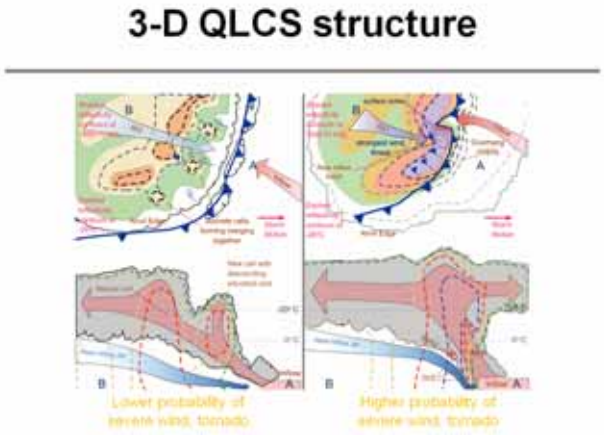

6. Initial convective modes leading to Bow Echoes

Instructor Notes: By the time you see the reflectivity echo of a multicell organize into a bow, it's already too late to issue a warning because the strong outflow has already been on the ground long enough to deform the precipitation shield. So it's useful to understand what kinds of convective structures lead to damaging bows. Here's a study by Klimowski, Hjelmfelt, and Bunkers in 2004 where hundreds of damaging bows were backtracked in time to see what created them. The most common evolution was the merger of small weakly organized multicells that were originally noninteracting. However, they quickly started interacting when one of the individual small multicells merged with another setting off a sequence of rapid cold pool production and subsequent bow. The fastest of the individual small cells or multicells usually corresponded to the motion of the bow. Sometimes the individual small multicells would briefly organize into a line on its way to a bow. Either way, the consolidation of individual cells likely helped create a similar consolidation of cold pools and helped to contribute to intense updraft and subsequent downdraft formation. The second most common evolution of a bow came from a squall line that persisted more than the pre-bow linear structures that we just talked about. In this type of evolution, the squall line is moving east changing relatively little in structure and then a trigger causes a forward surge in the gust front in a confined segment. Most often the trigger is an interaction with a pre-existing boundary or another convective storm. Sometimes the trigger is more subtle and may be manifested as a significant updraft surge somewhere along the line. By the way, the acronym of BE is defined as a classic bow echo whereas BEC is a Bow Echo Complex. The latter is when a bow echo is the primary, but not the only convective structure making up a multicell. The former is when the multicell is completely identified as a bow echo. Finally, a bow echo accompanying others along a line is called a Squall Line Bow Echo (SLBE), and has been also called a Line Echo Wave Pattern (LEWP). The third kind of bow echo evolves from a supercell when the bowing rear flank downdraft ignites strong convection along its gust front, and the mesocyclone begins to morph into a line end vortex, or QLCS vortex. Bow echoes originating from squall lines tended to have the longest lifespan (3.4 hr) vs. 2.9 hr from initial clusters. Bows originating from squall lines seem to be most common in the eastern US.

Student Notes:

Initial convective modes leading to Bow Echoes

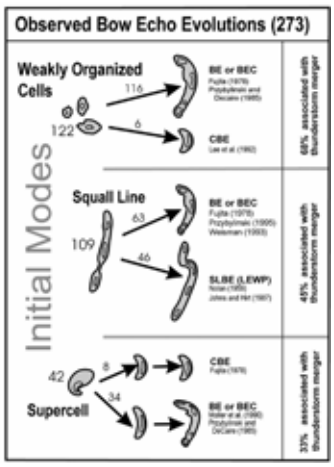

7. Initial convective modes leading to Bow Echoes – cool season

Instructor Notes: Another study by Burke and Schultz also investigated what kinds of convection led to bows, but only for cool season events. They're classification scheme added three new categories including an embedded line development, pairs of cells, and a squall line-cell merger. Like Klimowski et al., most of the bows originated as a linear squall line or a group of isolated cells. They also noted that merging cells or small multi-cells occurred frequently before bow echo genesis. For the cool season, supercells occurred in 43% of the formative and mature stages of bow echoes and 38% of squall-lines had supercells embedded. Nine of their 51 cool season cases were termed long-lived bow echoes (LBE's) that qualified as Derechos too. The number of cases for each storm type are listed in parentheses.

Student Notes:

Initial convective modes leading to Bow Echoes – cool season

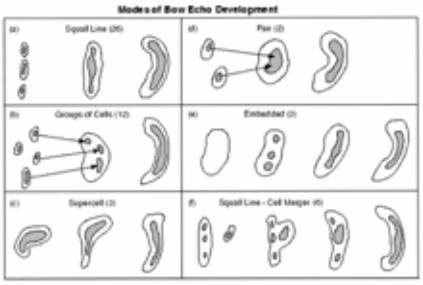

8. Initial stage of a damaging bow echo

Instructor Notes: The initial stage of a bow echo at the onset of severe damaging surface winds is a time when the precipitation area is not bowed at all. An updraft surge typically happens which then yields a severe downdraft. Also at the same time, anvil debris typically spreads rearward of the main convective line with respect to the steering layer flow. This anvil debris acts to initiate the rear inflow jet (RIJ). Assuming you're about to have a severe bow echo, the best time for initial warnings is in the tall echo state when updraft surges occur prior to the onset of the severe downdraft and RIJ. This is when you typically see strong, deep convergence, represented by the MARC (Mid Altitude Radial Convergence), along a segment of the line. Just before the bowing state, the descending RIJ hits the ground and begins to push forward. The most severe mesovortices may form at this time. The most severe surface winds occur when the mesovortex forms near the apex of the RIJ. As the convection morphs into a bow echo, the updraft depth often decreases, and a rear to front dry slot forms. The strong outflow from the RIJ is firmly established and has been on the ground for some time.

Student Notes:

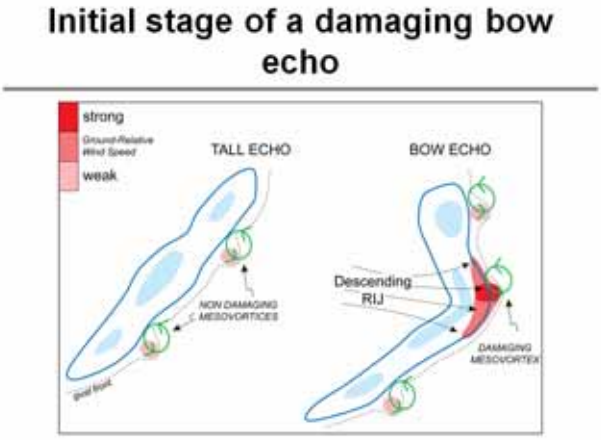

9. An example of a bow echo lifecycle: 10 June 2003 - STL

Instructor Notes: A flash-based looper will popup in a separate window in 10 seconds but first direct your attention to this main articulate slide. I'll wait until you get your bearings. This case of a bow forming shows the first cells at a very updraft-dominant stage. This is the time in which you first see the upscale organization of small multicells slowly consolidate and merge. If the shear is strong enough, then some of these small multicells may be supercells. Echo tops are usually high and the updrafts are deep. Notice the relatively high values of maximum expected hail size (MEHS). Next, the small multicells consolidate and new, strong updrafts begin to produce strong downdrafts. You can see the outflow already surging toward the radar. This is a time when the first warnings would've been out if you deem this event potentially severe, as in this case. In the

next image, this QLCS is still exhibiting tall reflectivity echoes, a sign of deep updrafts. However the RIJ is strong, and there have already been several severe mesovortices to the left of small surges of the gust front that have produced tornadoes and enhanced severe winds. The main precipitation shield has not yet deformed into the classic bow shape but it is about to produce the most severe winds yet. In this image there is the most faint hint of a rear inflow dry notch impinging inward from the west over Belleville, IL. This notch represents the most intense RIJ along this QLCS. The strongest mesovortex of this event forms to the north of the RIJ axis and that is where the most intense wind damage was observed along a belt northeast of Belleville to across the Mid America airport and Scott AFB and then southwest of Clinton, IL. It's clear there's a better association of the intense winds with the mesovortex, and not so much the RIJ axis. The last frame in this loop now shows a classic bow echo appearance though only well after the onset of the most damaging winds and most of the QLCS tornadoes. The echo tops have gone down as well as the MEHS, all indicating a trend toward shallower updrafts. The leading edge of the deep convection is still keeping up with the gust front and this bow echo is still more than just borderline severe. In the flash window loop, step through the frames to see the full evolution. Overlaid on the velocity panel, you'll see a box containing a detailed graphic of wind damage and tornadoes. The white shaded regions show wind damage of F0 (EF0) or greater while the white lines represent tornadoes. The small checkbox brings up the most relevant graphical conceptual model that corresponds to the stage of the QLCS in its lifecycle.

Student Notes:

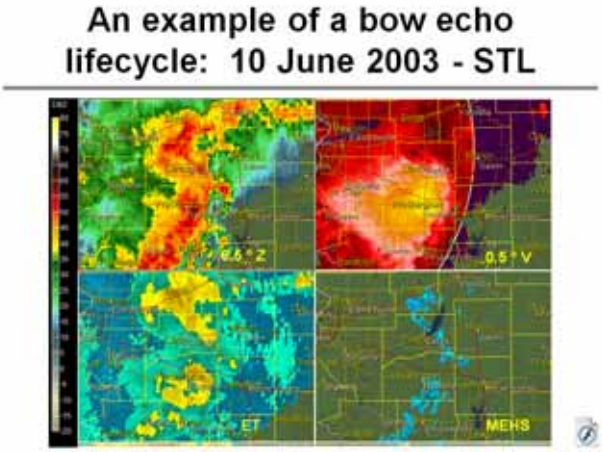

10. Early lifecycle of 4 Jul, 2004 Springfield, MO event

Instructor Notes: This event is an example of a bow echo originating from a multicell cluster. However, you could classify this evolution as an initial squall line since each multicell cluster was aligned on a common gust front. A popup window will appear with Ron Przybylinski, the SOO at WFO St. Louis, discussing the evolution of this severe bow echo from its inception. Ron has written and spoken extensively about QLCS severe weather events. Grab a drink and enjoy Ron's tour of this bow echo evolution. Ron's captions: Looking at reflectivity and storm-relative velocity from 10:02 - 10:24 - 10:37 UTC, you'll find that there was a weak vortex, not really well defined. You may come across

weak circulations during this initial isolated, to cluster phase of a bow echo. Nolan Atkins has documented these events back during BAMEX where we observed weak and short-lived vortices. Now we move forward to 1041 UTC we don't see much rotation but we do see inbounds behind on the backside of this cluster of storms. This is the tall echo stage. We start seeing some cyclonic shear in the midlevels. Mostly hail and high winds can be expected here around 1107 UTC. Moving forward, we see a vortex, now at the leading edge! We mentioned this particular vortex showing up around 11 UTC but now it's showing up nicely. Now the SRM data is showing a vortex in Cherokee county. We move closer in time (to the first tornado) and we see a multiple vortex structure. One to the southwest of Joplin and one to the northwest. It was this second vortex that spawned a tornado in northern Newton county. Note the location of the surface boundary (connecting with the tornadic vortex). We've seen this play a role with many QLCS tornadic events. Going back to reflectivity, we see a nice bowing structure with a rear inflow notch forming (at tornado time). We see multiple rear inflow notches where some lower Theta-E air penetrates into the leading convective line. Going back to SRM data, there's additional wind damage along the apex of the bow and the RIJ but to the south of the tornado. The damage was not so bad north of the tornadic vortex. Most of the wind damage was south and east across Neosho and counties directly downstream of the bow echo.

Student Notes:

11. Review of the 04 July 2004 evolution

Instructor Notes: The bow started as a multicell cluster on a gust front (a cross between the cluster and squall line origins in Klimowski et al. 2004 and Burke and Schultz, 2004) QLCS vortices were weak in the early stages before the RIJ formed QLCS vortices strengthened here after signatures of the RIJ form (rear inflow notch, inbounds) The leading boundary intersecting the bow was associated with a tornadic mesovortex. The most wind damage was along and north of the RIJ axis to the tornadic mesovortex.

Student Notes:

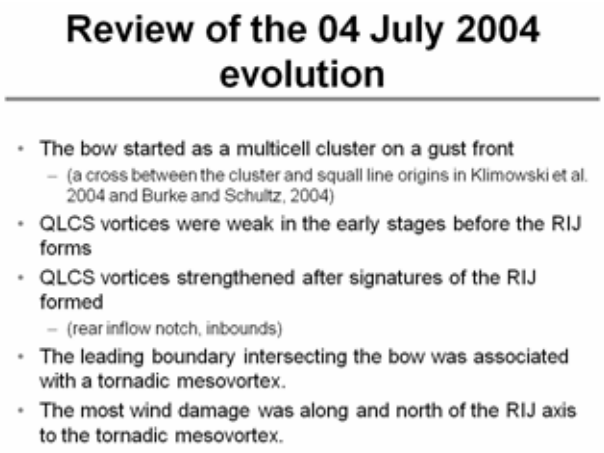

12. Early lifecycle of the 24 July, 2009 DVN QLCS

Instructor Notes: In this case, the bow echo starts off as two interacting supercells. Ron Przybylinski guides you through the evolution. Wait for the popup window and the video lasts two minutes. From Ron's captions: Another form of convective line evolution formed from supercell structures in the Davenport CWA. In this case, there are two supercells with strong mesocyclones positioned east-west. With time, these two supercells weaken in terms of their reflectivity structure though but the eastern one still has strong inflow notch. SRM data doesn't show much but some weak rotation on the eastern storm (near Scales Mound) and another is trying to form with the same storm at the head of the RFD push. As the storms continue moving southeast, and we see the bowing segment (especially with the RFD push) continue to evolve. The bowing segment continues to evolve and become dominant into Carroll county. SRM shows some weak rotation but nothing substantial at this time. Continuing further southeast and the main bow continues while a second bowing segment forms to the west.

Student Notes:

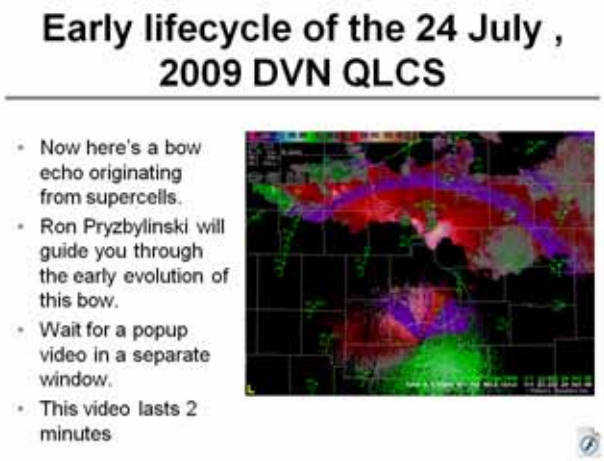

13. Review of the 24 July 2009 evolution

Instructor Notes: Two supercells exhibited HP characteristics, each with significant low-level mesocyclones The RFD of the eastern one erupted convection. Given the shape of the RFD gust front, the convection acquired a bow shape with an enhanced RIJ that was the RFD. Many times the primary mesocyclone occludes and drifts rearward

Student Notes:

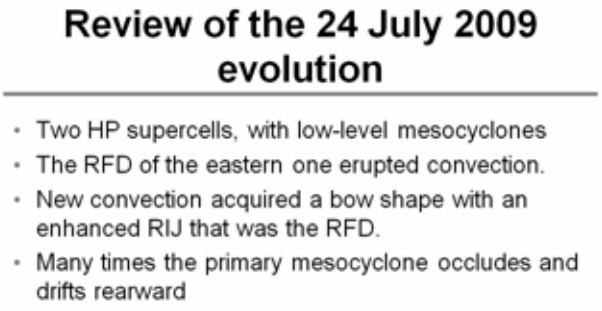

14. Supercell to bow echo motion

Instructor Notes: Watch the evolution of this supercell to bow echo as I move this loop using the feature following zoom following the supercell. As the supercells go on, you can see they're moving relatively closely to how I placed my 'drag me to storm' feature. As the supercell turns into a bow echo, you can see that the motion starts moving off to the left (of the distance speed tool). Now I'll move it faster so you can see the evolution in a different way.

Student Notes:

Change in storm motion from supercell to bow echo

15. QLCS-storm-interrogation-Quiz1

Instructor Notes:

Student Notes:

16. QLCS Mesovortex structure, evolution

Instructor Notes: While both the supercell mesocyclone and the QLCS mesovortex exhibit vertical vorticity at least partly colocated with updraft, they are structurally and dynamically different animals. You can see the differences with these two examples. At low-levels, the supercell features an obvious hook echo and broad, concave notch with a sharp reflectivity gradient. There is an occluding low-level mesocyclone, and enhanced inbounds further east signifying strong inflow into the RFD gust front indicating a new mesocyclone may be underway. The QLCS at low-levels shows a less obvious inflow notch and sometimes a rear inflow notch. The mesovortex forms along the gust front, and in this case, that's on the leading edge. At midlevels (15kft AGL), the supercell notch, or WER is closing off into a BWER while the inflow notch on the QLCS is less obvious. There are even more stark differences in SRM. Now you can see the occluded low-level mesocyclone is deep. The new mesocyclone is strongest at this level. Meanwhile, the QLCS mesovortex does not reach this level. The radar is sampling at the top of the gust front. Let me discuss a couple things you should know. First, the terminology, mesocyclone and mesovortex can be somewhat confusing. After all they are both mesovortices. These terms came about from different paths and often there is little coordination or reassessment to see if there would be ensuing confusion amongst the research community. So often it's useful to say supercell mesocyclone or QLCS mesovortex if this helps you to categorize their differing behaviors. Also, there is a term called bookend vortex. The mesovortex, such as this one, is not the kind of vortex that researchers from back to the days of Fujita called a bookend vortex. The bookend vortex refers to the circulation associated with the bow echo comma head and is quite a bit larger than a typical mesovortex. Sometimes mesovortices grow upscale to become bookend vortices.

Student Notes:

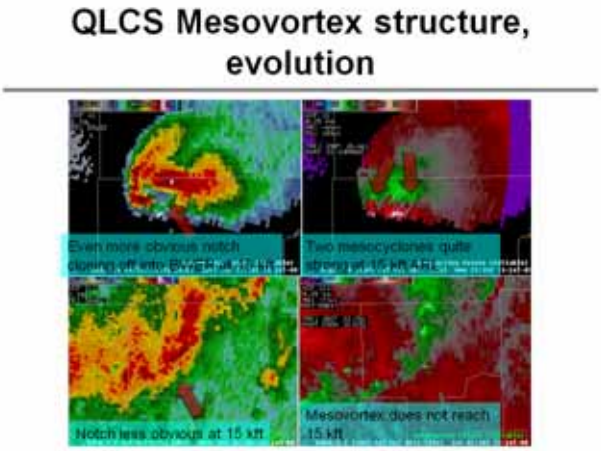

17. QLCS mesovortex structure and evolution: tracks

Instructor Notes: We'll take a closer look at the northern bowing segment for the June 10 case. Notice that the most intense mesovortices form well after the convective echoes congeal together to form a QLCS. We'll take a look at the initiation and evolution of mesovortex #6. If you'd like, please take a look at this case study written up by Atkins et al. 2005 titled "Damaging surface wind mechanism within the 10 June 2003 Saint Louis bow echo during BAMEX" in Monthly Weather Review.

Student Notes:

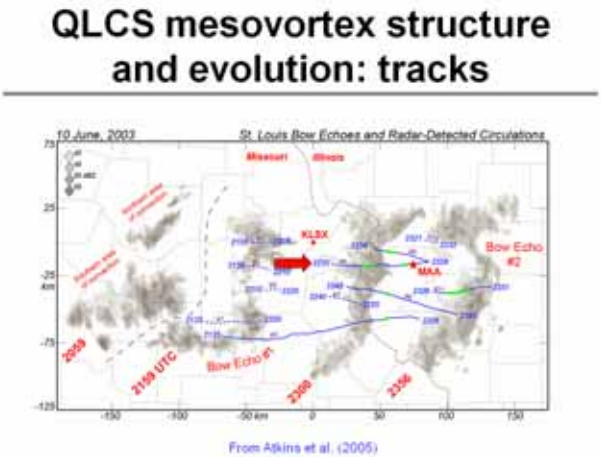

18. A typical severe mesovortex initiation (t=0 min)

Instructor Notes: At 2235 UTC on June 10, 2003, mesovortex #6 was initially tracked. You can see two elevations in this four-panel with SRM on the right, one at 5000' ARL and the other, 700' ARL (lowest elevation scan). Note that the lowest scan shows a gust front that's beginning to become kinked. Notice southwest of the kink, a strong RIJ with outbounds approaching 40 kts. Recall that this SRM display removed about 270 deg at 35 kts already. This mesovortex that's forming doesn't have an obvious maximum and minimum velocity core like you'd expect in a traditional mesocyclone, however there is a

local vorticity maximum that the updraft along the gust front can easily amplify. Let's take a look at two cross-sections, an Azimuthal one to see the mesovortex, and then a Radial one to see the QLCS structure.

Student Notes:

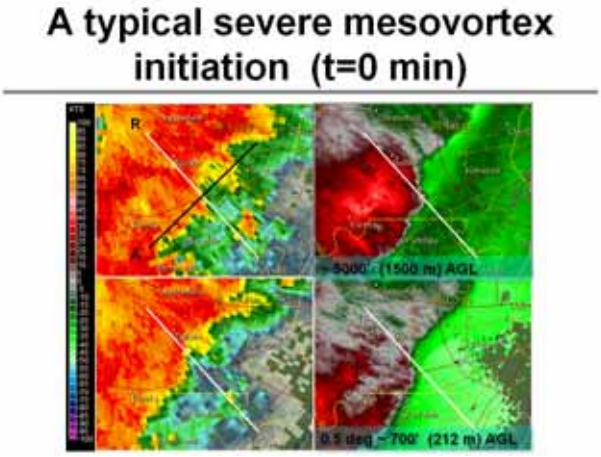

19. Azimuthal Cross-section: mesovortex initiation

Instructor Notes: First, the azimuthal cross-section shows heavy cores overlying a weak echo region. Remember that system motion may have caused an artificial WER. Going to velocity, the cross-section falls from within the protruding gust front then across it into the pre-storm air. The gust front at the kink is nearly vertical for the lowest 10 kft ARL with an abrupt cutoff. This structure is pretty typical and sometimes the mesovortex will be stronger down low. Spectrum width shows a zone of slightly higher values along the gust front interface, and then over the gust front. The high values above may simply be due to turbulence in the convective core.

Student Notes:

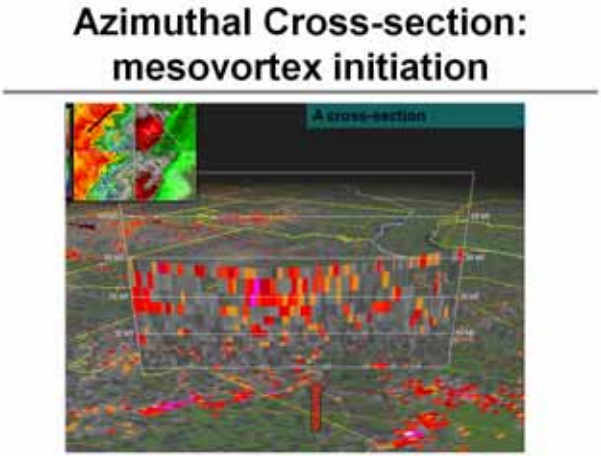

20. Radial Cross-section: mesovortex initiation

Instructor Notes: The Radial reflectivity cross-section shows that what may have been an artificial WER may be partly real since the strong echo overhang extends so far forward. The core is certainly at least led by a wall of high reflectivity gradient that typifies severe QLCSs. The SRM shows an intense nondescending rear inflow jet right up just behind the gust front of 10 kft depth. Note that there is an artificial forward tilt to the gust front due to system motion. Notice that the artificial displacement is not as far as the forward displacement of the intense reflectivity core so we are seeing true intense reflectivity echo overhang. Spectrum width shows again the most turbulence along, and above the gust front with low values in the RIJ core and in the pre-storm inflow. Signs that we will have a severe mesovortex event are already here. They include a nearby association of the intense RIJ with the low-level onset of the mesovortex, and a deep gust front and deep convection coincident with each other.

Student Notes:

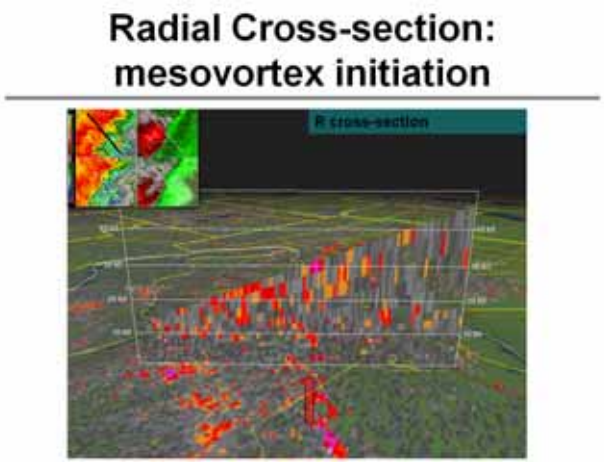

21. QLCS mesovortex structure and evolution: Time height

Instructor Notes: Adding a time-height profile, what you've just seen is marked by the arrow. In the upper-left panel, rotational velocity shows values peaking at 11 m/s (21 kts). But notice that the highest values are just above the lowest scan. This is a frequent behavior where scans above the ground up to 1-2 km have somewhat stronger values than at the lowest scan. So if you're radar is nearby, going up a scan or two may help show a more stout mesovortex. However, the mesovortex is still shallow and not exceeding 1.5 km AGL as documented by Atkins et al. 2005. The following 10 minutes show rapid deepening and strengthening of the vortex as you can see in the time trends of rotational velocity in the upper right. Notice that the azimuthal shear values in the lower right are right in line with any significant supercell mesocyclone (>10X10E-3 per second). Different than a typical mesocyclone, notice the diameter of this mesovortex is quite small, only 2 km (1.2 nm). The mesovortex occasionally peaked above 5 km as it

matured and produced a sequence of tornadoes. Intensification occurred prior to or at least during tornadogenesis, a typical behavior. Also notice the long lifespan of the mesovortex. It would be nice to take warn the initial deepening and intensification of this mesovortex before tornado time but you can also be more comfortable with followup warnings based on its persistence. Let's take a look at this mesovortex at a mature stage just prior to the first tornado.

Student Notes:

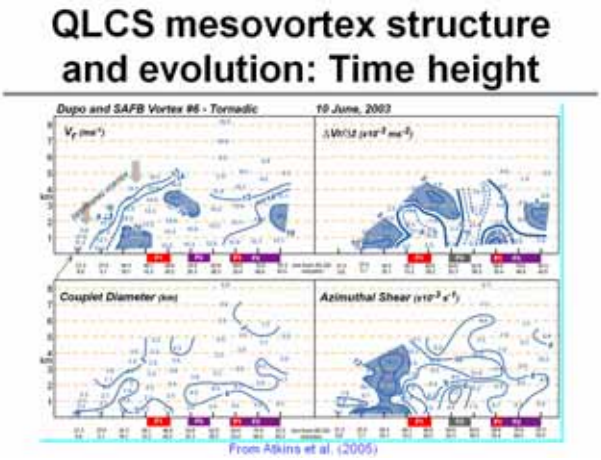

22. A typical severe mesovortex mature stage (t=15 min)

Instructor Notes: Shifting 10 minutes later, the mesovortex looks much stronger at the 5000' ARL level (top) with now what appears to be at least an isolated velocity minimum (inbound) on the top and even a hint of a core of maximum outbounds south of the center. The lowest scan also shows at least a maximum velocity core and even a hint that an azimuthal gate-to-gate velocity couplet is forming. These values were used to calculate the Vr in the time height trace. In the reflectivity, there's a little confusion in the picture. It appears that strong reflectivity has swallowed the mesovortex. However, there were some convective cells merging with the main line. So look left of the radial cross-section line and you see an S-shaped reflectivity gradient where the inflection point is right on the mesovortex. Also note southwest of the mesovortex you still see evidence of the RIJ in both the SRM and the rear inflow notch. All these are components of a severe mesovortex. Let's look at the cross-sections starting with the azimuthal one (A).

Student Notes:

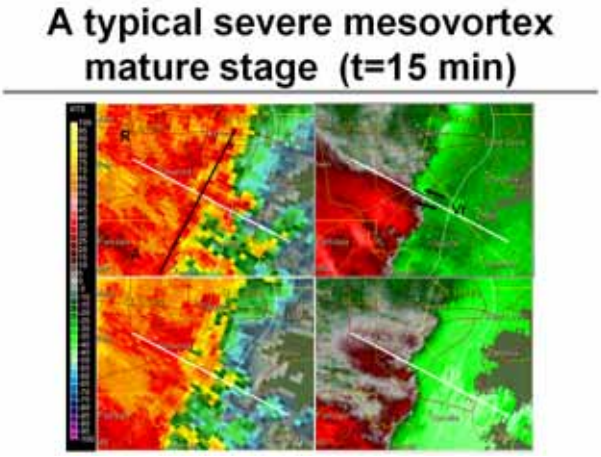

23. Azimuthal Cross-section: mature mesovortex

Instructor Notes: Again the reflectivity pattern looks a little muddy because of the merging cells. The SRM now shows the mesovortex extending to 15 kft (~5 km) ARL. The strongest rotational velocity still is in the lowest part of the mesovortex. This time the spectrum width highlights a bullseye of high values at the low-level mesovortex center.

Student Notes:

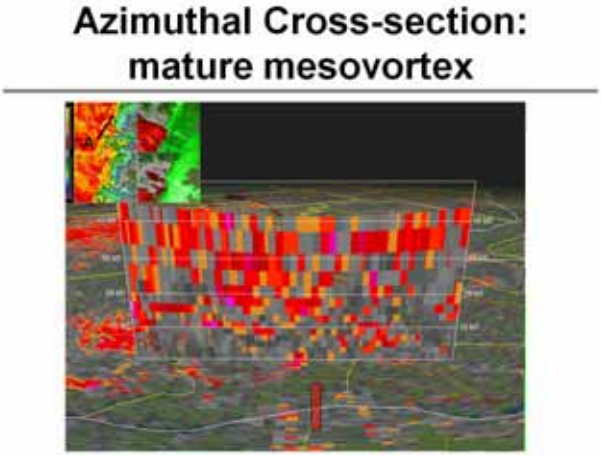

24. Radial Cross-section: mesovortex initiation

Instructor Notes: At 2245 UTC or initiation + 15 minutes, that same overhang is still visible, that is with the main convective line, and even the merging cell. Base velocity shows the RIJ right behind and leading into the south side of the mesovortex. The gust front has deepened behind the mesovortex, almost 15 kft ARL! All the winds in yellow are meeting severe thresholds or more. Notice in the SRM the big convergence down low, the strong rearward flow above the deep gust front and then the anvil layer outflow to the right. This is a pattern typical of a high-end severe QLCS. The SW shows again the vortex bullseye down low and the high values along and above the gust front inter-

face. But the inflow and initial updraft ahead of the gust front are relatively smooth, as is the RIJ core.

Student Notes:

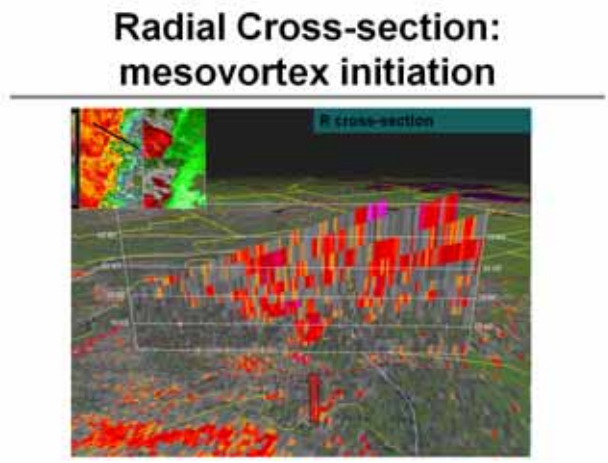

25. Interim summary: severe mesovortex evolution

Instructor Notes: To summarize, we had a nondescending vortex though it may appear weaker down in the lowest layer. The strong RIJ on the right side and behind the mesovortex is a serious precursor of a severe mesovortex. The mesovortex was not a classic Rankine combined archetype. We could see the deepening vortex as it matured and a more classic look as it garnered a min and max velocity. The convection was upright and even featured a WER. Front and rear inflow notches formed. SW was also useful to snag the vortex location as long as you know where to look since there's lots of other high SW centers.

Student Notes:

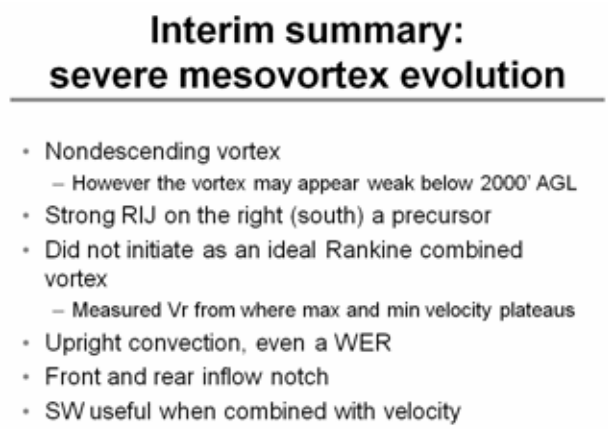

26. Mesovortex formation: Downdraft tilts vortex lines

Instructor Notes: Researchers have been trying to establish how QLCS mesovortices form and as expected there's more than one answer. This result that popped up in a sep-

arate window, featured one of the first theories and it's one that we still consider. That is a localized strong downdraft formed behind the gust front and depressed the vortex lines along the cold pool boundary eventually leading to a couplet. This evolution results in a vortex couplet with the anticyclonic member north or to the left if your pointed in the direction that the QLCS is moving. Not many warning forecasters have seen this kind of vortex couplet but there's evidence in BAMEX that they exist, perhaps mainly in the early stages of a QLCS before the RIJ really has a chance to mature. The anticyclonic member dies off quickly as it fights against Earth's vorticity.

Student Notes:

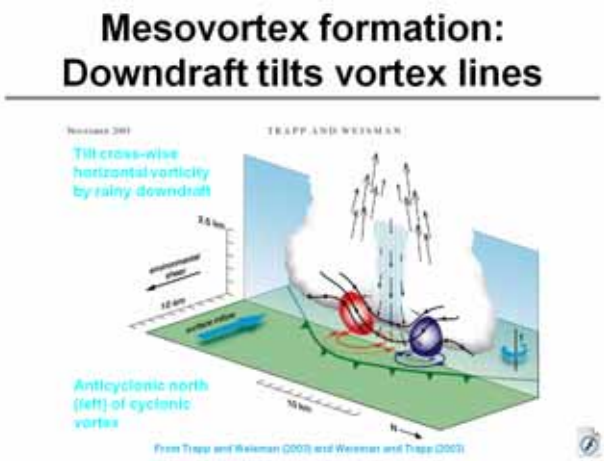

27. Mesovortex formation: Local updraft tilts vortex lines

Instructor Notes: More recently, Atkins and Laurent developed more than one theory for mesovortex formation because they saw different evolutions within the QLCS. This one requires a locally intense updraft along the gust front to tilt and stretch streamwise vorticity running down the boundary. The resulting vortex would be of a single sign and not a couplet. A similar theory for mesocyclone formation looks quite similar developed by Rotunno, Klemp, Davies-Jones and others. Instead of a QLCS gust front it's the forward flank gust front that helps. However mesocyclones happily form just tilting environmental streamwise vorticity without needing a forward flank gust front.

Student Notes:

28. Mesovortex formation: Local updraft tilts vortex lines

Instructor Notes: This other evolution in mesovortexgensis was found by Atkins and Laurent where instead of an isolated updraft pulling up streamwise vorticity, a local outward bulge in the gust front forms, possibly from the RIJ axis or a local downdraft. A horseshoe vortex arch forms with the cyclonic member on the north side (or left pointing ahead of the QLCS). This couplet is in the opposite sense to what Trapp and Weisman theorized and it's something we see more often, especially during the mature RIJ stage of the QLCS. Notice that this evolution is quite similar to what Markowski et al. 2008 theorized with the formation of a low-level mesocyclone in a supercell. In the supercell case, air from the downdraft descends, creates cross-wise vortex lines around its exterior, in the form of a horseshoe. Some of those vortex lines get entrained into the updraft. Notice that they distinguish those vortex lines from the environmental vortex lines that help create the midlevel mesocyclone.

Student Notes:

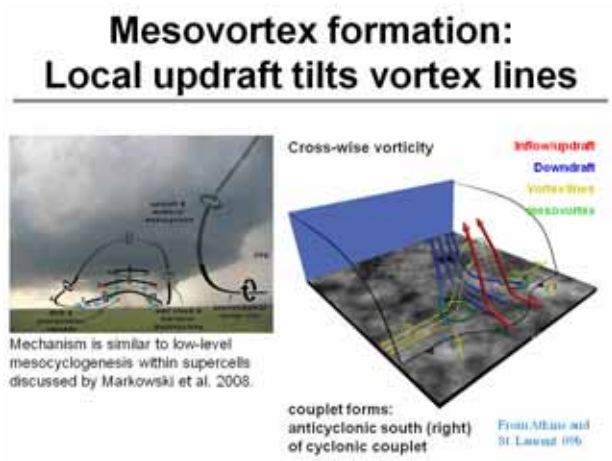

29. Mesovortex formation: Implications

Instructor Notes: So we described downdrafts directly tilting cold pool vortex lines to create a couplet with cyclonic (anticyclonic) member to the right (left). Then we talked about updraft tilting streamwise vortex lines to generate a singular cyclonic vortex, and we discussed the formation of vortex arches to create a couplet with the cyclonic (anticyclonic) member to the left (right). We didn't talk about horizontal shearing instability. Basically here the gust front vertical vorticity gets so large that it breaks down into regularly spaced vortices of the same sign, namely cyclonic. So the difference between this and the local updraft tilting streamwise vorticity is that first, we don't know how that vertical vorticity got there to be rolled up, and the local updraft tilting doesn't produce regularly spaced vortices at the same time. I think you've seen pictures of multiple waterspouts occurring simultaneously. That's a manifestation of shear instability, and the same thing could happen on a QLCS gust front.

Student Notes:

Mesovortex formation: Implications

Formation process	Implication (assuming westerly environmental shear)
Downdraft tilting cold pool vortex lines	Couplets: Anticyclonic mesovortex forms north of cyclonic mesovortex
Local updraft tilts streamwise vortex lines	No couplets: Multiple mesovortices irregularly spaced
Local updraft tilts crosswise vortex lines	Couplets: Anticyclonic mesovortex forms south of cyclonic mesovortex
Horizontal shearing instability	No couplets: Multiple mesovortices spaced at regular intervals

30. QLCS mesovortex tornado precursors – Vr profiles

Instructor Notes: There hasn't been a lot of work done in the field of discriminating tornadic vs. nontornadic QLCS mesovortices but what there is appears to be fairly applicable. The 10 June 2003 case had a clear discrimination between tornadic and nontornadic mesovortices. In this figure the mean rotational velocity of the tornadic mesovortices as a function of height shows how much stronger they were than for the nontornadic mesovortices, especially from 2 km AGL down toward the surface. So at least for this case, the mean Vr for tornadic mesovortices was around 24 kts (12 m/s). There needs to be more work to show how well this discrimination goes for a large sample of cases. However, the take home message is that the tornadic mesovortices are much stronger at low-levels.

Student Notes:

QLCS mesovortex tornado precursors – Vr profiles

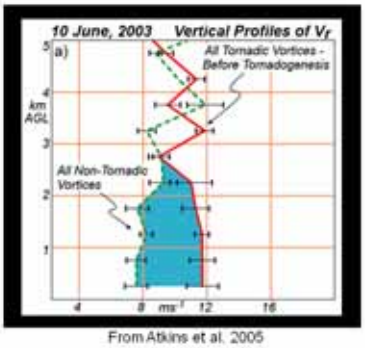

From Atkins et al. 2005

31. QLCS mesovortex tornado precursors: lifespans

Instructor Notes: In terms of longevity, the 10 June 2003 tornadic mesovortices lasted longer than those that were nontornadic. Again, the sample size is somewhat limited but there is evidence that this trend holds true for a larger set of cases too. As a warning forecaster, you don't have time to see if a particular mesovortex is going to last a long time, otherwise you'd have to sacrifice a lot of people before issuing a warning. But you can certainly increase your confidence in your warnings as the mesovortex continues to persist, and especially if its strong and long-lived.

Student Notes:

QLCS mesovortex tornado precursors: lifespans

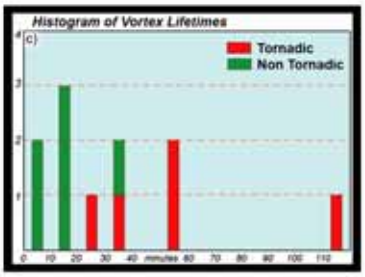

From Atkins et al. 2005

32. Mesovortex evolution: Back to 24 Jul 2009

Instructor Notes: Going back to the 24 July 2009 case, Ron will be walking you through the evolution of a particular mesovortex as he would do in a warning decision making mode. This video lasts about 3 minutes.

Student Notes:

33. Review: 24 July 2009 mesovortex

Instructor Notes: The main message from Ron's discussion is: This vortex also built up in time Stronger mesovortex: LLVr ~ 40 kts Rear inflow notch indicative of RIJ channels. Mesovortices most severe when adjacent to an RIJ Best tornado warning issuance time was when mesovortex exhibited rapid deepening

Student Notes:

34. Along-line variations: intersecting boundaries

Instructor Notes: As a final major topic, this lesson wouldn't be complete without discussing the impacts of heterogeneity (e.g., boundaries, mergers) on QLCS severity, especially on mesovortex behavior. There's quite a bit of work done on how boundaries and merging instability lines impact QLCSs but rather than recite all the work, let's apply it to this case, 04 July 2004, that we've been going through in this lesson. We already eluded to the presence of a pre-line boundary in this case extending to the southwest creating an intersection. Let's start at 1153 UTC and we'll see how the boundary has impacted the pre-storm environment. There's not much to go on except a couple METAR stations, Joplin and Springfield, and the Springfield WSR-88D VWP. The post boundary

air is important to sample because it'll determine how well the bow can survive on that side. But also equally important is how the boundary-bow intersection plays a role in enhancing mesovortexgenesis. For this page, we'll concentrate on the post-boundary air. I included the SGF raob hodograph at 12 UTC to show that there's a fairly complex shear profile from 0 – 3 km AGL and a general west-northwest bulk wind difference of 30 kts from 0 – 6km AGL. At 1153 UTC, the boundary has just passed Joplin and we can see the temperature hasn't dropped yet. The apex of the bow is directly in line with the boundary. At 1214 UTC, the KSGF wind profile shows a complex vertical wind profile but the VWP is not picking up the lowest level winds. There's perhaps a tendency for a northeasterly 0-3 km shear vector averaging the lowest few hundred meters within the surface and a similar layer around 3 km AGL. At 1240 UTC, the boundary passes over the radar and the surface winds go from southwest to northwest. The vertical shear is still complex. At 1300 UTC, There is a marked increase in southeasterly shear within the boundary layer with northwesterly surface winds and almost southerly 3 km winds. Above 3 km the wind shear reverses to northerly again. This feature persists through the end of the loop. The 0-3km shear is much stronger but in this case may not actually be conducive to enhancing the strength of the line since the predominant component of the shear is line-parallel, even front to rear. Notice that the northern end of the line never extends far beyond the boundary intersection. As far as instability is concerned, the SGF METARs eventually drop from 75 deg F just north of the boundary to 73 deg F an hour later. However the dewpoint remained higher than the pre-boundary air. It's not clear that the instability decreased rapidly north of the boundary but the shear could've had a negative impact on the QLCS survival. Had the shear been oriented from the WSW behind the boundary, the QLCS may have threatened Springfield with potential mesovortices. But most likely for the shear to be oriented from the WSW, the post boundary wind direction would've needed an easterly component, an attribute most commonly associated with a stalling, or even lifting outflow boundary.

Student Notes:

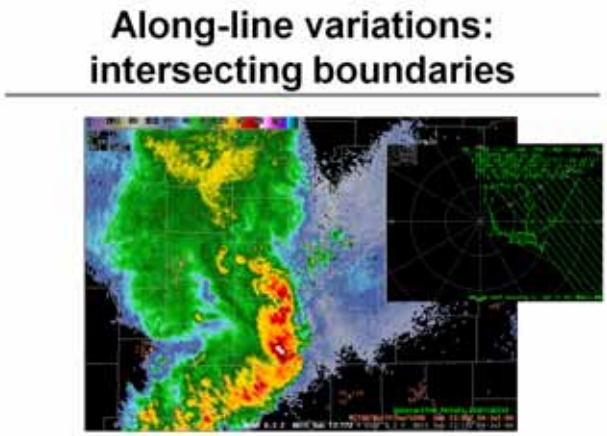

35. Along-line variations: Merging ascent zones

Instructor Notes: If the horizontal shear along and north of the boundary is not conducive for maintaining the QLCS, then perhaps another one or two other sources could

help to increase the threat of a severe mesovortex. One could be the enhanced convergence at the boundary intersection, and another could be the intersection of other convective cells, or the forcing mechanism producing them. In this case, there's a double intersection between an instability line forcing an axis of broken cells and the boundary at the same time. The locally stronger convergence here could easily have locally amplified any vertical vorticity lying along either boundary into a well defined vortex. Lese, 2006 noticed that the mesovortex that coincided with this double intersection resulted in a tornado while an adjacent mesovortex to the south did not. In the next slide, Ron will describe his thought process in warning forecaster mode.

Student Notes:

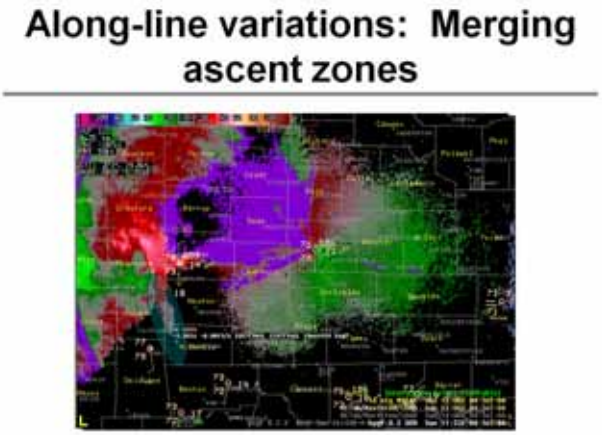

36. Along-line variations and mesovortices: 04 Jul 2004

Instructor Notes: Ron will be showing you the evolution of this particular mesovortex and how it relates to the surrounding intersections. Take note of his interrogation of its evolution with time and height too.

Student Notes:

37. Quiz-2

Instructor Notes:

Student Notes:

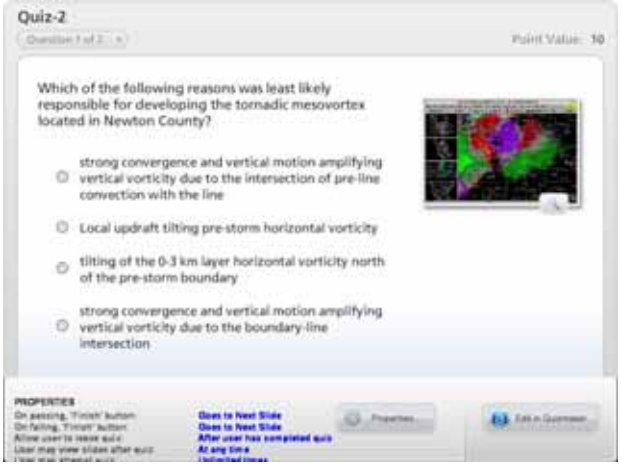

38. Along-line variations: Interim summary

Instructor Notes: Post-boundary air altered vertical shear, this time possibly in a negative way Boundary intersection likely enhanced convergence to amplify existing vertical vorticity Instability line manifested by merging line of cells created a double intersection with the other intersection and helped the one mesovortex become tornadic

Student Notes:

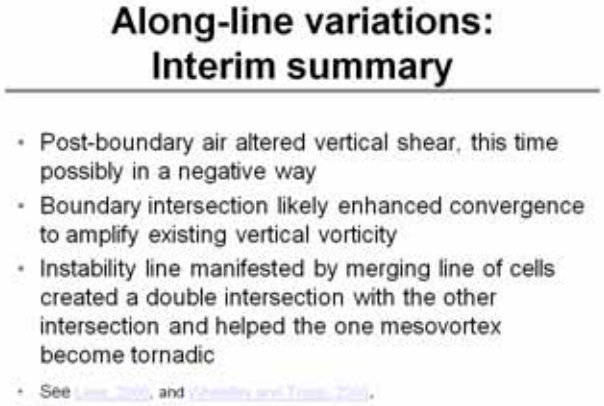

39. Summary

Instructor Notes: What stages in a QLCS lifecycle are most likely to produce the most severe wind (tornado) potential? During and after formation of the RIJ What kinds of 3-D structure are most related to the most intense severe wind (tornadic) events? Look for deep and steep gust front with a deep convergence zone and attached to a solid wall of

deep convection. What is a common evolution of convection preceding the formation of bows? Merging small multicells and associated cold pools What is the motion of typical bows? Typically with the mean convective layer wind and faster

Student Notes:

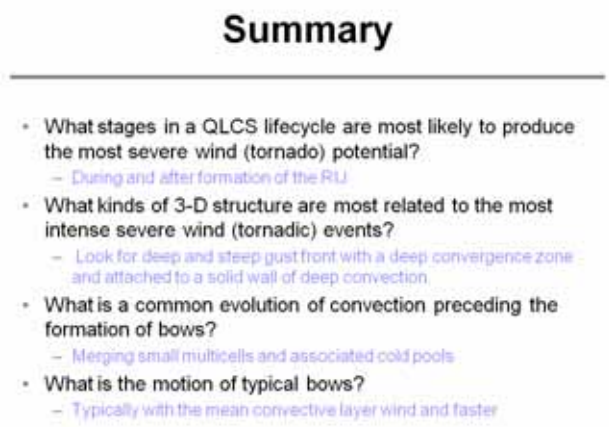

40. Summary - contd

Instructor Notes: How do mesovortices form? downdraft tilting vortex lines behind gust front, local updraft tilting streamwise vorticity on gust front, updraft tilting cross-wise vorticity over protruding gust front When are mesovortices most likely to become severe (wind and tornado)? After the RIJ forms and moves adjacent to a mesovortex How do I discriminate tornadic from nontornadic mesovortices? Stronger rotational velocity, depth, lifespan, environment When is the best time to issue a warning on a mesovortex? As the mesovortex begins to deepen

Student Notes:

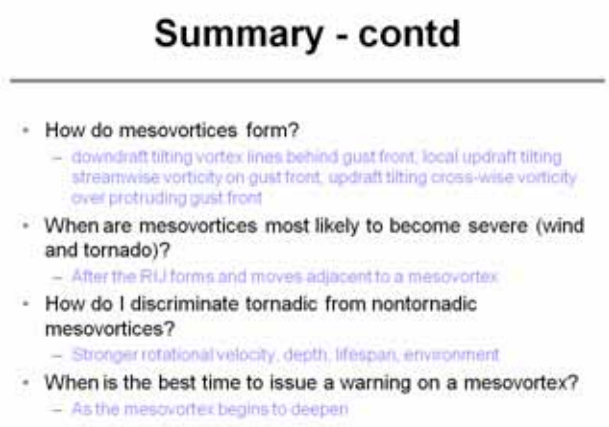

41. Summary - contd

Instructor Notes: How can a pre-storm boundary enhance mesovortices? Increasing pre-storm vertical shear, enhancing convergence at the intersection point Does a pre-

storm outflow boundary or warm front always enhance mesovortices? No, we need to worry about stability and shear changes as always

Student Notes:

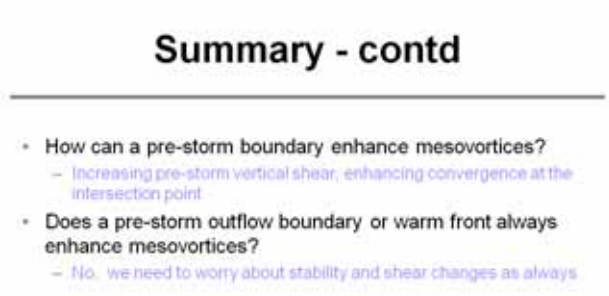

42. Credits

Instructor Notes:

Student Notes:

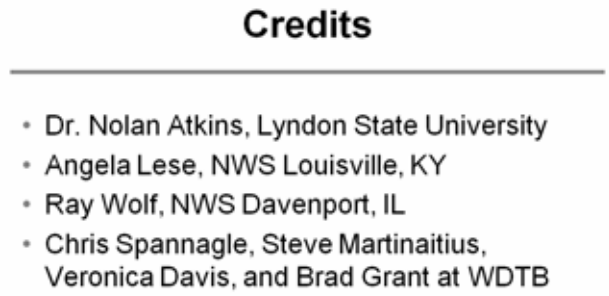

43. Contact Information

Instructor Notes: Get in touch with us should you have a question or would like to chat about severe weather.

Student Notes:

Contact Information

- awocsevere_list@wdtb.noaa.gov
  - Questions on any AWOC Severe lessons
- NWS-chat
  - wdtbchat chat room
- James G. LaDue
  - James.G.LaDue@noaa.gov
  - 405-325-3004

1. Tornado and Severe Thunderstorm Warning Best Practices

Instructor Notes: Hi, this is Brad Grant of the Warning Decision Training Branch. Welcome to a presentation Jim LaDue and myself have produced entitled, “Warning Decision Making Issues with Derecho-Producing QLCS Events”. A Quasi-Linear Convective System (or QLCS) is a name for a broad class of mesoscale convective systems that have various linear configurations. A high–end QLCS event can produce a derecho if there is a sufficient amount of wind damage. This training presentation will be about 45 minutes.

Student Notes:

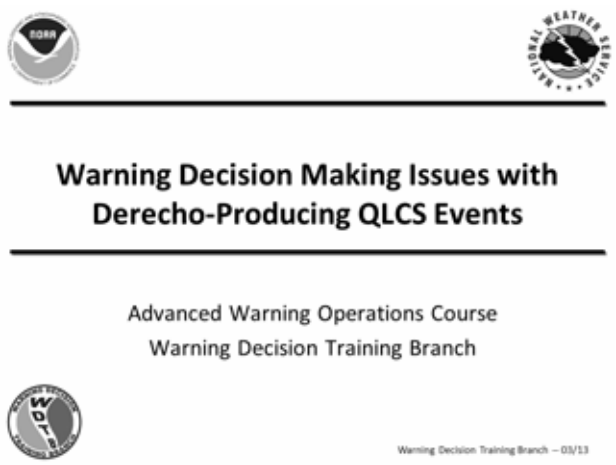

2. Training Rationale and Motivation

Instructor Notes: The motivation for this instruction is Finding 5 of the Historic derecho of June 29, 2012 Service Assessment. The finding from this assessment was that in trying to keep up with warnings for this large, fast-moving QLCS, some areas did not receive adequate lead time on the western edges of their polygons. In retrospect, one of the roots of this performance problem lies with correct anticipation of the types of threats and associated impacts with QLCS events. A QLCS event such as this was truly historic for this region but meteorological speaking, has some counterparts that can be use to illustrate important points in structure and phenomenology.

Student Notes:

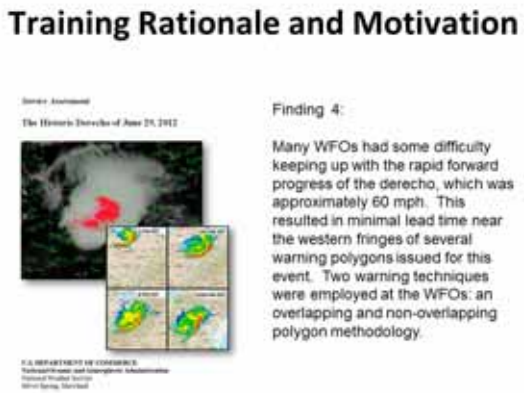

3. Solution Description

Instructor Notes: So, we have designed a learning plan called “Derecho Basics” that leverages existing WDTB training on threat assessment and storm interrogation strategies of QLCS events, especially with respect diagnosing the types of structures and life-cycle identification that can provide better impact-based warning services. These are the two learning objectives in the lesson. 1) Demonstrate the ability to identify synoptic- and/or mesoscale environments supportive of Quasi-Linear Convective Systems (QLCSs) including derechos. And 2) Demonstrate the ability to identify WSR-88D signatures associated with derechos and their associated severe weather hazards in order to facilitate effective impact-based warning decisions by both customers and partners.

Student Notes:

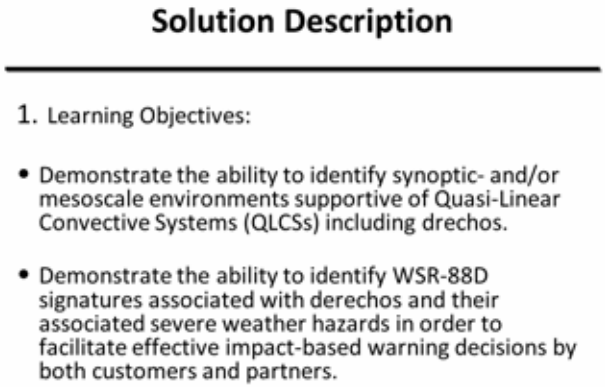

4. Climatology of Derechos

Instructor Notes: To start out this lesson, here’s a little review of the basics of the characteristics of this type of storm system. A derecho is defined as widespread, long-lived wind storm that is associated with a band of rapidly moving showers or thunderstorms. Although a derecho can produce destruction similar to that of tornadoes, the damage

typically is directed in one direction along a relatively straight swath. As a result, the term "straight-line wind damage" sometimes is used to describe derecho damage. By definition, if the wind damage swath extends more than 240 miles (about 400 kilometers) and includes wind gusts of at least 58 mph (93 km/h) or greater along most of its length, and if the wind damage swath extends more than 240 miles and includes wind gusts of at least 58 mph or greater along most of its length, then the event may be classified as a derecho. Here is a storm report plot of a classic multi-state derecho event from May 8, 2009. Derechos in the United States occur primarily along two axes. Based on a climatology developed from SPC, one axis extends along the "Corn Belt" from the upper Mississippi Valley southeast into the Ohio Valley, and the other from the southern Plains northeast into the mid-Mississippi Valley. During the cool season (September through April), derechos are relatively infrequent, but are most likely to occur from east Texas into the southeastern states. Although derechos are extremely rare west of the Great Plains, isolated derechos have occurred over interior portions of the western United States, especially during spring and early summer. There are two types of derechos, serial and progressive. The June 29, 2012 event fits more of the model for the progressive type. Progressive derechos are often associated with a relatively short line of thunderstorms (typically from 40 miles to 250 miles in length) that may at times take the shape of a single bow echo, particularly in the early stages of development. In some cases, the width of a progressive derecho and its associated bow echo system remain relatively narrow even though they may travel for hundreds of miles. In other cases, the progressive derecho and associated bow echo system begin relatively small, with a narrow path, but over time grow to exceed 250 miles in width. The line of thunderstorms of a progressive derecho often begins as a single bow echo that evolves into a short squall line, typically with more than one embedded bowing segment. Progressive derechos may travel for many hundreds of miles along a path that is relatively narrow compared to those of serial derechos. Often they are associated with an area of weak low pressure at the surface.

Student Notes:

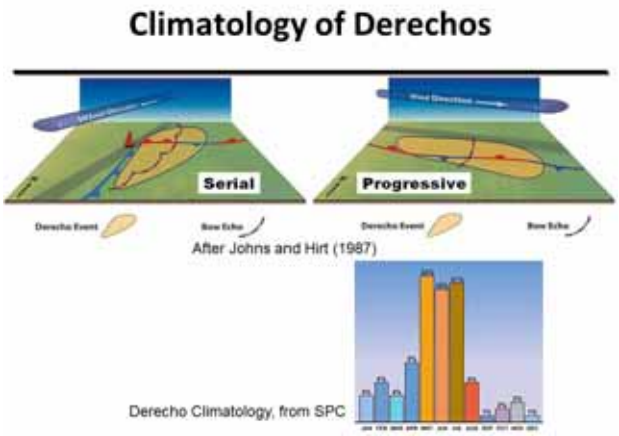

5. Forecasting Maintenance/Decay of QLCSs (factors sustaining QLCSs to Atlantic)

Instructor Notes: One of the challenges with forecasting maintenance or decay of QLCSs is the ability to identify which environmental parameters hold the key. In a study from Lombardo and Colle (2012) of 59 QLCS events that occurred in the Northeastern U.S., they grouped QLCS events into 3 classes based on radar evolution as they moved toward the Atlantic Coast: decaying, slowly decaying, or sustaining. It was found that 900 to 800 mb warm air advection maximum was collocated with QLCSs that were able to sustain themselves all the way to the Atlantic Ocean. The vertically localized low-level warm air advection maximum was thought to be important in destabilizing the atmosphere just above the shallow marine layer. Other factors contributing to deep midlevel synoptic scale ascent were not as pronounced, such as 500 mb convergent Q vectors or frontogenetical forcing. In addition, mean low-level shear (0- 3 km) was found to increase by around 10 kts for sustaining coastal linear convection over decaying events. In fact, the average 0-3 km shear was largest for QLCS events that are maintained over the Atlantic waters. This is in contrast to Coniglio et al. (2010) , who found no significant difference in the low-level vertical wind shear values between short-lived (< 5 h) and long-lived (< 8 h) MCSs over the central United States, within 200 km downstream of the composite system location.

Student Notes:

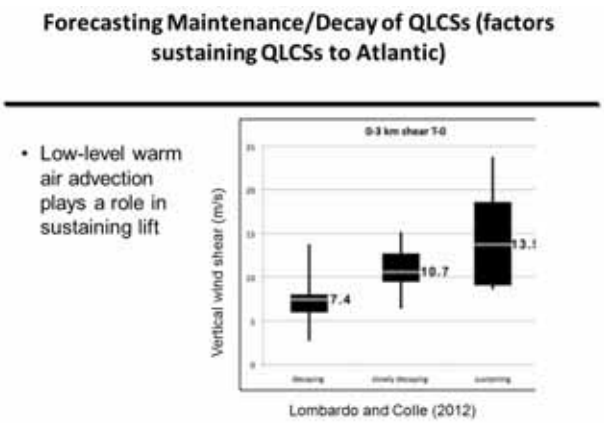

6. Forecasting Maintenance/Decay of QLCSs (crossing Appalachians)

Instructor Notes: In another study by Letkewicz and Parker (2010) , they evaluated various sounding parameters for QLCSs that crossed the Appalachian Mountains. In attempt to differentiate environments that supported QLCS maintenance, they were able to stratify events into two categories which led to 20 crossing and 20 noncrossing MCS cases. The cases were largely similar in terms of their 500-hPa patterns, MCS archetypes, and orientations with respect to the barrier. Analysis of radiosonde data, however,

revealed that the environment east of the mountains discriminated between case types very well. The thermodynamic and kinematic variables that had the most discriminatory power included those associated with instability, bulk shear vector magnitudes, and mean tropospheric wind. Crossing cases were characterized by higher instability, which was found to be partially attributable to the diurnal cycle. However, these cases also tended to occur in environments with weaker shear and a smaller mean wind. To summarize findings from a table shown here from their study, the environment that the MCS is moving into is more important for its maintenance than the one in which it originally developed. Downdraft CAPE (DCAPE) was the parameter that best separated crossing from non-crossing MCSs west of the Appalachians. Crossing cases on average contained higher amounts of DCAPE, which can be associated with the potential for stronger (i.e., deeper) outflow, due to more evaporational cooling. This could lead to a greater chance for the MCS's cold pool to retrigger convection to the lee of the mtns. The authors warned forecasters, though, to still be somewhat wary of using DCAPE, because of the large spread of midlevel moisture values observed in the cases. SBCAPE and MUCAPE were also considerably higher in the crossing cases. The upstream kinematic parameter that best separated case types was the 0–1 km shear, which was on average, smaller for crossing cases. These results are not immediately clear. There were also several wind speed and shear vector magnitude parameters that separated crossing and noncrossing cases well. These include 0–3 km and 0–6 km shear, and maximum bulk shear, but the relationship was not always clear, as the average of each of these parameters was smaller for crossers than noncrossers.

Student Notes:

Forecasting Maintenance/Decay of QLCSs (crossing Appalachians)

Location	Parameter	Crossing Avg	Non-Crossing Avg
Upstream	DCAPE (J/kg)	-612	-510
	0-1 km shear (m/s)	9	12
Downstream	SBCAPE (J/kg)	2371	519
	MUCAPE (J/kg)	2660	903
	Sfc-500hPa θ_e(K)	18	6
	0-3 km lapse rate (K/km)	7	6
	0-3 km shear (m/s)	9	16
	Sfc θ_e(K)	345	332
	0-6 km shear (m/s)	12	20
	LCL height (m AGL)	903	622
	Mountain-perpendicular 0-3 km shear (m/s)	5	9
	MLCAPE (J/kg)	513	318
	MUCIN (J/kg)	-18	-63

From Letkewicz and Parker (2010)

7. Using MUCAPE/MUCIN to Forecast MCS Mountain-crossers

Instructor Notes: The relationship between MUCAPE and MUCIN is illustrated in this figure from Letkewicz and Parker, 2010, showing that their poor correlation is due to a wide range of MUCAPE values when MUCIN is near zero and a wide range of MUCIN values when MUCAPE is small. If a forecaster were to use a MUCAPE threshold of 1000 J/kg, then 16 of the 20 cases with values in excess of the threshold would be correctly

diagnosed as crossers. Furthermore, if a forecaster were to also impose a MUCIN threshold of -50 J/kg, six of the seven cases with more than -50 J/kg of MUCIN and less than 1000 J/kg of MUCAPE would be correctly forecasted as noncrossers. Overall, they found that crossing cases tended to have thermodynamic environments in the lee of the mountains that were more favorable for convection, where MUCAPE and MUCIN are recommended as the most important operational ingredients.

Student Notes:

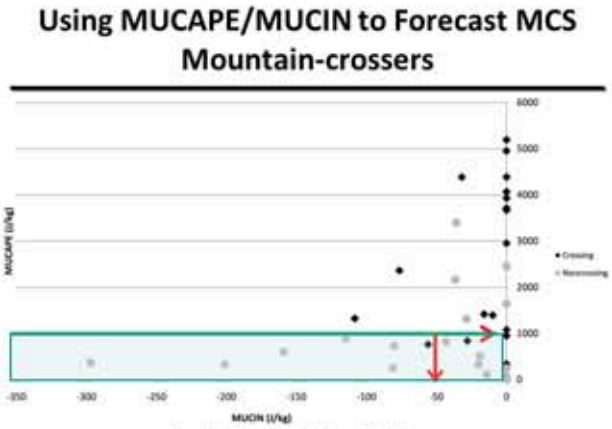

From Letkewicz and Parker (2010)

8. Why the Fast Movement for Some Derechos like June 29, 2012?

Instructor Notes: So, to review, a high–end QLCS event can produce a derecho if there is a sufficient amount of wind damage. On the lower right is a Google Map of warning polygons issued for the June 29, 2012 derecho. Darker boundaries are where multiple polygons shared a common boundary. Blue polygons are severe thunderstorm warnings, red are tornado warnings. The derecho travelled at a rapid speed (50-60 mph) and thus warnings became large. So, how do some QLCSs move so rapidly? Well, it's a function of cold pool strength, mean winds, and buoyancy. Based on Corfidi's research on propagation of multicells, as a cold pool develops and elongates, repetitive storm growth on the downwind-moving progressive part of the gust front comprises the derecho-producing convective system. It helps to perpetuate the system as long as there is sufficient buoyancy for lifting air parcels downstream. This is seen in the plan view figure. Now, the vertical wind profile is conceptual and is based on mean winds of documented downwind producing QLCSs. The key point is that the vector magnitude and direction supports movement in the downshear direction and the movement is going to be much faster than just the mean wind. Let's next talk a little about the factors at play in modulating a downwind-propagating, or forward propagating QLCS.

Student Notes:

9. Review of Main Factors at Play with Forward-Propagating QLCS Events

Instructor Notes: Let's take a few moments to review the main factors at play with forward propagating QLCS events. First, deep layer shear is a discriminating ingredient in MCSs that are weak or non-severe versus those that become a derecho. The mean hodograph from Coniglio clearly shows that shear becomes more stretched and straight-line along the x-axis (MCS-motion) as you go from the weak MCSs to the derecho MCSs (the colored numbers along the hodographs are kilometers Above Ground Level (AGL)). You can also see the huge increase in low-level storm-relative inflow for the derecho MCSs. Buoyancy and other measures of convective instability are equally important . The role of CAPE is multifaceted. Not only is sufficient CAPE necessary to maintain intense updrafts along the leading edge of the cold pool, but the larger the CAPE the more intense the updrafts and resultant supply of moisture and energy to the overall MCS. This in turn increases the subsequent downdrafts and strengthens or at least maintains the cold pool momentum. If CAPE weakens or the outflow surges into an environment with little or no CAPE and/or significant convective inhibition, then the convective system can quickly lose its energy source and diminish quickly. Thus, vertically integrated buoyancy is often used as a convenient measure of potential cold pool intensity, but there are limitations as the computations do not account for the role of midlevel dry air. In the case of the evening of June 29, 2012, there was ample CAPE downstream to perpetuate and intensify the system as you can see from this AWIPS D2D screen capture of the 12 hr forecast of CAPE from the NAM valid at 00z on the evening of June 29. Values above 3000 J/kg are every image contour inside the yellow color in the image and values > 4000 are annotated. These values actually stayed pretty high throughout the evening.

Student Notes:

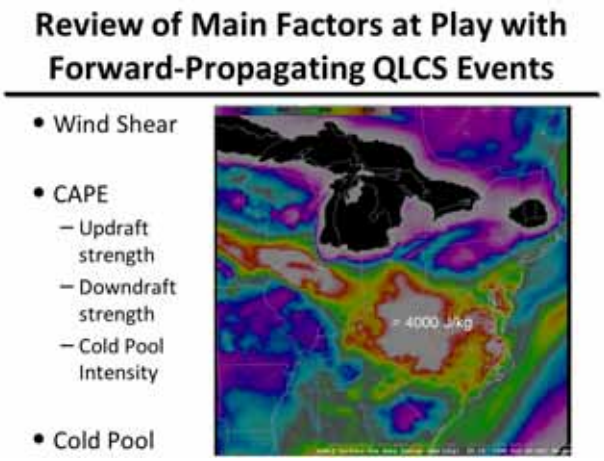

10. Other Factors Related to QLCS Maintenance

Instructor Notes: There are other factors that are related to QLCS maintenance. These factors (as previously noted in AWOC IC Severe 2 lesson 3) have been found to encourage downwind propagation: (1) Rich boundary layer moisture --- Moisture-rich air fosters new storm development by lowering the LCL and enhancing precipitation drag (2) Steep low-level lapse rates --- Steep lapse rates enhance both CAPE and downward momentum transfer (3) Minimal Convective Inhibition or CIN --- The potential for storm initiation is maximized when CIN is low (4) Fast cloud-layer flow --- Fast flow increases gust front speed by strengthening storm outflow; fast flow also fosters the development of embedded supercells and their associated severe threats (5) Deeply unidirectional flow --- Unidirectional flow encourages elongation of the system cold pool in a preferred direction, thereby enhancing storm-relative inflow in that direction (6) Slightly-backed near-surface winds relative to the mean flow --- Backed low-level winds enhance storm-relative inflow and the rate of downwind cell development

Student Notes:

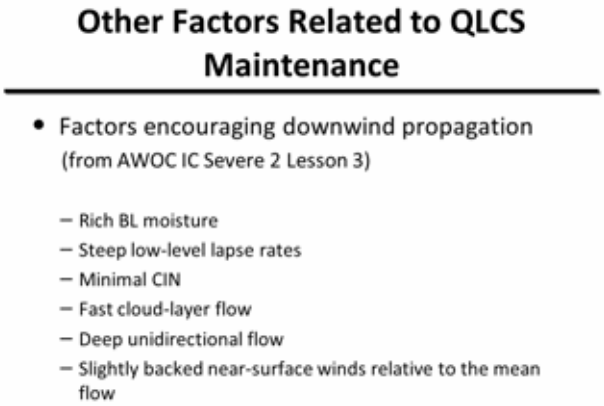

11. Can Extreme Buoyancy Compensate for Lack of Strong Shear in Modulating QLCS Events?

Instructor Notes: Based on the 00z IAD sounding, there was over 5000 J/Kg of SBCAPE. Corfidi forward propagating vector = 301 deg/48 kts. DCAPE values from the observed sounding was 1512 J/kg. Some other forecast soundings had close to 2000 J/Kg of DCAPE. So, shear was not impressive but CAPE was huge, leading to a strong and deep cold pool. In RKW theory, if the shear is weak, a cold pool/shear balance is achieved with the RIJ which seems to allow the system to last a long time. Here is a NSHARP AWIPS-2 sounding which points to some more details.

Student Notes:

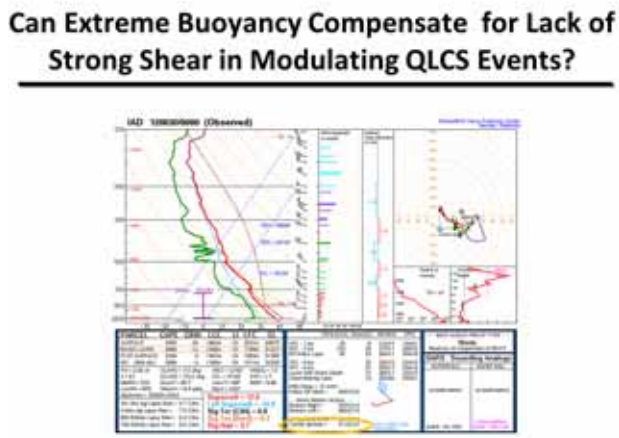

12. Other Proximity Soundings Showed Favorable Thermodynamics

Instructor Notes: From a 0100 UTC RAP sounding for DC, note the steep lapse rates, low LCL , and no CIN.

Student Notes:

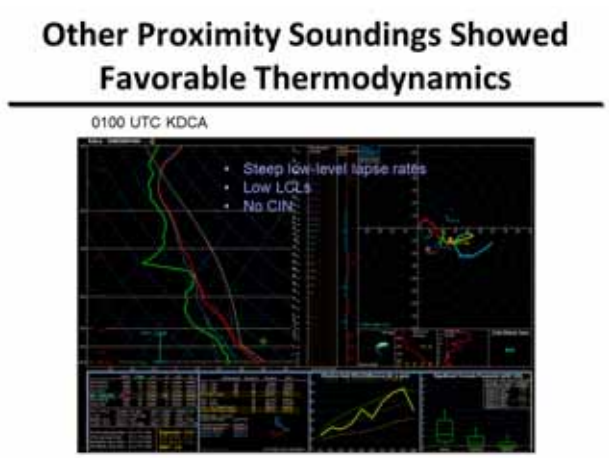

13. Cold Pool Strength

Instructor Notes: Due to the extreme instability out ahead of progressive derechos, there usually are some large, temperature contrasts which are indications of the strength of the cold pool and subsequent strong winds. By 0100 UTC, the analysis showed temperature drops of greater than 26F due to the QLCS cold pool.

Student Notes:

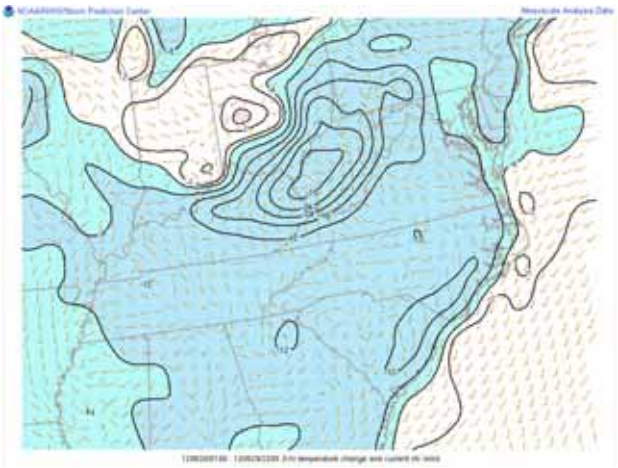

14. Initial Stage of a Damaging Bow Echo

Instructor Notes: The initial stage of a bow echo at the onset of severe damaging surface winds is a time when the precipitation area is not bowed at all. An updraft surge typically happens which then yields a severe downdraft. Also at the same time, anvil debris typically spreads rearward of the main convective line with respect to the steering layer flow. This anvil debris acts to initiate the rear inflow jet (RIJ). Assuming you're about to have a severe bow echo, the best time for initial warnings is in the tall echo state when updraft surges occur prior to the onset of the severe downdraft and RIJ. This is when you typically see strong, deep convergence, represented by the MARC (Mid Altitude Radial Convergence), along a segment of the line. Just before the bowing state, the descending RIJ hits the ground and begins to push forward. The most severe mesovortices may form at this time. The most severe surface winds occur when the mesovortex forms near the apex of the RIJ. As the convection morphs into a bow echo, the updraft depth often decreases, and a rear to front dry slot forms. The strong outflow from the RIJ is firmly established and has been on the ground for some time.

Student Notes:

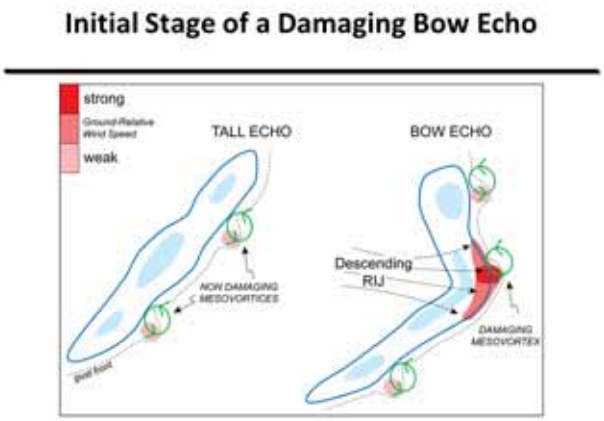

15. Storm Interrogation Best Practices 3-D QLCS structure

Instructor Notes: This next section is from IC Severe 3, a lesson produced with Jim and Ron P. on QLCS Storm-interrogation, first published in 2010. The most severe QLCS events typically have an upright updraft with almost slab-like appearance along a deep gust front. The convection is able to remain attached to the gust front and so on radar, you may not actually see a separate fine line from the intense reflectivity cores. A deep convergent zone accompanies the gust front. On some occasions, and after accounting for system motion during volume scanning, you may see a strong echo overhang leading the reflectivity core. Rear inflow notches signify intense RIJ channels. The RIJ remains elevated to descend only immediately behind the convective line. Lightning often precedes the arrival of the line. Mesovortices are common with these structures as there is plenty of deep updraft over their formation regions. The less severe events exhibit more isolated convective cells often displaced well behind the gust front. A separate fineline is often visible ahead of the first reflectivity cores. The gust front is often severely sloped with a shallow leading edge. The RIJ often descends well behind the leading convective cores. Deep, severe mesovortices would be extremely rare with a sloped system like this.

Student Notes:

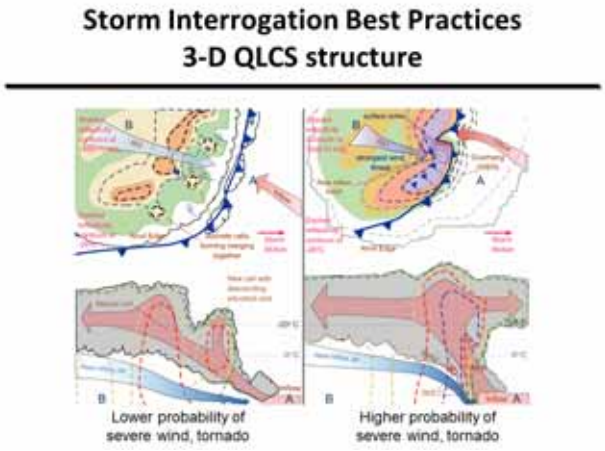

16. Derecho ComparisonSimulated: reflectivity (top)?(bottom)

Instructor Notes: There are subtle, but important, differences even amongst QLCSs with slab-like lifting. To illustrate, here is a comparison between the infamous 29 June 2012 derecho and the Superderecho of 08 May 2009. Both derechos are similar in age but differ in the strength of the cold pool. Consequently their structures differ as well as the locations and types of hazards. The most typical structure is the one represented by the 29 June 2012 event here in Ohio. Note that the cold pool dominates its organization with temperature deficits ranging to 10 to 13 deg C. We find a large region of strong winds whose components are typically normal to the gust front with the highest values immediately behind. A poorly defined comma head of high reflectivity appears on the north side and a pool of surface-based vorticity lies along the gust front to its north and east. The midlevel representation of this vorticity is stronger and lies rearward over the low-level cold pool. As such there is no surface representation of this MCV. The more unusual structure came from the 08 May 2009 case where a much stronger bookend vortex appears in the reflectivity. This derecho's cold pool is much weaker with a temperature deficit of only 4 to 6 deg C. In this case, there is a well defined low-level vortex directly inside the reflectivity comma head. The strongest winds now don't lie just behind the gust front but instead are more focused around the west to south sides of the vortex. Essentially the loss of the cold pool allowed the MCV's pressure minimum to reach the surface and create a hurricane-like warm core low. These plots are courtesy of successful 3 km WRF runs that simulated the structures of both derechos studied by Weisman (2012) for 29 June 2012 and Weisman and Evans (2012) for 08 May 2009.

Student Notes:

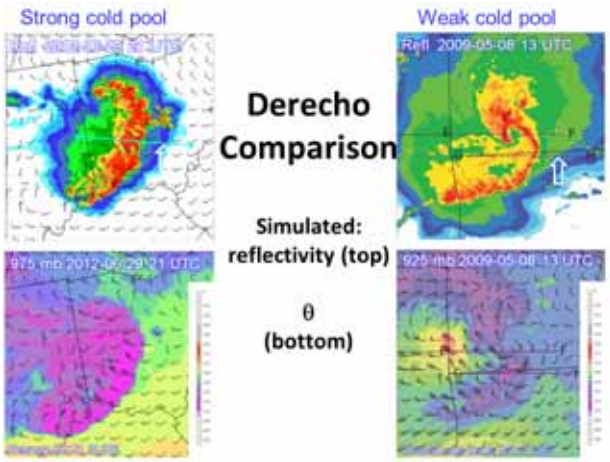

17. June 29, 2012 Storm-Scale Model

Instructor Notes:

Student Notes:

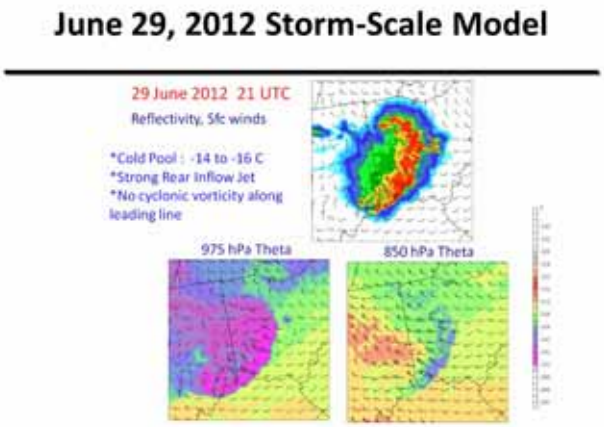

18. Slide 18

Instructor Notes: When we look at the cross-sections, we see that the strength of the cold pool (seen by the rise in isentropes in the top panels) is much higher for the 29 June case in Ohio whereas there's a much smaller rise for the 08 May event. So what did the environment do to create such a radical difference in structure. One possibility is that the 29 June case featured much higher ?e in the pre-storm boundary layer, but weaker shear. Notice the rather weak pre-storm wind profile for 29 June vs. 08 May. However other important factors include those that could've weakened the cold pool in 08 May and one of these may include higher boundary-layer relative humidity.

Student Notes:

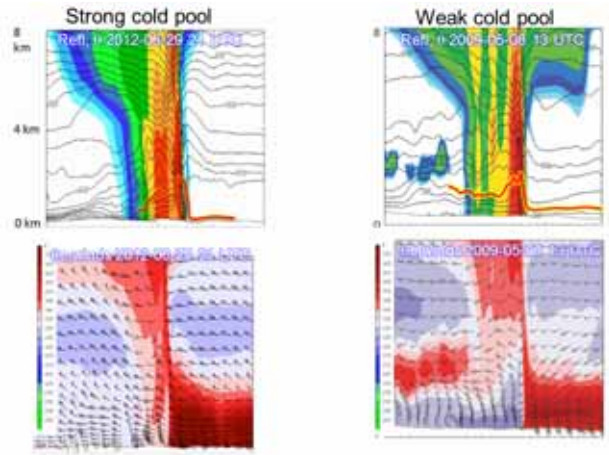

19. Strong Shear, Weak Cold Pool Derecho

Instructor Notes: A strong derecho with a relatively weak cold pool, such as May 8, produces several regions of interest affecting your warning decisions, regions 1-5. In region 1, the midlevel shear induced by strong low-level inflow and MCV-enhanced mid-level winds, has caused the convection to tilt downshear and become fragmented and somewhat shallow as seen in the DVIL product. The gust front follows the fragmented convection. In region 2 the vertical shear in the pre-storm air has become balanced with that at the cold pool boundary and the convection has become upright and deep (see the DVIL product). The gust front lies on the leading edge of a solid line of heavy convective precipitation. Down to region 3 and here the gust front has begun to pull ahead of the convective line. The DVIL product again shows shallower convection. All of these structural changes have big implications for the warning strategies and much of it is related to the orientation of the cold pool boundary with the pre-storm vertical shear. The fourth region has much to do with what we talked about before regarding the MCV penetrating to the surface and allowing a warm-core vortex to generate strong circulating winds around the low pressure. The weakened cold pool allowed this to happen. Region 5 represents the more traditional rear inflow jet and an axis of high winds trailing well behind the gust front. We'll take a closer look at these regions, what they mean for warning strategy and how to identify them coming up.

Student Notes:

Strong Shear, Weak Cold Pool Derecho

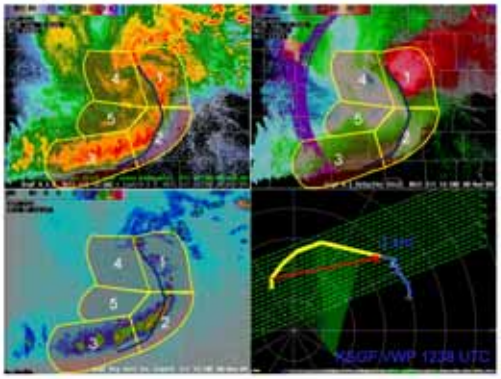

20. Region 1: Shear Dominance

Instructor Notes: This is a region where the gust front spawns relatively discrete convective cells whose tops are sheared rear to front (relative to the cold pool) and the updrafts are somewhat shallow. Going back to the shear we can see why. We overlay the 0-3 km shear vector across region 1 and then the location of the cold pool boundary. The 0-3 km bulk wind difference is 30 m/s. But we notice that the shear vector is not exactly perpendicular to the boundary; instead there is a 70 degree angle. Thus, the component of the total shear is rather 28 m/s. This is an unusually high value that is responsible for the character of the convection here. What does this mean for you at the warning desk? Take a look at the velocity and you'll see the gust front in this region occupied by strong horizontal shear. The discrete convective updrafts were rooted to the gust front and quickly broke up into supercell-like structures as a result of this strong line-normal vertical shear. Mesovortices formed within these updrafts. However their formation may have been more akin to that of traditional supercell mesocyclones. Multiple tornadoes formed in this region shortly after this radar scan. As a warning forecaster, when you see the gust-front normal component of the 0-3 km shear exceed roughly 15 – 20 m/s, watch out for convection to become discrete and for mesovortices or supercellular mesocyclones to form. Tornadoes are likely if at least 10 m/s of that shear is within the 0-1 km layer in the presence of other favorable thermodynamics that were covered in IC2. Why does the convection become so discrete and somewhat shallower in the face of stronger shear? We'll revisit the theory of shear vs cold pool balance.

Student Notes:

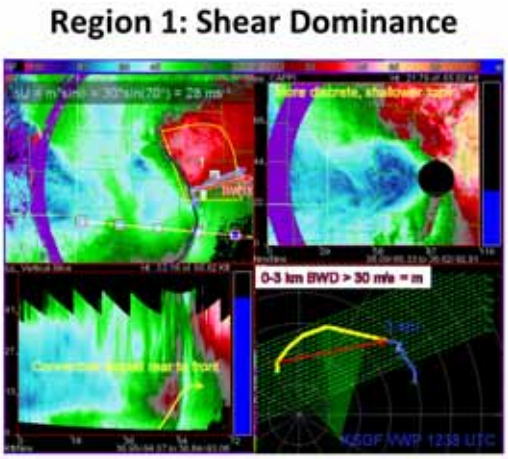

21. Recap of RKW Theory

Instructor Notes: RKW theory goes quite a ways to explain the structural characteristics of derechos and likely hazards. All derechos produce damaging wind (by nature of the definition), however, the presence of mesovortices can change the intensity and shape of the severe winds. We just saw an example of a shear-dominant segment of the gust front where more discrete, shallower convection led the gust front. The imbalance between the strong environmental line-normal shear and weak cold pool shear led to weak lifting as updrafts are quickly tilted downshear. The value of delta-U we got 28 m/s fell into the shear dominant regime. Mesovortices or supercellular mesocyclones are likely unless the shear is strong enough to completely shred updrafts. Tornadoes are likely contingent on favorable thermodynamics and 0-1 km shear. Damaging winds are not going to be widespread, but mesovortices will likely have some. Decreasing the environmental vertical line-normal shear into the 15-20 m/s range will lead to a more balanced state given the same cold pool strength. When this happens then the ensuing updraft along the convergence zone strengthens and becomes more erect. The gust front lies underneath the updraft and immediately in front of the heavy convective precipitation. This regime allows for almost unbroken convective updraft above the gust front. Mesovortices and tornadoes are all likely in this regime, the latter contingent on favorable thermodynamics and sufficient low-level (0-1 km) vertical shear. Damaging wind is also likely to be widespread thanks to the unbroken convective line. As the environmental line normal vertical shear decreases further below 15 m/s, or the cold pool strengthens, the convective updraft is likely to slope front to rear. Now the gust front begins to race out ahead of the line of convective precipitation. The slab-like lifting may become more broken and much of the ascent will be elevated above the cold pool. Mesovortices become rare, and so do tornadoes, no matter the actual value of the environmental vertical shear. Recall it's the line-normal component that matters. The only way to improve the line-normal vertical shear is for part of the line to surge forward producing a more favorable orientation to the convective line. Even with this imbalance, derechos are possible. This dominant cold pool regime can occur in parts of a curving derecho producing QLCS or the entire QLCS could be cold pool dominant. Let's take a look at the other regimes of the sample derecho.

Student Notes:

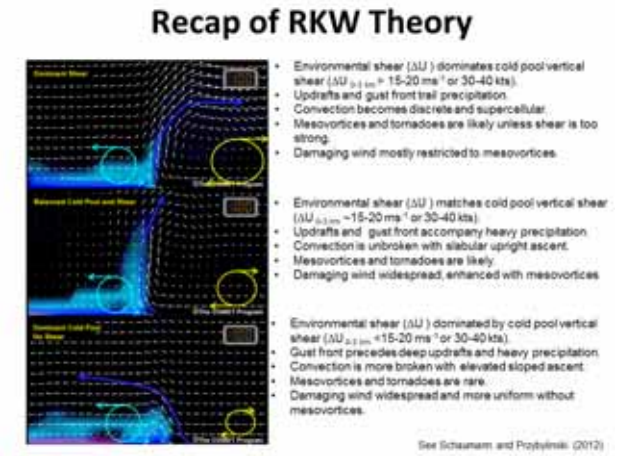

22. Region 2: Balance

Instructor Notes: The gust front changes orientation further south from region 1 such that it's oriented NE to SW. Let's assume the 0-3 km BWD is the same in region 2 (a dangerous assumption to be mentioned later). In this new location the environmental shear vector is oriented roughly 45 degrees to the gust front. This results in a delta-U of 21 m/s. This new orientation is closer to the typical values associated with 'balanced' systems. The visual manifestations are obvious as the convection is deeper, more slab-like (continuous) and vertically erect. The velocity data shows a deep convergence zone in the cross-section that extends along a line exceeding 21 kft ARL in the CAPPI. That's impressive! This region is likely going to contain widespread damaging winds along with focused regions of enhanced wind damage with mesovortices. Watch this area carefully for mesovortices that may also strengthen enough to become tornadic. So the delta-U appears somewhat large and yet the radar data shows deep upright slab-like convective line that suggests balance. If the RKW theory is correct, then either the cold pool is unusually strong to create balance with the delta-U, or the delta-U is smaller. We've seen a strong suggestion from the model data that the cold pool isn't any stronger in region 2 and so we can rule that out. But what about the delta-U? Well it could be weaker. One possibility is that the environmental BWD is somewhat weaker here because this location is somewhat south of the strongest mid-level flow wrapping around the convectively-generated MCV. Note in the 21 kft velocity in the CAPPI there is a zone of very strong winds with a rather sharp southern edge. This edge appears to be on the north side of region 2. It is possible that weaker midlevel flow to the south may contribute to weaker environmental vertical shear and thus a higher chance of a shear/cold pool balance.

Student Notes:

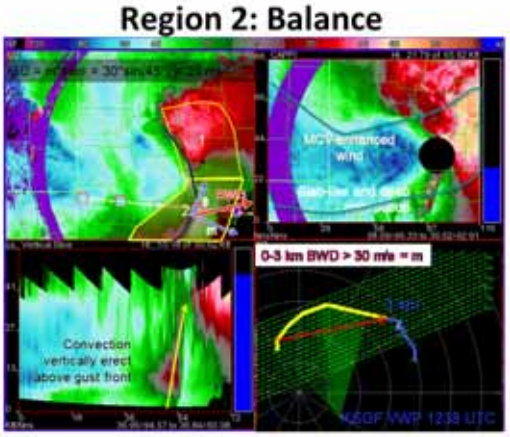

23. Region 3: Balance

Instructor Notes: On to region 3 and the gust front orientation (WSW-ENE) rapidly diminishes delta-U. Playing a conservative stance and plugging in a 20 degree difference between the BWD direction and the gust front orientation yields a delta-U of 10 m/s. That's less than the typical optimal values of 15-20 m/s and thus this segment of the derecho should feature a cold pool dominant structure. Indeed the radar shows that with diminished reflectivities at 20 kft and in the cross-section also shows the same. The velocity shows the gust front position extending further ahead of the convective line and the line itself appears more broken in the CAPPI. This is the region where mesovortices and tornado threat is minimal, not worth a tornado warning. Wind damage is certainly possible though this area is typically south of the RIJ and so the wind is likely not as widespread as directly ahead of the strongest portion of the RIJ.

Student Notes:

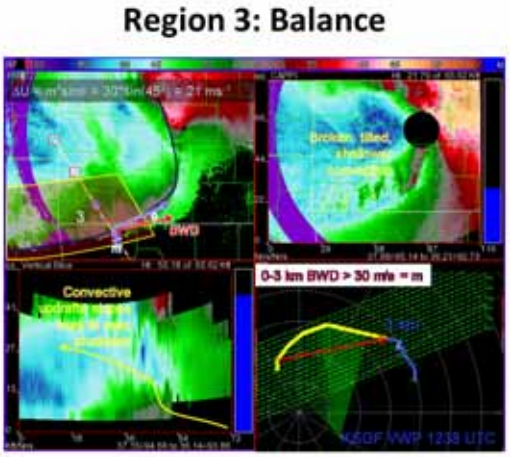

24. Regions 4 and 5

Instructor Notes: Going back to the northwest we see what made this derecho so special. The weak cold pool allowed the low pressure associated with a powerful midlevel

MCV to be reflected at the surface. The result was an intense circulating wind storm around a meso-? vortex. Thus, a wide area of hurricane force winds formed around the vortex center in region 4. The radar could see this circulation because it was deep. Most of the time the cold pool would limit the lower extent of this circulation above a shallow layer. But not this time. What complicated the situation was the presence or introduction of mesovortices along the curling convective band towards the MCV. Some of these were tornadic. Region 5 represented the more traditional region of the rear inflow jet axis. This is a nearly ubiquitous feature in derechos. However the RIJ in this case was certainly influenced by the presence of the MCV. Both of these areas produced severe winds requiring a warning. But what type of warnings should be issued? After all, some of these winds lasted for more than 20 minutes and were not necessarily associated with active convection, especially in the southern portions of region 4 and region 5.

Student Notes:

Regions 4 and 5

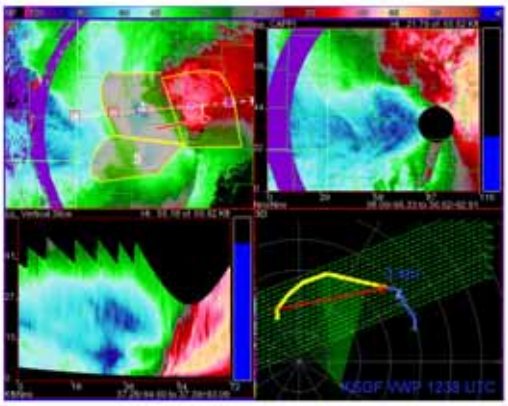

25. Weak Cold Pool Derecho Warning Strategy

Instructor Notes: If this derecho were a tropical cyclone then the answer would be that either high wind warnings or an inland hurricane wind warning would be issued. But this is an organized thunderstorm and so traditionally severe thunderstorm warnings were issued with the occasional tornado warning to address that threat. Notice that severe thunderstorm warnings covered much of regions 4 and 5 as the MCV and RIJ began to produce severe winds. Yet the high winds in much of these regions were not associated with a thunderstorm, especially just south of the MCV center where descending air eroded precipitation.

Student Notes:

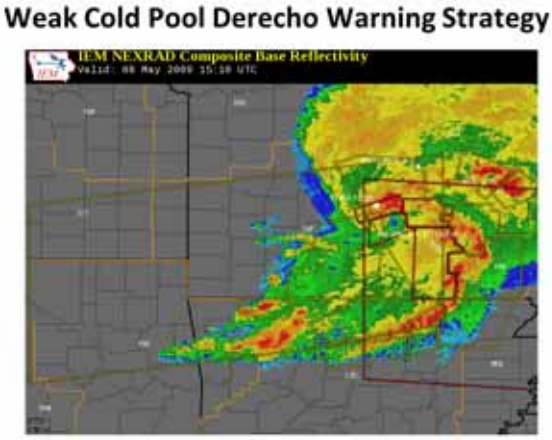

26. High Wind Warning: Another Option

Instructor Notes: Perhaps a high wind warning would also be an option to cover those areas of damaging winds that are not also experiencing active convection. There are criteria that have to be met including high winds at 35G50 kts or more lasting for at least an hour. The meteogram from KSGF on that day shows indeed that such criteria were met. In fact, the Springfield office issued a high wind warning just ahead of the derecho as it became apparent that it was becoming a big show. The text in their warning described that the winds would occur behind the severe thunderstorms. However the final winds were significantly stronger than anticipated. This is understandable since this event was rare. Rare, but not unprecedented. Other derechos have also been cold pool deficient with severe (hurricane force) swirling winds around an MCV including one famous event on 2003 July 21 in NW PA and W NY.

Student Notes:

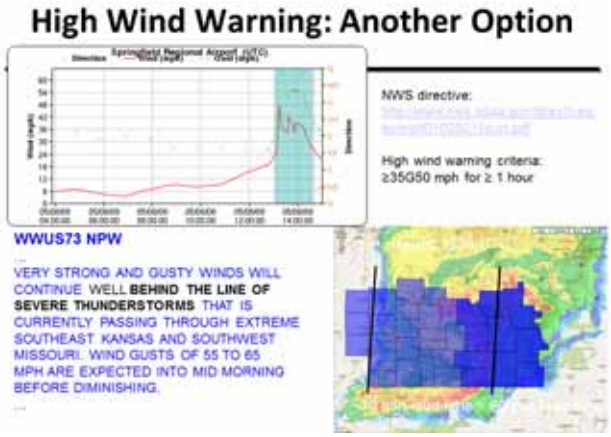

27. 2009 May 08 Event Reports

Instructor Notes: As you can see this derecho was widespread, but the worst of the wind damage from the combined RIJ , MCV, and downbursts was from MO to southern

IN. Do notice that the derecho was responsible for significant flash flooding too as a result of slow moving convection ahead of the MCV and then the intense convection on the north side of the MCV. Much of the worst wind damage resulted from sustained hurricane force winds over a period of an hour. This duration is what makes the derecho potentially more damaging.

Student Notes:

28. 2012 July 03 DLH

Instructor Notes: The majority of derechos don't transition into a cold pool deficient state. Instead they appear much like this one did west of Duluth, MN on 2012 Jul 03. The shape is the same as the derecho of 2009; it's that of a large bow with a bookend vortex to the north. But the differences begin when you notice that the most solid portion of the line (see DVIL) is now north of the apex. Notice that now the cold pool boundary is leading the heavy convective precipitation everywhere, but is adjacent north of the apex and is well separated to the south. This structure makes sense as the hodograph from the KDLH VWP shows a weaker 0-3 km shear even though it's from the same direction. The weaker shear means the cold pool has an easier time to at least achieve balance north of the apex in region 1. As a result, this derecho is somewhat less complex than the one on 2009 May 8. The MCV is apparent but not as intense, and it is uncertain as to whether it extends to the ground. However the RIJ appears strong with inbounds at 2-3 kft ARL reaching 80 kts. In addition, a developing mesovortex is located on the north side of the RIJ apex along the cold pool boundary.

Student Notes:

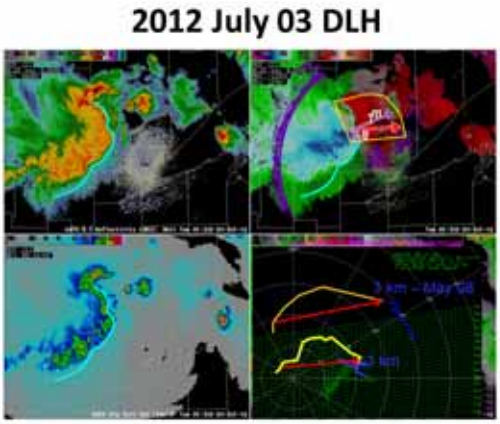

29. Detailed View of Region 1 - DLH

Instructor Notes: Zooming in, see that the cross section shows vertically erect strong echoes in this region 1, the strongest is with an isolated cell well out ahead of the line and along a warm front. Along the convective line, an almost unbroken line of ZDR columns at 20 kft ARL highlights the almost slab-like lifting occurring over the low-level outflow boundary.

Student Notes:

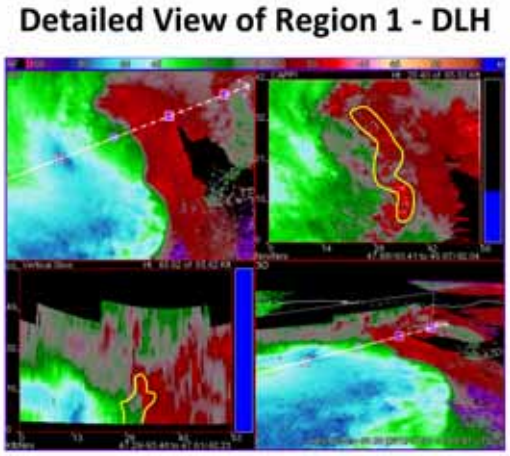

30. 2012 July 03 DLH

Instructor Notes: In region 2, the orientation of the gust front reduces the boundary-normal shear (m) far enough that the cold pool dominates. In this case to the point where the cold pool boundary outruns the convective cores and the lifting becomes more sloped with less slabular lifting and more discrete deep updrafts. As a result, this derecho is somewhat less complex than the one on 2009 May 8. The MCV is apparent but not as intense, and it is uncertain as to whether it extends to the ground. However the RIJ appears strong with inbounds at 2-3 kft ARL reaching 80 kts. In addition, a developing mesovortex is located on the north side of the RIJ apex along the cold pool boundary.

Student Notes:

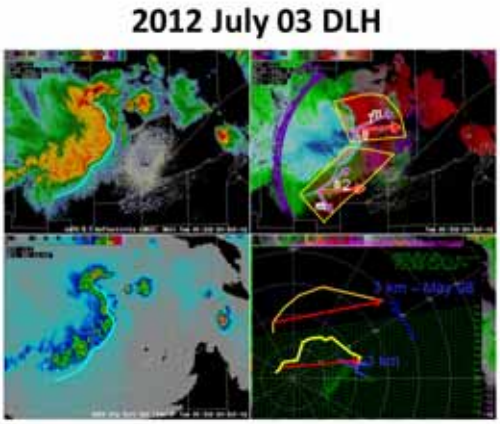

31. Region 2: Cold Pool Dominance - DLH

Instructor Notes:

Student Notes:

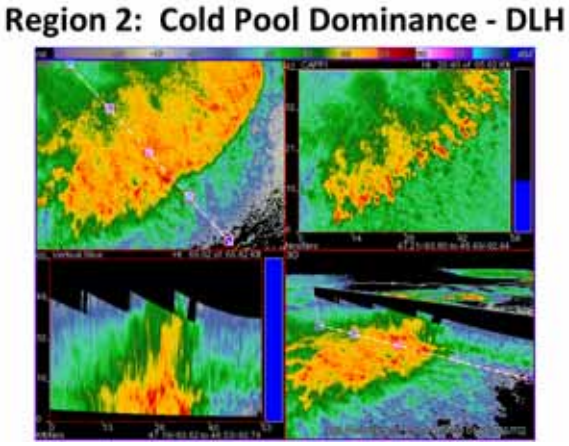

32. 2012 July 03 DLH

Instructor Notes: We look behind the line and see that the MCV is apparent, but not as intense as the super derecho of 2009, and it is uncertain as to whether it extends to the ground. However, the RIJ appears strong with inbounds at 2-3 kft ARL reaching 80 kts and here we label this area region 3. The RIJ is sufficiently strong enough to cause damaging winds, especially in conjunction with local downbursts and mesovortices. However, it's unknown to what extent those winds remain damaging as one goes further behind the line. This uncertainty certainly affects the decision of whether or not to keep severe thunderstorm warnings behind the line or introduce a high wind warning. A high wind warning has the advantage of lead-time, but at the cost of a false alarm should the wind duration not verify. Severe thunderstorm warnings have the advantage of higher resolution, more appropriateness with a severe thunderstorm, but the cost is lead time. As a reminder, these regions are not meant to represent suggestions for warning polygons. They are

highlighting areas representing common structures. For a recap of the actual warnings issued, let's go on.

Student Notes:

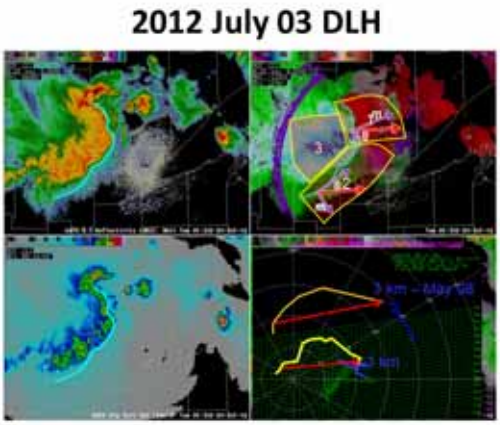

33. Slide 33

Instructor Notes: This is a Base Reflectivity mosaic radar loop of the derecho, beginning with the cluster of disorganized multi- and supercells east of Grand Forks near 00 UTC. The warning polygons were small to begin but the content of the warnings was definitely high end (excess of 80 mph, dangerous situation). The northern warnings focused on more discrete supercellular structures extending east of the developing bookend vortex. The southern warnings handled the primary developing derecho. By 0128 UTC, WFO DLH opted for one large warning encompassing the entire derecho. This strategy of laying out large severe thunderstorm warnings continued until the derecho exited their CWA. The key here is to remember that the high end threat language began before the classic bowing shape of the derecho began.

Student Notes:

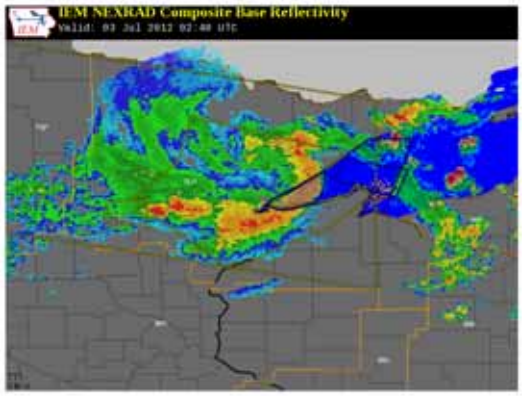

34. Slide 34

Instructor Notes: At this beginning stage is when the updrafts are more discrete and tall, but convective initiation became too aggressive and adjacent cold pools merged. At 2330 UTC is when cells merged across a region at least 100 km long. At this scale, and in an environment of high CAPE and strong shear, the merging cold pools strongly suggest the onset of a damaging bow. In less than an hour, the multicell cluster morphed into the classic bow of the derecho. But the damaging winds were already well established.

Student Notes:

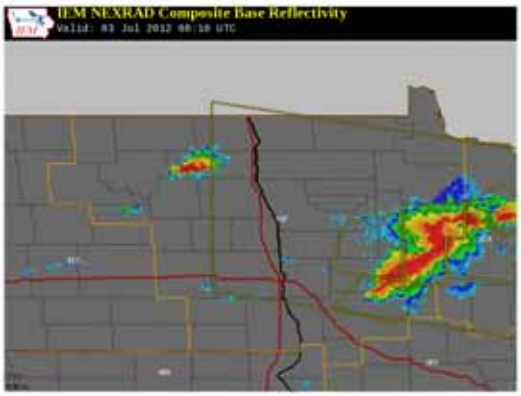

35. July 3, 2012 Phases of Development

Instructor Notes: At this beginning stage is when the updrafts are more discrete and tall, but convective initiation became too aggressive, and adjacent cold pools merged.

Student Notes:

36. Storm Interrogation Best Practices

Instructor Notes: Which stages in a QLCS lifecycle are most likely to produce the most severe wind and tornado reports? - During and after formation of the RIJ. What 3-D structure is associated with the strongest severe wind and tornado events? - A deep and steep gust front with a deep convergence zone attached to a solid wall of deep convection. What is a common convective evolution preceding the formation of a bow echo? - Merging small multicells and their associated cold pools What is the motion of a typical bow echo? - Identical to the mean convective layer wind and faster

Student Notes:

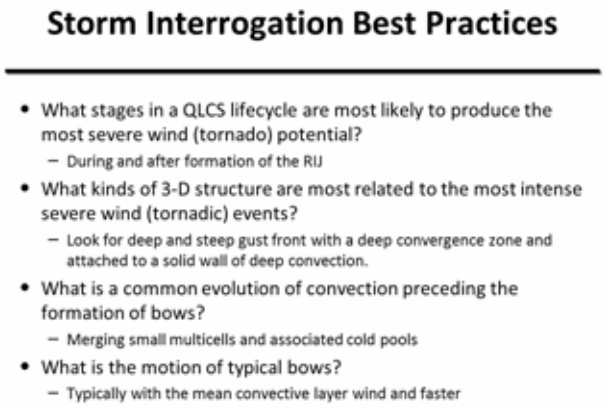

37. Warning Considerations

Instructor Notes: A fast-moving QLCS can present warning polygon issues for forecasters. From our Tornado and Severe Thunderstorm Warning Best Practices and Advanced Storm-Based Warning courses, we illustrated warning strategies for fast-moving storms, most of which were supercells. I will now present an example on how to issue polygons for a fast-moving mature QLCS producing damaging winds due to a very strong cold pool in balance with a RIJ.

Student Notes:

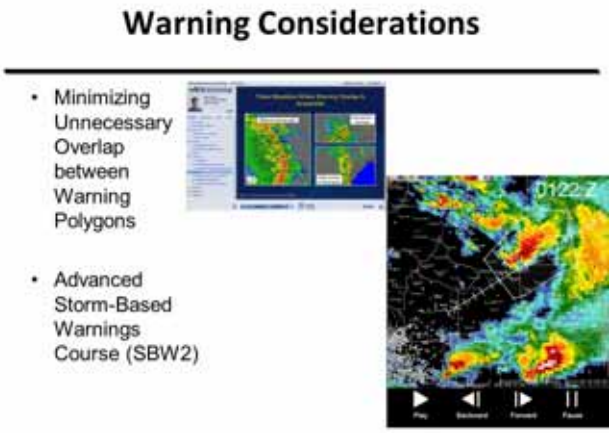

38. Example of a Warning Strategy

Instructor Notes: Here is a recommended warning polygon strategy for a fast-moving QLCS. This example is from the 2012 June 29 derecho. Step 1 is evaluate the environment to determine potential threats such as tornado, wind, hail, and flash flood. As was discussed previously, this environment's main hazard was it's high severe wind potential. Step 2 is determine threat motion. Recall from the 00z IAD sounding, the SBCAPE was over 5000 J/kg and the 00z RUC forecast indicated that there was >4600 J/kg of SBCAPE ahead of the line across a large area. The NSHARP AWIPS 2 sounding (also available with BUFKIT) displayed a forward-propagating Corfidi Vector, which in this case was from 301 degrees at 48 kts (much faster than the 0-6 km mean wind). Unidirectional flow above the LFC is encouraging elongation of the system cold pool in a preferred direction, thereby enhancing storm-relative inflow in that direction. Because of extreme downstream instability and shear vector orientation, a strong, convectively-generated cold pool was contributing to a system-relative flow. All of this provides a good first guess approximation to the threat motion as shown. Step 3 is determine polygon orientation. Mesovortex potential is low because the effective bulk shear is 35 kts and the QLCS is cold-pool dominant. Thus, our storm interrogation strategies will emphasize severe thunderstorm warning. Steep upright updrafts are noted along the leading edge and there is a strong RIJ most pronounced behind the northern apex of the bowing segment as noted previously. Discrete cells are forming and merging along the leading edge of the reflectivity gradient with the gust front located just ahead of the gradient. The preferred warning strategy in this situation is to orient the polygons along the line of motion with a flaring out on the downstream end. Allow for some overlap to ensure adequate downstream lead time for locations on the entrance region of the polygon. And, if given the opportunity, within the constraints of workload warning management, it would be a good idea to break up the warning polygons to minimize excess text. The next slide provides more detail.

Student Notes:

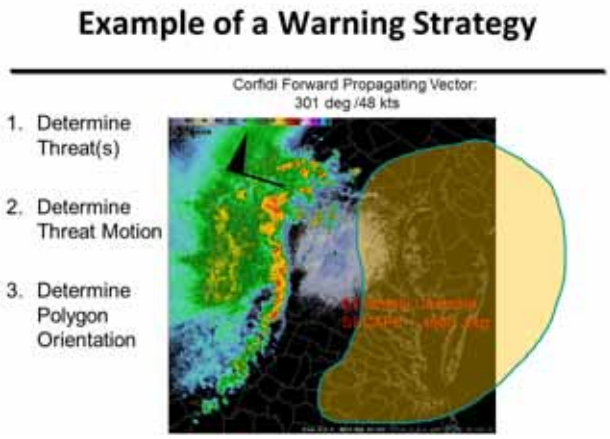

39. Slide 39

Instructor Notes: Here's an example of a typical Severe Thunderstorm Warning issued along a squall line. The strategy is to warn along a large portion of the line using polygons with a 3 to 1 length to width ratio. Each warning's duration is approximately one hour which provides lead time and covers the severe wind threat behind the line. Warnings must be reissued about half-way into each warning, which obviously creates some polygon overlap.

Student Notes:

40. Changing Orientation of Polygon to Decrease Length to Width Ratio

Instructor Notes: Here's a different warning polygon strategy which cuts down on overlap and obtains maximum lead time for locations on the entrance side of the polygon. These are big polygons so you'll have to watch for text overload. We start the warnings at 0109z, with the assumption that there is an existing warning out for threats to the west of the three new polygons.

Student Notes:

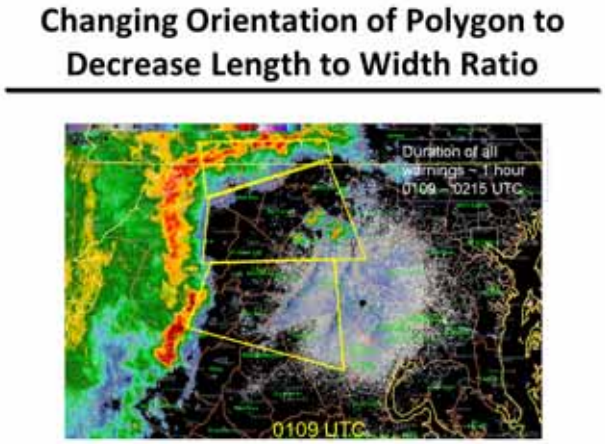

41. 3 Volume Scans Later

Instructor Notes: No , 3 volume scans later.

Student Notes:

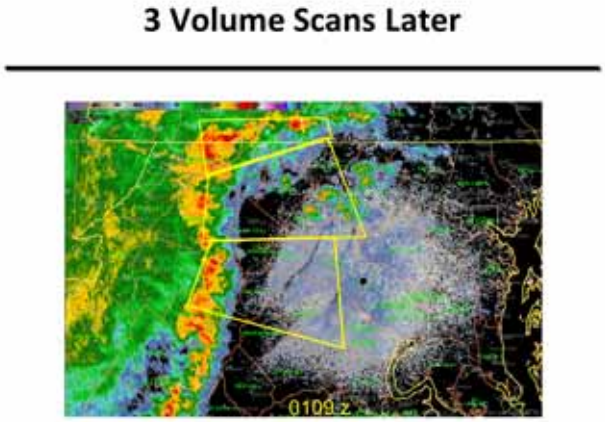

42. 6 Volume Scans Later

Instructor Notes: Now, the storms and proposed polygons issued 6 volume scans later.

Student Notes:

6 Volume Scans Later

43. 6 Volume Scans Later:Base Velocity

Instructor Notes:

Student Notes:

6 Volume Scans Later:
Base Velocity

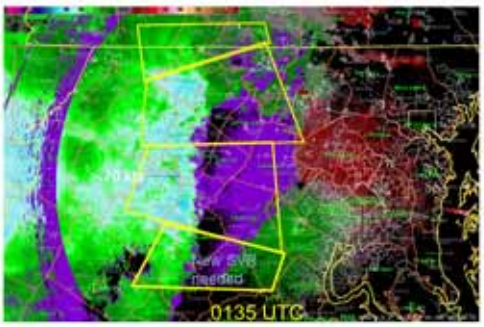

44. Time to Extend?(Warning Expires in 30 min)

Instructor Notes: No, the warning still has 30 minutes remaining and plenty of downstream lead time. Compare this situation with what you would have had with a 3 to 1 length to width ratio warning we showed earlier. The next slide shows how I'd update with downstream warnings.

Student Notes:

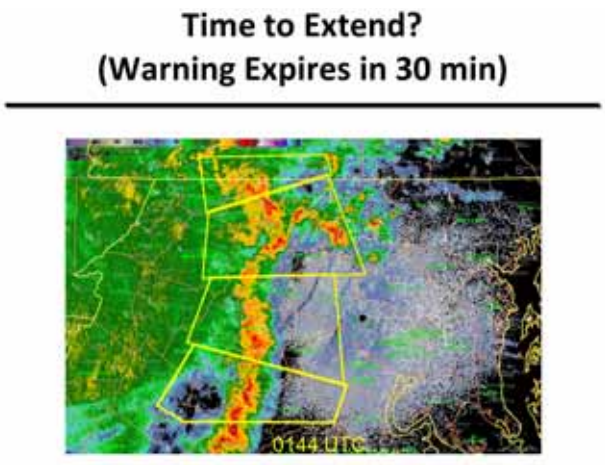

45. Following-Up with New Warnings

Instructor Notes: I've re-centered the display at the RDA, zoomed in to view the most intense part of the line, and overlaid the approximate locations of the warnings of interest which expire at 0215z. At this point, you can consolidate some warning threats into the three white polygons shown. These three new warnings hit most of the Washington D.C. metro areas with adequate lead times of the impending threat. Again, you can continue the smaller length to width ratio for polygon size. Note, the warning at the northern-most part of the screen shot is oriented with a smaller length as there is some slower movement near the bookend part of the line. Also, given the velocity data, this might be a possible location for mesovortex development. Hence. This polygon might go red.

Student Notes:

46. RIJ Sampled at Higher Tilts Approaching Leading Edge Suggests Stronger Wind Potential and Acceleration of Line

Instructor Notes: Now, we are examining a 2.4 reflectivity tilt at 0205 UTC which is well past the time for an update to the previously shown initial warnings. But the main point here is to illustrate the structure of the QLCS has changed with the intensification of the cold pool and resulting push of the RIJ toward the leading updrafts such that individual updrafts have consolidated and we are seeing more slab-like lifting with the line as well as development of weak echo channels behind the leading edge. As we zoom into a 0.25 km base velocity product, we can see the leading edge of the RIJ just west of the radar, which has increased the ground-relative winds to > 83 kts. These measurements verify the change in the QLCS structure and denote an impending increased intensity of the winds. Thus, I would consider using enhanced wording in the warnings to highlight high-impact winds exceeding 80 kts in the DC metro area by 0230-0245 UTC.

Student Notes:

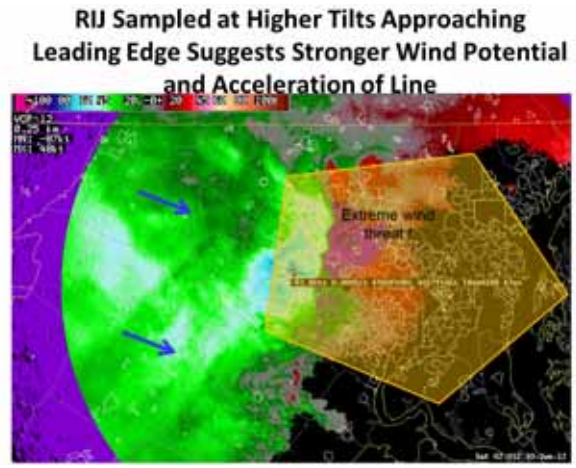

47. Summary

Instructor Notes: Warning challenges are related to good evaluation. Threat Assessment starts with climatology and uses an evaluation of the types of QLCS that occur. Downstream instability is a big factor in intensity and maintenance of the system. Some QLCS will fit models that are: High shear dominated Cold pool dominated Balanced. (the RIJ helps to restore the balance). Storm interrogation strategies should be based on the type of balance. Warning polygon strategies should take the shape of the threat motion and maximize lead times for expected impacts in the polygons. Some overlap is acceptable given these warning goals.

Student Notes:

Summary

- Warning challenges related to lack of proper evaluation
- Threat Assessment starts with climatology and uses an evaluation of the types of QLCS that occur
  - Assesses downstream instability is big factor
  - High shear
  - Cold pool dominated
  - Balanced

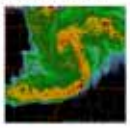

- Warning polygon strategies take the shape of the threat motion and maximize lead times for expected impacts

48. Contact Information

Instructor Notes:

Student Notes:

Contact Information

Warning Decision Training Brar
120 David L. Boren Blvd.
Norman, OK 73072
(405) 325-3190

WDTB Instructional Developers

Brad Grant
bradford.n.grant@noaa.gov
405-325-2997

James LaDue
james.g.ladue@noaa.gov
405-325-3004